

NGU Report 2012.005

**Tropical Weathering
in Norway,
TWIN Final Report**

Report no.: 2012.005		ISSN 0800-3416	Grading: Open	
Title: Tropical Weathering In Norway, TWIN Final Report				
Authors: Odleiv Olesen, Dag Bering, Marco Brønner, Einar Dalsegg, Karl Fabian, Ola Fredin, Jomar Gellein, Berit Husteli, Christian Magnus, Jan Steinar Rønning, Terje Solbakk, Jan Fredrik Tønnesen & Jon Arne Øverland			Client: Geological Survey of Norway and Norwegian Petroleum Directorate	
County: Vestfold, Vest-Agder, Sogn & Fjordane, Nord-Trøndelag, Nordland, Finnmark			Commune:	
Map-sheet name (M=1:250.000) Skien, Mandal, Florø, Ulsteinvik, Trondheim, Svolvær, Andøya			Number of pages: 188 Price (NOK): 645,-	
Fieldwork carried out: 2009-2011	Date of report: 02.05.2012		Project no.: 3307.00	Person responsible: <i>Øystein Nordgalen</i>
<p>Summary:</p> <p>The Geological Survey of Norway and the Norwegian Petroleum Directorate established the TWIN Project (Tropical Weathering In Norway) in 2009 to improve the understanding of deep weathering on mainland Norway as well as offshore. All known reports of deep weathering in Norway have been reviewed and registered in a GIS database. We have selected four representative locations for more detailed studies in southern Norway (Kjose, Lista, Vågsøy-Stad and Inderøya) and another four locations in northern Norway (Vestvågøya, Hadseløya, Andøya and Hamarøya). Geophysical studies (2D resistivity and refraction seismic) reveal fairly continuous saprolite layers with a thickness up to 100 metres in Vestfold (Kjose), Lofoten-Vesterålen, Hamarøya and Varangerhalvøya. The results also show that the degree of weathering varies extensively over short distances. An offshore petroleum reservoir consisting of weathered basement rocks is most likely equally heterogeneous. The deep weathering in the Lofoten-Vesterålen and Hamarøya occur most likely on the basement surface of rotated fault blocks, whilst the weathering in southeastern Norway and eastern Finnmark seems to occur in a stable and more distal part relative to the Mesozoic rift basins. The remnants of deeply weathered basement on the mainland of Norway occur as accumulations of clay minerals along structurally defined weakness zones and locally as up to c. 100 m thick continuous saprolite layers. Weathering extending down to more than 200 m depth is observed in fracture zones. XRF analysis and mass balance calculations (degree of leaching) commonly show a high degree of mineral alteration with bulk leaching of main elements (Si, Al, Na and K) in the range of 30-65%. The pervasive alteration of large volumes of bedrock is indicative of chemical weathering caused by percolating acidic groundwater in a humid climate, possibly during tropical to sub-tropical conditions in the Mesozoic. Subsequent erosion and denudation have largely removed the evidence of deep weathering on the mainland. The deep weathering process can also explain some of the enhanced concentrations of heavy metals and REE in some Norwegian tills. Understanding these processes is consequently a key to a successful mineral exploration programme as well as an efficient planning of new tunnels and other rock constructions in Norway.</p>				
Keywords: Geofysikk (Geophysics)	Kontinentalsokkel (Continental shelf)	Tolkning (Interpretation)		
Berggrunnsgeologi (Bedrock geology)	Dypforvitring (Deep weathering)	Magnetisk metode (Magnetic method)		
Paleomagnetisme (Palaeomagnetism)	Elektrisk metode (Electrical method)	Fagrapport (Scientific report)		

CONTENTS

1	INTRODUCTION	7
1.1	Saprolite – deep tropical weathering	8
2	GEOPHYSICAL METHODS	19
2.1	Resistivity and induced polarisation.....	19
2.1.1	Acquisition	19
2.1.2	Inversion.....	20
2.2	Refraction seismics.....	21
2.3	Amager method	22
2.4	Palaeomagnetic dating.....	23
2.4.1	Sampling.....	24
2.4.2	Sampling procedure for weathered rocks at Hadseløya	24
2.4.3	Palaeomagnetic measurements.....	26
3	GEOLOGICAL AND GEOCHEMICAL METHODS.....	27
3.1	Geochemical and mineralogical analyses.....	27
3.1.1	Introduction	27
3.1.2	Sampling locations	28
3.1.3	Analytical methods.....	28
3.1.4	Results	29
3.1.5	Conclusions	30
3.2	Remote sensing mapping of deep-weathered bedrock	30
4	REVIEW OF PREVIOUS DEEP-WEATHERING REPORTS.....	33
4.1	Geophysical data	35
4.2	Profiles.....	36
5	SOUTHERN NORWAY	37
5.1	Lista	37
5.2	Kjose.....	47
5.2.1	Geochemistry, clay mineralogy and granulometry	48
5.2.2	Electric resistivity measurements.....	50
5.3	Vågsøy – Stad – Inderøya.....	55
5.3.1	Vågsøy.....	55
5.3.2	Stad.....	66
5.3.3	Inderøya.....	71
6	NORTHERN NORWAY	77
6.1	Introduction	77
6.2	Geological framework of the Lofoten-Vesterålen-Hamarøya region	78
6.3	Vestvågøya	79
6.3.1	Resistivity profiling.....	81
6.3.2	Seismic profiling	83
6.3.3	Comparison of seismic and resistivity profiling and conclusions.....	85
6.4	Hadseløya	87

6.4.2	Palaeomagnetic sampling.....	91
6.5	Sortland	94
6.5.1	AMAGER results	94
6.5.2	Resistivity profiling.....	95
6.6	Hamarøya	98
6.6.1	Resistivity profiling.....	99
6.7	Andøya	100
6.7.1	Resistivity profiling.....	102
6.7.2	Palaeomagnetic sampling, Ramså.....	108
6.7.3	Seismic profiling, Staveheia,.....	111
6.8	Conclusions from Lofoten-Vesterålen and Hamarøya	117
7	REGIONAL GEOMORPHOLOGY AND DEEP WEATHERING	120
8	DISCUSSION	126
9	CONCLUSIONS	130
10	RECOMMENDATION FOR FURTHER WORK.....	132
11	REFERENCES	133

Appendix 1

XRD-analysis by Alf Olav Larsen.....	149
--------------------------------------	-----

Appendix 2

Mehuken windpower park, mapping of drillcores from five sites for windpower plants.

Bergab – Berggeologiska Undersökningar AB.....	157
------------------------------------------------	-----

1 INTRODUCTION

The Norwegian Petroleum Directorate and the Geological Survey of Norway launched the joint research and mapping project TWIN (Tropical Weathering in Norway) in 2009 to study the numerous occurrences of deeply weathered bedrock in Norway. The two institutions had realised that this phenomenon is widespread in parts of mainland and offshore Norway. Remnants of weathered basement have an increasing impact on society and economy in Norway as they can be responsible, on the one hand, for rock avalanches and tunnel hazards but also have a considerable potential as hydrocarbon and groundwater reservoirs. An improved understanding of these supergene processes is also a key to interpreting some of the geochemical anomalies in mineral exploration programmes. The TWIN project involves mineralogical, chemical and petrophysical characterisation of known occurrences of weathered bedrock or saprolite, as well as the development and testing of age dating techniques and geomorphological and geophysical mapping tools.

The remnants of deeply weathered basement on the mainland occur both as accumulations of clay minerals, including smectite and kaolinite, and as coarse-grained grus along structurally defined weakness zones (faults and fracture zones) and locally as continuous layers. Clay-rich zones with thicknesses of more than 200 metres have been observed (Palmstrøm *et al.* 2003, Olesen *et al.* 2007), e.g. in the Lieråsen and Romeriksporten tunnels. More extensive layers of saprolite have been reported in some areas such as at Kjøse in Vestfold. The partial or total alteration of bedrock to clay minerals is to a large extent the result of chemical weathering caused by percolating acidic groundwater in a humid climate. When using the studies in southern Sweden, on Andøya and offshore Norway (Lidmar-Bergström *et al.* 1997, Sturt *et al.* 1979 and Roaldset *et al.* 1993) as analogues, it is likely that the most extensive weathering on mainland Norway occurred during tropical to sub-tropical conditions in the Mesozoic. Subsequent erosion and denudation have partly removed the evidence of deep weathering on the mainland. Moreover, several offshore exploration wells have recently detected coarse-grained grus weathering below Mesozoic sedimentary rocks (Carstens 2011). This type of weathering has often been interpreted to be of Quaternary age on the mainland (e.g. Peulvast 1985, Sørensen 1988, Paasche *et al.* 2006). Hydrothermal activity has, locally, also caused alteration of the bedrock to clay minerals, especially within the Oslo Graben (e.g. Ihlen *et al.* 1982, Ihlen & Martinsen 1986).

We have selected eight representative locations for more detailed studies: Kjøse-Larvik, Lista, Vågsøy-Stad and Inderøya in southern Norway, and Vestvågøya, Hadselsøya, Andøya and Hamarøya in northern Norway (Fig. 1.1). Several of the areas are located adjacent to offshore areas with seismic indications of deep Mesozoic weathering. We have also included some locations from Finnmark in the discussion chapter to complete the regional review of deep weathering in Norway. Offshore oil exploration wells, shallow boreholes or sea bottom sampling may provide crucial information with regard to timing, extent and character of the weathering. Andøya in Vesterålen is of special interest since weathered basement occurs immediately below outcropping Mesozoic sedimentary rocks.

An improved understanding of the age and nature of weathering and alteration of basement bedrock has a wide range of applications onshore (e.g. rock stability of natural mountain slopes and man-made construction sites and tunnels in addition to groundwater utilisation and mineral exploration) as well as offshore (e.g. bottom seal of hydrocarbon traps over basement highs, migration paths of hydrocarbons and potential petroleum reservoirs). The locations of numerous sounds, inlets, islands and skerries along the Norwegian coast can, to a large extent, have been controlled by exhumation and erosion of weathered basement. The study provides a connection between geomorphological elements along the Norwegian coast onshore and offshore.

1.1 Saprolite – deep tropical weathering

Lidmar-Bergström (1989, 1995) proposed that the joint-controlled valley landscape of southwestern Sweden was formed during Neogene denudation. She demonstrated how erosion of a thick Jurassic/Early Cretaceous saprolite along regional fault and fracture zones had caused the formation of extensive valleys in the northern Scania region (Figs. 1.1 & 1.2). This system of joint-aligned valleys could be traced northwards along the west coast of Sweden all the way to eastern Norway and farther west along the coast of southern Norway (Fig. 1.1). The weakness zones in this sub-Cretaceous etch-surface are partly due to the presence of clay minerals such as kaolinite and smectite which are, to a large extent, the result of chemical weathering under subtropical conditions in the Jurassic and Early Cretaceous (Lidmar-Bergström 1982; Lidmar-Bergström *et al.* 1999). The weathering occurred originally across the entire palaeosurface, but gradually penetrated deeper into pre-existing fracture zones (Fig. 1.2). The saprolite was partially eroded before the Cretaceous, and the remnants of this chemical weathering were preserved below shales and carbonates deposited during the Late Jurassic and Cretaceous transgressions (c. 400 metres higher eustatic sea level). Up to 60 metre-thick bodies of saprolite have been found in joint valleys in Scania (Lidmar-Bergström 1999). Interpretations of aeromagnetic data in the Oslofjord region indicate the presence of saprolite exceeding 200 m in thickness in fracture zones (Olesen *et al.* 2007). Exhumation of the Mesozoic erosion surface in southeastern Norway was initiated during the Early Cainozoic and the uplift and erosion accelerated during the Neogene (Riis 1996, Lidmar-Bergström *et al.* 1999).

There has previously been a widespread view that clay-bearing weathering surfaces in Scandinavia formed during the Mesozoic whilst the gravelly, so-called ‘grus’-weathering is much younger, perhaps of Quaternary or Plio-Pleistocene age (Peulvast 1985, Sørensen 1988, Lidmar-Bergström *et al.* 1999). Olsen (1995) and Paasche *et al.* (2006) have suggested a Tertiary age for the kaolinitic weathering of the Precambrian on Finnmarksvidda and coarse-grained weathering in Vesterålen, respectively. The blockfields that occur frequently in the mountainous regions of Norway have been suggested to represent collapsed saprolites (Riis 1996, Lidmar-Bergström *et al.* 1999) but their origin is not fully understood.

Riis (1996) concluded from a correlation between offshore geology and onshore morphological elements that a peneplain with related deep weathering had formed during the Jurassic. His study supported the conclusions from Lidmar-Bergström (1995) that the relief in Sweden bordering southeastern Norway had an extensive cover of Late Jurassic and Cretaceous sediments. Remnants of subtropical weathering can also be found below Mesozoic sedimentary rocks on Andøya, northern Norway (Sturt *et al* 1979) and on the continental shelf (Roaldset *et al.* 1993, Mørk *et al.* 2003).

More than a hundred years ago Reusch (1902, 1903a) suggested that the Oslo Region had been covered with Cretaceous sedimentary rocks (Fig. 1.3). He based his hypothesis on a geomorphological feature defined as ‘superimposed valleys’. He argued that the Numedalslågen river could not have eroded through the relatively high Skrim mountains (700-800 metres above sea level, Fig. 1.3) if the course had not already been defined in relatively soft sedimentary strata lying on the crystalline rocks. Reusch (1902, 1903a) also concluded that a SSE-NNW-trending palaeo-river had been flowing from Valdres through Nittedal and Øyeren to the coast. This drainage system was changed after exhumation and erosion along the fault systems of the Oslo Rift and in the softer, low-grade metamorphic, Cambro-Silurian rocks of the Ringerike-Hadeland district. Reusch (1902, 1903a) argued further that the eroded sedimentary sequence could be of Cretaceous age since flintstones were found in Østfold county and he knew that the Cretaceous rocks in Denmark were flintstone-bearing. Holtedahl (1953a) disagreed with the conclusions presented by Reusch (1902, 1903a) and suggested that the valleys in the Oslofjord region developed primarily along regional fracture zones. Aeromagnetic maps (Lundin *et al.* 2005, Olesen *et al.* 2007), however, do not indicate any regional fracture zones along the valleys of Lågendalen and Nittedal or the Drammenfjord.

Reusch (1878) had earlier also concluded that the landscape was relatively little affected by the glacial erosion. He especially referred to a location at Ødegårdsbukta 2-3 km to the east of Nevlunghavn in Vestfold where a large block of limestone has been removed by the inland ice (Fig. 1.4, UTM 32 coordinates: 552 080 - 6536 860, WGS 84 datum, on 1:50 000 map-sheet 1712 I Langesund). No weathering surface has been formed on the new exposed bedrock surface during the last 10,000 years, indicating that the typical limestone weathering in the Oslofjord region must be much older than Pleistocene. It could, in principle, represent the base of the original Mesozoic weathering.

Reusch (1903b) also studied kaolinite deposits in Norway (including deposits in Hurdal, Seljord and Flekkefjord). He arrived at the conclusion that the Flekkefjord deposit was a result of hydrothermal activity related to volcanism (Reusch 1900). There is also undisputed hydrothermal clay alteration (commonly referred to as propylite and argillic alteration) associated with subvolcanic complexes and ore-forming processes in the Oslo Region (Olerud & Ihlen 1986) and some deep-seated (>1000 m) clay-bearing veins in Norwegian

mines and hydropower plants (Sæther 1964, Rokoengen 1973). There is, consequently, no evidence that all clay-bearing fractures in the Norwegian bedrock are related to subtropical weathering. However, Lidmar-Bergström (1989) and Lidmar-Bergström *et al.* (1999) have shown that clay alteration associated with many of the fracture zones in the greater Oslofjord region represents remnants of an originally extensive saprolite layer.

During tropical weathering, iron oxides such as magnetite alter to hematite and iron hydroxides at the same time as silicate minerals are converted into clay minerals (e.g. Henkel & Guzmán 1977, Grant 1984). Ferro-hydroxides have also been observed in clay-alteration zones in the greater Oslofjord Region, in Vestfold (Låg 1945), and in Østfold (Kocheise 1994, Banks *et al.* 1994). Deep weathering will therefore create a negative deviation in the Earth's magnetic field. Olesen *et al.* (2007) and Olesen & Rønning (2008) utilised this phenomenon to produce a tunnel planning awareness map of the Oslo region. If the bedrock holds a reversed magnetisation, the breakdown of the remanent minerals will, however, cause a positive anomaly as, for example, observed by Beard & Lutro (2000) in the Krokskogen area to the northwest of Oslo.

It is generally observed that the thick layer of weathered rock (saprolite) in tropical areas can be subdivided into several weathering zones (Acworth 1987, Scott & Pain 2008). The deeper zones are commonly dominated by granular friable layers of disintegrated crystal aggregates and rock fragments whilst a shallower zone has a massive accumulation of secondary minerals (clays), though some stable primary minerals may still be present in their original form. The shallow zone has low permeability whereas the deeper zone has an intermediate permeability (Fig. 1.5).

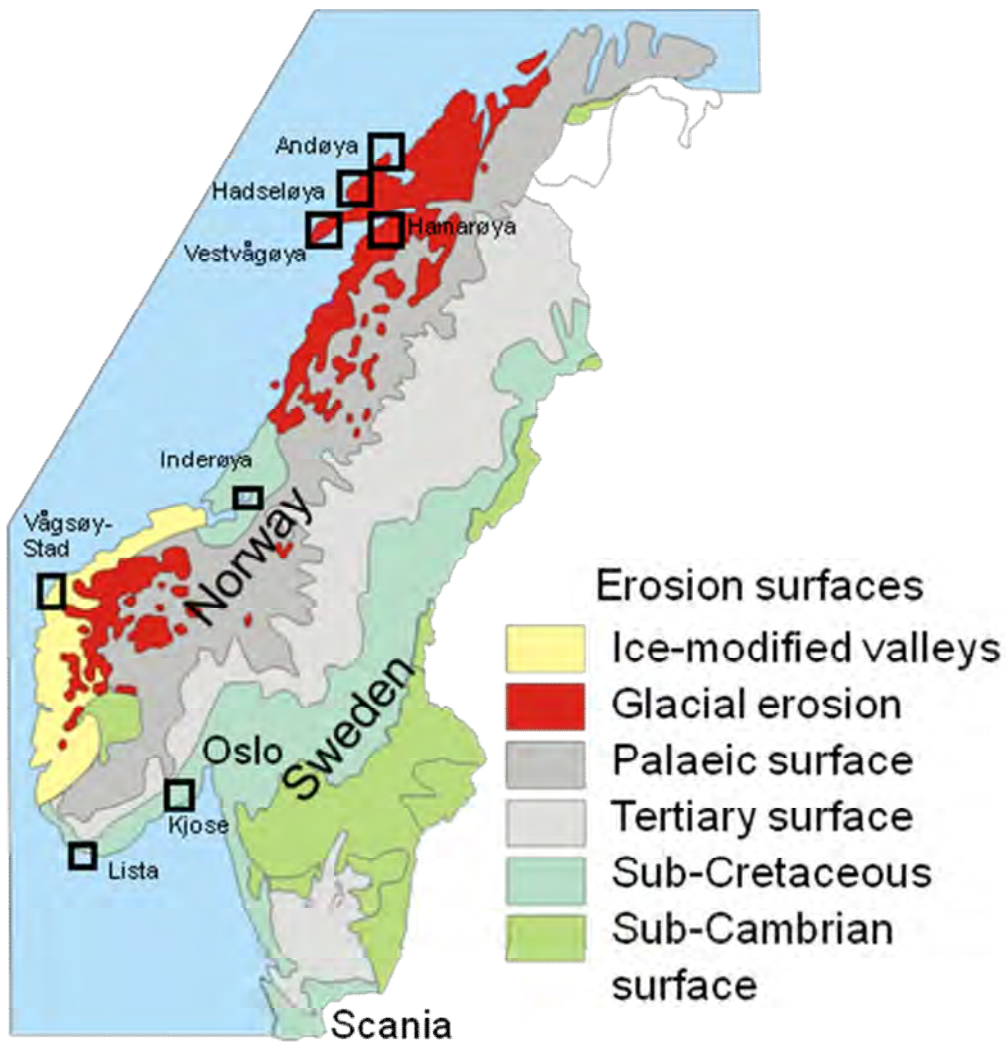


Figure 1.1 Geomorphological map of western Fennoscandia (Lidmar-Bergström et al. 1999). The eight representative locations selected for more detailed studies are depicted: Kjøse, Lista, Vågsøy-Stad and Inderøya in southern Norway and Vestvågøya, Hadselsøya, Andøya and Hamarøya in northern Norway.

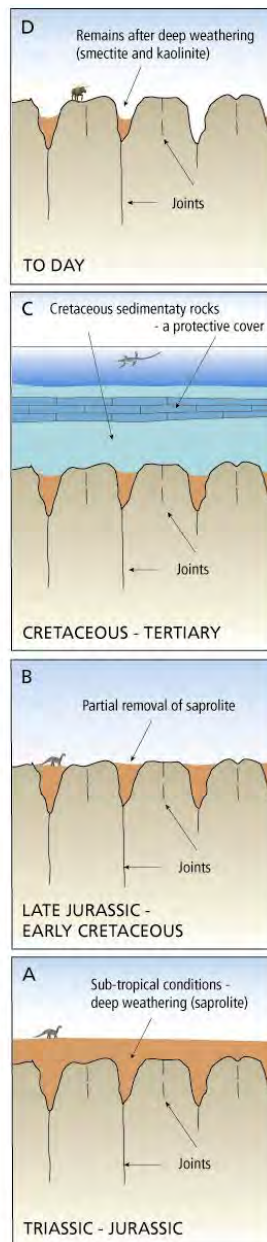


Figure 1.2 Schematic illustration of Lidmar-Bergström's model for the development of deep-weathering products. A) Triassic-Jurassic sub-tropical weathering (etching) across the entire palaeo-surface with deeper penetration into pre-existing fracture zones. B) Partial erosion of the weathered material during Late Jurassic or Early Cretaceous. C) Preservation of chemical weathering below shales and carbonates deposited during the Late Jurassic and Cretaceous transgressions. D) Uplift and erosion during the Neogene. The bulk of the chemical weathering products was removed leaving an immature etch-surface landscape with joints and faults as valleys. The clay zones containing smectite and kaolinite have been preserved at depth along the fracture zones (modified after Lidmar-Bergström 1995). In some areas such as Kjøse, Lofoten-Vesterålen, Hamarøya and Varangerhalvøya, more extensive saprolite layers are preserved.

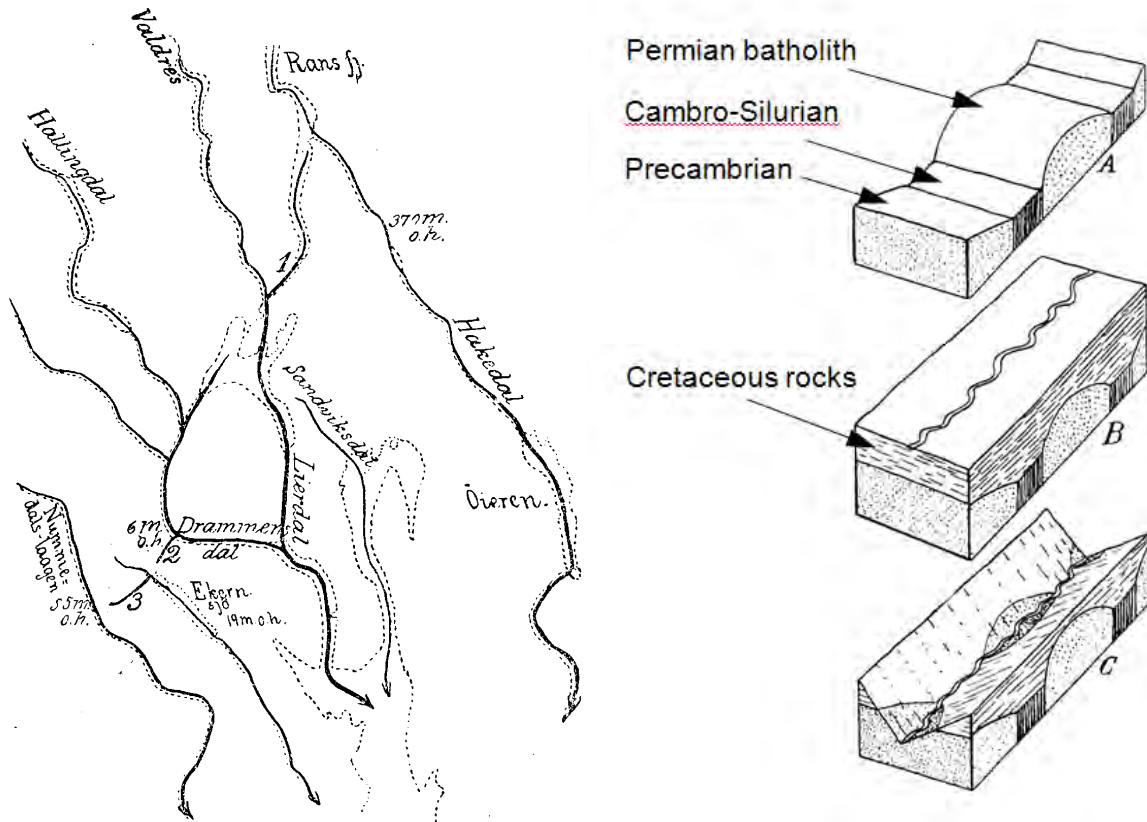


Figure 1.3 Based on the hypothesis of 'superimposed valleys' Reusch (1902, 1903a) suggested that the Oslo Region had been covered by Cretaceous sedimentary rocks. He argued that the Numedalslågen river could not have eroded through the relatively high Skrim mountains if the course was not already defined in relatively soft sedimentary rocks. He also concluded that a SSE-oriented palaeo-river had been flowing from Valdres through Nittedal and Øyeren to the coast. This drainage system was changed after exhumation and erosion along the fault systems of the Oslo Rift and in the softer, low-grade metamorphic Cambro-Silurian rocks of the Ringerike-Hadeland district. Reusch argued further that the eroded sedimentary succession could be of Cretaceous age since flintstones were found in the Østfold county.

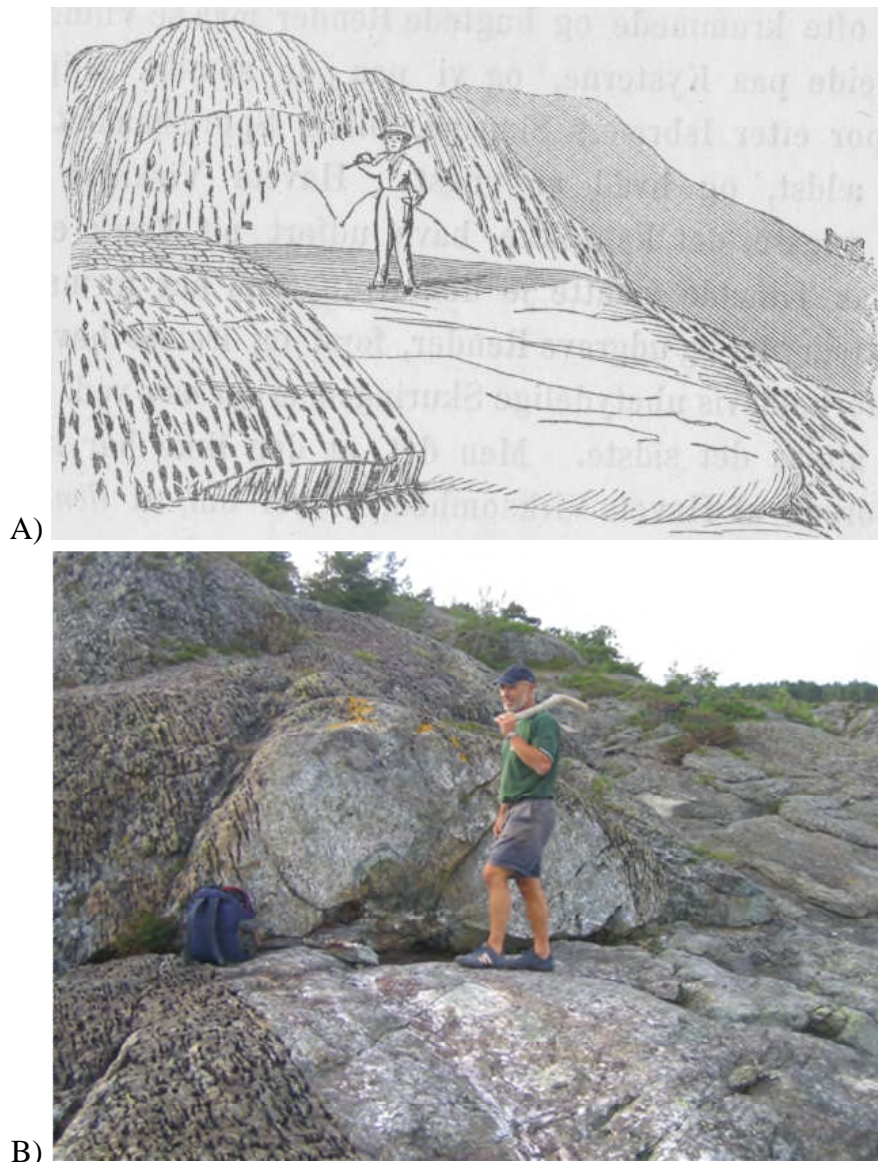


Figure 1.4 Large block of weathered limestone removed by the inland ice at Ødegårdsbukta (UTM 32 coordinates with WGS 84 datum: 552 080 - 6536 860 on 1:50 000 map sheet 1712 I Langesund), 2-3 km to the east of Nevlunghavn in Vestfold. A) Drawing by Reusch (1878). B) Photograph of the same location in 2006. No weathering surface has been formed at the exposure during the last 10,000 years indicating that the typical limestone weathering in the Oslofjord region must be much older than Pleistocene. Reusch (1878) concluded that the erosional effect on the topography during the Pleistocene glaciations was relatively low.

The relatively flat-lying terrain in Finnmark has also been interpreted as an originally weathered surface (Fjellanger & Nystuen 2007). Areas with competent bedrock such as quartzite and gabbro occur frequently as ridges and mountains (e.g. Duolbagáisá, Rásttigáisá, Čohkarášša, Iškoras, Ádjit, Biggevárri, Øksfjord, Seiland and Stjernøya). Glacial erosion has later sculptured the inselbergs in western Finnmark and Troms to an alpine landscape. Fig. 1.5 illustrates how quartzites in light colours occur as elevated ridges on the Nordkinn Peninsula whereas the thinner bedded sandstones and pelitic rocks in grey and green colours coincide with flat-lying terrain at a lower altitude. The low-altitude terrain might represent a palaeoweathering surface (etch surface) with deeply weathered fracture zones. The quartzitic ridges are interpreted to represent so-called inselbergs that are also common in areas with pervasive tropical weathering. The overburden in the area may therefore represent a glacially reworked saprolite. The observed anomalous high concentrations of REEs and heavy metals such as Cr, Ni, Mo, Zn and Pb (Reimann *et al.* 2011, 2012) can be partly caused by a weathering process where main elements such as K, Na and Ca have been partly removed by leaching. Similar geochemical patterns with reduced concentrations of main elements and increased concentrations of heavy metals and REEs in till relative to the adjacent bedrock have also been reported in southeastern Norway (Roaldset 1975, Reimann *et al.* 2007).

Deep weathering has also been observed in trenches as well as on refraction seismic data in the Sádgejohka (Sargejokk) area located 50 km to the south of Karasjok (Dalsegg 1987, Olsen 1998). The weathered basement occurs below a complex Quaternary stratigraphy including several palaeosols, the oldest being more than 300,000 years (Olsen 1998). Gjeldsvik (1956) reported a preglacial weathering of copper minerals in the Čierte area farther to the west on Finnmarksvidda. Chalcopyrite and bornite in a breccia have been replaced by supergene minerals such as chalcocite, covellite, malachite, chrysocolla and limonite. Dalsegg *et al.* (1986) found also secondary copper minerals such as chalcocite and native copper in a copper mineralization in the Riednjjav'ri area in the southern part of the Kautokeino Greenstone Belt. Lindahl (1983) has argued that the Njallaav'zi uranium deposit in the Čierte area is of supergene origin and was formed during late Precambrian weathering. Åm (1994) reported weathering minerals such as vermiculite, smectite, kaolinite and goethite in the Stuoragurra postglacial fault at Máze (Masi) farther to the north on Finnmarksvidda.

Alnæs & Hillestand (1989) described extensive layers of kaolinite-bearing Quaternary overburden and sandstone in the eastern part of the Varanger Peninsula (Fig. 1.6). They carried out an extensive programme consisting of six refraction seismic profiles and ten drillholes and found a kaolinite content of up to 15 % and further concluded that the weathering had a regional distribution in the area. Kaolinite occurs in the Quaternary overburden as well as in the highly fractured reddish sandstone. We have included results from an extensive research programme in Australia to illustrate that the relationship between *in situ* and transported regolith can be rather complex – even without glacial erosion and transport (Fig. 1.7).

Riis (1996) and Fjellanger & Nystuen (2007) suggested a Tertiary age for the paleic surface in eastern Finnmark based on correlation with subsurface unconformities in the Barents Sea and correlation with the regional plains in northern Sweden and Finland dated by Eocene fossils from clays in bedrock depressions (Tynni 1982, Fenner 1988). An older, Mesozoic age, however, cannot be ruled out. It is further possible that the Alta and Reisa canyons were originally formed as superimposed valleys, as described in eastern Norway by Reusch (1902, 1903a). See Section 1.1 in the present report.



Figure 1.5 Perspective view of the Nordkinn Peninsula seen from the north (www.norgei3d.no). The psammitic rocks in light colours (mostly quartzites) occur as elevated ridges whereas the thinbedded more pelitic rocks in grey and green colours coincide with flat-lying terrains at a lower altitude. The difference in altitude is approximately 200-300 metres. The low-altitude terrain represents most likely a palaeoweathering surface (etch surface) with deeply weathered fracture zones (referred to as joint valleys by Lidmar-Bergström (1989, 1995)). The ridges are interpreted to represent inselbergs that are also common in areas with pervasive tropical weathering. The same type of quartzite inselbergs can also be found farther south in the Gaissa Mountains and in the Precambrian of Finnmarksvidda (e.g. Iškoras, Ádjit, Biggevárri). For the geology of the Nordkinn Peninsula, see Siedlecka & Roberts (1996).



a)



b)

Figure 1.6 Outcrop of kaolinite-bearing sandstone in Leirelva, a tributary to Komagelva on the Varanger Peninsula in Finnmark (from Alnæs & Hillestad 1989). Kaolinite occurs in the Quaternary overburden as well as in the highly fractured reddish sandstone.

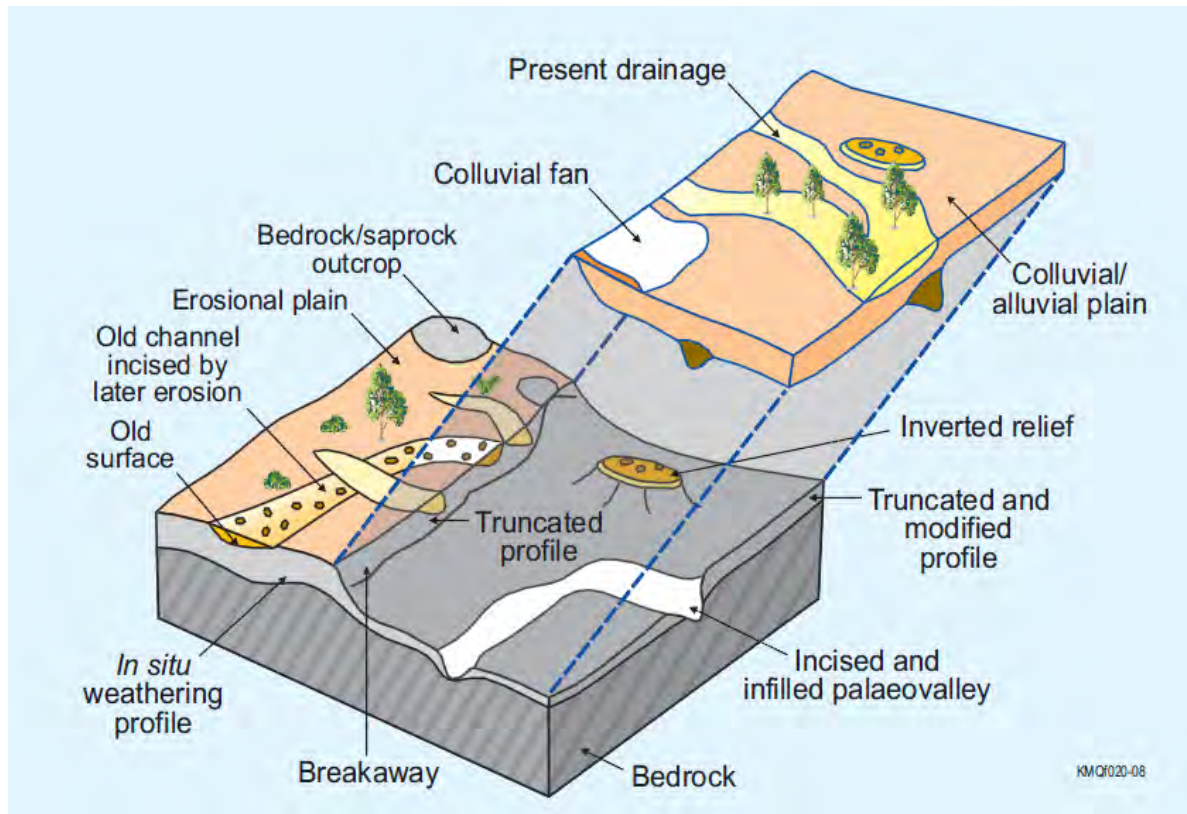


Figure 1.7 *Block diagram summarizing the main regolith-landform components of the Cobar region in Australia (McQueen 2008). The figure illustrates a complicated pattern of both in situ and transported weathering.*

2 GEOPHYSICAL METHODS

Marco Brønner, Einar Dalsegg, Karl Fabian, Odleiv Olesen, Jan Steinar Rønning & Jan Fredrik Tønnesen

2.1 Resistivity and induced polarisation

The 2D electric resistivity traversing (ERT) and induced polarisation (IP) methods have been applied in the TWIN project. The combined IP and resistivity measurements extended the survey time slightly. The combination of the two kinds of data, however, significantly reduced the risk of misinterpretation. The methods are briefly described below and a detailed description is available at

<http://www.ngu.no/no/hm/Norges-geologi/Geofysikk/Bakkegeofysikk/Elektriske-metoder/>
(in Norwegian).



Figure 2.1 Acquisition of electric resistivity data south of Ramsåa at Andøya (Andøyatorv peat extraction plant).

2.1.1 Acquisition

Data are collected using a cable system developed by the Institute of Technology of Lund University, called the Lund system (Dahlin 1993). The system consists of a relay box (Electrode Selector ES10-64 C) and of two or four multi-electrode cables. The ABEM Terrameter SAS 4000 (ABEM 1999) resistivity and IP instrument contains an integrated PC for full control of the data acquisition process and storage of data. In this survey, four cables were used with a GRADIENT electrode configuration and 10 m electrode spacing. A maximum depth range of about 120 metres may be reached with the latter configuration. The resolution decreases with depth and resistivity data deeper than c. 80 metres are by experience less reliable. The entire system can be rolled along the profile such that the extent of a profile is almost unlimited.

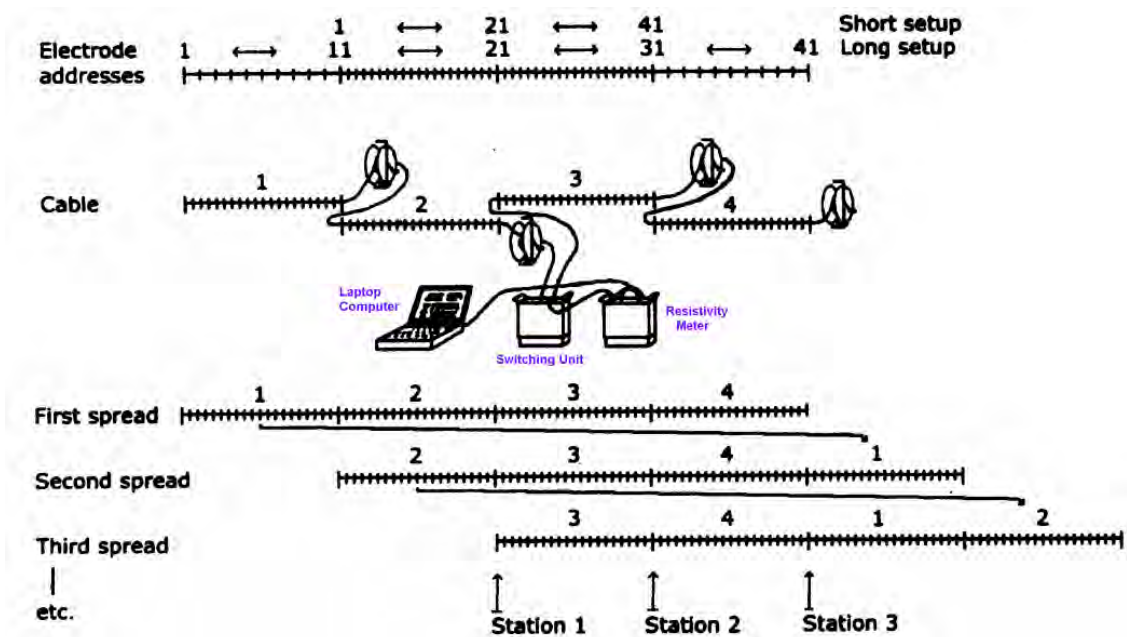


Figure 2.2 Sketch outline of the ABEM Lund Imaging System. Each mark on the cables indicates an electrode position (Dahlin 1996). The cables are placed along a single line (the sideways shift in the figure is only for clarity). This figure also shows the principle of moving cables when using the roll-along technique.

2.1.2 Inversion

All resistivity measurements give an apparent resistivity value that represents a weighted average resistivity which resulted from the resistivity of each heterogeneous volume in the surrounds of the measurement points (note: heterogeneous volume in terms of resistivity and size for the purpose of this study). To find the specific resistivity of each part of the heterogeneous investigated volume, the data are inverted. This is done by dividing the profile into blocks each characterised by specific resistivity values. The resistivity values of the blocks are adjusted following an iterative procedure until the theoretical model fits the measured data.

Resistivity measurements were inverted using the computer program RES2DINV (Loke, 2010). Different methods of inversion are applied ("Least Square" and "Robust") with variations in the inversion parameters, attenuation factors and filters. This did not result in any fundamental changes in the main features of the inverted profiles.

The resistivity of the bedrock, which is obtained by ERT, depends on the porosity, water saturation and resistivity of groundwater in cracks and fracture zones, as well as the clay content that is produced by weathering and other geological phenomena.

2.2 Refraction seismics

Similar to geoelectric investigations, seismic measurements are also often carried out in exploration geophysics. Seismic refraction measurements are based on the times of arrival of the initial ground motion generated by a source recorded at different distances. Complications related to late arrivals in the recorded ground motion are discarded. Thus, the dataset derived from refraction measurements consists of a series of times versus distances. These are then interpreted in terms of the depths to subsurface interfaces and the velocities at which motion travels through the subsurface within each layer. These velocities are controlled by a set of physical constants, called elastic parameters that describe the material. Any change in rock or soil property will result in changes to the seismic velocities (Redpath 1973).

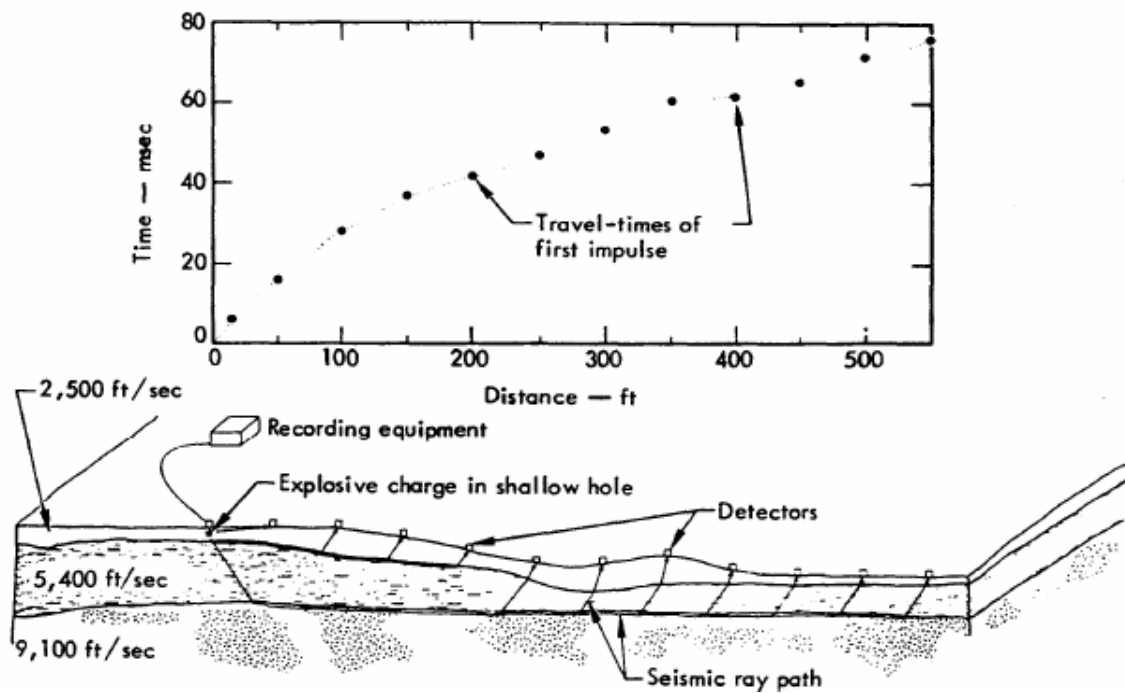


Figure 2.3 Schematic diagram illustrating the shallow refraction seismic method (Redpath 1973).



Figure 2.4 The seismic recording system ABEM TERRALOC MK6.

2.3 Amager method

The AMAGER method (AeroMAGnetic and GEomorphological Relations) was developed and published by Olesen *et al.* (2007) and comprises a correlation of morphological depressions and magnetic lows. The method is based on the not necessarily, but for Norway, common observation that deeply weathered basement shows a noticeably reduced magnetisation (Figure 2.5) as compared with the parent material and is moreover easily erodible. Relative magnetic lows which correlate with topographic depressions in eroded and exposed basement landscapes are thus likely to indicate the location and distribution of deep weathering.



Figure 2.5 Magnetic measurements of weathered and un-weathered bedrock on Hamarøya. The remaining magnetisation of the altered rocks is reduced to a third compared to the parent material.

The method requires good-quality aeromagnetic data and digital elevation grids to achieve reliable results. Furthermore, detailed geological maps and a profound knowledge of the geology are useful in order to delineate areas with Quaternary overburden.

For the TWIN project we modified and developed the AMAGER method and applied it to the two areas of Lista and Langøya, where both weathering locations had been reported and high-quality, high-resolution aeromagnetic data were on hand. We carried out a 1 km Gaussian high-pass filtering of both the reduced-to-pole magnetic and topography grids. Subsequently, we used the Geosoft's CET Grid Analysis extension to automatically detect the minima from both grids. This extension was developed by the Centre for Exploration Targeting (CET) at the University of Western Australia and provides a rapid and unbiased workflow for texture, phase analysis and structure detection. The advantage of using this modified method rather than the original one (Olesen *et al.* 2007) is that we do not use a defined single value threshold to include or exclude a minimum, and we also applied a qualitative approach, which is better adapted to the relative lateral changes of the magnetisation. However, we also

applied an automatic gain control (AGC) to scale the magnetic and topographic data, which was especially beneficial for areas of rather subdued morphology.

The solutions for both grids were correlated and coinciding solutions in the two high-pass filtered datasets were used as indications of deep weathering.

2.4 Palaeomagnetic dating

A lack of age dating hampers the reconstruction and understanding of deep weathering events. Here, we present results from a pilot study to use palaeomagnetic techniques to infer age constraints from two, deep-weathered sites at Hadseløya and Andøya, Lofoten-Vesterålen islands, Norway. The general idea behind this approach is to use palaeomagnetic dating in an analogous way as the studies by Parnell *et al.* (2004) and Elmore *et al.* (2010). Parnell *et al.* (2004) reconstructed the direction of a chemical remanent magnetisation (CRM) acquired during a hot fluid-flow event channelled through a thrust zone. The timing of kaolin formation has been constrained by palaeomagnetic analysis at two localities, where a coeval relationship between the kaolin and a diagenetic intergrowth of hydrothermal hematite could be demonstrated (Fig. 2.6). Elmore *et al.* (2010) used a similar approach to date brecciation and associated fluid-induced diagenetic alteration, probably related to Mesozoic extension.



Figure 2.6 Palaeomagnetic determination of the timing of hydrothermal hematite formation during a fluid flow event at Kishorn (Fig.8 from Parnell *et al.* 2004). Solid circle, square, and triangle indicate palaeomagnetic pole positions determined from CRMs at sites mineralised by hydrothermal hematite and kaolin. Comparison with an apparent polar wander curve for Europe indicates that the poles lie at or near the curve in Permian time.

In the setting of deep weathering, palaeomagnetic measurements may, in a similar way, be able to pick up a magnetisation overprint that occurred during the weathering event. If fluid flow related to the weathering induces a diagenetic formation of magnetic minerals, like hematite, these would acquire a CRM reflecting the magnetic field at the time of the weathering event.

By reconstructing a palaeomagnetic direction from the CRM, and comparing this to the apparent polar wander path, it should be possible to narrow down the time window for the weathering event. In theory, there even is an advantage of the deep weathering study over the above fluid-flow studies, in that it is possible not only to sample the weathered material, but also the undisturbed parent material at the same site. A deviation between the palaeomagnetic directions of these two materials can then provide independent evidence for a secondary CRM formation at a later time.

2.4.1 Sampling

Hard-rock sampling was carried out according to standard palaeomagnetic procedures as described in Butler (1992). Inch cores were drilled and oriented using a Pomeroy orientation tool and a Brunton compass. The preferable sun-compass orientation method could not be applied for meteorological reasons.

2.4.2 Sampling procedure for weathered rocks at Hadseløya

Weathered material was sampled following the sampling procedures described by Schnepf *et al.* (2008) for baked clay and soft sediments. Because the weathered material at Hadseløya was extremely loose, a nose of in-situ weathered rocks was prepared by removing the material around it. Using plaster, and plaster bandages, the nose was surrounded by a tight cast with a flat surface. After the plaster had dried, this surface could be magnetically oriented using the Brunton compass.

After orienting, the material was carefully removed and packed together with the plaster cast. At the NGU laboratory the unconsolidated material was then soaked with water glass, Na_2SiO_3 , and kept soaked for several weeks to obtain optimal consolidation. The “Wacker OH” silica rock hardener, recommended for consolidation by Schnepf *et al.* (2008), was not available. This led to some problems during re-sampling of the material at Leoben, because the water glass often penetrated only 1-2 cm into the rock. Fortunately, enough hardened material was available for the palaeomagnetic measurements.

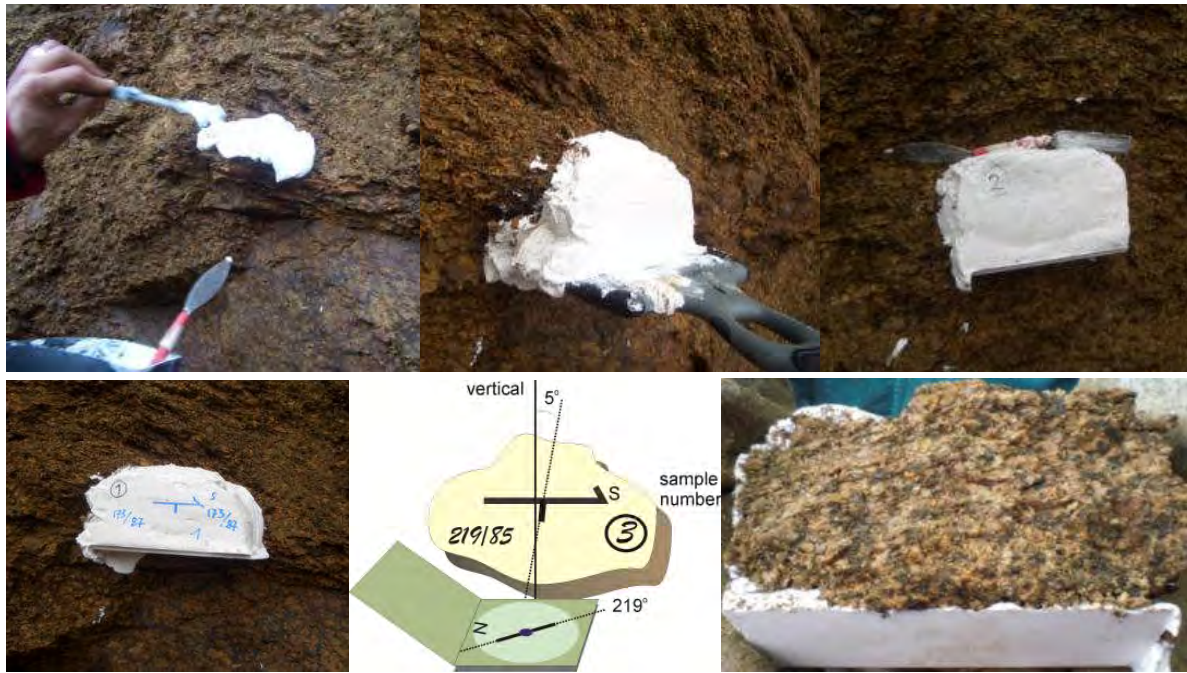


Figure 2.7 Oriented sampling of unconsolidated weathered bedrock at Hadseløya using the technique recommended by Schnepf et al. (2008).

The deep weathered layer at Ramså, Andøya, lies in a river bed and is covered by fluvial sediments. Therefore, the sediment cover first had to be removed and then non-magnetic aluminium tubes were driven into the unconsolidated bedrock below. The tube cores were magnetically oriented and carefully dug out.



Figure 2.8 Oriented sampling of unconsolidated weathered bedrock at Ramså, Andøya.

2.4.3 Palaeomagnetic measurements

Due to the unstable structure and weak magnetic signal of the samples, it was necessary to use a cryogenic magnetometer for the palaeomagnetic measurements. Because of the long experience and optimal equipment of the palaeomagnetic laboratory of the University Leoben, Austria, with unconsolidated continental sediments all palaeomagnetic measurements of drillcores and weathered plaster samples have been performed at this laboratory. Additional whole core measurements on the aluminium tubes from Ramså were performed at the drill-core palaeomagnetic laboratory of the LIAG in Grubenhagen, Germany. This was necessary because the diameter of the measurement coils in the cryogenic magnetometer at Leoben, designed for palaeomagnetic inch-cores, was too small for these samples, whereas the instrument at LIAG is designed for large diameter drillcores.

3 GEOLOGICAL AND GEOCHEMICAL METHODS

Ola Fredin

3.1 Geochemical and mineralogical analyses

3.1.1 Introduction

Characterisation of saprolites through geochemistry, clay content and grain size has proven to be a powerful tool in understanding past weathering processes. The potential for dating (palaeo-) weathering of samples from the crystalline basement has also been investigated. By quantifying the change in element concentrations from the fresh host bedrock to the saprolite, the amount and character of the weathering can be established. Through analysis of clay minerals, which represent the end stage of weathering in the saprolite, a better understanding of weathering processes can also be achieved. Finally, dating of clay diagenesis can potentially provide information on when the weathering processes were active.

Geochemical and clay analyses have been used at several locations to study deep weathering in the Scandinavian countries and elsewhere. XRD analysis of clay minerals is a difficult and time-consuming process and several studies have yielded ambiguous results. Examples of such ambiguous results have been reported for Norwegian sites by Rea *et al.* (1996a) and Paasche *et al.* (2006). The clay mineral kaolinite, which by many is regarded as a strong indicator of pervasive feldspar weathering, has commonly been reported even though the XRD procedure used cannot exclude the presence of chlorite as well as or instead of kaolinite. There has thus been a tendency, in particular in some Scandinavian scientific literature, to overestimate the presence of kaolinite in inferred weathering profiles. However, several extensive studies of clay mineralogy in Scandinavian saprolites have also been made where the presence of kaolinite is well established (e.g. Roaldset *et al.* 1982, Lidmar-Bergström *et al.* 1997). In order to avoid the difficulties and pitfalls involved with XRD analysis, this project has relied heavily on geochemical quantification of elements both in fresh host bedrock and saprolite. In this way, it is straightforward to see which elements have been affected by weathering and to calculate the mass loss (chemical leaching) during the weathering process (Brimhall *et al.* 1985).

For dating the clay minerals a number of methodologies were considered. K/Ar and $^{40}\text{Ar}/^{39}\text{Ar}$ dating of manganese oxides (Vasconcelos *et al.* 1992), alunite (Itaya *et al.* 1996), jarosite (Vasconcelos *et al.* 1994) and illite (Pluijm *et al.* 2001) has been used in a number of studies, with variable degrees of success. Other methodologies include (U-Th)/He dating of goethite (Schuster *et al.* 2005) and measurement of Radiation Induced Defects derived from the decay of U and Th (which is based on principles similar to Fission Track Dating). Because NGU has its own laboratory for $^{40}\text{Ar}/^{39}\text{Ar}$ dating, our focus has mainly been on investigating the presence of manganese oxides, alunite, jarosite and illite.

3.1.2 Sampling locations

Most of the sites from which samples were collected within the TWIN project were previously described by Peulvast (1985). Samples were collected from Hamarøya, Hadseløya, and from a site approximately 5 km to the north-northeast of Leknes. Material with a weathered appearance was collected from these sites, as well as bedrock with a fresh appearance for comparison. Ramså, Andøya, was visited as well, and core samples had been collected previously from this site.

3.1.3 Analytical methods

All samples were first dried and then examined under a binocular microscope. Grain size, SEM, XRF and XRD analyses were completed at the laboratory of the Geological Survey of Norway in Trondheim. Grain sizes were determined on dried samples with a Coulter LS Particle Size Analyzer. Scanning electron microscopy analyses were performed on surface bulk fine matrix samples and semi-quantitative analyses of grain chemistry and mineralogy were completed according to energy dispersive spectrometer techniques (Goldstein *et al.* 2003).

Samples were prepared according to standard techniques for XRF examination at the laboratory of the Geological Survey of Norway. The analytical techniques are described in the accreditation documentation of the NGU laboratory ([NGU - XRF 2008](#)). Precision of the analysis depends on the element that is analysed but concentrations are generally determined with error margins on the order of ppm or better. In this study, all sampled localities were sampled for both fresh bedrock and saprolite. In some localities (Kjose, Vågsøy) a series of samples was taken in the saprolite to see if the degree of weathering varies with depth in the profile. The principle behind the analysis is described by Brimhall *et al.* (1985), Brimhall & Dietrich (1987) and Chadwick *et al.* (1990) where the element composition of fresh bedrock is compared with the element composition of the saprolite. This comparison allows a quantification of the degree of weathering that the bedrock has been subjected to and which of the main elements that have been leached. A major obstacle for this analysis is that the saprolite undergoes changes in density and volume during the weathering process, which hampers a straight calculation of mass loss from the fresh bedrock. To overcome this, an immobile element (usually Zr or the oxide TiO₂) is used as a reference to which all other elements are compared (Brimhall *et al.* 1985, Brimhall & Dietrich 1987, Chadwick *et al.* 1990). As long as the immobile element has a weathering rate that is an order of magnitude slower than other elements, this method yields reliable results.

XRD analysis is described in the accreditation documentation of the NGU laboratory ([NGU - XRD 2005](#)). The <2 mm size fraction of each sample was separated by settling, Mg-saturated and purified with a ceramic filter to produce oriented samples. An initial XRD scan was performed at 2–69°2 ϕ with a scan speed of 0.02°2 ϕ s and a step size of 0.04°2 ϕ . Second and third scans were performed following ethylglycol saturation and heating of the samples to

550°C, respectively. These scans were performed at $2-35^{\circ}2\theta$ with a scan speed of $0.0067^{\circ}2\theta$ -1 and a step size of $0.04^{\circ}2\theta$. Diffraction peaks were analysed with peak search software and manually reviewed following Brindley & Brown (1980) and Moore & Reynolds (1997).

3.1.4 Results

The localities with the most pervasive weathering in the study (Vesterålen, Hamarøya, Vågsøy and Kjøse) are generally found in intermediate to mafic rocks. Lithologies range from (quartz-)monzonite to syenite and finally to gabbro. So far, few signs of weathering have been found in the more felsic lithologies. Only very small amounts of clay minerals were found in our samples, and few sure signs of advanced weathering clay minerals were found. In many samples, the amount of clay minerals was too small to be analysed with the present XRD methodology. However, in some samples primary clay minerals such as illite and chlorite were easily identified. Intermediate weathering minerals such as vermiculite and smectites could also be found, as well as trace amounts of typical saprolite clay minerals such as kaolinite and gibbsite (Kjøse area and Vågsøy samples). Optical microscope inspection of material with a weathered appearance indicated that weathering-prone minerals such as feldspars were still looking quite fresh. A brownish tinge, oxidisation, in samples that had the most weathered appearance appears to be superficial. SEM studies of fine grains confirmed the impression from optical microscopy that very little chemical etching has been taking place in silica-rich minerals such as quartz and feldspars. However, biotite quite commonly seems to have been altered in diagenesis into vermiculite and smectite.

Grain-size distribution in all investigated soil profiles is dominated by sand and gravel with very little silt and clay (generally <5%). In some cases we also sampled glacial till overlying the saprolite; these samples often contained more clay and silt, showing an incorporation of finer material from elsewhere.

On the other hand, XRF analysis and mass balance calculations (degree of leaching) commonly show a high degree of mineral alteration with bulk leaching of main elements (Si, Al, Na and K) in the range of 30 - 65%. The upper range can be considered as indicative of intense leaching. Since optical microscopy and SEM studies show limited etching on silicate-rich minerals, it appears likely that phyllosilicates (mainly biotite) and other 'dark' minerals such as hornblende and pyroxene have been chemically altered. In some samples there are signs of reprecipitation of oxides and hydroxides, which is in agreement with saprolite formation.

In none of our samples did we find clay material that would be suitable for dating. Either there were too small amounts of clay, or the clay mineralogy was not suitable for dating using the methods described above. We suspect that any attempt at dating the clay minerals would only have yielded ages approximating to the age of the host rock.

3.1.5 Conclusions

The XRF data shows that intense leaching processes have occurred at all localities with the most extreme values in Vesterålen/Lofoten and at Lista. The XRD analysis is ambiguous with analytical problems involved with the very clay-poor samples. There are definite signs of alteration of biotite into vermiculite and smectite, and at some localities small amounts of feldspar have been altered into kaolinite. It seems likely that the main weathering process in the investigated saprolites involved alteration of biotite into vermiculite and smectite. This process causes expansion and exerts pressure on the surrounding mineral grains. The process can be likened to physical weathering causing disintegration of the rock into gravelly-sandy saprolite (Nesbitt & Young 1989). This disintegrated rock (gravelly-sandy saprolite), in turn, is then much more porous and rainwater can penetrate far down into the profile causing chemical alteration mainly of the mafic minerals.

Because no new dates have been obtained, we cannot confirm or disprove an 'old' age for any of our samples. In principle, the characteristics of our samples could be the result of recent weathering under the present-day climatic conditions. An argument against a recent age (i.e. Quaternary?) could be the actual penetration of weathering down into the crystalline basement, which on both Hamarøya and Hadseløya is in the order of several tens of metres.

3.2 Remote sensing mapping of deep-weathered bedrock

Remote sensing data (satellite and aerial imagery) have been used to map deep weathering foremost in arid environments in Australia and South Africa where this phenomenon has economic implications for geochemical exploration for mineral deposits and in terms of supergene ores (Buckingham & Sommer 1983, Amos & Greenbaum 1989, Cunningham *et al.* 2005). The method builds upon the fact that different minerals and deposits have different spectral reflectances. Hence, minerals reflect electromagnetic radiation back to the satellite sensor differently depending on the mineral lattice (Sabin 1996, Fig. 3.1). In principle, this means that each mineral has its own spectral 'fingerprint' as seen for example in Fig. 3.1. This implies that mineral phases derived from chemical weathering processes theoretically show up as distinct patterns in multi- and hyperspectral, remote sensing data (Sabins 1996).

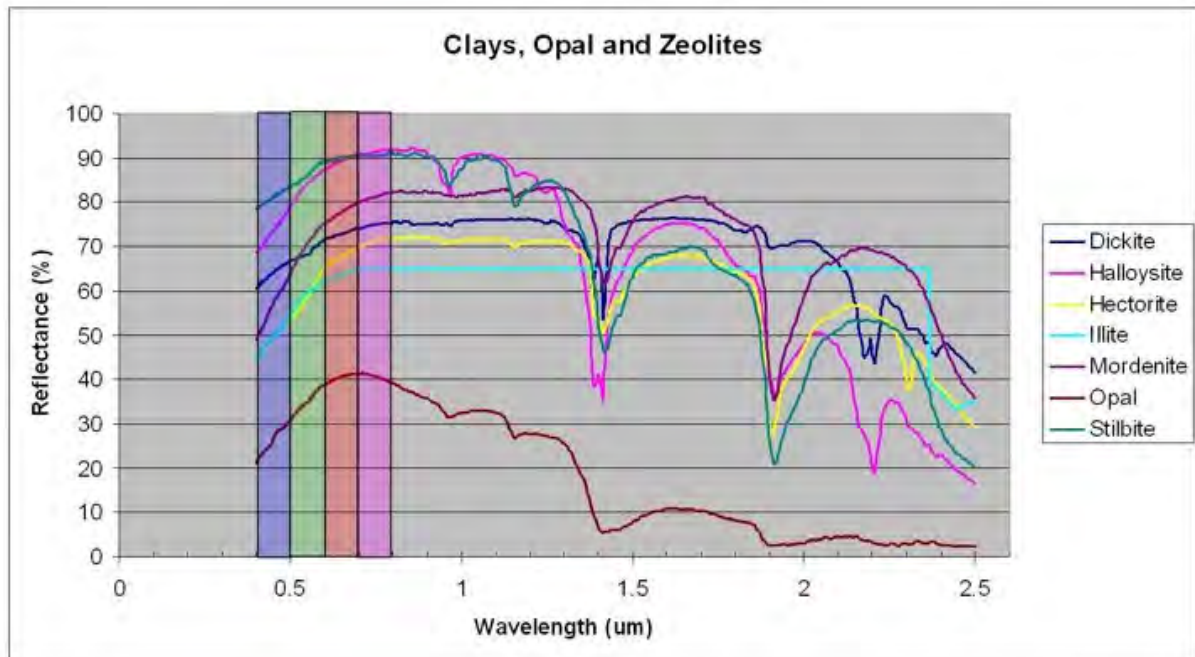


Figure 3.1 A selection of minerals and clays and their spectral signature (reflectance) at different wavelengths. The spectral signature of a wealth of minerals has been compiled by the USGS (<http://speclab.cr.usgs.gov/spectral-lib.html>). Note that the visible (to the naked eye) reflectance is just a narrow part of the electromagnetic spectrum used. Wavelengths far out into ultraviolet and infrared are used in multispectral and hyperspectral remote sensing.

The spectral reflectance from Earth can be recorded in a number of narrow wavelength bands. If data are recorded in 4-25 bands the data are called multispectral, and if they are recorded in more narrow bands (often more than 200) the data are referred to as hyperspectral. Hyperspectral data obviously have a greater potential to differentiate different spectral signatures in detail; however, they demand much more data processing and also might have problems with signal-to-noise issues.

In the TWIN Project an attempt was made to test mapping of known weathering localities using hyperspectral data from the sensor “Hyperion” onboard the Earth observing satellite “EO-1”. Documentation about Hyperion and EO-1 can be found at the NASA website (<http://eo1.gsfc.nasa.gov/>). A data acquisition request (DAR) was forwarded to NASA with the intent to program the EO-1 satellite to record data while passing over Hamarøy in the spring of 2010. It was judged feasible to obtain usable data of weathering 'signatures' since much of the saprolite in the area is exposed in large quarries and is used locally as gravel fill on roads. The DAR was specified so that allowable data acquisition was from April to June to benefit from little snow cover and little vegetation. Unfortunately, no usable scenes were obtained from the satellite, on account of either too much snow cover or clouds obscuring large parts of the scene. We then tried using archived Hyperion data from southern Sweden covering some of the localities in the county of Småland visited during the TWIN excursion. These data proved to be very difficult to work with since they were recorded on a day in late October (2008) with low sun elevation. Shadows and a low signal-to-noise ratio in the narrow

spectral bands made detection of specific minerals very difficult. No conclusive identification of alteration minerals or saprolite could be made with these data. We conclude that mapping of saprolite using hyperspectral remote sensing data is feasible in arid climates with a long summer season (bright days with strong reflectance) on sparse vegetation. Such careful spectral analysis is difficult in the Nordic countries with a very short summer season after the snow has melted and before dense vegetation obscures a view of the ground surface.

4 REVIEW OF PREVIOUS DEEP-WEATHERING REPORTS

Ola Fredin & Berit Husteli

Previous studies on weathering phenomena in Norway have been compiled into an ESRI geodatabase (ESRI ArcMap filegeodatabase v. 10) where known localities have been registered as points (Feature class: *Saprolite*). The database can be downloaded from ftp.ngu.no/pub/TWIN.

Literature containing information about weathering in Norway has been examined systematically for localities. Relevant literature is listed in the reference list at the end of the present report (Chapter 11). Every paper contributed to adding one or more new sources to the list, the result being that the amount of literature related to descriptions of possible preglacial weathering remnants is comprehensive. Each weathering locality is digitised as a point feature with potentially 16 attributes. The attribute table is presented in the following and a summary of it is listed as Table 4.1.

Table 4.1 The attributes described in each saprolite point.

Point attributes	What
Object ID	Consecutive numbering
Shape	Point feature
Locality name	Name of the locality
Weathering type	Integer
Description	150 characters concerning its appearance and distribution
Landscape type	Description of general morphology of the area
Date of visit	Date
Sampled	Yes or No
Clay type	Clay mineral(s)
Chemistry	characters
Geophysics	What type of geophysical investigation
Rem.mag	Result from palaeomagnetic studies
Stratigraphic relation	Older than/younger than/minimum age/inferred age
Source	Publication(s) or persons contributing with information
Bedrock	Bedrock in the area (if differing from source, given in parenthesis)
Positional accuracy	1,2 or 3

Attributes assigned to these data are, *Object ID*, which has a consecutive numbering from the order it was added to the database. *Shape* is a mandatory field added by GIS to indicate feature type. *Locality name* is either the locality name given in the literature, or a name given by its geographical location. Deep-weathering localities are grouped into seven different type categories based on their characteristics. They were numbered 1-7 and the different classes are 1) Saprolite with a matrix consisting predominantly of clay, 2) Saprolite with a grussy

composition, 3) Unequivocal weathering, which means localities included in the database but where composition and origin are uncertain. This class often contains clay veins, in otherwise fresh bedrock. 4) Secondary weathering in jointed bedrock, secondary referring to the presence of clay minerals formed in situ. 5) Weathering pits and caverns and other morphological features associated with differential etching of rocks by chemical weathering. 6) Includes tors and associated morphology, and 7) Autochthonous blockfields, probably of pre-Pleistocene origin. An overview of the categories is given in Table 4.2.

Table 4.2 Summarised description of the different weathering type categories.

Weathering type	Description
1	Saprolite with a matrix consisting predominantly of clay
2	Saprolite with a grussy composition
3	Dubious or nondescript saprolite
4	Secondary weathering in jointed bedrock
5	Weathering hollows
6	Tors and associated weathering morphology
7	Autochthonous block field, of pre-Pleistocene origin

Description is a 150-character field describing the locality appearance, distribution or other interesting attributes. The *landscape type* in the area is described briefly, if visited by persons affiliated with the TWIN Project; *date* is stated under visited. If sampled when visited, yes or no is indicated under the field *sampled*. *Clay mineral(s)* is written under clay type if investigated either by the TWIN project or in research carried out by the reference. If *geophysics* has been performed the type of method is stated. The recordings and interpretation of the geophysics are not added under saprolite, but have their feature category under geophysics. If palaeomagnetism has been measured, results are briefly written in *rem.mag*. *Stratigraphic position* of the weathering residue is described either as the position relative to other geological units, minimum geological age according to dating, or age inferred by source. *Publication*, which the locality is taken from, is cited under source. If the source is not published, personal communication or 'heresay' is indicated. As the type of weathering is partly dependent on the composition of the *bedrock*, the main bedrock type occurring in the area is extracted from bedrock map at www.ngu.no. If the local bedrock differs from the bedrock stated in the paper, it is written in parenthesis. Finally, the positional accuracy of the locality is grouped into three categories 1-3. 1 is the highest level of accuracy, meaning that GPS coordinates were used to plot the position into the database and it is possible to return to the locality aided by a GPS receiver. Level 2 is used when the locality is digitised according to a map with a decent scale or a good description. When the source of the locality had neither a map nor a good description of the geographic location, level 3 is employed. Based on the relatively poor description, level 3 localities might be difficult to find in the field.

When descriptive pictures, drawings, maps, logs or tables presenting the results of analyses are available, they are added as attachments to the point.

4.1 Geophysical data

Geophysics performed in areas of suspected deep weathering has been added to the database either as a line or raster. Seismics and resistivity measurements have been added as a line at its respective locality, but AMAGER data have been added as raster data.

Each registration has potentially nine attributes associated with it. Attributes assigned to these data are summarised in Table 4.3 and described in the following. *Object ID*, which has consecutive numbering from the order in which the geophysics was added to the database, and *shape* as mentioned above. Under *type*, the type of geophysics presented is described briefly, whether it is resistivity, refraction seismic, AMAGER or magnetic susceptibility. Under *locality*, the name of the locality is stated. The person responsible for the recording of the geophysics is named in under *operator* and the date of recording is plotted under *date*. Normally this is teamwork and several persons are involved.

The *Quality* attribute is meant to indicate which results can be expected, considering the type of equipment that was used. For instance, with electrical resistivity, we would note the array which the cathodes are arranged in and what separation they had. AMAGER data and quality of topography data are indicated, noting the grid, line spacing and flight altitude of aeromagnetic surveys and filtering of results. In refraction seismic, the spacing of the geophone and the source are indicated as well as the type of equipment used. *Shape length* is automatically calculated in the GIS software when the profile is plotted. Depending on the accuracy of the position given, it might not match with the profile itself. Where several profiles are recorded in one area, transects are named and numbered according to how these were organised by the operator. This generally reflects the order of recording.

The geophysics results are added as an attachment, and if more interesting extra information is available, this is also attached.

Table 4.3 The attributes described when geophysics is added to the database.

Line attributes	What
Object ID	Consecutive numbering
Shape	Polyline or raster
Type	What kind of geophysics
Locality	Where was the geophysics obtained
Operator	Who is responsible for the recording
Date	When was the geophysics recorded
Quality	What kind of array/how densely spaced/energy level
Shape length	Length of transect
Line number	If several transects, order of recordings

4.2 Profiles

Profiles have been added to achieve an impression of large-scale morphological and stratigraphical relationships. Literature containing information about the relief of Norway has been examined, in the same manner as for the saprolites. Profiles of various forms are scanned, and plotted into the database as polylines at their respective locations. Profiles rarely come with exact coordinates, thus the locations of the profiles are approximate, placed by the aid of an overview. Each registration has five attributes, which are presented in Table 4.4. *Object ID* is numbered consecutively from the order in which it was digitised, *shape* as mentioned above, and under *name*; the name of the profile. The publication from which the profile is taken is cited under *references* and the length of the profile is automatically calculated in ArcMap.

The profile itself is added as an attachment, and if more information regarding the construction of the profile is available, this is also attached.

Table 4.4 The attributes described when a profile is added to the database.

Line attributes	What
Object ID	Consecutive numbering
Shape	Polyline
Profile name	Name of the profile
References	Source where profile is published
Shape length	Length of profile

5 SOUTHERN NORWAY

5.1 Lista

Jon Arne Øverland, Dag Bering, Marco Brønner, Einar Dalsegg, Ola Fredin, Christian Magnus, Terje Solbakk.

The name Lista is here used both for the Lista Peninsula (bounded by Krossnessundet, Helvikfjorden, Framvaren, Indre Pollen and Eidsfjorden) and the surrounding areas to the east (Ravneheia and Spind), see Fig. 5.1A. The bedrock of the southern part of the Lista Peninsula consists of banded heterogeneous gneiss, the northern part of the Lista Peninsula and Ravneheia of charnockite and the Spind area of hornblende granite. The southern part of the Lista Peninsula is covered by Quaternary sediments creating a flat or slightly undulating topography (Fig. 5.1C). In contrast, the northern part of the Lista Peninsula, Ravneheia and the Spind area consist of a hilly landscape where a thin Quaternary cover is found only in the many small valleys.

Lista is situated in the hinge zone between the uplifted Norwegian mainland and the subsiding North Sea Basin. An attempt to reveal the fundamental feature of the surface topography of Lista was made by calculating a simple three dimensional “*summit height envelope*” (Doré 1992), this corresponds to the “*summit-level surface*” described in Barth (1939b). The summit height envelope of Lista is based on the three most elevated points relative to the envelope, which were found to be:

Point	E (UTM 32 WGS84)	N (UTM 32 WGS84)	Height (m)
Storefjell	365348	6448107	346
Havika	366155	6437962	28
Lofjell	360508	6446825	193

The constructed summit height envelope shows a dip of 2.3° , with a dip direction of 215° (southwest). At least seven peaks have heights that come within 20 m below the constructed envelope. Comparing the topography with the envelope level shows that the landscape level in the barren northern and eastern areas is seldom lower than 100 m below the envelope level. In the southern part of the Lista Peninsula the Quaternary sediments cover the bedrock. Three Vibroseis lines recorded in 1995 (by the University of Bergen for NPD) in the southwestern part of the Lista Peninsula reveal that the bedrock is dipping in the same southwestern direction as the summit height envelope surface. Two of these lines are shown in Fig. 5.1B, and their position is shown in Fig. 5.1A. The base of the Quaternary sediments is represented by the uppermost strong reflector. It must be emphasised that the constructed envelope represents a local level limited to Lista, and cannot be extrapolated to surrounding areas.

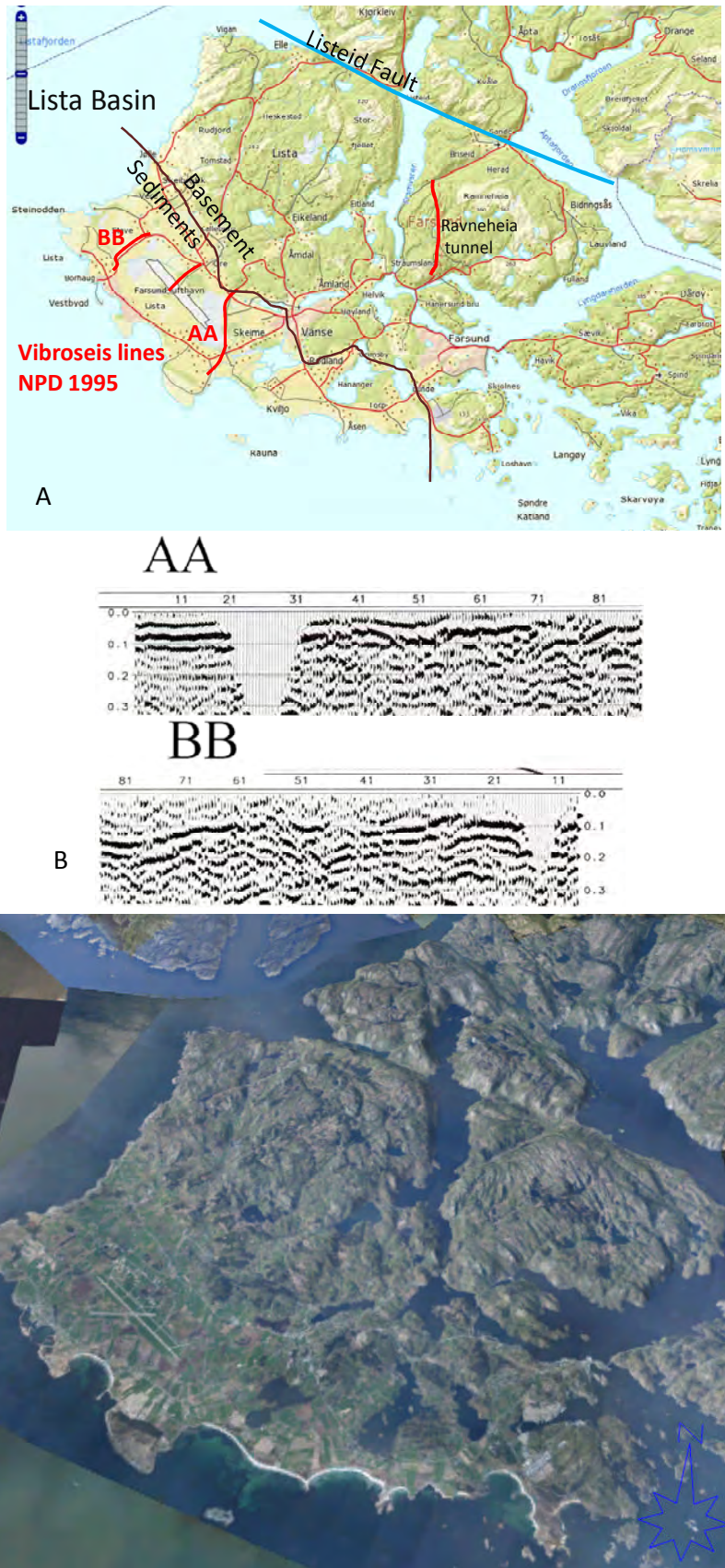


Figure 5.1 A) Lista, overview map. B) Vibroseis lines AA and BB, recorded by the University of Bergen for NPD in 1995. Line locations are marked on Fig. 5.1A.' C) Perspective view of the Lista Peninsula visualised from the south (produced with www.Norgei3D.no). Note the joint valleys in the central part of the figure.

The landscape level in Vest-Agder and its connection to older peneplains has been discussed by Barth (1939b), Andersen (1960), Holtedahl (1988) and Riis (1996). The landscape in Vest-Agder originated as the sub-Cambrian peneplain (the 'old paleic surface'), modified by later erosion and uplift in Mesozoic and Cainozoic time (Lidmar-Bergström *et al.* 1999). Based on correlation with saprolites and landforms in south Sweden and Denmark, along with the association with covering strata offshore (Lidmar-Bergström *et al.* 1999, Riis 1996), it is likely that the area was deeply etched in pre-Cretaceous time, later covered with sediments and finally stripped in the Plio-/Pleistocene. The landscape thus represents a dissected peneplain and could be termed a joint valley landscape.

Several features of the landscape in northern part of the Lista Peninsula, Ravneheia and the Spind area indicate that the glacial influence on the landscape is weak compared to other parts of the Norwegian mainland. Several hills and small mountains have marked steep peaks, as for example Snarefjell (364168E, 6444269N, UTM zone 32, WGS84 datum), Fig. 5.2A upper and Bukkefjellan (361698E, 6448333N), Fig. 5.2A lower. On Ørnasede (371734E, 6441578N) the peak consists of a huge disconnected block which has remained in its original position.

Preservation of tor-like features adds to the impression of either minor or no glacial erosion. Fig. 5.3B shows stacks with weathering surfaces at Nørskår (369342E, 6444196N). On a smaller scale, a weathering pit (Fig. 5.2B) located at Kjelen (364706E, 6450357N) has reached dimensions that might indicate a start of weathering before the latest glaciation (Øverland 2011). Barth (1939a,b) referred to a forthcoming publication by Wettergreen Jensen about the lack of glacial striations on Lista. We have not been able to locate this publication. The probable explanation for the absence of an erosive ice sheet over part of Lista is that the ice movements were largely concentrated in the surrounding fjords, Fedafjorden, Eidsfjorden, Framvaren and Lyngdalsfjorden as well as in the offshore Norwegian Channel (Skagerrak ice stream). The fjords have been overdeepened during the Pleistocene glaciations.

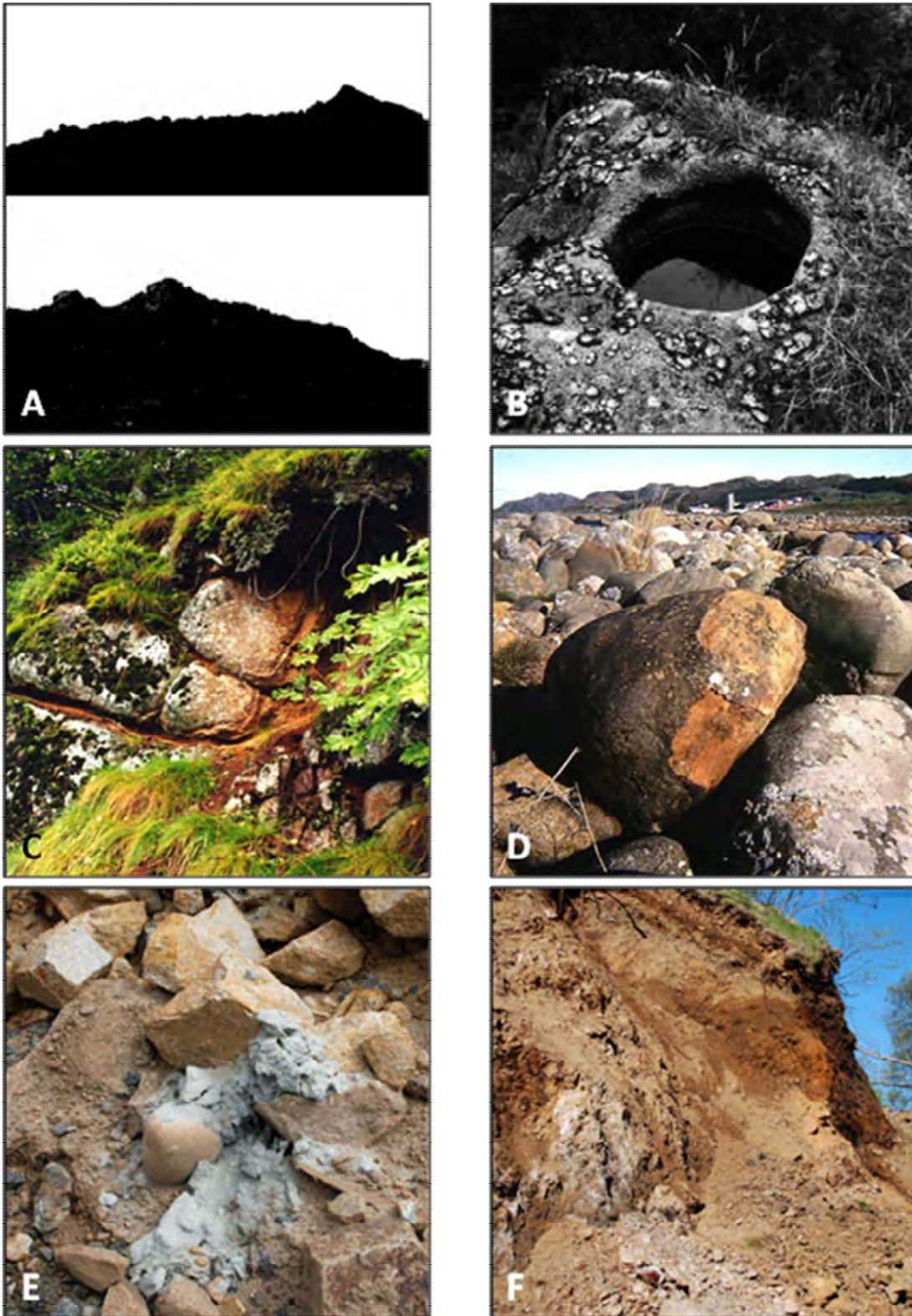


Figure 5.2 A) Profiles of Snarefjell and Bukkefjellet. B) The weathering pit Kjelen. C) Corestones, Gullsmedbakk. D) Corestone, north of Stavestø. E) Dump from rock fall in the Ravneheia tunnel. F) Core of fault zone, Listeid Fault.



Fig. 2. Forvitret bergart ved Ullgjell. På dette sted har den vært tatt ut med hakke og spade og brukt som veigrus. På toppen ligger almindelig morene.



Figure 5.3 A) From Barth (1939b) – Fig. 2. B) Tor with weathered surface, Nørskår. C) Fractured and weathered bedrock, Knutstad.

The occurrence of weathered bedrock and weathering products on Lista was noted by Reusch (1901): “*Bergarten syntes i det hele taget at være tilbøielig til at sprække op og er meget forvitret*” Reusch described the thin till layers in the northern part of the Lista Peninsula to

”... består fornemlig af kantede og mest forvitrede stene at stedets egen bergart; ...” H. Bjørlykke (1929) described the extension of different soil types on Lista, and noted soil layers of weathering products in the hilly areas: *”Steddannet forvittringsjord kan man dog finne lokalt i de østlige og nordlige deler, særlig i bergskråningene, men de har for liten mektighet og utstrekning til å være av nogen større betydning.”*

Barth (1939a) described two locations (Eikelandkleiva and Ullgjell, Fig. 5.3A) with weathered bedrock centrally situated on the Lista Peninsula: *”Den faste bergart er ”råtnet”: den er lokalt blitt løs og leiraktig slik at den kan tas ut med spade. Utseende er ganske eiendommelig, idet produktet ved første blick synes å bestå av fast fjell. Det har fjellets farge og struktur; årer og lag optrer akkurat som en ser dem i en fast fjellvegg, og når en kommer nærmere, kan sogar de enkelte mineralkorn, som bygger op fjellet, skjelnes. Men går en helt hen, viser det seg at en med spade kan skave skiver ut av 'fjellet'.”* Barth identified the clay fraction of the weathered rock as belonging to the beidellite group. He compared the weathering on Lista to weathering in the southeastern USA, and discussed briefly the origin and timing of the weathering. He elaborated on these subjects in Barth (1939b), and concluded by proposing a Tertiary age for the weathering. Isachsen & Rosenqvist (1949) were sceptical to the definition of beidellite as a mineral and reclassified the clays as a mixture of montmorillonite and different bauxite minerals.

It has not been possible to positively identify the two locations described by Barth, but there are clear indications of weathering in the area. To illustrate this, we have chosen a location at Gullsmedbakk (363568E, 6445337N, UTM 32 WGS84), near to, but probably south of Barth's location Eikelandkleiva). At this location (Fig. 5.2C) there are partly developed corestones surrounded by reddish saprolite.

Two fully developed corestones are found on the cobble beach north of Stavestø. This beach consists of stones and blocks left after marine erosion of till. The more accessible of the two corestones (358565E, 6446036N) is shown in Fig. 5.2D. The corestone has a crust of iron oxides. Directly under this shell only the quartz grains remain of the original rock, feldspars and other minerals having been removed. It is surprising that these corestones, fragile compared to fresh bedrock, have endured both glacial transportation and marine erosion with only minor damage. There is, of course, no possibility of identifying the precise origin of these corestones. The major ice streams (the Skagerrak Glaciers) followed the coast towards the northwest, probably also covering the southern part of the Lista Peninsula. It is therefore not unlikely that the corestones originate from weathered bedrock on Lista or areas farther to the east in Agder.

A road tunnel was driven through the Ravneheia mountain plateau in 2007 (Moen 2007). A major rock fall (3,000 m³) occurred 900 m from the southern entrance. The rock fall consisted of blocks, rock fragments and clay, all of which had a noticeable lighter colour than the fresh bedrock. Fig. 5.2E shows an example from the rock fall found at a dump outside the

tunnel. Some of the blocks were partly covered by a deep brown coating (lower right corner in Fig. 5.2E). XRD-analysis carried out by Alf Olav Larsen in 2007 (Appendix 1) shows clays in the rock fall consisting of montmorillonite, minor amounts of albite, biotite and traces of kaolinite. The brown coating consisted of hisingerite ($\text{Fe}^{3+}_2\text{Si}_2\text{O}_5(\text{OH})_4 \cdot 2\text{H}_2\text{O}$), a mineral often associated with weathering or hydrothermal alteration.

The rock fall in the Ravneheia tunnel occurred in a weakness zone consisting of crushed and weathered rock. The weakness zone appears on the surface as a NW-SE-trending valley (Fig. 5.5). Electric resistivity measurements were carried out by NGU (Rønning *et al.* 2009) across this valley at the location of the rock fall. The measurements showed low resistivity across the valley down to a depth of approximately 140 m from the surface (Fig. 5.6), which represents the maximum depth of penetration by the method. The rock fall in the tunnel is situated approximately 180 m below the bottom of the valley.

The Listeid Fault is a major fault which can be recognised in the landscape from Hidra in the west to Herad in the east. The centre of the fault is exposed in the distinct narrow valley of Listeid. On the southern side of this valley the intensively fractured fault zone is quarried for stone and gravel. At the western end of the quarry the deeply altered core of the fault is exposed (Fig. 5.2F, 366043E, 6450011N). The fault core consists of a brownish soil enriched in iron and manganese oxides. Embedded in this substance are parts of less altered bedrock, with slickensides and remnants of mineral veins. No attempts have been made to investigate if the alterations in the fault core are caused by deep-seated hydrothermal activity and/or weathering from the surface.

The Listeid Fault is associated with dense fracturing in the adjacent area. Fig. 5.3C shows fractured bedrock at Knutstad (364954E, 6450204N), located approximately 300 m from the fault. The fractures are filled with a reddish, fine-grained material. XRD analysis (Appendix 1 – the location is named *Sigerslottet*) shows that the fine-grained fracture fill consists of montmorillonite, some illite, quartz and traces of kaolinite. XRD analysis was, in addition, made on fine-grained samples from Gullsmédbakk. This analysis was made at the NGU laboratory with procedures described in Chapter 3 in the present report. The content of fine-grained material suitable for clay analysis was unfortunately low. However, clear signals from illite, chlorite and vermiculite were detected. The occurrence of kaolinite is possible but not proven with the present analytical technique. Geochemical analyses were performed on saprolite samples from Gullsmédbakk and Åmdal, approximately 1 km south of Gullsmédbakk. Soil samples were taken for XRF analysis at the NGU laboratory and compared with the chemistry of host bedrock according to methods described earlier. The results are outlined in Table 5.1.

Table 5.1 Loss of elements (%) in saprolite compared to host bedrock with Zr used as an immobile reference element.

	SiO ₂	Al ₂ O ₃	Fe ₂ O ₃	TiO ₂	MgO	CaO	Na ₂ O	K ₂ O	MnO		Si+Al+Na+K	SUM
Gullsmedbakk	-43,9	-7,8	0,1	-0,2	0,8	-1,1	-2,2	-4,0	0,3		-57,9	-58,1
Åmdal	-52,2	-8,9	-1,1	-0,6	0,6	-2,7	-2,2	-2,8	-0,1		-66,1	-70,0

Table 5.1 shows an unusually high degree of elemental loss with ~60% mass lost at Gullsmedbakk and 70% at Åmdal. This implies that a majority of the host rock has been lost as solutes through chemical weathering, and the mechanical break-up of rock is clearly of subordinate importance at the sampled localities on Lista. Since both localities show this high degree of chemical weathering, it is unlikely that the results are erroneous due to the Zr 'nugget effect'. Regional geophysical mapping of deep-weathering zones using the AMAGER method (described earlier) shows a distinct pattern of areas with potential deep weathering following joints and valleys (Fig. 5.4). Saprolites are confirmed in the Ravneheia tunnel and at several other localities described above, and the model is thus confirmed in these areas. However, in other areas the model is difficult to verify due to soil and peat cover. We consider the model robust on a regional scale.

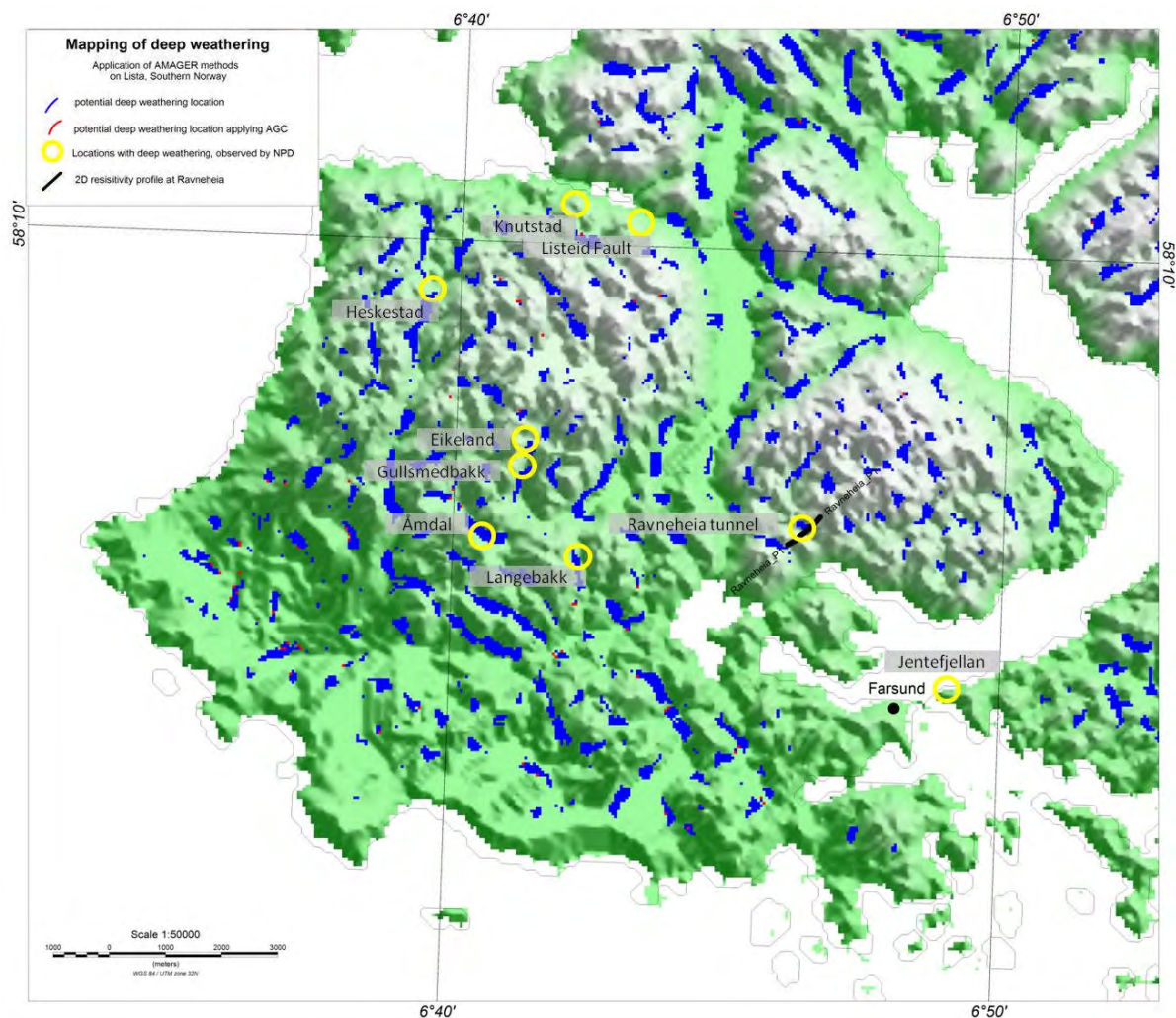


Figure 5.4 Potential deep weathering on Lista based on the AMAGER method.

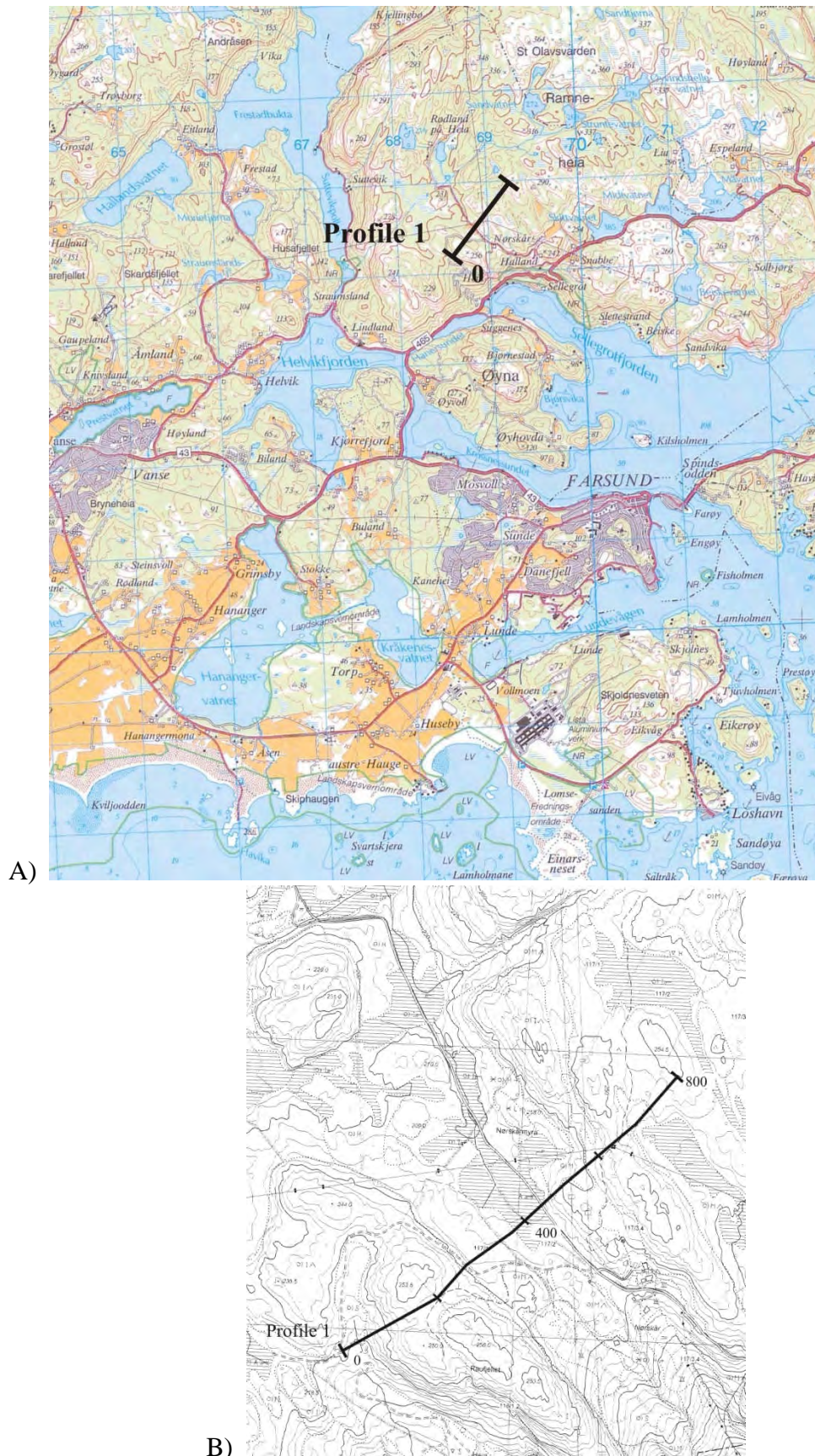
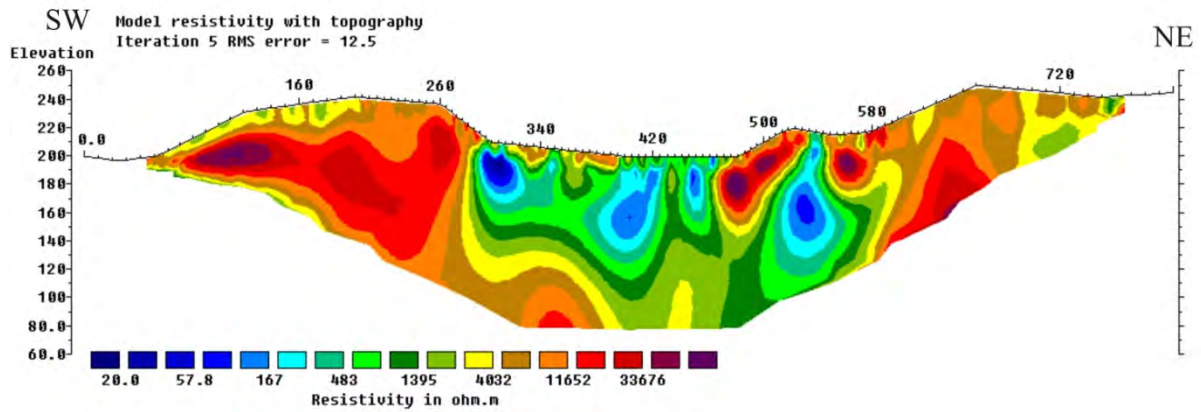


Figure 5.5 Location of the 2D resistivity profile (Rønning et al. 2009) at Ravneheia plotted on A) a M711 map (originally at a scale of 1:50,000) and B) on a detailed economic map (originally at a scale of 1:5,000).

Profile 1

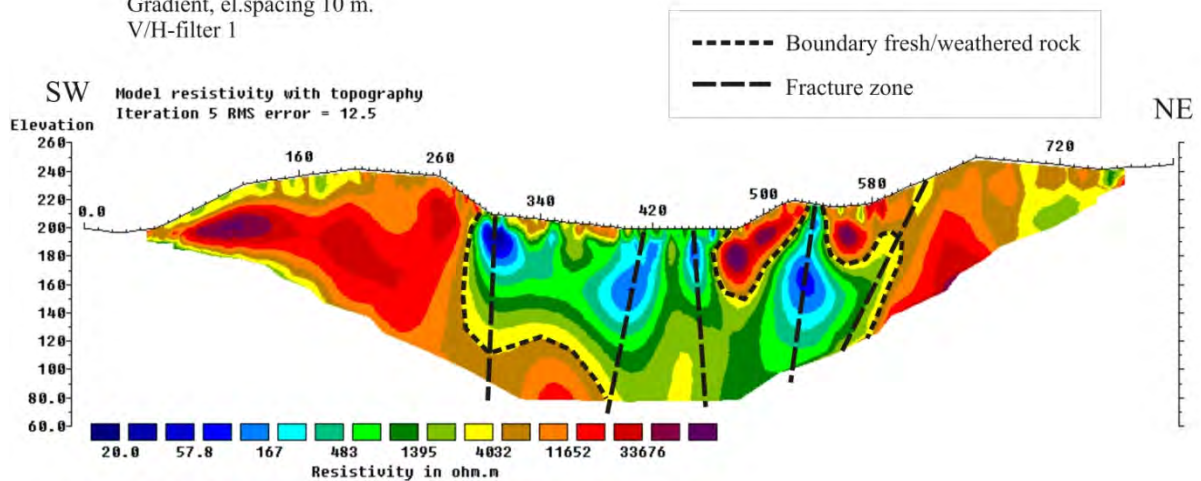
Resistivity
Gradient, el.spacing 10 m.
V/H-filter 1



Horizontal scale is 6.06 pixels per unit spacing
Vertical exaggeration in model section display = 1.00
First electrode is located at 0.0 m.
Last electrode is located at 800.0 m.

Profile 1

Resistivity
Gradient, el.spacing 10 m.
V/H-filter 1



Horizontal scale is 6.06 pixels per unit spacing
Vertical exaggeration in model section display = 1.00
First electrode is located at 0.0 m.
Last electrode is located at 800.0 m.

Figure 5.6 Electrical Resistivity Traversing (ERT) Profile 1. Upper panel shows raw data and the lower panel shows normalised data with the interpreted transition from fresh bedrock to weathering soil (from Rønning et al. 2009). The low-resistivity zones are interpreted to represent fractured and weathered bedrock.

5.2 Kjose

Ola Fredin, Marco Brönnner, Einar Dalsegg, Bart Hendriks, Odleiv Olesen & Jan Steinar Rønning

Clay alteration of crystalline bedrock in the greater Oslo Region has been studied by a large number of geologists, e.g. Låg, (1945, 1963), Sæther (1964), Selmer-Olsen (1964), Rokoengen (1973), Bergseth *et al.* (1980), Sørensen (1988), Banks *et al.* (1992a,b, 1994) and Kocheise (1994). Some of these sites have been difficult to locate since they are most likely covered by vegetation today. Most of the authors favour low-temperature fluids related to the formation of the Permian Oslo Rift as the dominating alteration agent. We think, however, that Lidmar-Bergström *et al.* (1999) provide a more plausible explanation for the widespread occurrence of clay minerals in the coastal areas of southern Norway and western Sweden. The strandflat that is formed by an erosion mechanism involving freezing, thawing and wave abrasion (e.g. Høltedahl 1958) does not cut into the etch-surface area of southern Norway and western Sweden, indicating that exhumation of the surface can be quite young, perhaps only a few hundred thousand years.

The Kjose area is mostly situated within the 'Larvikite region' west of lake Farris, close to the town Larvik in southern Norway. The bedrock consists of syenites and monzonites. Deep weathering and saprolites from this area has been described by Reusch (1901), Låg (1945) and Sørensen (1988). Professor Jul Låg at the University of Ås observed back in the 1940s that rye and potatoes could be cultivated in weathering soil within an area covering several square kilometres in the Kjose area (Figure 6B and 6C and Låg 1945). This soil was however too dry for many other useful plants.

The most comprehensive review of the spatial distribution, granulometry, clay minerals and other characteristics of the Kjose saprolites is found in Sørensen (1988). He concluded that the probable main weathering process is alteration of biotite to vermiculite and finally into smectite. This reaction sequence results in a 40% expansion of the original biotite mineral grains and thus a physical break-up of the rock mass (Nettleton *et al.* 1969). Sørensen (1988) also considered sericitisation (hydrothermal processes) of feldspars and pyroxenes an important process in the weathering of the larvikite. He argues that sericitisation likely took place during formation of the Oslo Rift in the Permian and thus rendered the larvikite susceptible to further surface weathering. Moreover, Sørensen (1988) reported the mainly presence of the clay minerals vermiculite, illite and chlorite. Traces of kaolinite cannot be excluded but is unlikely.

5.2.1 Geochemistry, clay mineralogy and granulometry

Samples from Kjose were analysed for geochemical composition using XRF techniques at the NGU lab (see previous section). Fresh rock samples adjacent to saprolite were sampled and the element composition in the saprolite versus fresh rock indicates how much of the respective elements have been leached through weathering processes (Brimhall *et al.* 1985, Brimhall & Dietrich 1987, Chadwick *et al.* 1990). Fig. 5.7 shows elemental mass loss for a saprolite section close to the railway crossing in Kjose. Four samples were taken, whereof three from saprolite and one from fresh host rock. All major elements show increasing loss through weathering higher up in the profile. This is to be expected since a higher degree of weathering is common higher up in a saprolite profile. Fig. 5.7 also shows precipitation of hydro-/oxides ('rust') that is also expected in a weathering profile. A mass loss of about 30% was calculated for the 5 m higher profile at Kjose.

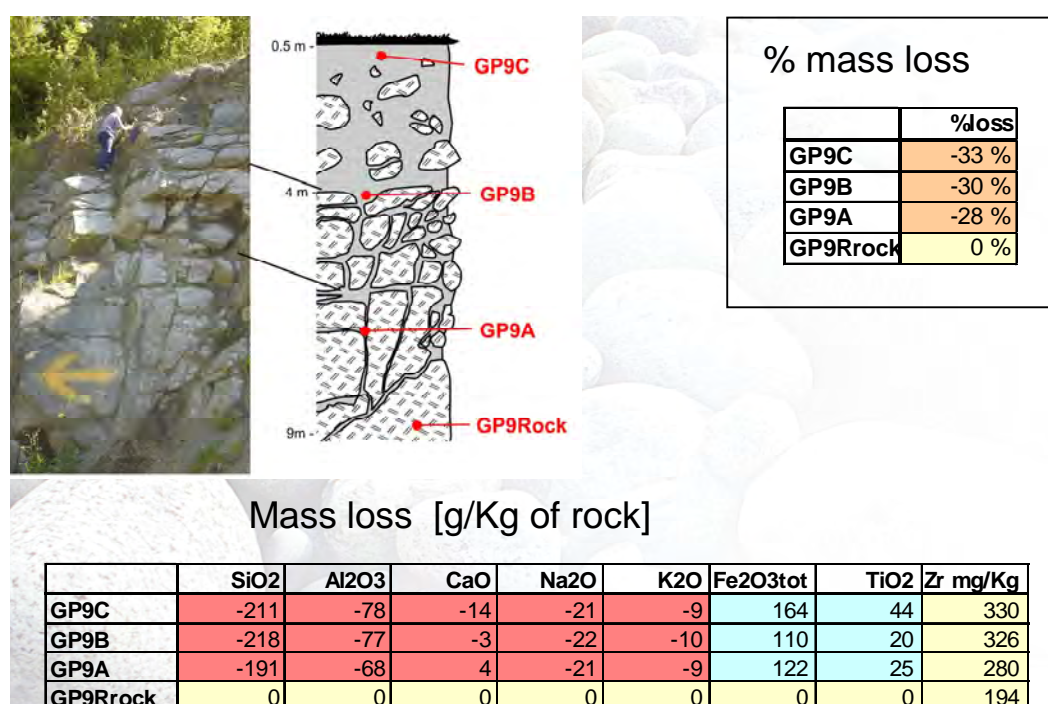


Figure 5.7 Geochemical mass balance calculations for a saprolite profile close to Kjose railroad station. About 30% of elements have been lost through chemical weathering in the ~5 m-high profile. Some reprecipitation of oxides and hydroxides can be observed (marked blue in table). The Brimhall *et al.* (1985) mass balance calculations are described in section 3.1.3.

XRD analysis was performed on the same saprolite from Kjose and the XRD spectrum is shown in Fig. 5.8. Sample preparation was made on fines (<2µm) and the X-ray diffraction spectrum recorded for an untreated sample, then treated with ethylene glycol and finally after heating to 550°C according to laboratory procedures described above. The spectrum was analysed using [peak search software](#) at NGU.

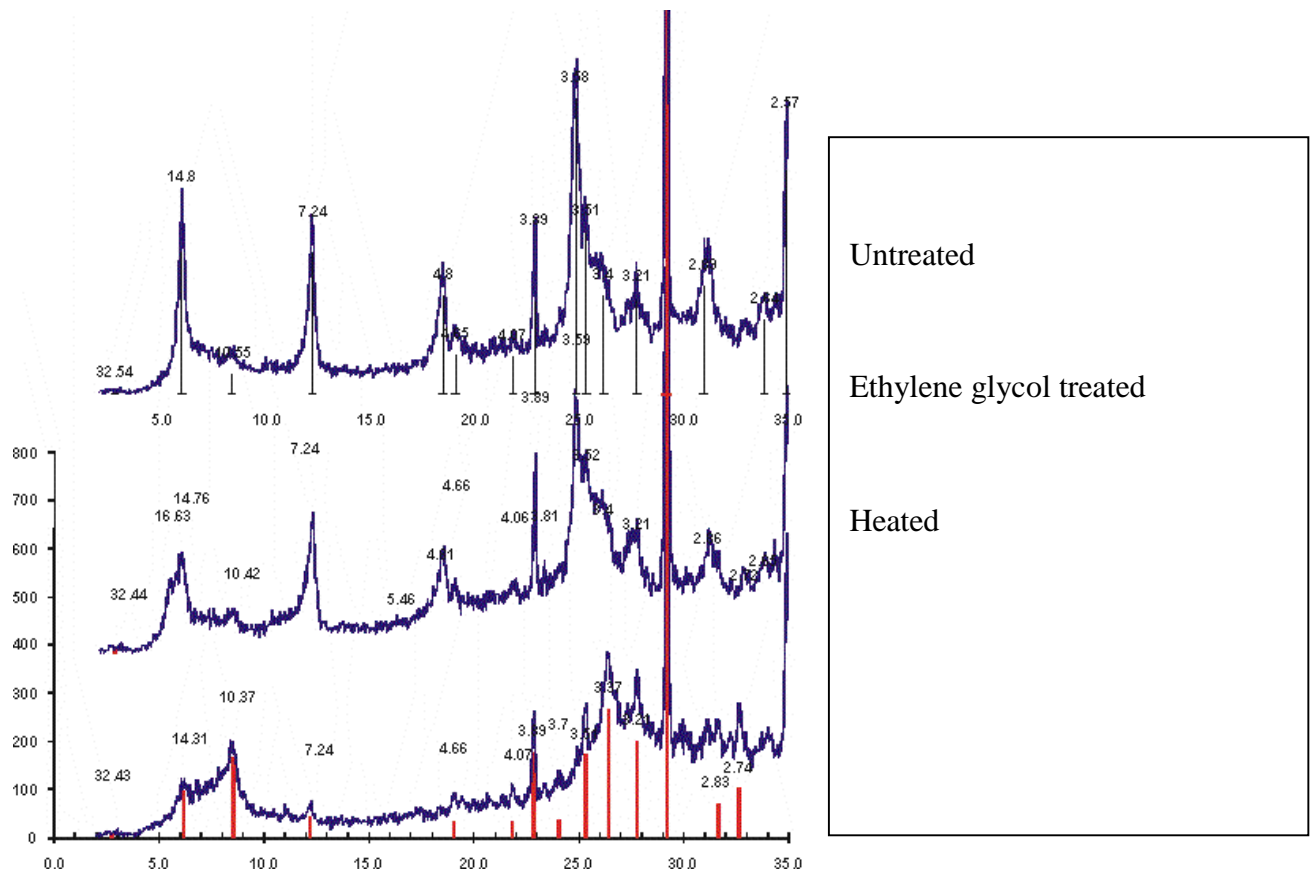


Figure 5.8 XRD spectrum for saprolite sample at Kjose.

The XRD analysis yields definite indications of chlorite, illite, vermiculite and smectite. Moreover, kaolinite and gibbsite are possibly present in the samples, but these phases cannot be identified with confidence with the present methods (Moore & Reynolds 1997) (Fig. 5.8).

Grain-size distribution analysis was performed on several soil samples from the Kjose and Larvik areas and samples were taken both from what was interpreted as palaeosoils (saprolite) and from glacial till with recent soil development. The grain-size distribution is shown in Fig. 5.9.

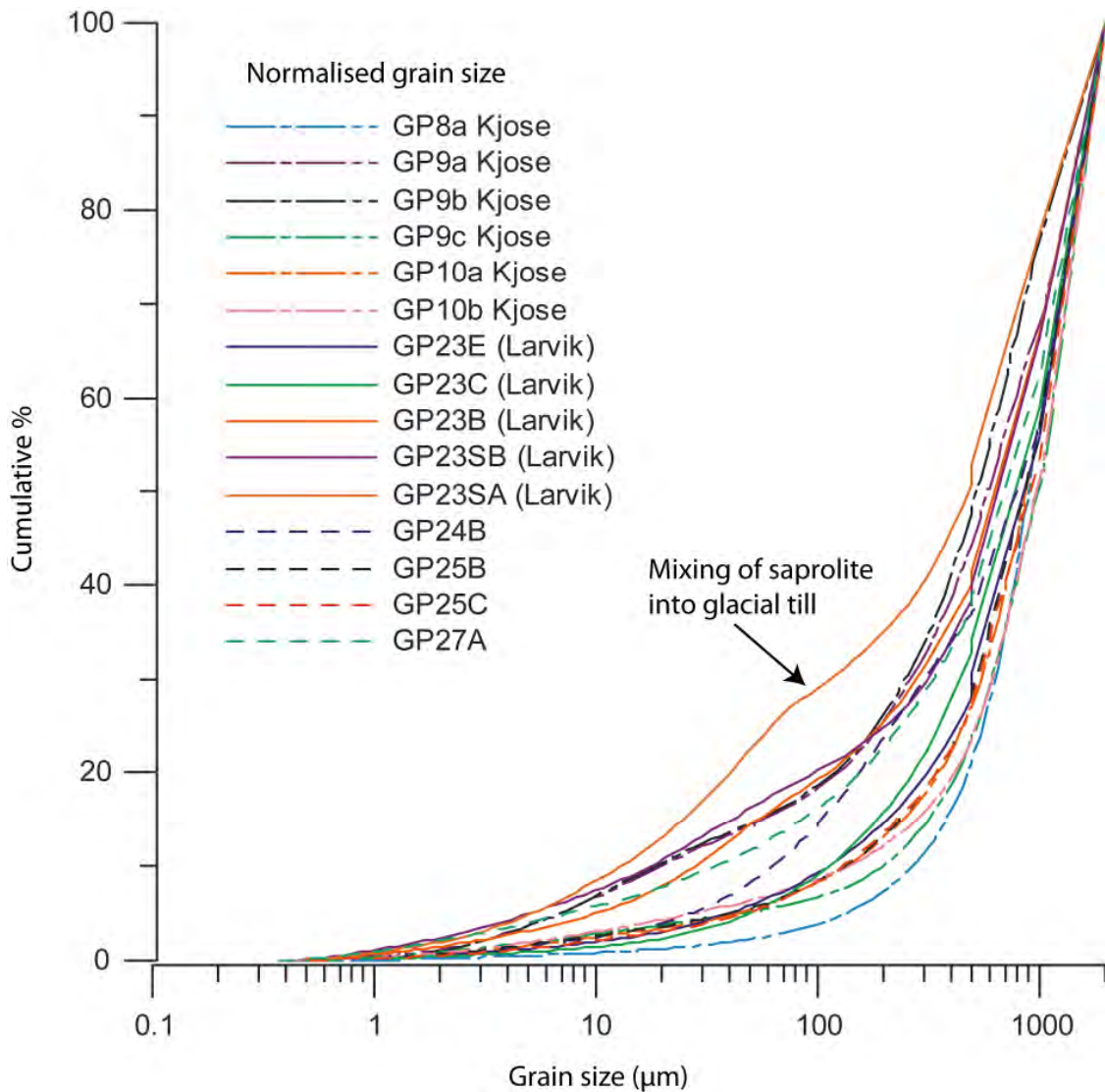


Figure 5.9 Grain-size distribution for 15 soil samples from Larvik/Kjose and nearby locations in south Norway.

The grain size distribution for saprolites shows a distinct bias towards sand and gravel with little mass in the silt and clay fractions, whilst till samples contain more fine-grained material (Fig. 5.9). The saprolites at Kjose/Larvik can thus be described as gravelly/sandy (Fig. 5.10) with a similar grain-size distribution as grussy saprolites on the South Småland Peneplain in southern Sweden (Lidmar-Bergström *et al.* 1997).

5.2.2 Electric resistivity measurements

Electric resistivity traversing (ERT) along four profiles (Fig. 5.10) was carried out to elucidate the spatial distribution and depth of potential deep weathering in the area. Låg (1945) and Sørensen (1988) reported extensive occurrences of saprolite in the Kjose/Farris area, which was later confirmed during field visits through the TWIN project. ERT was thus carried out in core areas of deep weathering (Fig. 5.11), and the results are presented in Figs. 5.12-5.15.



a)



b)

Figure 5.10 a) Perspective view of the Kjose area visualised from the south (produced with www.Norgei3D.no). Note the north-south trending joint valleys. B) Grussy weathering of syenite in a gravel pit at Kjose (UTM 549 110 – 6555 430, zone 32, WGS84 datum, 83 m a.s.l.). The location is situated immediately to the west of the intersection of Profile 4 and the main road through the Kjose hamlet (Fig. 5.11) and is shown by the yellow star in Fig. a) above.

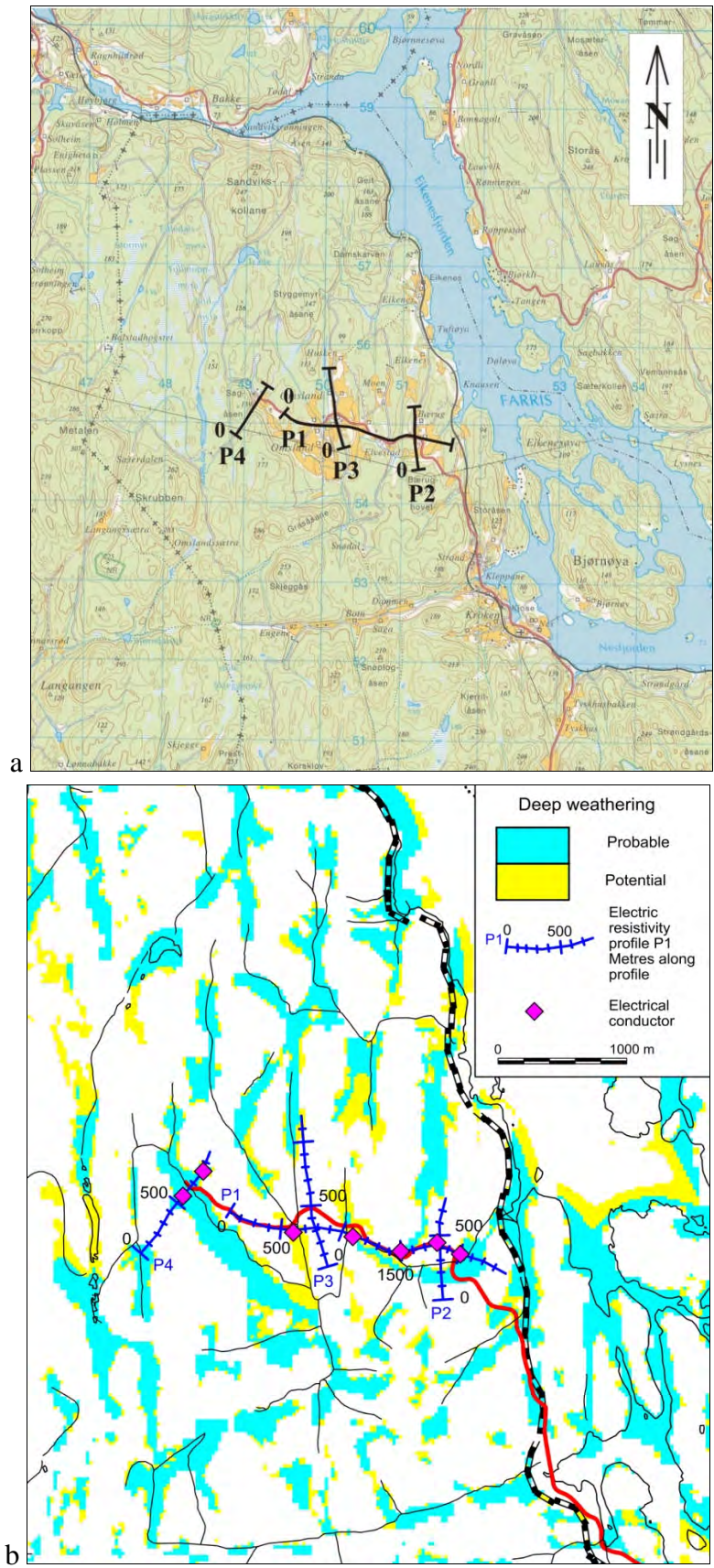


Figure 5.11 a) Map of 2D electric resistivity profiles at Kjose. b) Interpretation of deep weathering from Olesen (2006) and Olesen et al. (2007) and location of electrical conductors interpreted as deeply weathered fracture zones.

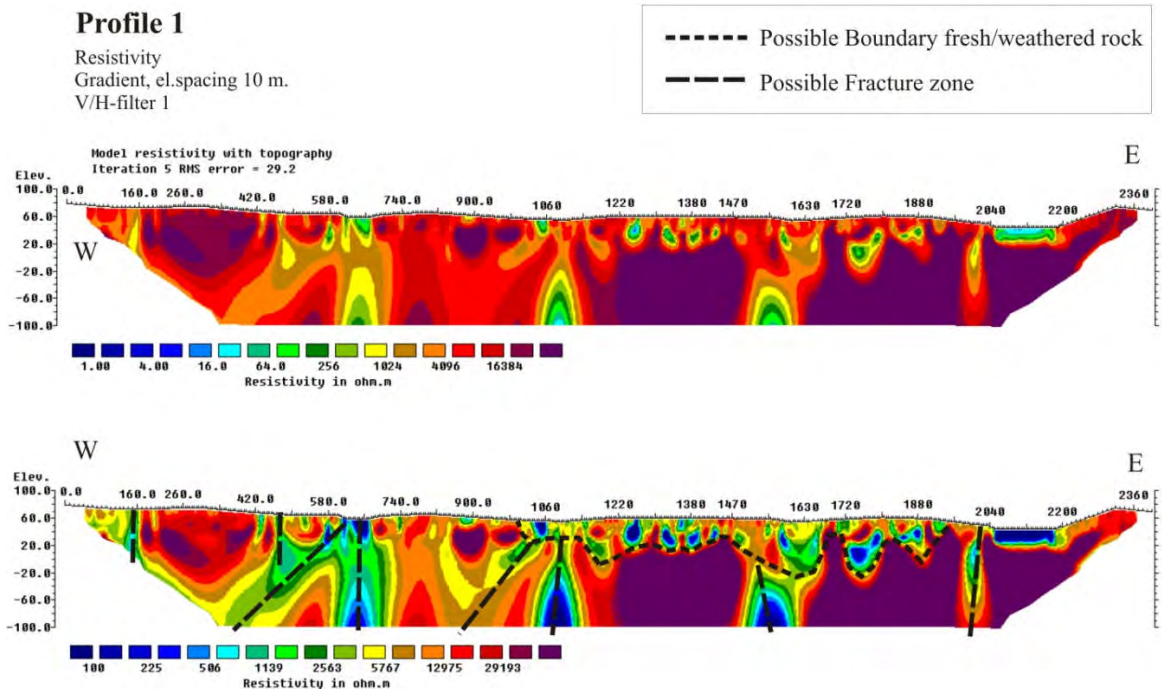


Figure 5.12 Electrical resistivity traversing (ERT) Profile 1 at Kjose. Upper panel shows raw data and the lower panel shows normalised data with the interpreted transition from fresh bedrock to weathering soil with low resistivity values (Note change in colour scales).

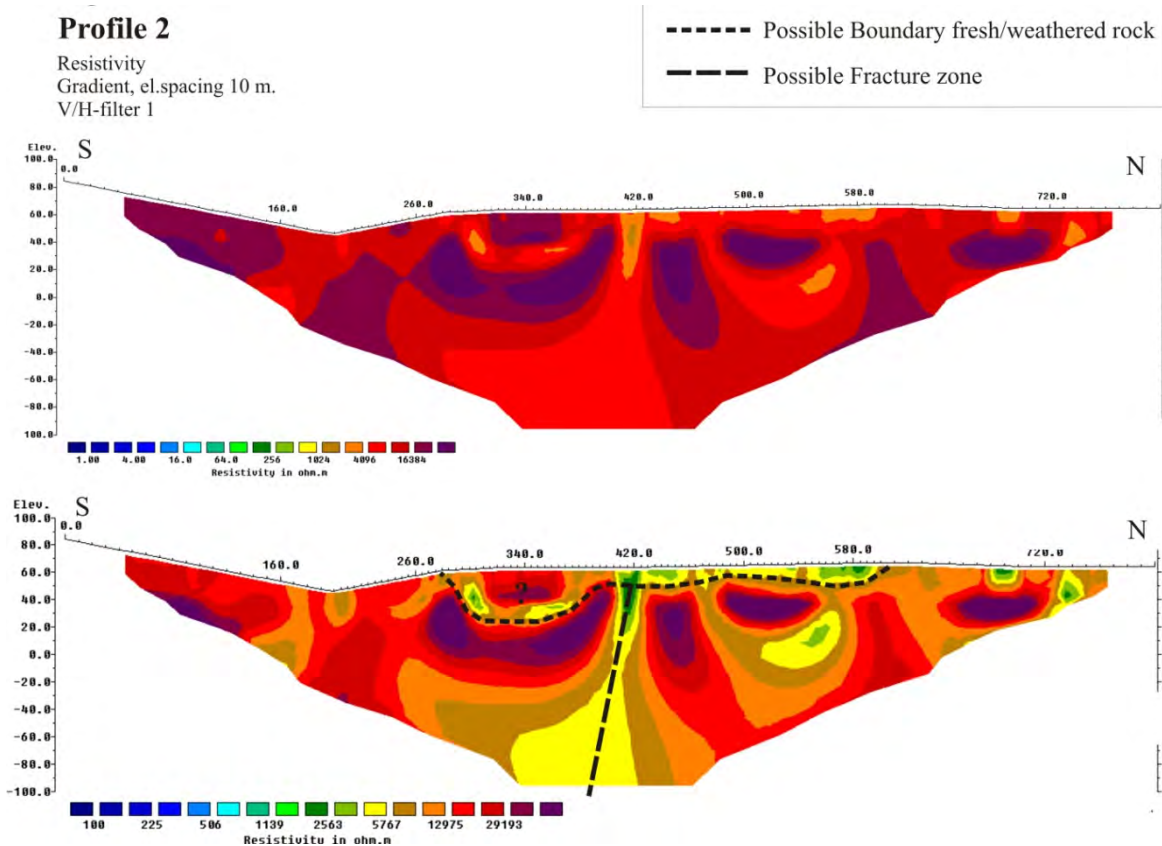


Figure 5.13 ERT Profile 2. Upper panel shows raw data and the lower panel shows normalised data with the interpreted transition from fresh bedrock to weathering soil (Note change in colour scales).

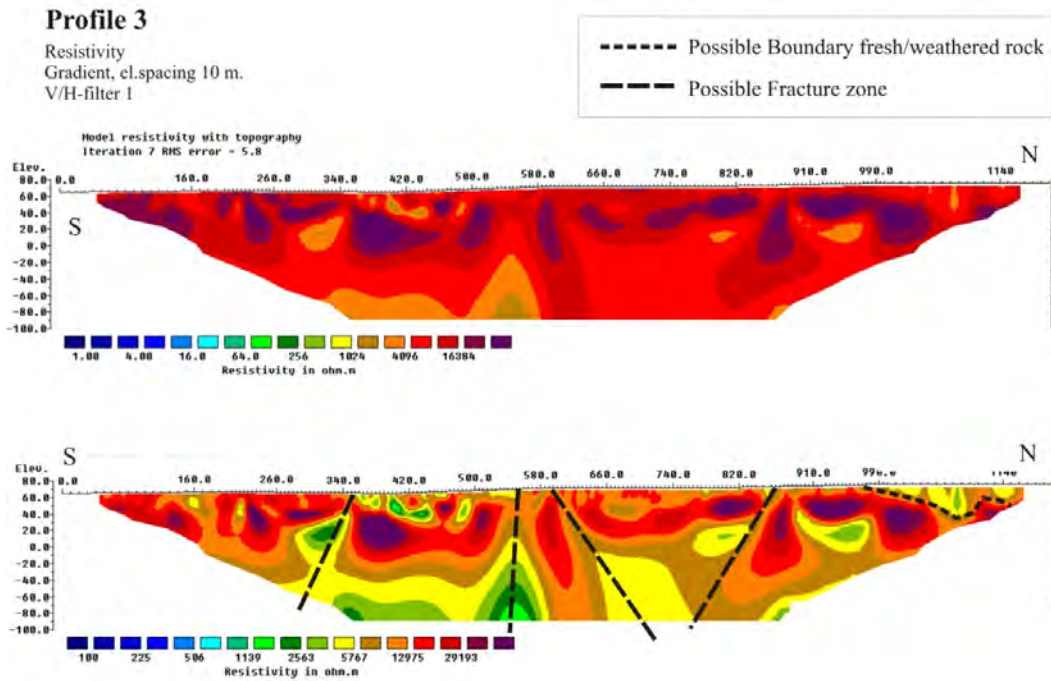


Figure 5.14 ERT Profile 3. Upper panel shows raw data and the lower panel shows normalised data with the interpreted transition from fresh bedrock to weathering soil (Note change in colour scale).

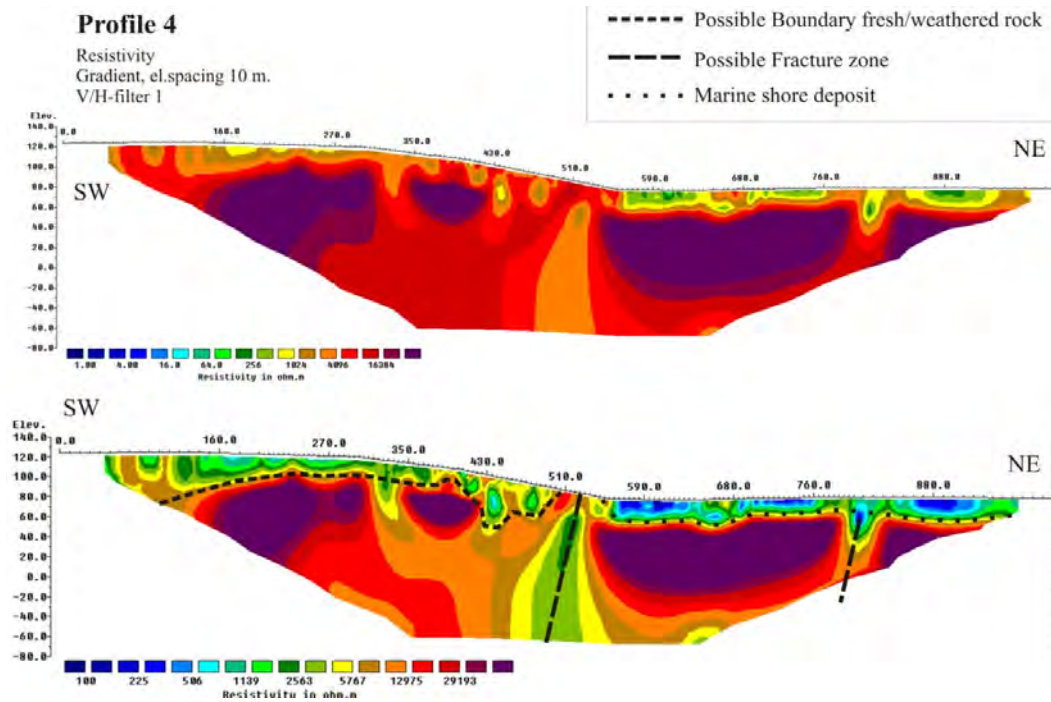


Figure 5.15 ERT Profile 4. Upper panel shows raw data and the lower panel shows normalised data with the interpreted transition from fresh bedrock to weathering soil (Note change in colour scale).

The profiles in Figs. 5.12-5.15 show what is interpreted as a 40 m thick layer of weathered bedrock (saprolite) with lower resistivity values. The profiles are complicated with an undulating bedrock/saprolite interface and several major fault zones cutting through the bedrock yielding very deep structures with low resistivity values. The ERT profiles suggest extensive weathering at depth over the investigated area. The electrical conductors coincide with the deep weathering interpreted by Olesen *et al.* (2007) using the Amager method. As Sørensen (1988) suggested, it also seems plausible that weathering has been localised around fault zones where meteoric and juvenile water have been circulating through geological time.

5.3 Vågsøy – Stad – Inderøya

Odleiv Olesen, Marco Brønner, Einar Dalsegg, Ola Fredin & Jan Steinar Rønning

5.3.1 Vågsøy

These locations were originally described in a master thesis by Larsen & Longva (1979) and later studied by Roaldset *et al.* (1982). The weathered gabbro in an open pit at Movatnet (Figs. 5.16 & 5.17a) on Vågsøy was investigated in detail. It is c. 5 m deep (Figs. 5.17b & 5.18) and contains the clay minerals vermiculite, illite and smectite (Roaldset *et al.* 1982). The 2D resistivity profile (Fig. 5.20) located 100 m to the west of the open pit indicates that the weathered gabbro is limited to a weakness zone in the bedrock. The resistivity profile indicates that the weathered and fractured zone may have a width in the order of 10-20 m. Profile 2 (Fig. 5.20) located 1.1 km to the west of Profile 1 does not have a similar low-resistivity zone. Profile 2 (Fig. 5.21) is located c. 300 m above sea level and 200 m from a steep cliff. The groundwater in fracture zones in this profile may consequently have drained away. The result could be a high-resistivity zone, as observed in the small valley that represents the location for the possible extension of the fracture zone in Profile 1.

The geological investigations associated with the foundations of eight windmills in the adjacent area (Göthfors 2010) (Fig. 5.22-5.24) indicate that the deep weathering is restricted to the fracture zone running through Movatnet. Cores from a total of five boreholes down to a depth of c. 20 metres show that the bedrock consists of fresh gneiss and amphibolite. Clay minerals are, however, observed along fractures and joints. The report by Göthfors (2010) is included as Appendix 2 in the present report.

Photographs from the construction sites have been provided by Ragnar Hagen who was the local consultant and advisor during the planning and construction of the Mehuken II windmill park. Figs. 5.23-5.25 reveal relatively fresh bedrock with minor fracture zones and infills of clay minerals and support the conclusion of the presence of fresh bedrock outside the main fracture zone. The bedrock in the foundation sites consists mainly of grey, foliated, augen gneiss with smaller zones of amphibolites (Göthfors 2010). The augen gneiss is rich in mica

minerals. The dominant joint set is parallel to the foliation. The cores indicate a relatively fresh bedrock, but a few zones with heavily fractured or totally crushed bedrock occur locally. Chlorite, calcite and clay minerals occur locally as fracture fillings.

The perspective aerial photograph (Fig. 5.16) produced using www.norgei3D.no indicates palaeosurfaces at Vågsøy and Stad. The observed weathering at Movatnet, however, seems to be preserved along weakness zones where the weathering originally extended to greater depths and was hence protected against glacial erosion.

The mass balance has been calculated for both weathered and fresh gabbro at Movatnet (Table 5.2). The loss of mass through chemical weathering is estimated to 37 %. The Zr content has been used as a reference immobile element in the calculations (Brimhall et al. 1985). Roaldset et al. (1982) suggested that the weathering at Movatnet occurred in a warm, humid climate based on the occurrence of smectite and kaolinite.

Fig. 5.17B shows measured in situ magnetic susceptibility (10^{-5} SI) at the Movatnet locality. The measurements were carried out using the portable Microkappa (Model KT-5) from ZHstruments. It is based on electromagnetic induction utilising an air-cored coil with a diameter of 55 mm. The accuracy of the instrument is 1×10^{-5} SI. A total of 13 measurements were carried out with intervals of c. 25 cm from the turf and overburden down through the weathered gabbro to the fresh gabbro. The average susceptibility for the clay alteration and the relatively fresh gabbro is 190 and $2750 \cdot 10^{-5}$ SI, respectively, showing that the magnetite in the gabbro is altered to other iron-containing minerals such as hematite and iron-hydroxides with a lower susceptibility. During tropical weathering, iron oxides alter to iron hydroxides at the same time as silicate minerals are converted into clay minerals (e.g. Henkel & Guzmán 1977, Grant 1984). Olesen (2006) and Olesen *et al.* (2007) utilised this phenomenon in compiling the awareness maps for tunnel planning in the Oslofjord region.

Clay-infected bedrock was a problem during the construction of the Sindre radar on Vågsøy around 1990 (R. Hagen, pers. comm. 2010). A report describing the bedrock conditions was prepared for the military authorities. We have checked the military archives in Bergen, Hamar and Oslo but have unfortunately not been able to recover the report.

Results from the ERT measurements at Vågsøy are shown in Figs. 5.20 & 5.21. Interpretation of the two measured lines is given in the figure texts.



Figure 5.16 Palaeosurfaces at Vågsøy and Stadlandet visualised from the north (produced with www.Norgei3D.no). The Vestkapp plateau is located to the far right. Vågsøy can be seen in the background with the white frame.

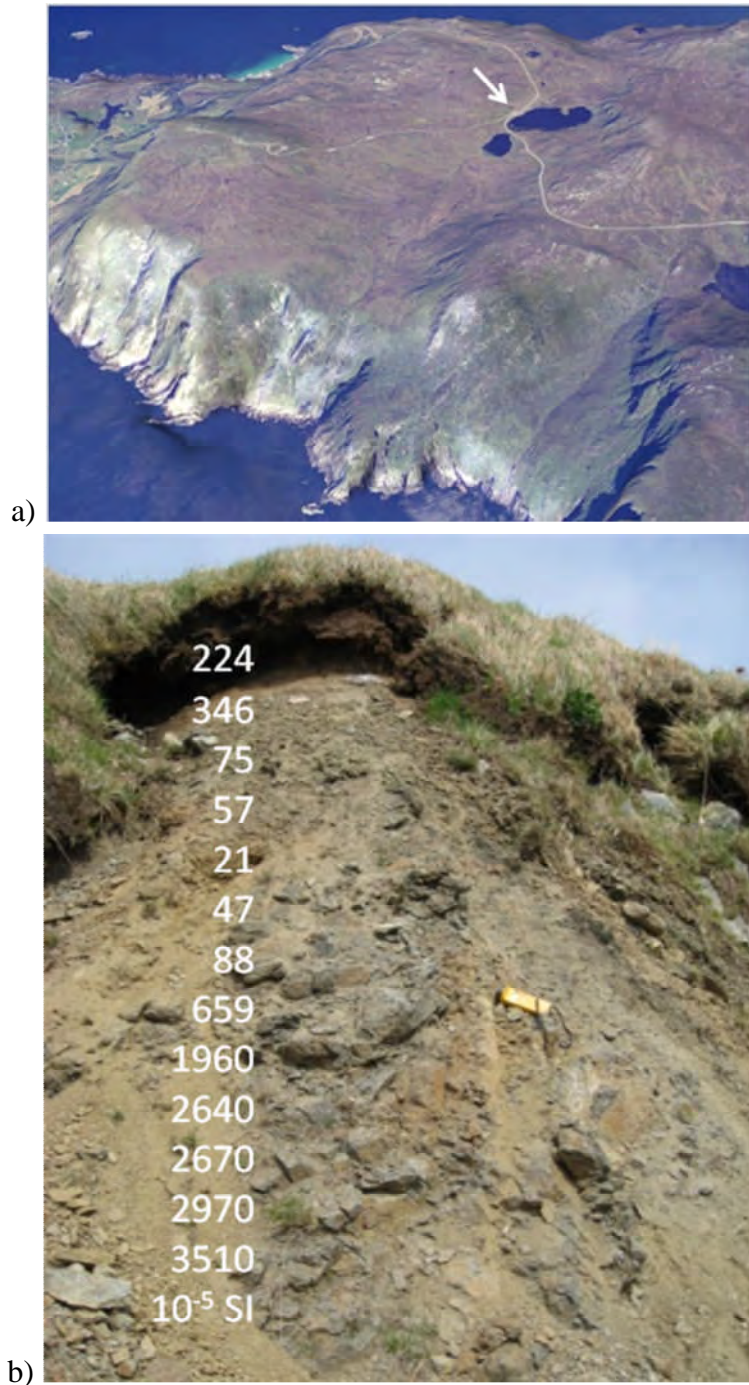


Figure 5.17 Deeply weathered gabbro at Movatnet on Vågsøy, Sogn & Fjordane. a) The palaeosurface at Vågsøy seen from the south. The open pit is located immediately to the north of the road passing along the lake and is shown by the white arrow. The weathering occurs in a fractured gabbro along an E-W trending lineament. The aerial photograph is produced using www.Norgei3D.no. b) Photograph of weathered gabbro. The white numbers show the variation of in situ magnetic susceptibility (10^{-5} SI) from the turf down through the weathered gabbro to the relatively fresh gabbro. The average susceptibility for the clay alteration and gabbro is $185 \cdot 10^{-5}$ SI and $2750 \cdot 10^{-5}$ SI, respectively. The 20 cm-long Kappameter KT-M instrument illustrates the scale.

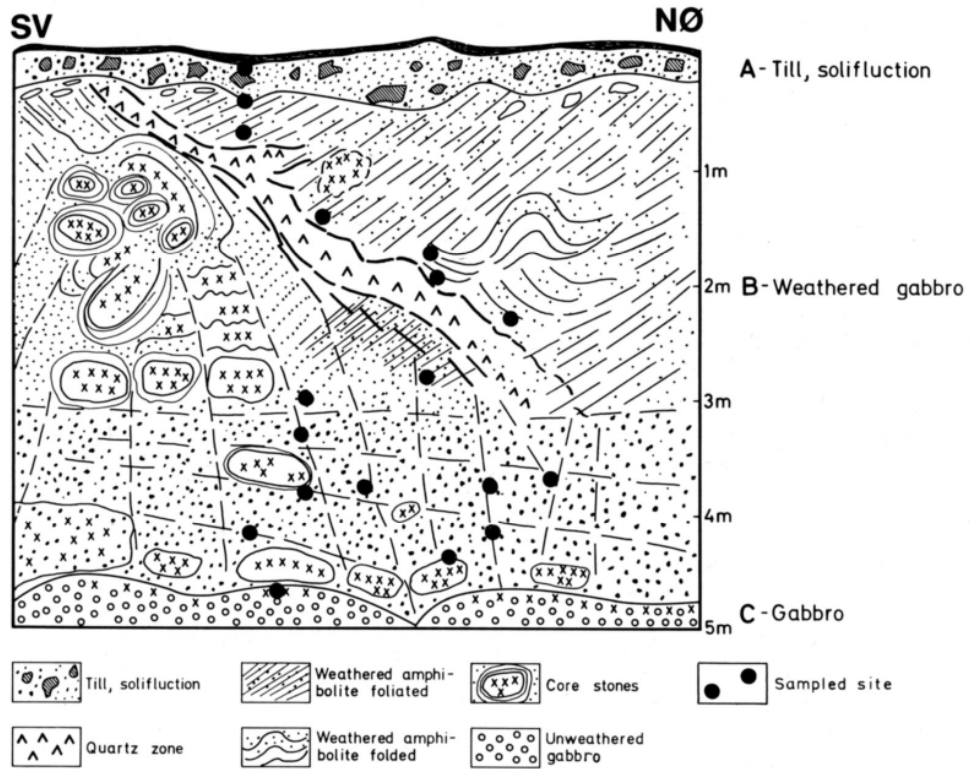
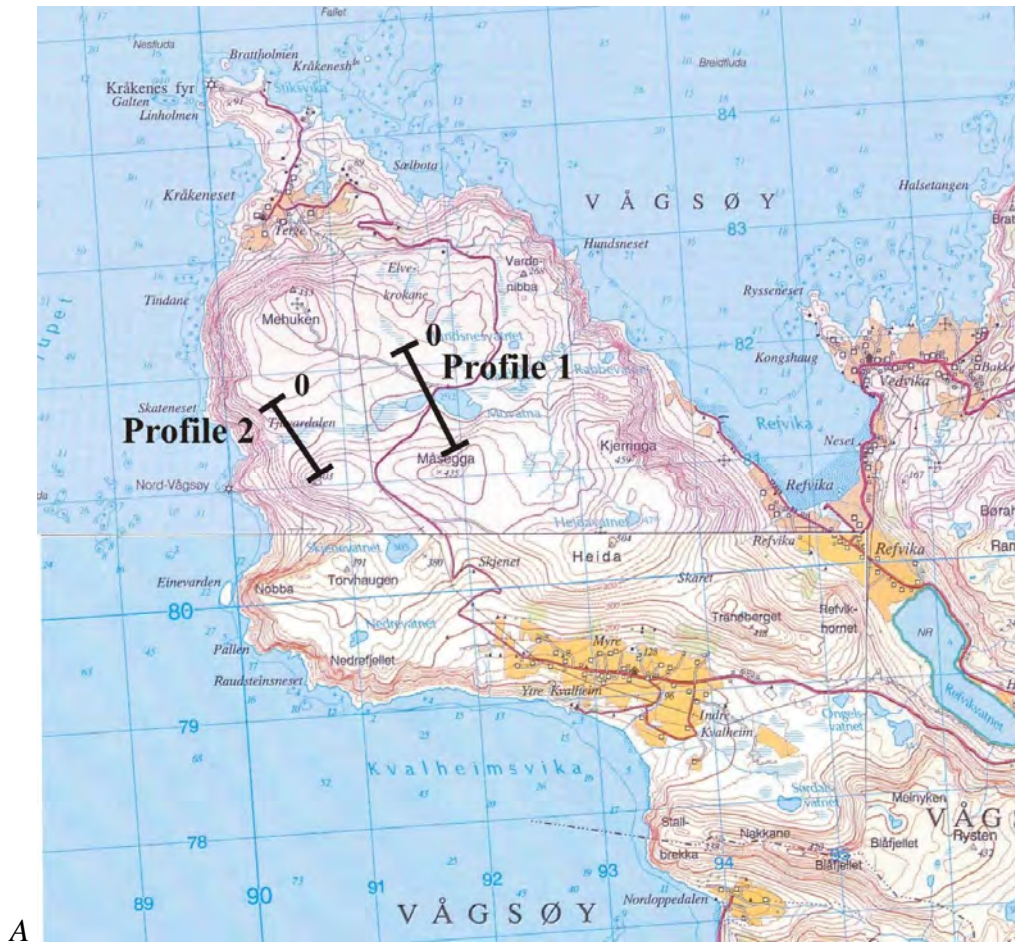


Figure 5.18 Exposure of the 5-m deep zone of weathered gabbro at Movatnet, Vågsøy (from Roaldset et al. 1982). Erratic blocks of augen gneiss occur in the Quaternary overburden.

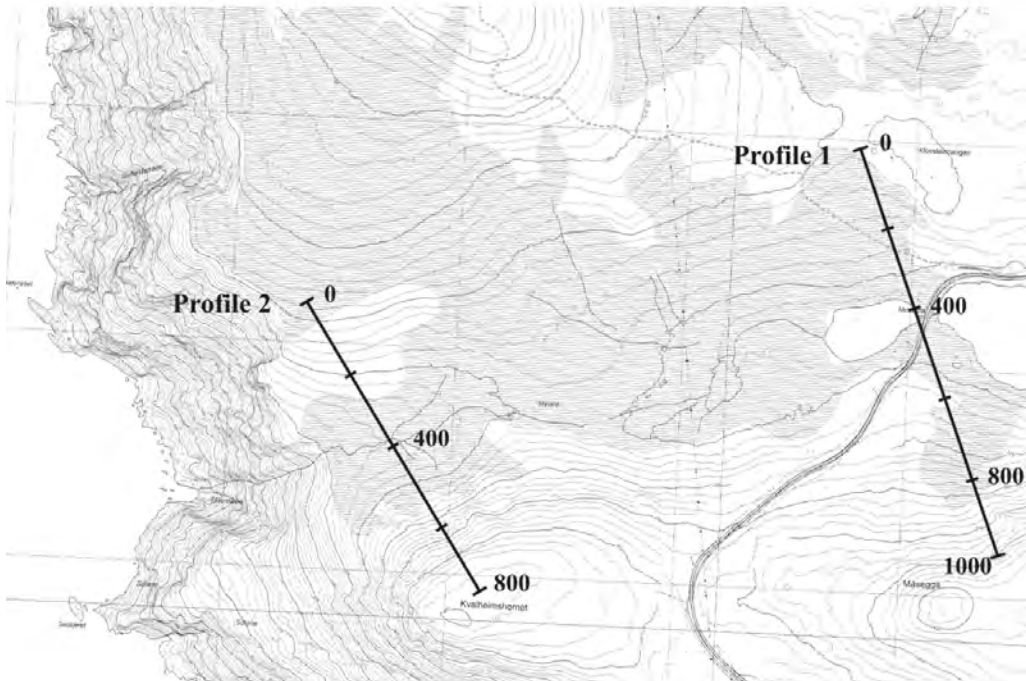
Table 5.2 Brimhall mass balance calculations for weathered and fresh gabbro at Movatnet. The loss of mass through chemical weathering is estimated to 37 %. The Zr content has been used a reference immobile element in the calculations (Brimhall et al. 1985).



Leached in 100 g of rock												
	SiO ₂	Al ₂ O ₃	Fe ₂ O ₃	TiO ₂	MgO	CaO	Na ₂ O	K ₂ O	MnO		SUM Si+Al+Na+K	SUM
3. Saprolite	-13.9	-4.0	-9.3	-1.7	-2.4	-4.6	-1.0	-0.1	-0.1		-19.0	-37.1
2. Core boulder rim	-12.4	-4.2	-4.9	-1.0	-1.0	-3.9	-0.9	-0.1	0.0		-17.6	-28.4
1. Fresh rock	0	0	0	0	0	0	0	0	0			

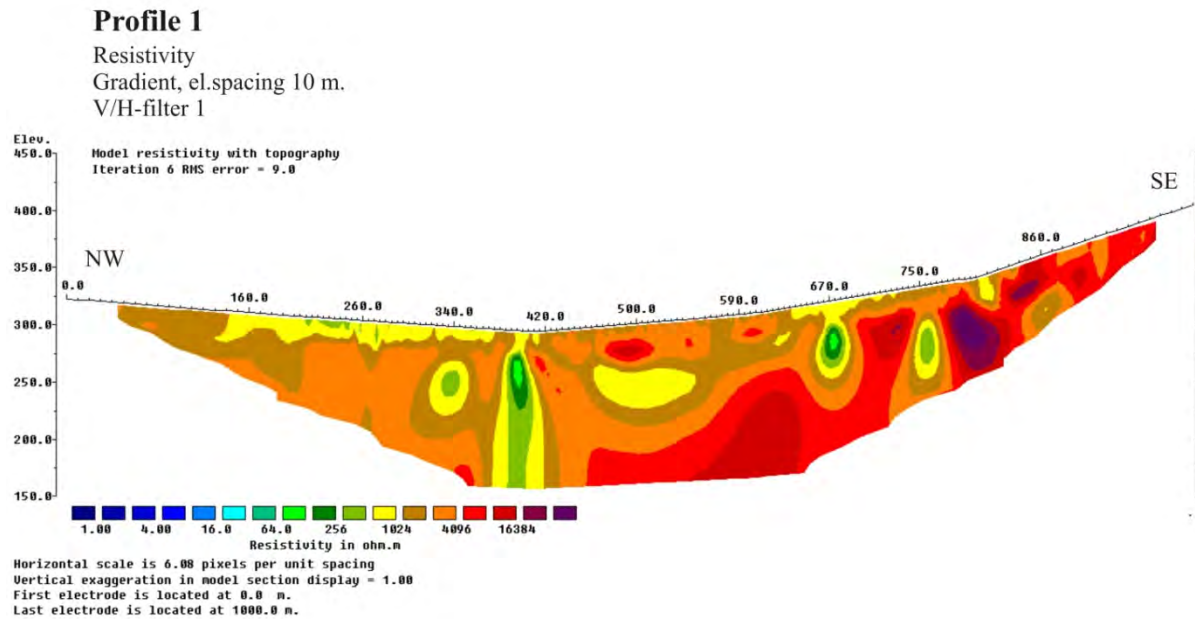


A



B

Figure 5.19 A) Location of two 2D resistivity profiles on Vågsøy plotted on a M711 map (originally at a scale of 1:50,000 and B) on a detailed economic map (originally at a scale of 1:10,000). The open pit with the weathered gabbro is located immediately to the north of the road to the far east in the latter map.



b)

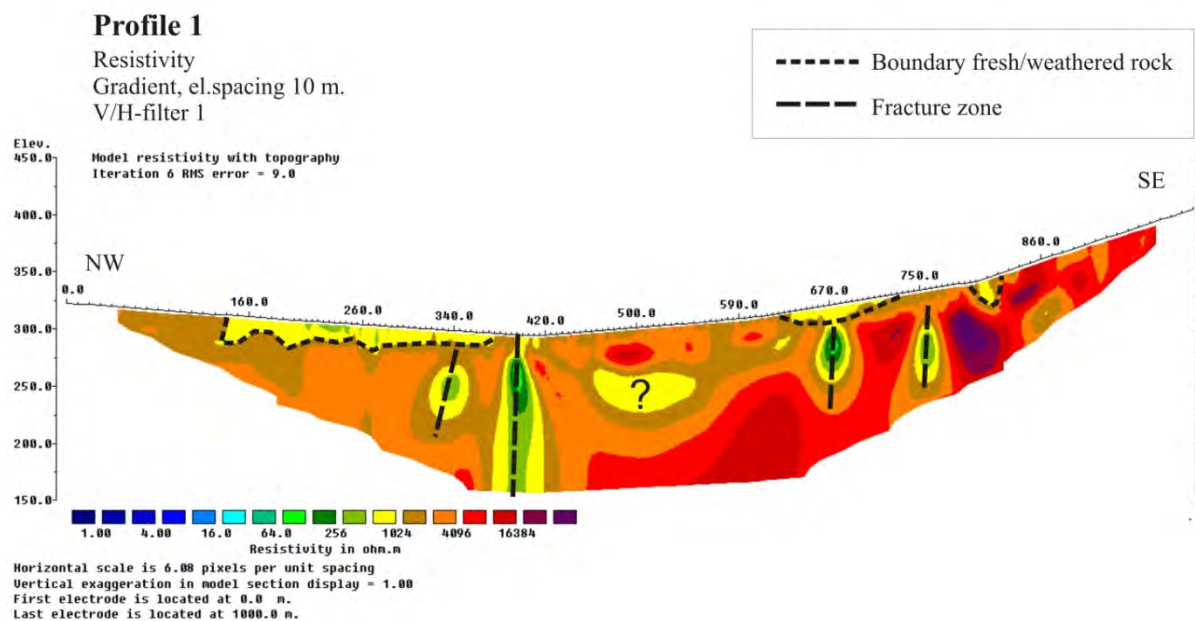
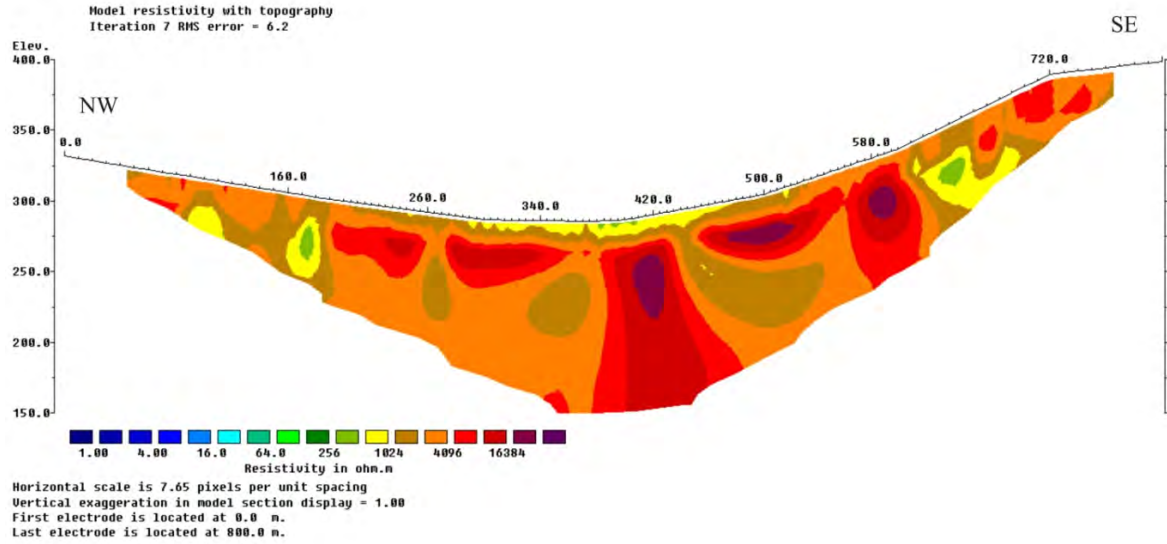


Figure 5.20 Resistivity (ERT) Profile 1 on Vågsøy. (See Figs. 5.19A and 5.19B for location).
a) Observations and b) Observations with superimposed interpretations. The dotted lines show the interpreted bedrock surface and dashed lines indicate possible fracture zones. The c. 10-15 m-wide low-resistivity zone at c. 400 m most likely represents the continuation of the observed weathered gabbro located in the open pit 100 m to the east (Fig. 5.17). The thickness of the overburden seems to increase to 25 metres in the northwest.

a)

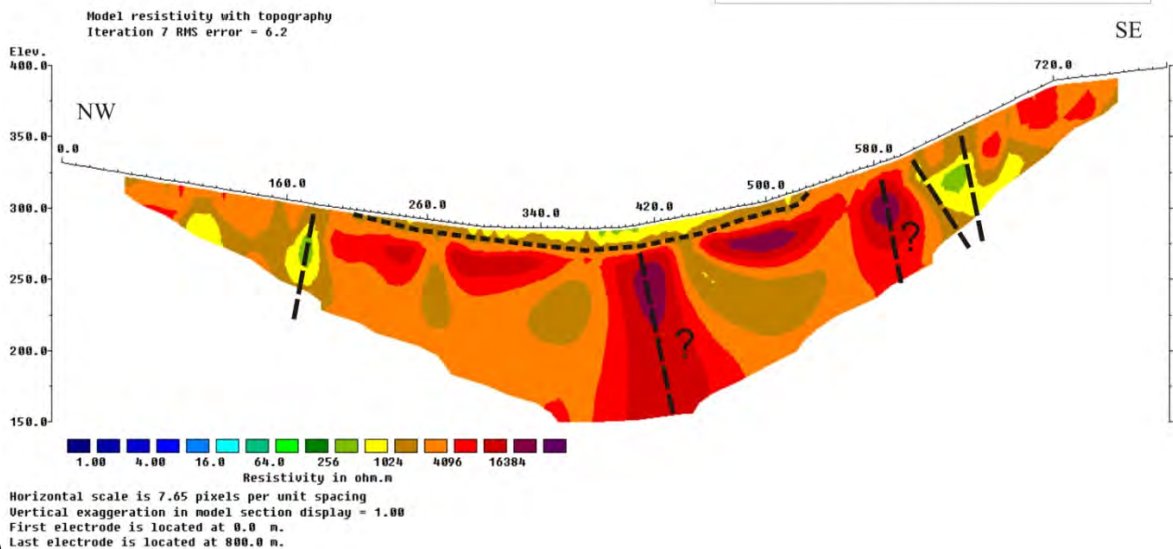
Profile 2

Resistivity
Gradient, el.spacing 10 m.
V/H-filter 1



Profile 2

Resistivity
Gradient, el.spacing 10 m.
V/H-filter 1



b)

Figure 5.21 Resistivity profile 2 located 1.1 km to the west of profile 1 (See Figs. 5.19A and 5.19B for location). a) Observations and b) Observations with superimposed interpretations. The dotted line shows the interpreted bedrock surface and dashed lines indicate possible fracture zones. A total of five minor fracture zones with varying dip have been interpreted. The fractured and weathered gabbro interpreted in Profile 1 does not, however, seem to occur along this profile. The Quaternary overburden seems to have a thickness of c. 10 metres. High resistivity in the zones at coordinates 420 and 580 may be caused by water drainage from these zones close to the steep hillside.

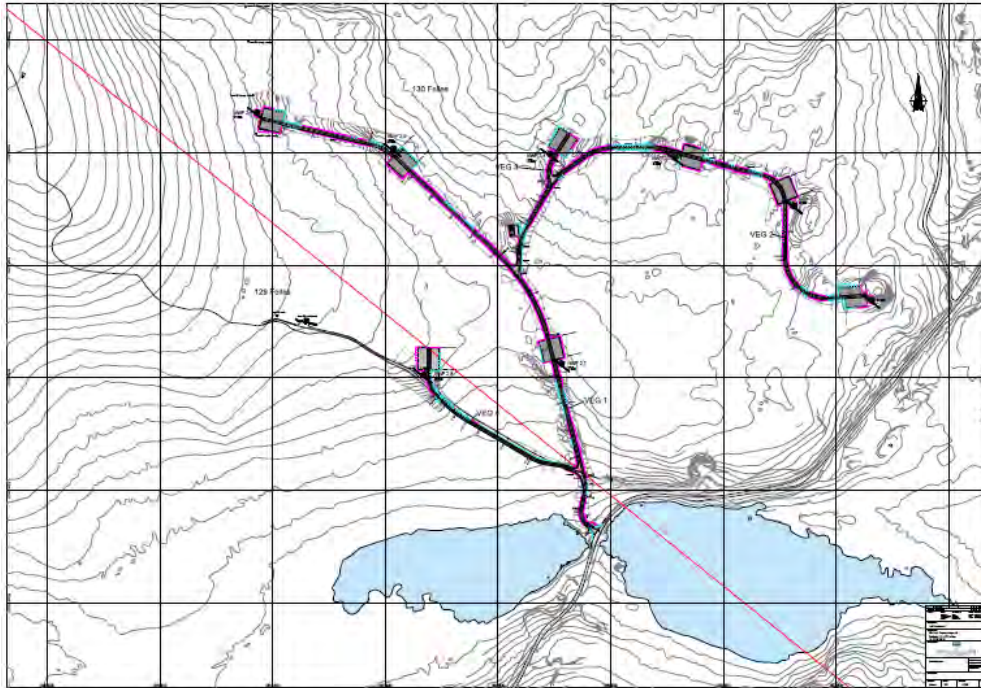


Figure 5.22 The foundations of the Mehuken II windmill park are numbered from 2.1 to the far east to 2.6 to the northwest. Foundations 2.7 and 2.8 are located farther south and closer to Movatna, to the SE and SW, respectively.



Figure 5.23 Oblique aerial photograph of the Mehuken-Movatna area on Vågsøy. The view is from the east. The open pit containing the weathered gabbro is located adjacent to the road along Movatna and can be seen to the far left in the picture. The original five windmills and the foundation sites for the eight new windmills in the Mehuken windmill park can be seen in the central part of the picture.



Figure 5.24 The bedrock in foundation 2.6 in the Mehuken II wind mill park consists of relatively competent amphibolite (Photo: Ragnar Hagen). The bedrock was investigated at depth through a 21,75 m long drill core that has been drilled towards the southwest with an inclination of 70 degrees from the horizontal (Göthfors 2010 and Appendix 2). The drill core consists of grey foliated augen gneiss. There are also some smaller segments of amphibolite. The augen gneiss is rich in mica minerals. The eyes are light in colour and often slightly extended in the foliation plane. The colour of the amphibolite varies from grey to greyish green to carbon black. The carbon black amphibolite is soft and crumbly. The dominant joint set is parallel to the foliation in the core. The core indicates a relatively fresh bedrock, but there are a few zones where the drill core is heavily fractured or totally crushed. There are not much secondary mineral filling in the fractures. Occurring fracture minerals are chlorite and calcite.



Figure 5.25 The bedrock of foundation site No. 2.8 in the Mehuken II windmill park consists of augen gneiss and amphibolites (Photo: Ragnar Hagen). The 21.6 m-long core indicates competent bedrock, except for a few zones where the drillcore is very heavily fractured or totally crushed (Göthfors 2010 and Appendix 2). These fracture zones contain an abundance of clay minerals. Otherwise there are very few fillings in the fractures. Fracture minerals present are clay minerals and chlorite. See Appendix 2 for further details.

5.3.2 Stad

Larsen & Longva (1979) and Roaldset et al. (1982) described *in situ* weathered granitic gneiss on the mountain Kjerringa at Vestkapp, Stad peninsula (Fig. 5.26). The mountain is located on a plateau which most likely constitutes a remnant of a palaeosurface. The plateau is bounded by high, vertical cliffs formed by wave action (Figs. 5.26) and is covered by an up to 10 m-thick sediment layer consisting of weathered bedrock overlain by basal tills and solifluction deposits (Roaldset et al. 1982). The reported high content of gibbsite in addition to the occurrence of smectite and kaolinite led Roaldset et al. (1982) to conclude that the bedrock has been exposed to laterite/bauxitic weathering in a warm and humid climate.

The 1 km-long, 2D resistivity profile (Figs. 5.27) indicates three fracture zones with varying dip and a relatively thin (1-3 m) overburden along the profile. This is consistent with the trenching results reported by Larsen & Longva (1979) and Roaldset et al. (1982). We have interpreted the apparent low-resistivity zone at the summit of Kjerringa (approximately at location 780 m along the profile in Fig. 5.27) to be an artefact produced by the weather radar system at this site.

A

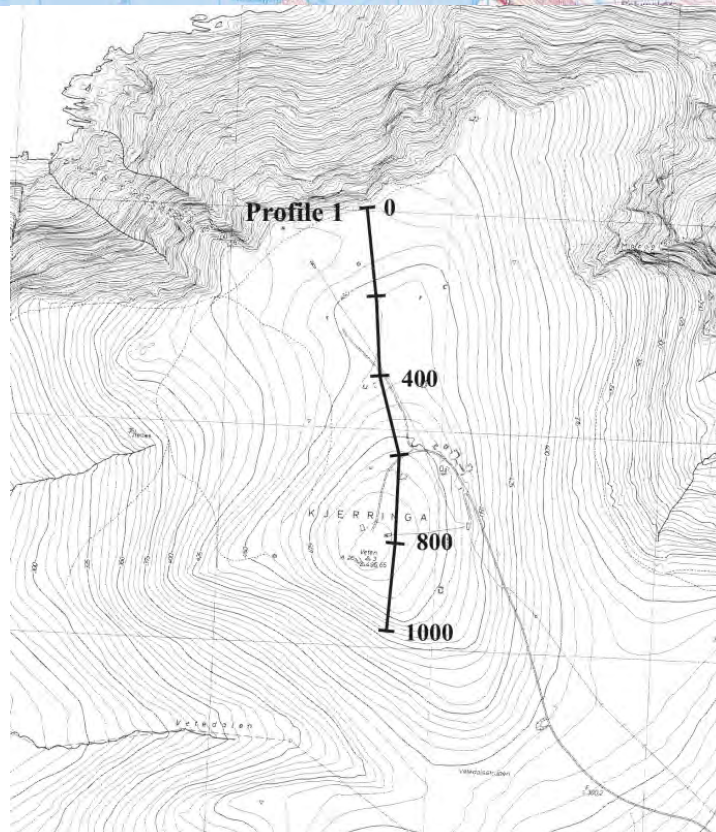
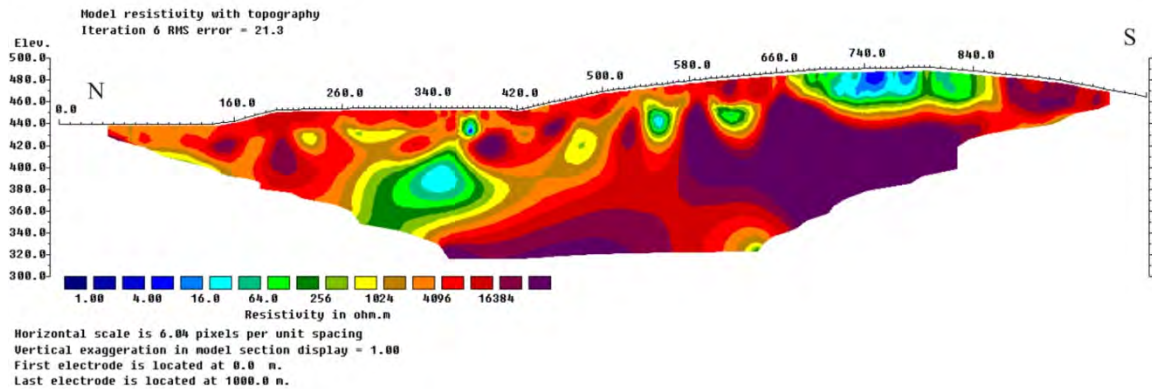


Figure 5.26 Location of 2D resistivity profiles on Stad plotted on A) a M711 map (originally at a scale of 1:50,000) and B) on a detailed economic map (originally at a scale of 1:10,000). A weather radar system is located along the profile across the mountain Kjerringa at approximately coordinate 780 m.

Profile 1

Resistivity
Gradient, el.spacing 10 m.
V/H-filter 1



Profile 1

Resistivity
Gradient, el.spacing 10 m.
V/H-filter 1

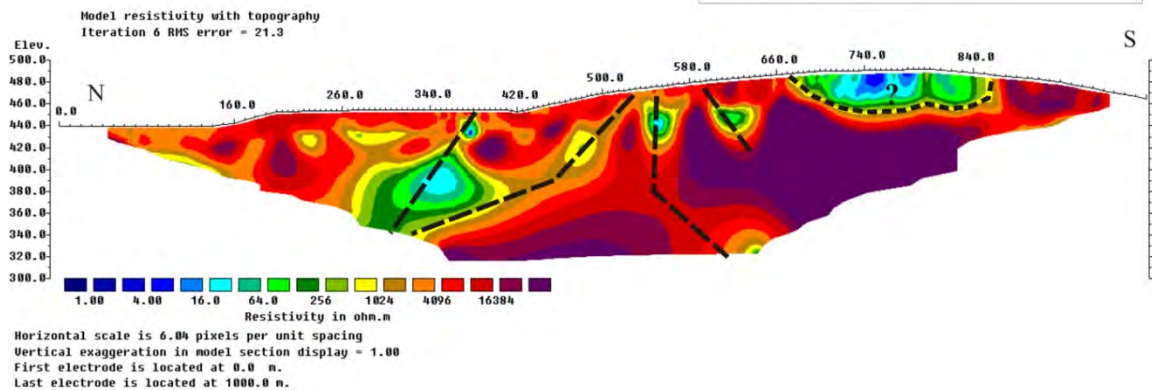


Figure 5.27 Resistivity profile on Vestkapp, Stad. (See Fig. 5.26 for location). a) Observations and b) Observations with superimposed interpretations. The dotted line shows the interpreted bedrock surface and dashed lines indicate possible fracture zones. Three weakness zones with varying dip have been interpreted. The Quaternary overburden seems to be relatively thin along the profile. A weather radar system is located close to the profile at approximately 790 m (Kjerringa) and is most likely the cause of the apparent low-resistivity zone at this location.

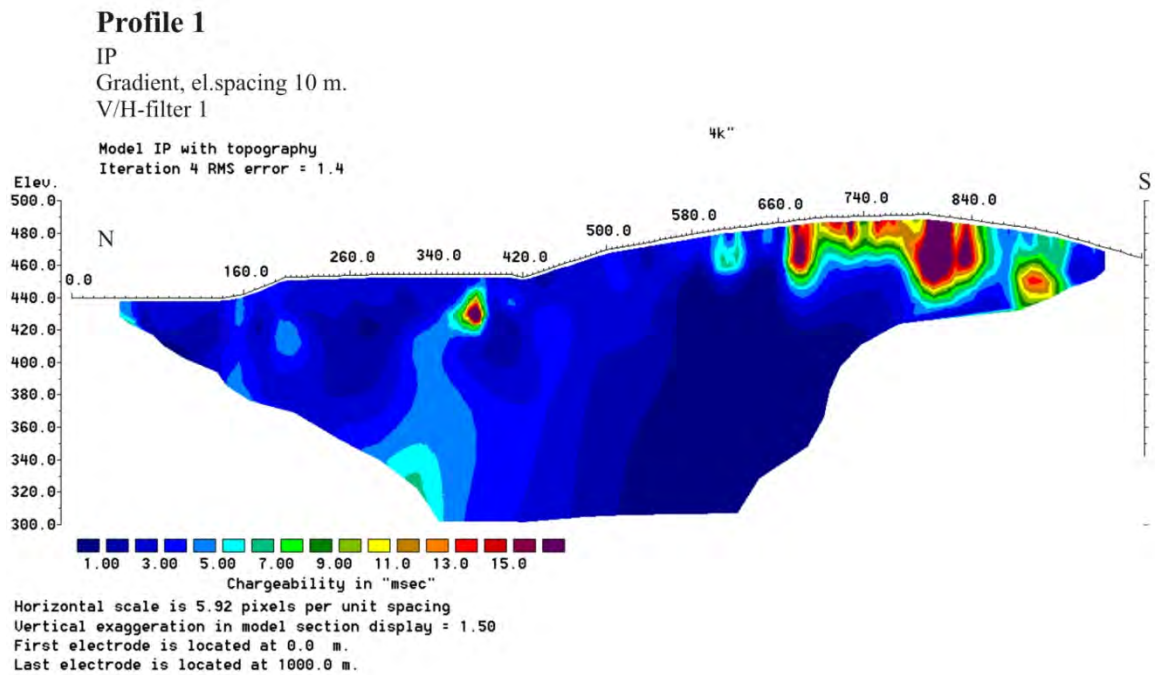


Figure 5.28 Induced polarisation (IP) along the profile at Vestkapp. The pronounced IP anomaly between 670 m and 840 m is located in the vicinity of the weather radar at coordinate 790 m and is most likely related to disturbances from this installation.

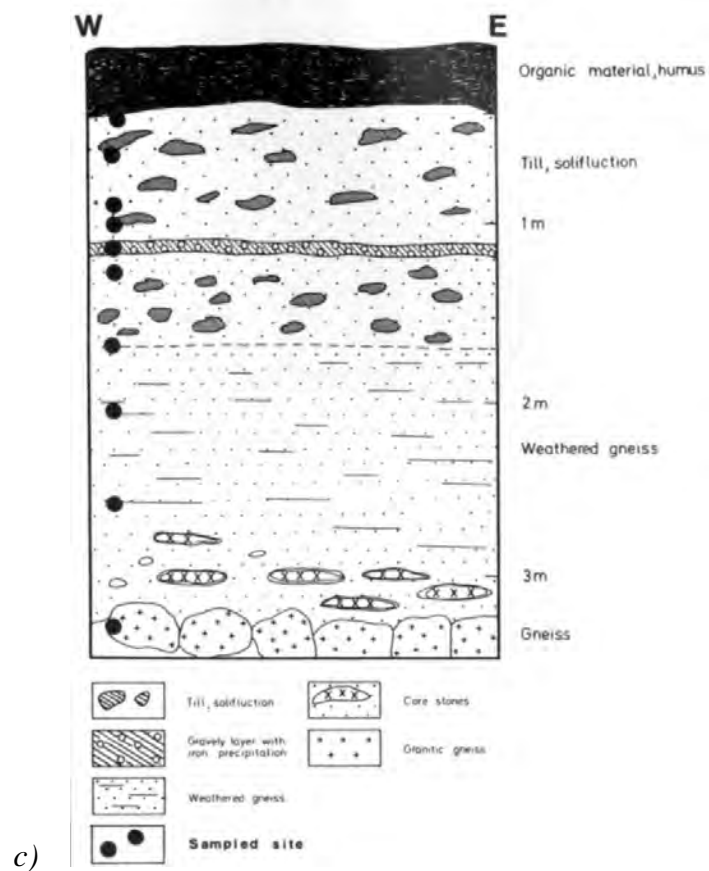
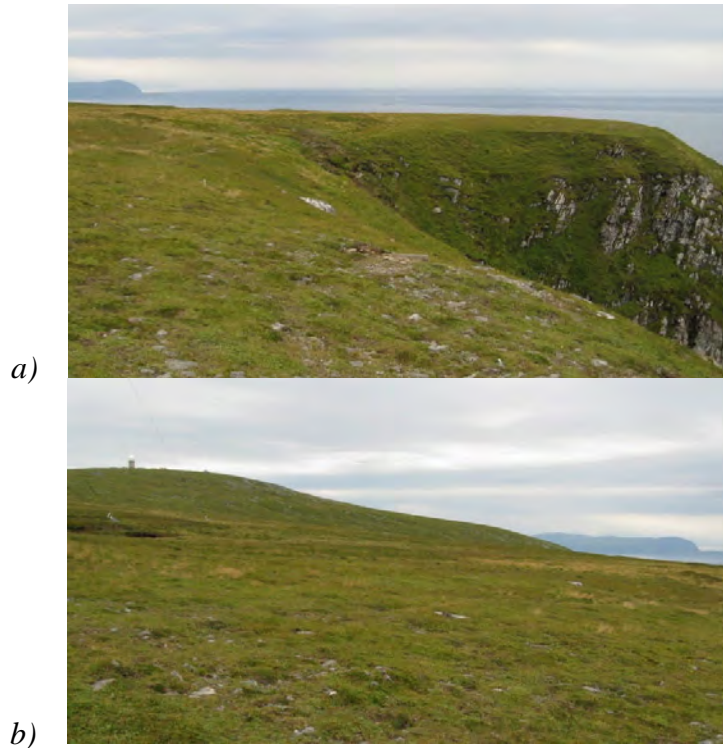


Figure 5.29 a) Palaeosurface at Vestkapp plateau. b) Palaeosurface at Vestkapp. The Kjerringa with the weather radar can be seen to the far left. c) Geological section through deep-weathered soils in a trench on the mountain Kjerringa at Vestkapp, Stad (Roaldset et. al. 1982).

5.3.3 Inderøya

The Inderøya area in Nord-Trøndelag was chosen for closer investigation because of the previously mapped areas of weathered bedrock. Sveian (1985), Reite (1997) and Sveian *et al.* (in press) registered large areas of discontinuous and thin weathering in the municipalities of Inderøya and Mosvik (Figs. 5.30 & 5.31). Inderøya constitutes part of the basement to the Beitstadfjorden Basin to the northwest (Polak *et al.* 2004, Bøe & Bjerkli 1989, Bøe *et al.* 2010) (Fig. 5.32) where Jurassic and Cretaceous sedimentary successions form the infill in a c. 1500 m-deep half-graben located along the Verran Fault (Bøe *et al.* 2010). These sedimentary rocks must have extended across the Inderøya peninsula in the Mesozoic (Bøe *et al.* 2010) and could have delayed the erosion of Triassic-Jurassic weathering until the Tertiary or even Quaternary. We regarded the potential for finding remnants of tropical weathering on Inderøya as fairly high.

Field observations along the main roads on Inderøya and farther to the southwest revealed a number of rusty and fractured schists, especially in the Mosvik area (Fig. 5.33). Two other locations on the nearby Fosen Peninsula occur along road-cuts between Storvatnet and Skaugdalen (J. Cramer, pers., comm. 2011) and at Ålvatnet in Leksvik. The UTM coordinates (zone 32, WGS 84 datum) of the two locations are 561700 – 7059725 and 581200-7068740, respectively. We could not, however, find any localities with clay-rich alteration. One possible exception, however, occurs along another road cut to the south of Bulandsvatnet in the Stjørdal municipality (UTM coordinates 608400 70499500).

We have interpreted eight fracture zones with varying dip along the 1.6 km-long, 2D resistivity profile on Inderøya (Figs. 5.34 & 5.35). The linear depressions in the terrain (Fig. 5.34) seem to coincide with low-resistivity zones that may represent deeply weathered zones. The Quaternary overburden seems to be relatively thin along the profile.

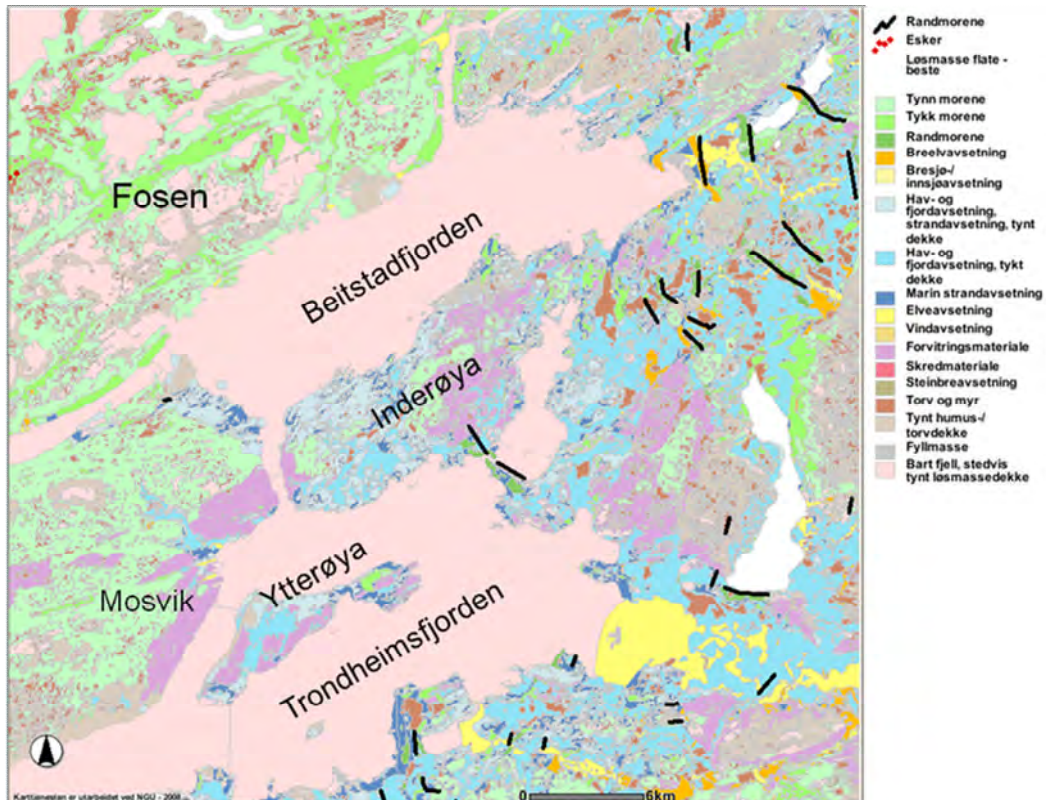


Figure 5.30 A subset of the Quaternary map of North Trøndelag (Sveian et al. in press) produced from NGUs map database. Substantial areas of weathering ('forvittringsmateriale' in the map legend) have been mapped on Inderøya and near Mosvik to the south of Beitstadfjorden.

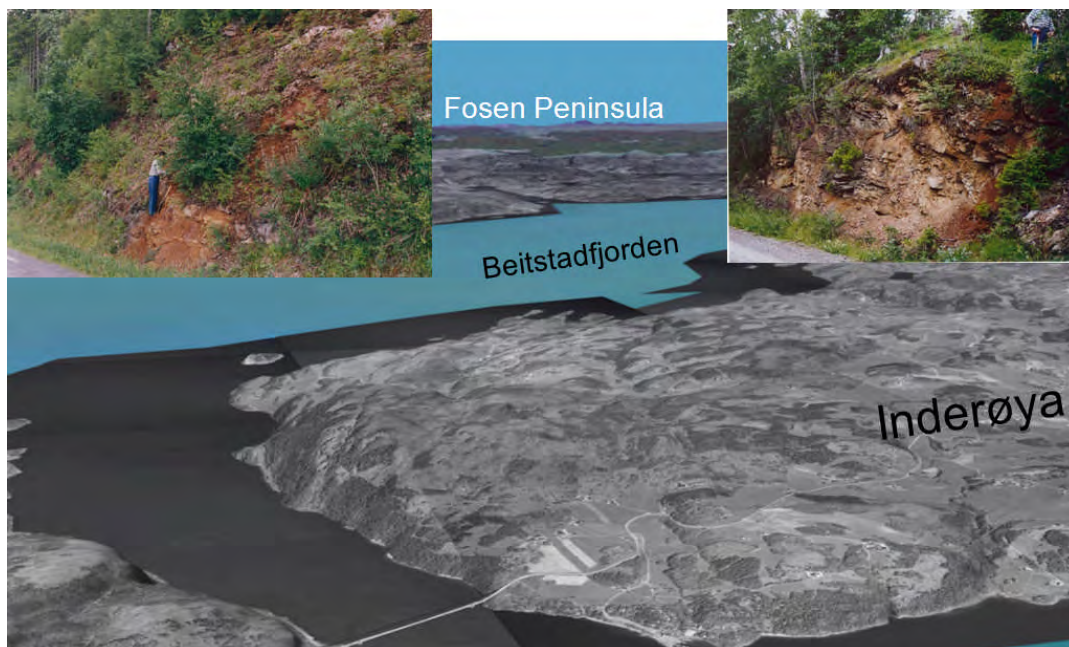


Figure 5.31 Perspective aerial photograph of the Inderøya peninsula looking to the north. Linear depressions in the terrain may represent weathered fracture zones. The two inset pictures show weathered rocks from the Inderøya area (Sveian & Solli 1997). We have not been able to relocate the two sites. They are most likely covered by vegetation today.

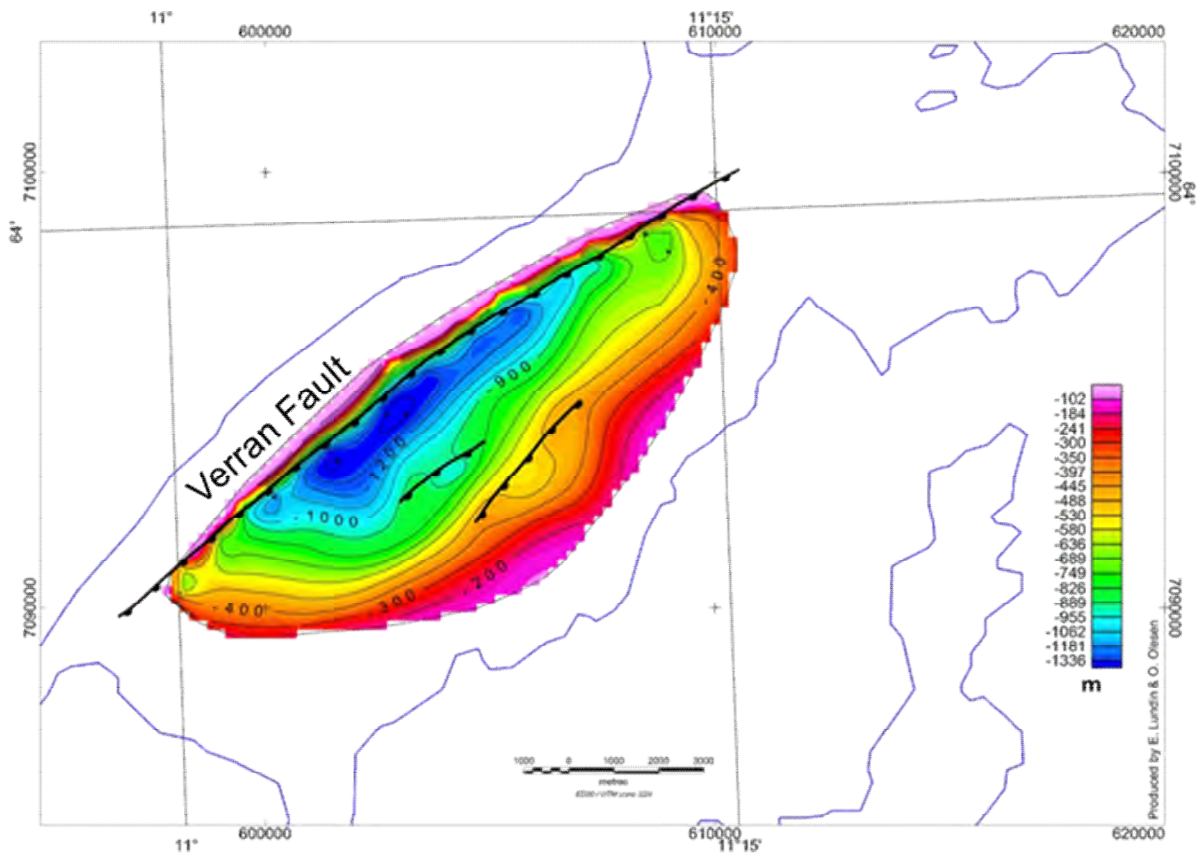
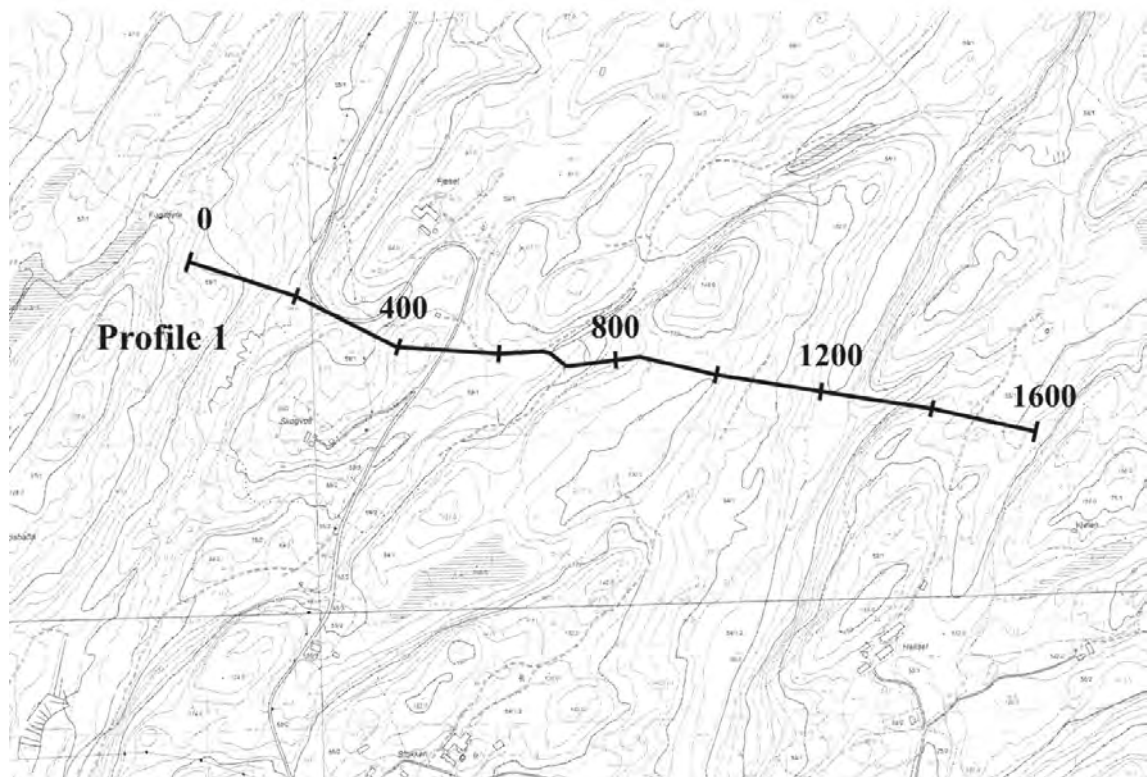


Figure 5.32 Jurassic basin in Beitstadfjorden to the northwest of Inderøya (Polak et al. 2004). The sedimentary rocks almost certainly extended across Inderøya before they were eventually removed by erosion.



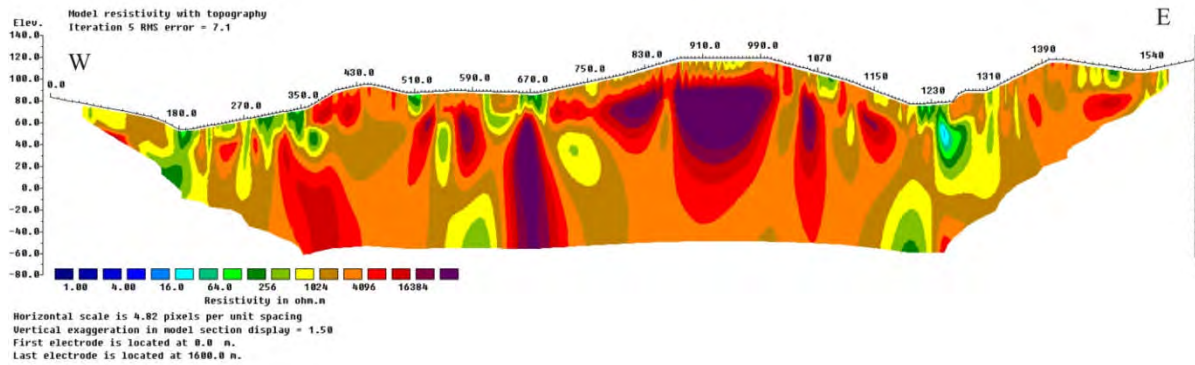
A



B

Figure 5.33 Location of a 1600 m-long 2D resistivity profile on Inderøya on A) a M711 map (originally at a scale of 1:50,000) and on B) an economic map (originally at a scale of 1:10,000).

a)
Profile 1
 Resistivity
 Gradient, el.spacing 10 m.
 V/H-filter 1



b)
Profile 1
 Resistivity
 Gradient, el.spacing 10 m.
 V/H-filter 1

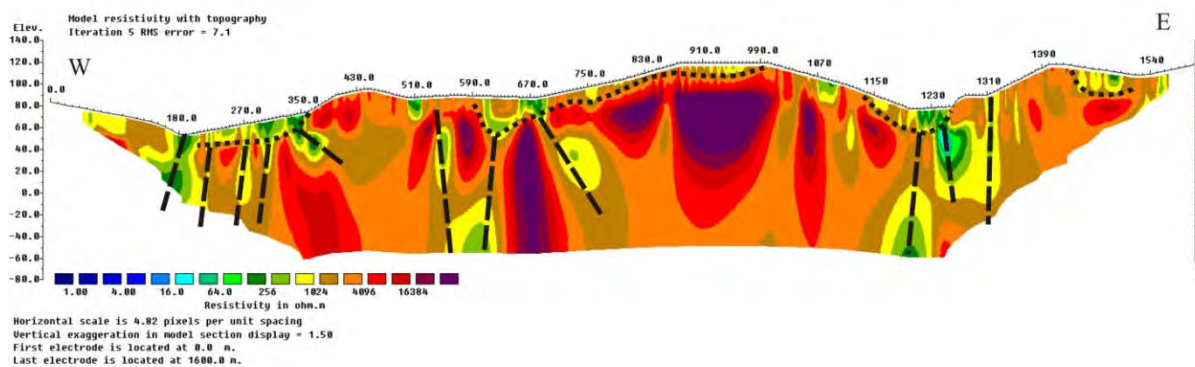


Figure 5.34 Resistivity profile on Inderøya. (See Fig. 5.33 for location). a) Observations and b) Observations with superimposed interpretations. The dotted line shows the interpreted bedrock surface and dashed lines indicate possible fracture zones. A total of eight fracture zones with varying dip have been interpreted. The linear depressions in the terrain (at locations 100, 670 and 1200 m, Fig. 33b) seem to coincide with low-resistivity zones that may represent deeply weathered zones. The Quaternary overburden seems to be relatively thin along the profile.



Figure 5.35 Fractured and fragmented mica schist along a road-cut at Dørgåsen in Mosvik (UTM 32, WGS84 593800-7078550). The clay content appears to be low even though the rock seems to be totally disintegrated. This type of weathering is typical for the soil that is identified as weathered material (forvitningsmateriale) on the Quaternary map (Reite 1997, Sveian & Solli 1997, Sveian 1985, Sveian et al. in press).

6 NORTHERN NORWAY

Marco Brønner, Einar Dalsegg, Karl Fabian, Ola Fredin, Jomar Gellein, Jan Steinar Rønning, Terje Solbakk & Jan Fredrik Tønnesen

6.1 Introduction

Saprolitic bedrock in the Lofoten-Vesterålen area and on Hamarøya is used by local farmers to construct and maintain small gravel roads and only few of the locations have been reported in the scientific literature. During the mapping we investigated publications and old construction reports, visited known quarries and former pits and interviewed local people. Furthermore, recent air photographs were used to detect more locations with possible weathered rocks. We found three locations onshore on Lofoten-Vesterålen, on Vestvågøya, Hadseløya and Andøya, with remarkably deep penetration of weathering into the bedrock. Moreover, an open pit on Hamarøya was studied. These locations were further investigated and resistivity profiling was undertaken to estimate the thickness of the weathered zones.

For Langøya, modern high-resolution aeromagnetic data were on hand which were selected for testing of the AMAGER method (Chapter 2.3) to map possible deep weathering on the island. The results were subsequently compared with resistivity and excavation profiles.

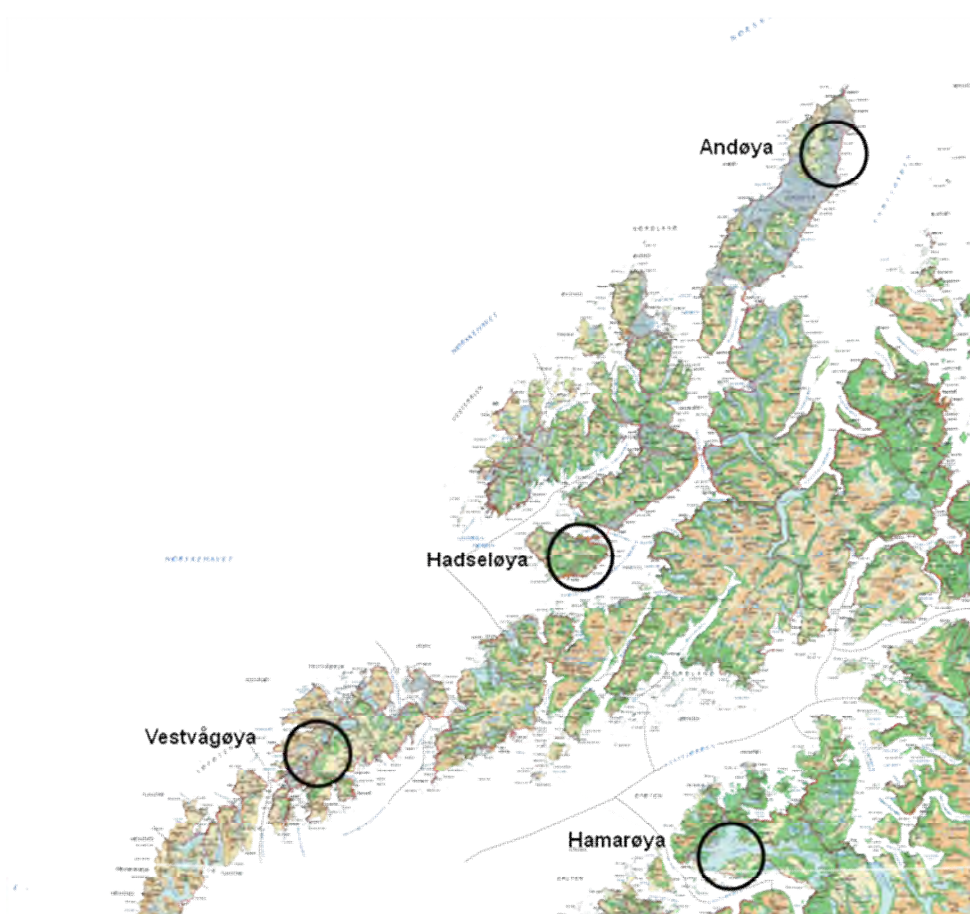


Figure 6.1 Overview map of the studied locations in the Lofoten-Vesterålen and Hamarøya areas.

Severe problems occurred during the construction of the 726 m-long Rørvikskaret road tunnel (E 10) on Austvågøya in Lofoten in the early 1970s. The tunnel caved in during the construction and the collapse extended along a weakness zone with high swelling clay content all the way to the top of the mountain pass (Grønhaug 1975, Palmstrøm *et al.* 2003). In the end there was an open hole from the tunnel to the top of the pass located 100 metres above the tunnel. The tunnel project was delayed by three years and was not completed until 1974 after five years of construction. We think that the tunnel collapse most likely occurred along a deeply weathered major fracture zone where the silicate minerals had been altered to clay minerals. The total cost of the tunnel increased from a budgeted 3 MNOK to a final total of 6.5 MNOK (Palmstrøm *et al.* 2003).

6.2 Geological framework of the Lofoten-Vesterålen-Hamarøya region

Erosion of the sedimentary succession and various tectonic processes with fault block rotations and uplift have often been inferred to explain the relief of the landscape in the Lofoten-Vesterålen archipelago, northern Norway (Fig. 6.1). Recent studies, however, have shown that these processes are not sufficient to explain the magnitude and variation in relief (Lidmar-Bergström 1995, 1997, Lidmar-Bergström & Näslund 2005, Bonow *et al.* 2007). The locations of numerous sounds and islands, not only in the Lofoten-Vesterålen area, but also along the Norwegian coast, could to a large extent be the result of exhumation and erosion of weathered basement. Deep weathering in Norway commonly occurs along structurally defined weakness zones and thus played, and still plays, a decisive role in the genesis of the relief of the landscape.

The Lofoten-Vesterålen archipelago is a NNE-SSW to NE-SW oriented basement high (Åm 1975, Blystad *et al.* 1995, Løseth & Tveten 1996, Olesen *et al.* 1997, Tsikalas *et al.* 2001), situated between 67°24'N and 69°20'N latitude at the narrowest part of the Norwegian continental shelf. It is flanked by a system of deep Late Palaeozoic/Early Mesozoic grabens and half-grabens (Tsikalas *et al.* 2008, 2005, Mjelde *et al.* 1993) which experienced major phases of extension during the Jurassic to Tertiary. The crustal thickness is on average c. 26 km with a maximum at c. 30 km beneath Andøya in the north and an upwarping Moho to c. 20 km beneath Moskenesøya to the south (Nysæther *et al.* 1969, Olesen *et al.* 2002, Tsikalas *et al.* 2005).

The basement of the Lofoten-Vesterålen islands and on Hamarøya is dominated by Proterozoic and Archaean, polymetamorphic, migmatitic gneisses and intrusions of mangeritic to charnockitic composition (Heier & Compston 1969). The Caledonian effect on the region was previously assumed to be limited (Griffin *et al.* 1978). Later work by Steltenpohl *et al.* (2004, 2009, 2011), however, has shown that the Precambrian rocks of the Lofoten-Vesterålen archipelago as well as the adjacent mainland have been affected both by the Caledonian collision in Silurian time and by a subsequent gravity collapse. Sellevoll &

Thanvarachorn (1977) and Olesen *et al.* (2010) compiled rock density maps for the Lofoten-Vesterålen area showing noticeable high basement densities for the Lofotens and Langøya of up to 2870 kg/cm³. This is also well expressed in the gravity map (Olesen *et al.* 2010) and point to an originally deep-seated or deeply buried crustal block, subsequently exhumed relatively quickly to a shallow depth. Aeromagnetic data (Åm 1975) show a similar boundary caused by high-magnetic migmatites and intrusions of granulite facies on Lofoten, Langøya and western Hamarøya and amphibolitic-facies rocks in the Vesterålen region, mainly derived by retrograde metamorphism (Griffin *et al.* 1978). Neither the structures nor the major element chemistry of the migmatites on either side of the isograd show any obvious differences (Heier & Thoresen 1971), and the observed granulite-facies assemblage was most probably superimposed on already migmatized rocks (Olesen *et al.* 1991).

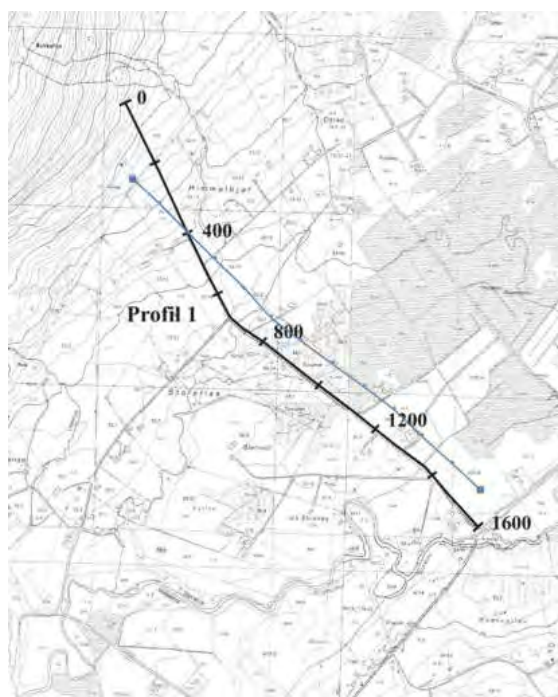
The landscape of the Lofoten-Vesterålen islands results from a complex tectonic history, characterised mainly by normal faulting, extension and blockwise vertical movements (Griffin *et al.* 1978, Peulvast 1986) which were especially active during Mesozoic and Cainozoic times (Hendriks *et al.* 2010, Bergh *et al.* 2007, Løseth & Tveten 1996). Rotated and tilted, fault-bounded blocks form a diversified landscape which shows both an alpine-type morphology with steep cliffs and mountains rising up from sea level to more than 1200 m above sea level (western Hinnøya and Moskenesøya), and Paleic surfaces of a smooth hilly landscape (Langøya), wide valleys (Vestvågøya) and large strandflats at sea level. Peulvast (1986) described the main morphostructural features as 'NE-SW oriented mountains or plateau ridges arranged *en echelon* between longitudinal fjords, sounds and basins, which are cross-cut by oblique or perpendicular features, splitting the islands into smaller blocks'.

6.3 Vestvågøya

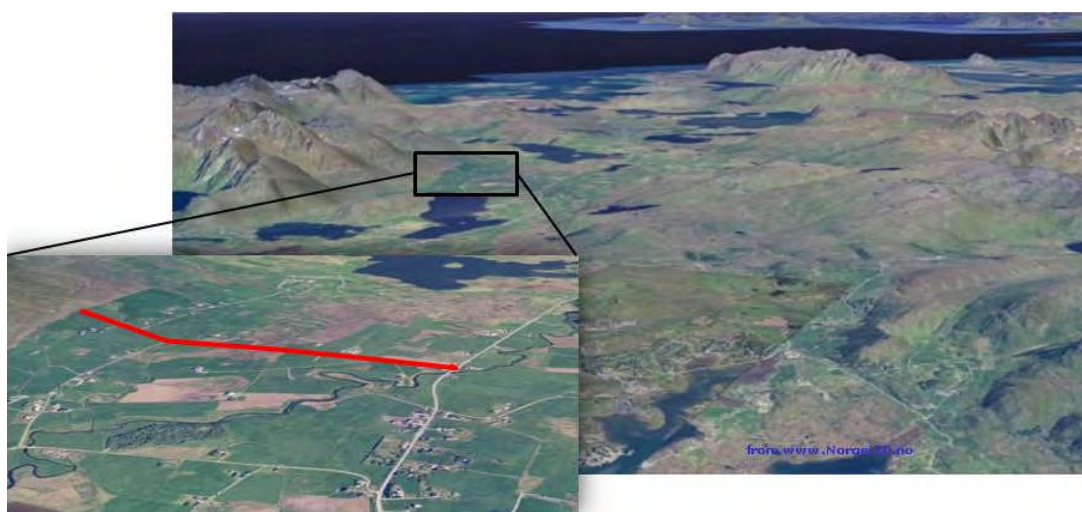
A probably rather wide area of weathered basement was already discovered and mapped on Vestvågøya by NGU in the 1980s. The site is located at Rise, an agrarian area situated in a rather wide and flat NE-SW-striking valley (Fig. 6.2b). During the project only small outcrops with weathered material were found, but photos and reports from NGU staff (Fig. 6.3, P-R. Neeb, pers. comm. 2010) witnessed a significant amount of saprolite in this area, close to the surface and covered by only a thin layer of soil. Resistivity and seismic profiling were carried out and indicate a thickness of weathered and fractured basement of more than 100 m. The primary bedrock type is mangerite. The observed weathered basement shows both physical and chemical weathering and is of a clay-poor sandy to gritty nature. The colours are brown to black with a metallic glint. The saprolite is very similar to the ones observed on Hadseløya and Hamarøya. The locality between Saup and Tangstad was sampled and the porosity and permeability of the sample were measured at NPD to 24.3 % and c. 300 mD (Table 6.1), respectively (at 20 bar NCP/20°C).

Table 6.1 Analysis of permeability and porosity (at 20 bar NCP/20°C) of a sample from a locality between Saup and Tangstad at Vestvågøya. The measurements are carried out at Weatherfords laboratory in Stavanger.

Sample id.	Length	Diameter	Klinkenberg corr. gas permeability	Pore volume	Grain volume	Grain density	Porosity
	(cm)	(cm)	20 bar NCP/20°C	20 bar NCP/20°C	atm/20°C	atm/20°C	20 bar NCP/20°C
	(cm)	(cm)	(mD)	(ml)	(ml)	(g/ml)	(g/ml)
Saup-2	2,20	3,60	291	4,71	14,71	2,67	0,243



a



b

Figure 6.2 a) Overview map with the position of the resistivity and seismic profile (blue). Blue dots show the seismic shotpoints; b) an aerial photo of Rise and surroundings seen from the southwest shows the position of the profiles across a valley plain (produced with www.norgei3d.no).

6.3.1 Resistivity profiling

Interpretation of resistivity profiles is hampered by certain ambiguities and the resistivity values for igneous rocks from the literature show a large range of 100 – 1,000,000 ohm·m (Palacky 1987). Intensive studies in Norway have revealed values between 1,000 and 10,000 ohm·m for metamorphic and igneous rocks (Fig. 6.4, Elvebakk 2011). A c. 800 m deep borehole at Skulbruheia, Leknes, close to the study area, is located in a lithology similar to the one at Rise (monzonitic gneisses, originally derived from mangerites) and shows resistivity values as high as 3000-7000 ohm·m (Elvebakk 2011). The lithology of the Kontiki borehole at Leknes consists of granodioritic orthogneisses in the uppermost c. 50 m and monzonitic gneisses from 60 m to 250 m. The P-wave velocity within the upper 240 m increases slightly from c. 5000 m/s to 5800 m/s (Fig. 6.4). The resistivity decreases abruptly to c. 3000 ohm·m at c. 60 m depth, which correlates fairly well with the change in lithology. The observed bedrock in the borehole shows significant fracturing.



Figure 6.3 A photograph (Peer-Richard Neeb, pers. comm.) from the 1980s shows a local quarry at Rise with a clay-poor saprolite with a minimum thickness of c. 6 m. Translation: Jord – soil;; mangeritt – mangerite, forvittr. – weathered.

The observed resistivity values along the profile are much lower (Fig. 6.5), which might indicate that the top of unweathered bedrock was not reached by the resistivity measurements. From the resistivity measurements a southeastward dipping resistivity contrast could be observed along the profile until approximately at position 1100 m. It was interpreted as a near-top-bedrock horizon (dotted line in Fig. 6.5), since the observed resistivity values below are too low to represent unweathered bedrock (<3000 ohm·m). In the vicinity of the northwestern termination of the profile, an outcrop of weathered and fractured basement was observed, which correlates with the higher resistivity values at the surface (pos. 80-140 m) and can thus confirm the weathered characteristics of the underlying rock. The horizon is truncated by three deep-seated zones with low resistivity, most likely associated with fracture zones. The resistivity data show large lateral variations, which indicate a very thick layer of regolith with corestone, interspersed saprolite, saprorock and weathered and fractured basement. The rather low resistivity values along the entire profile also point to a water-saturated system of noticeable porosity and permeability.

Leknes

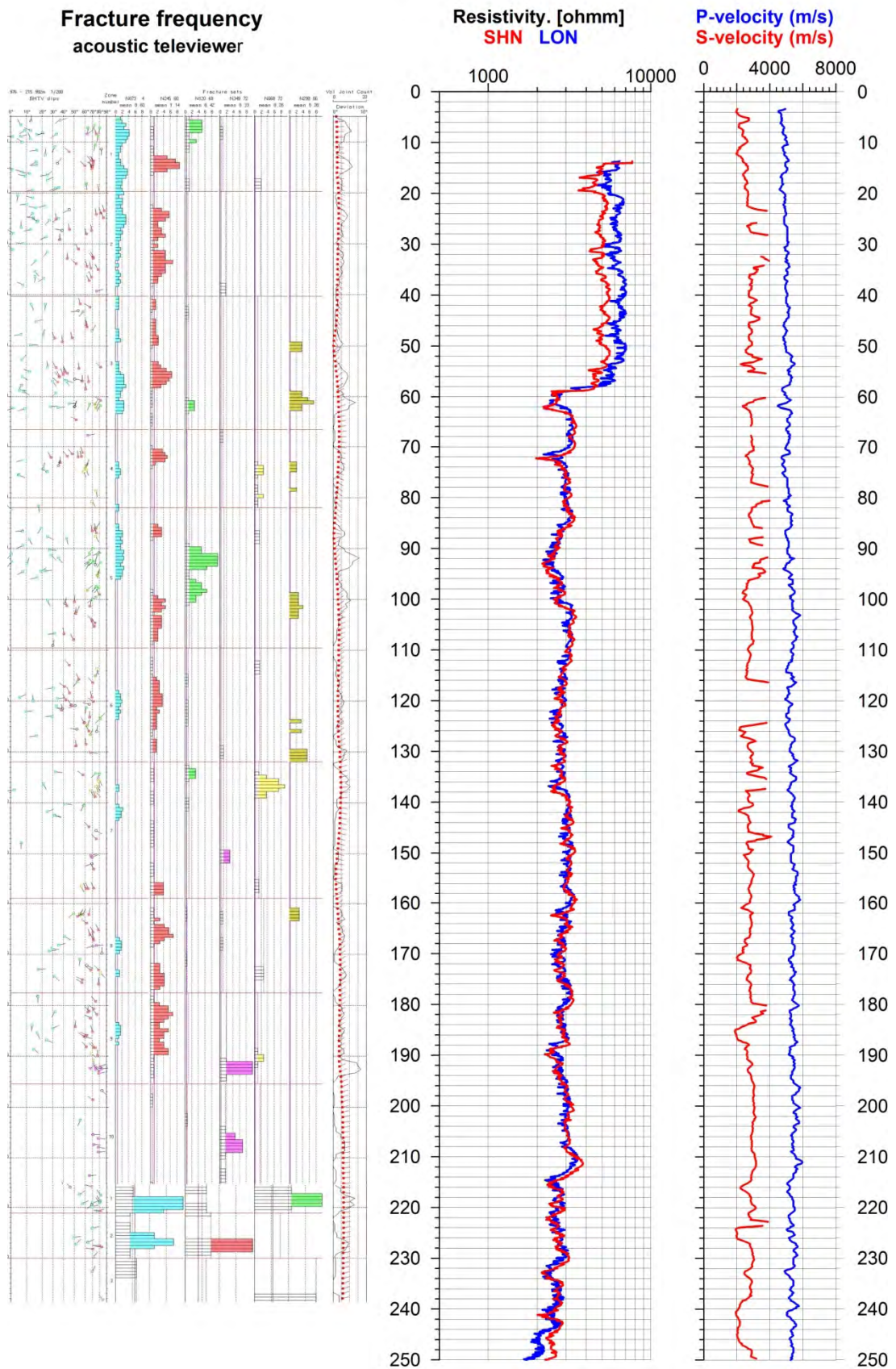


Figure 6.4 Resistivity and P-wave velocity logs (0-240 m) from a borehole at Skulbruheia close to Leknes, together with a fracture frequency diagram (Elvebakk 2011).

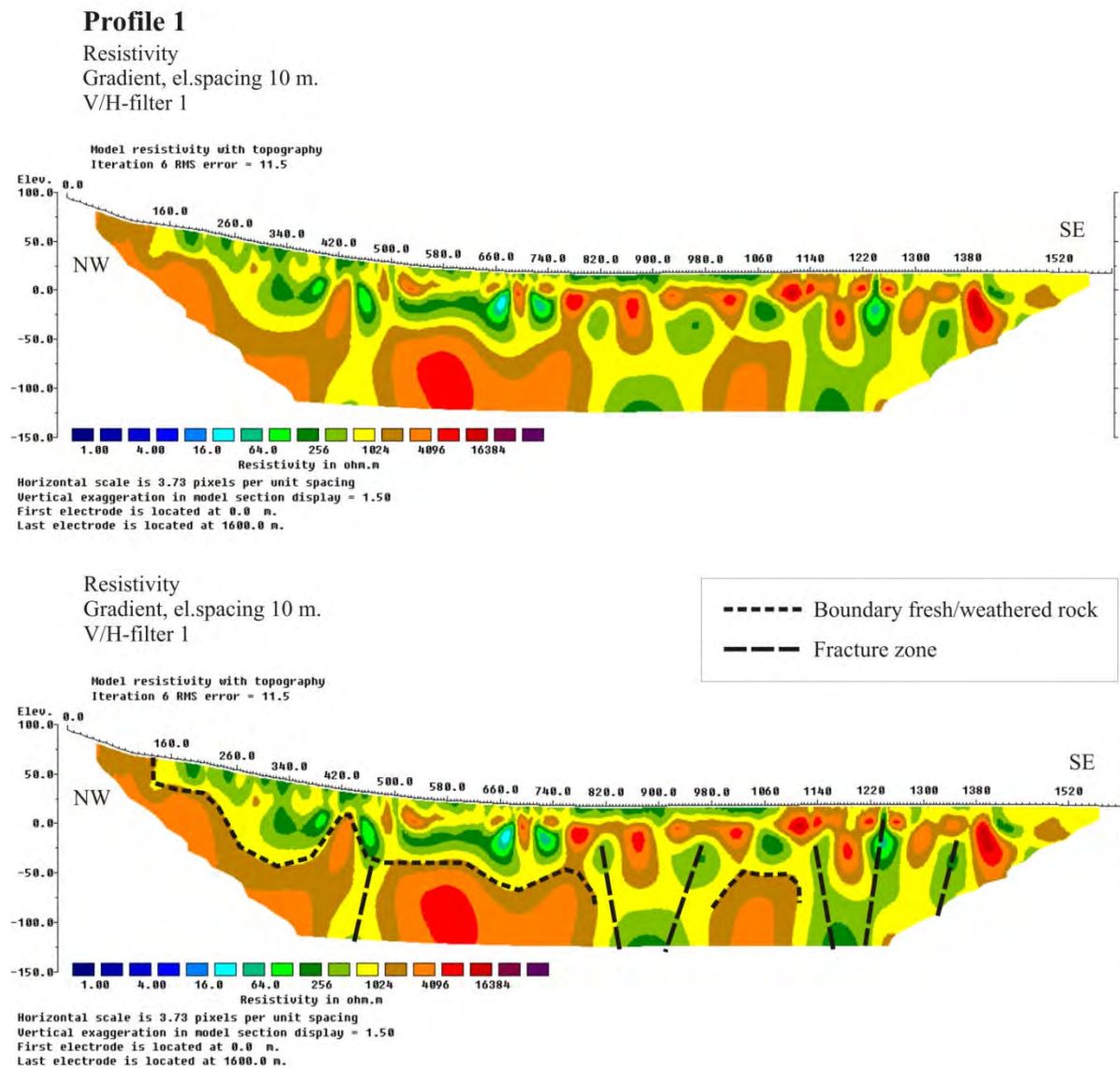


Figure 6.3 Resistivity profile from Rise, Vestvågøya. A horizontal resistivity boundary was interpreted as the near-top-bedrock horizon, which is truncated by several fracture zones of low resistivity. The saprolite layer is thickening towards the southeast.

6.3.2 Seismic profiling

The location of the seismic profile is shown in Fig. 6.2a (blue line). The geophysical interpretation of the refraction seismic profile S1 is shown in Fig. 6.6. Three velocity layers are detected along the profile, but the middle layer is indicated only at some of the shot points as it is too thin to be registered everywhere (blind zone). It is anticipated that the middle layer is continuous through the whole profile. The seismic velocity in this layer has at some places been determined to be 1900- 2000 m/s, but in another place it was registered as c. 1600 m/s. Both velocities can be related to water-saturated sediments where the higher values can be in till material and the lower values in better sorted material such as sand/gravel or clay, but there is also a great possibility that the velocities can represent strongly weathered or fractured/crushed bedrock. The seismic velocities in the surface layer seem to be highly

variable and have values from 300 to 900 m/s. The velocities indicate dry or only partly water-saturated sediments and the highest values (up to 900 m/s) can represent till material. The lower values (down to 300 m/s) may represent sand/gravel or possibly bog and peat material. The velocities for the upper and middle layer can only be determined in the vicinity of the shot points.

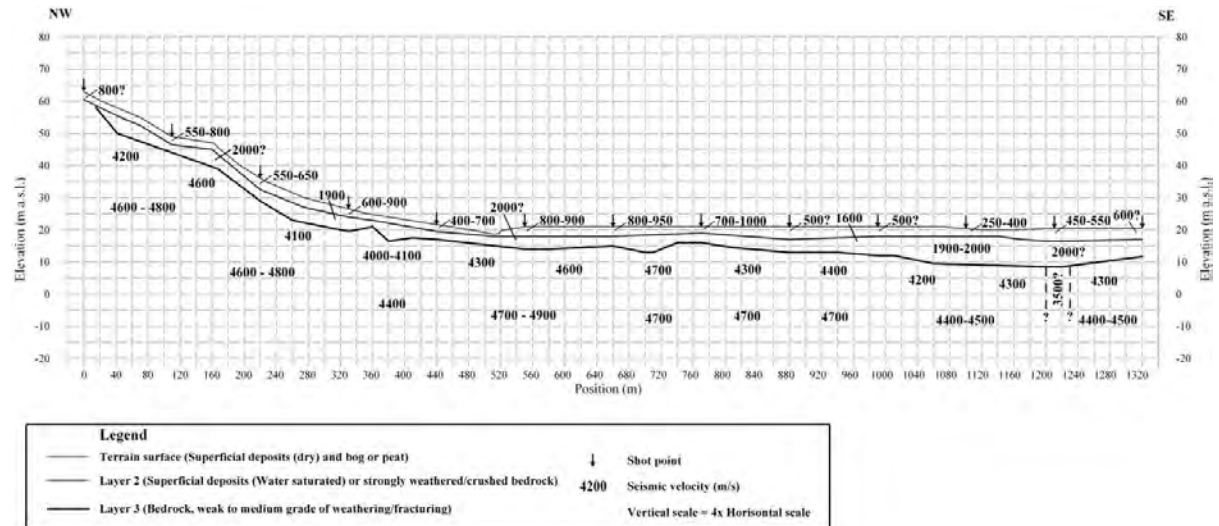


Figure 6.2 Refraction seismic profile from Rise, Vestvågøya.

The seismic velocity of the bottom layer is also highly variable and is determined to have values from 4000 to 4900 m/s. These values most likely represent bedrock, but the variations indicate a highly variable degree of weathering and/or fracturing.

The thickness of the surface layer is estimated to vary from 2 to 4 m. The thickness of the surface layer and the middle layer together seems to vary from 2-3 m up to a maximum of 11-12 m, and the thickness is greatest in the southeastern part of the profile (position 1040-1260 m). Uncertainties in the velocities of the two layers, the great velocity contrast between the layers and the relatively small thicknesses produce quite large uncertainties when determining the depth to layer 3. It is estimated that the uncertainty in the determined depth from the surface down to bedrock with a seismic velocity of 4000 m/s and higher at some places can be 2-3 m.

In addition to the great lateral variation in the seismic velocity of the bedrock along the profile there are also some vertical variations, and the velocity is generally increasing with depth. The velocities in the bedrock are determined from forward and reverse shootings along the profile. The velocity values indicated close to the top of the bedrock surface are determined from shots with a spacing of 110 m and at some places 220 m. The velocity values produced from deeper in the bedrock are determined from shots with a distance of 330 m and greater (up to 770 m). It is considered that with greater shot-receiver distance the acoustic waves penetrate deeper into the high-velocity bedrock than with a small spacing where the seismic waves will mostly follow the bedrock surface. From the relatively simple

measuring system and interpretation procedure applied in the present study it has only been possible to confirm the increasing velocity with depth qualitatively. Depth detection to massive bedrock with a seismic velocity higher than 5000 m/s has not been possible.

With short shot distance, the highest seismic velocity along the bedrock surface (4600-4700 m/s) is indicated in an area to the northwest along the profile (position 110-220 m) and in a central area (pos. 550-770 m), and it is anticipated that the top bedrock has a low degree of weathering/fracturing at these two locations. The lowest seismic velocities (4000-4100 m/s) occur in the area between 220 m and 440 m and there it is expected that the top of the bedrock has a high degree of weathering/fracturing. The velocity in the northwesternmost area (pos. 0-110 m) is estimated to 4200 m/s, whilst it varies between 4200 and 4400 m/s southeastwards along the profile (from pos. 770 m). There are indications of a local low-velocity zone to the southeast (position 1200-1230 m) with an uncertain velocity value of 3500 m/s.

With long shot distance the highest seismic velocity (4600-4800 m/s) is determined along the northwestern part of the profile (pos. 0-300 m) and in the central part (pos. 440-990 m). Weathering/fracturing for the deeper bedrock appears to be limited. At position 330-440 m the seismic velocity is as low as 4400 m/s and there it is anticipated that extensive weathering/fracturing is extending to a much greater depth. The same is assumed southeastward from pos. 990 m along the profile where the seismic velocity is determined to 4400-4500 m/s. The low-velocity zone indicated at position 1200-1230 m with a short shot-spacing has no significant influence when using long shot spacing and it is assumed that the zone has relatively limited depth extent.

6.3.3 Comparison of seismic and resistivity profiling and conclusions

Refraction seismic data and resistivity measurements definitely have different resolution and the uncertainty of the geoelectric measurements is much greater with depth than for the refraction seismic data. Although the locations of the two profiles are not identical (Fig. 6.2a), they are positioned close enough to allow a joint interpretation.

In contradiction to the resistivity profile the seismic data clearly identify two layers of rather low velocities (< 1000 m/s and ~2000 m/s) and a seismic boundary with higher velocities underneath (Fig. 6.7).

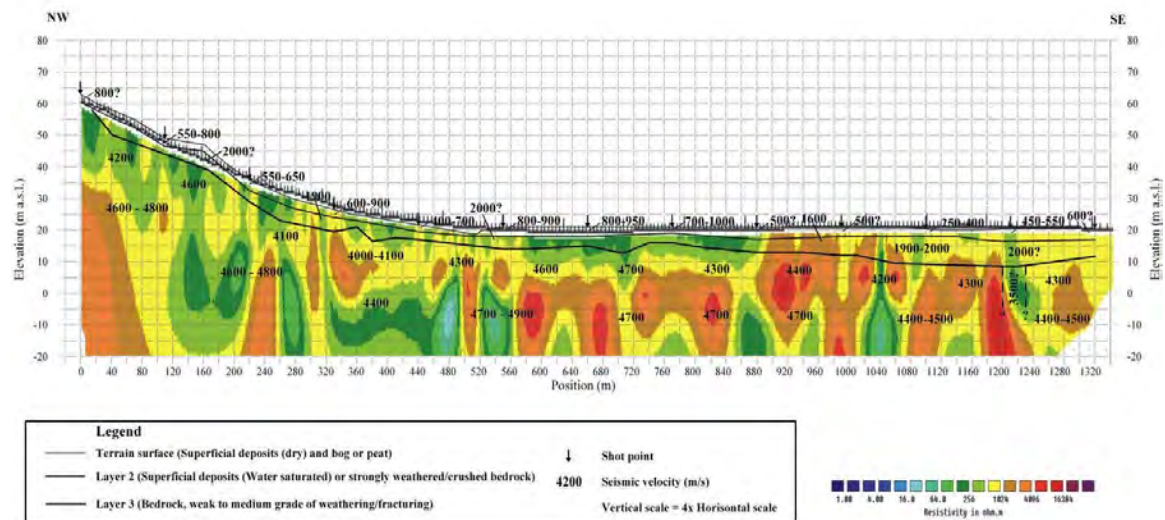


Figure 6.3 Resistivity data clipped to the seismic profile depth extension with superimposed seismic interpretations and observed velocities.

The uppermost layer probably corresponds to soil and intermediate, barely compacted material of soil and saprolite, whilst the second layer mostly represents a more compacted, sandy to gritty saprolite, maybe with varying compaction and porosity, which could explain relatively small changes in resistivity. Below this layer, seismic velocities jump up to about 4000 m/s and more, corresponding to fractured and weathered basement rocks. The heterogeneous fracturing of this layer is well expressed in the resistivity data by significant and irregular changes in resistivity. The apparent contradictive distribution of resistivity and seismic velocities can be explained by the different nature of the two methods. In simple terms, the seismic refracted waves tend to take the shortest/fastest route whereas the electric current prefers the layer with the lowest resistivity. Apparent resistivity values and variations must therefore be evaluated qualitatively rather than quantitatively.

In the Rise area, our interpretations show an up to 11-12 m-thick layer with rather unconsolidated material that most likely represents the same type of weathered rock as reported in the 80s (Fig. 6.4). The saprolite may consist of deeply weathered mangerite that is thickening towards southeast. The weathered zone is most likely interspersed with corestones and covered by only a thin layer of soil (~ 1m) on top. The thickness of the regolith along the profile ranges from 0 m in the northwest to more than 150 m at its southeastern end. Very low resistivity noted locally along the profile indicates that the thickness of saprolite probably varies significantly and has a greater thickness within the three, larger, inferred fracture zones.

6.4 Hadseløya

On Hadseløya, a quarry with deeply weathered basement rocks of c. 14 m thickness was investigated. The locality is situated south of Stokmarknes (Fig. 6.8a) on the flank of a wide valley and is covered by only a thin layer of soil (< 1m). The parent rock type that can be observed on-site in some corestones is mangerite. The crystalline fabric of the primary basement rocks is very well preserved and a quartz vein was observed within the saprolite, which indicates the in-situ character of the weathered material. The site shows a rather homogeneous, clay-poor, granular material with only a few corestones (Fig. 6.8b).

Samples were taken for geochemical analysis. The mass balance has been calculated for both weathered and fresh mangerite on Hadseløya (Table 6.2). The Zr content has been used as a reference immobile element in the calculations (Brimhall *et al.* 1985) and an extraordinary high mass loss of c. 64 % was observed.

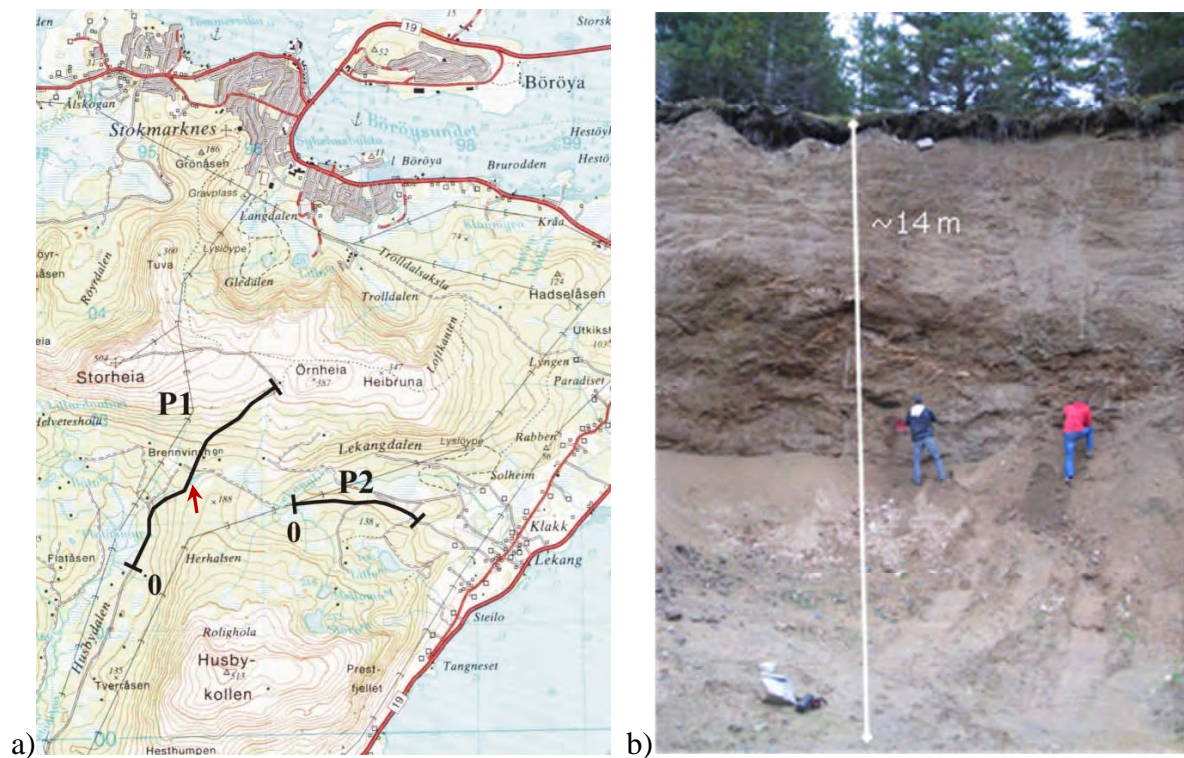


Figure 6.4 a) Map showing the location of the quarry on Hadseløya (red arrow) and resistivity profiles at Hadseløya. b) Picture showing a c. 14 m-thick layer of saprolite in the quarry. A quartz vein and the preserved fabric of the original rock confirm the in situ state of the material.

Table 6.2 Brimhall mass balance calculations for weathered and fresh mangerite at Brennvinsaugen on Hadseløya. The loss of mass through chemical weathering is estimated to 64 %. The Zr content has been used as a reference immobile element in the calculations (Brimhall *et al.* 1985).

	SiO ₂	Al ₂ O ₃	Fe ₂ O ₃	TiO ₂	MgO	CaO	Na ₂ O	K ₂ O	MnO	P ₂ O ₅	Gl.tap
58959	60,3	13,4	8,03	0,596	1,18	1,47	3,35	4,20	0,166	0,224	4,95
58990	69,0	14,3	4,45	0,397	0,505	1,01	4,10	5,53	0,073	0,058	0,202

$$\text{Transp } \tau = \left[\frac{C_{j,w} / C_{i,w}}{C_{j,p} / C_{i,p}} \right] - 1$$

REFERENCE MATERIAL

	Zr
58959	819
58990	310

Transport τ

	SiO ₂	Al ₂ O ₃	Fe ₂ O ₃	TiO ₂	MgO	CaO	Na ₂ O	K ₂ O	MnO	P ₂ O ₅	Gl.tap
58959	-0,67	-0,65	-0,32	-0,43	-0,12	-0,45	-0,69	-0,71	-0,14	0,46	8,28
58990	0,00	0,00	0,00	0,00	0,00	0,00	0,00	0,00	0,00	0,00	0,00

Leached in 100g of rock													
	SiO ₂	Al ₂ O ₃	Fe ₂ O ₃	TiO ₂	MgO	CaO	Na ₂ O	K ₂ O	MnO			Si+Al+Na+	SUM
58959	-46,2	-9,2	-1,4	-0,2	-0,1	-0,5	-2,8	-3,9	0,0			-62,2	-64,3
58990	0	0	0	0	0	0	0	0	0				

6.4.1.1 Resistivity profiling

From resistivity measurements, the zone with fractured and weathered bedrock seems locally to be more than 100 m thick (Figs. 6.9 & 6.10). Two resistivity profiles were measured along existing roads (Fig. 6.8a). P1 is oriented NE-SW along the road, which runs parallel to the quarry. The resistivity data show a c. 50 m-thick layer of mostly low resistivity, which is thinning towards the northeast. The layer is underlain by blocks of high resistivity with a rather irregular surface truncated by at least five steep zones with low resistivity. The quarry is situated at c. 450 m and coincides with one of these vertical low-resistivity zones.

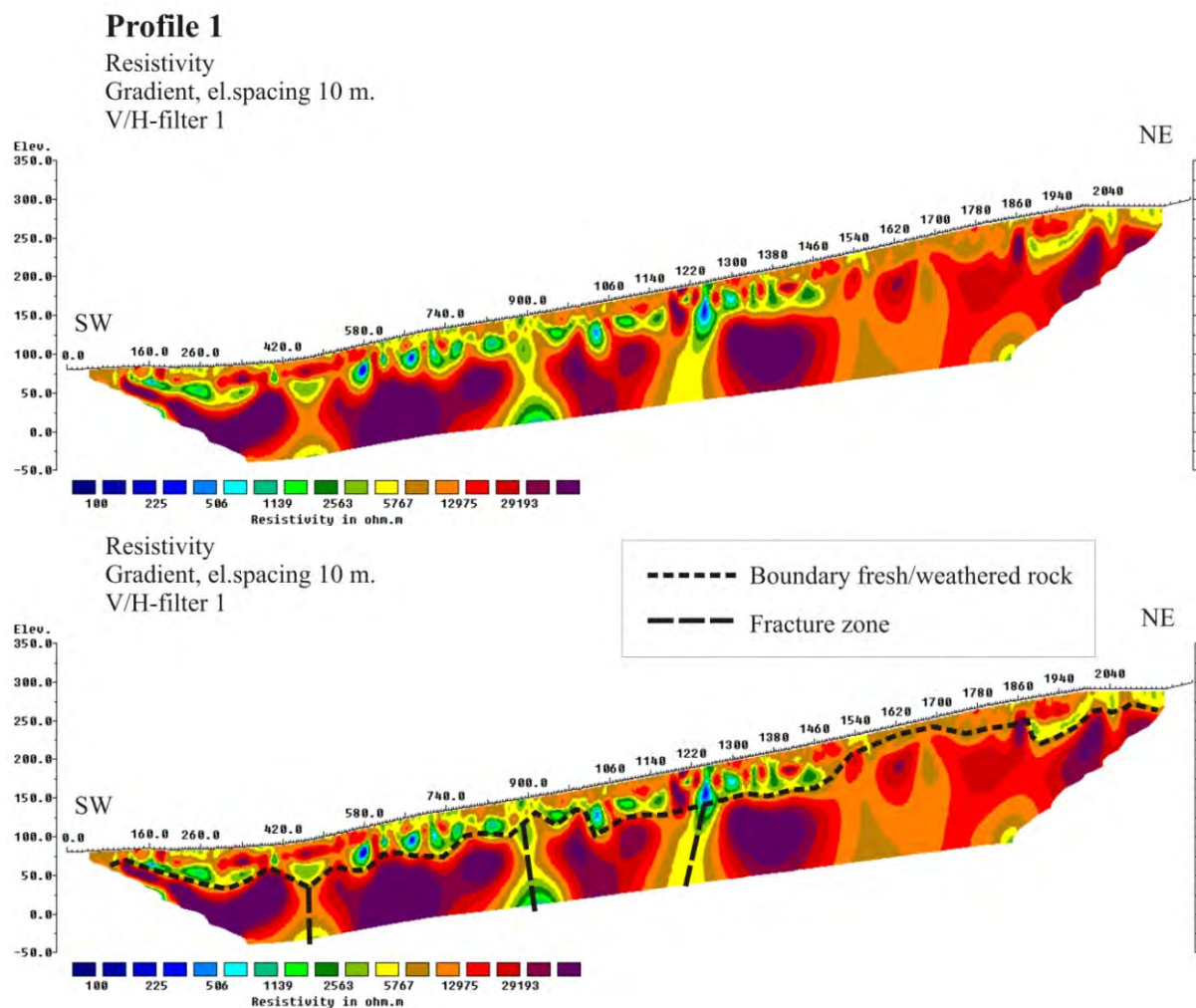


Figure 6.5 Resistivity profile P1 on Hadseløya shows a c. 50 m-thick layer of low resistivity underlain by high resistivity unweathered basement with a rather irregular surface and truncated by at least three, steep, fracture zones with low resistivity.

Profile P2 is oriented c. E-W and shows mostly high resistivity values with lateral variations of steep to vertically oriented zones with lower resistivity. In the centre of the profile (520 – 660 m) a larger low-resistivity zone on top of a system of almost vertical and very deep zones with low resistivity.

Profile 2

Resistivity
Gradient, el.spacing 10 m.
V/H-filter 1

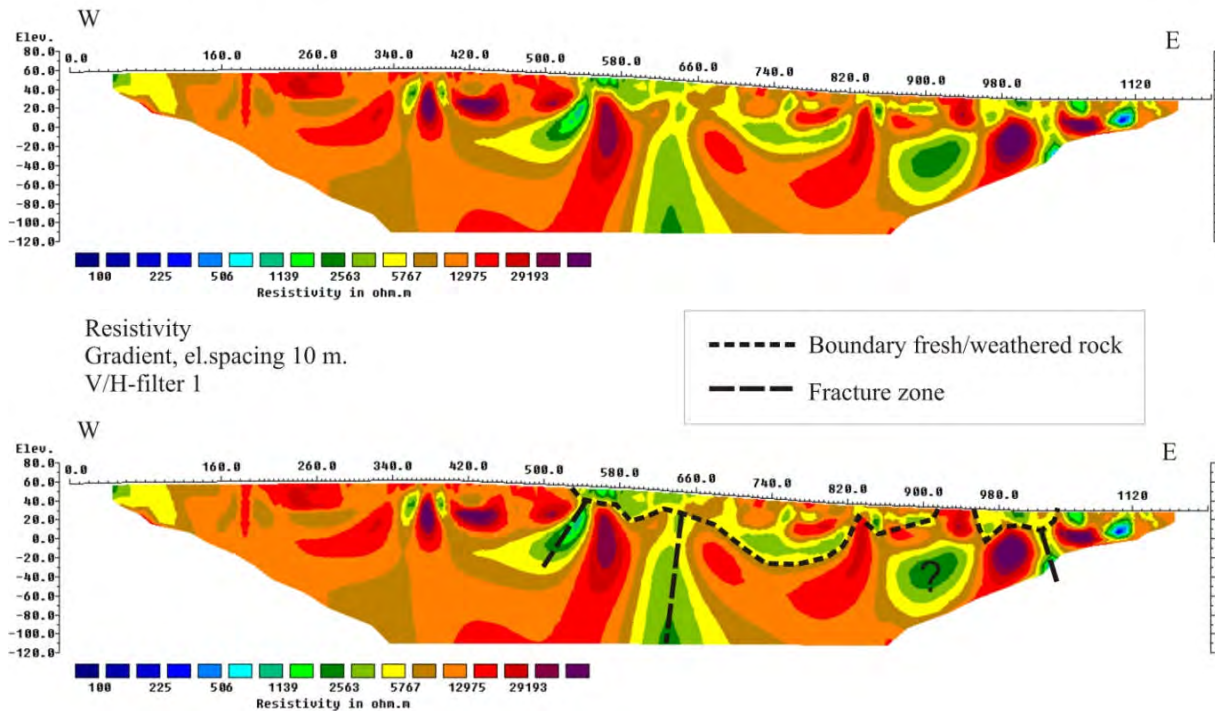


Figure 6.6 Resistivity profile P2 shows mostly high-resistivity values with lateral variations into step or vertically oriented low-resistivity zones. This is likely due to fractured and/or slightly weathered basement with a larger low-resistivity zone in the central part on top of a system of almost vertical low-resistivity zones.

The high-resistivity values most likely represent bedrock that is unaltered or little affected by weathering. The irregular surface of the high-resistivity bodies along Profile P1 (Fig. 6.9) probably reflects the transition of saprolite/saprorock to barely fractured and unweathered basement. The zones of low resistivity in between represent larger fractures and weakness zones probably filled with deeply weathered rock. The lateral variations within rather high resistivity along P2, however, remain unclear. Except for some features where the resistivity contrast is large and obviously related to fracturing and advanced weathering, the variations could simply be caused by variations in fluid saturation, but – and this seems to be more likely regarding the observed large amount of saprolite – it could also indicate fractured bedrock.

6.4.2 Palaeomagnetic sampling

As described in Section 2.4, we collected samples on Hadseløya for age dating of the deep-weathered material, exploiting the palaeomagnetic characteristics and differences of collected weathered and unweathered samples.

On Hadseløya, samples were taken from two sites and measured and evaluated regarding the remanent magnetisation.

Site A (Hadseløya)

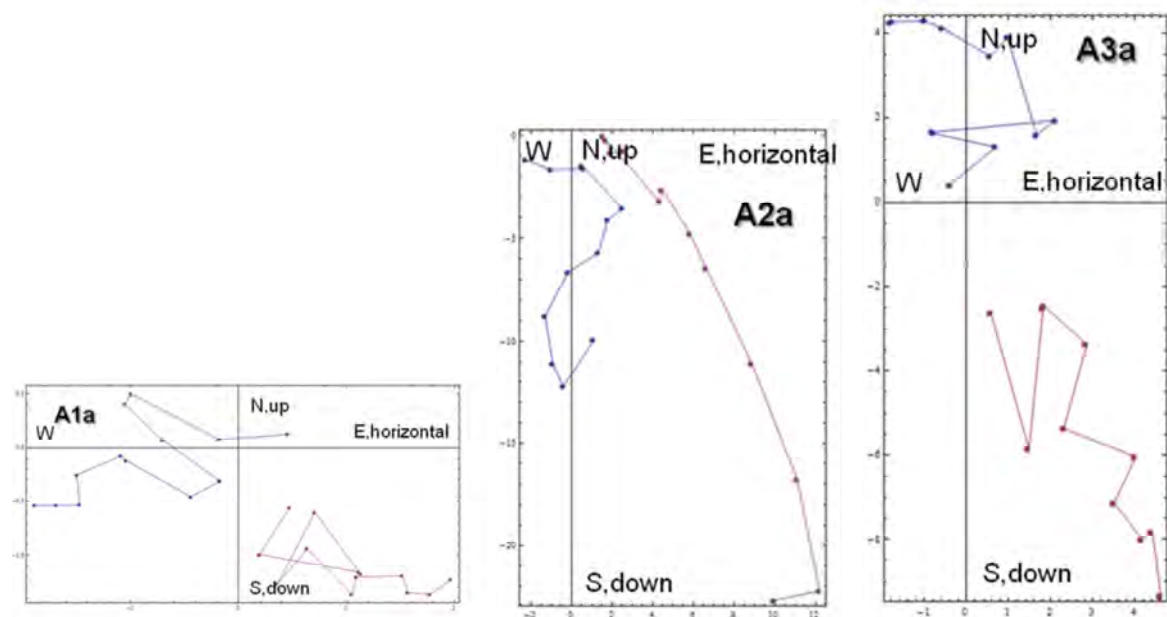


Figure 6.7 Zijderveld diagrams of AF demagnetisation results on three weathered rock specimens from site A at Hadseløya. Red: inclination plots of up-component versus horizontal component. Blue: declination plots of E-W component versus N-S component of the horizontal projection of the magnetisation.

At site A only three samples from unconsolidated weathered rock could be recovered. As shown in Fig. 6.11, none of them shows a demagnetisation pattern that clearly goes to the origin and defines a reliable direction. Moreover, crude estimates of the characteristic remanence (ChRM) of specimen A1a and specimens A2a and A3a result in different palaeomagnetic directions. Whilst A1a yields a shallow ChRM with SE orientation, A2a and A3a both have steep magnetisation directions, with reverse (A2a) and normal (A3a) field orientations. If interpreted as representing true palaeomagnetic directions, this could mean that A1a represents an older component, which either is a primary remanence or due to an early alteration event, whilst A2a and A3a are due to recent alteration in an inverse field (at least 780 ka old) and a normal field that could be younger.

Site B (Hadseløya)

At site B it was possible to recover six drillcores from solid rock bodies and two weathered rock samples. The sampling positions are shown in Fig. 6.12.



Figure 6.8 Relative position of solid bedrock samples and weathered rock samples at site B in Hadseløya.

Solid rock samples

The three specimens B4b, B5a, and B6b come from three drillcores at the same solid rock face.

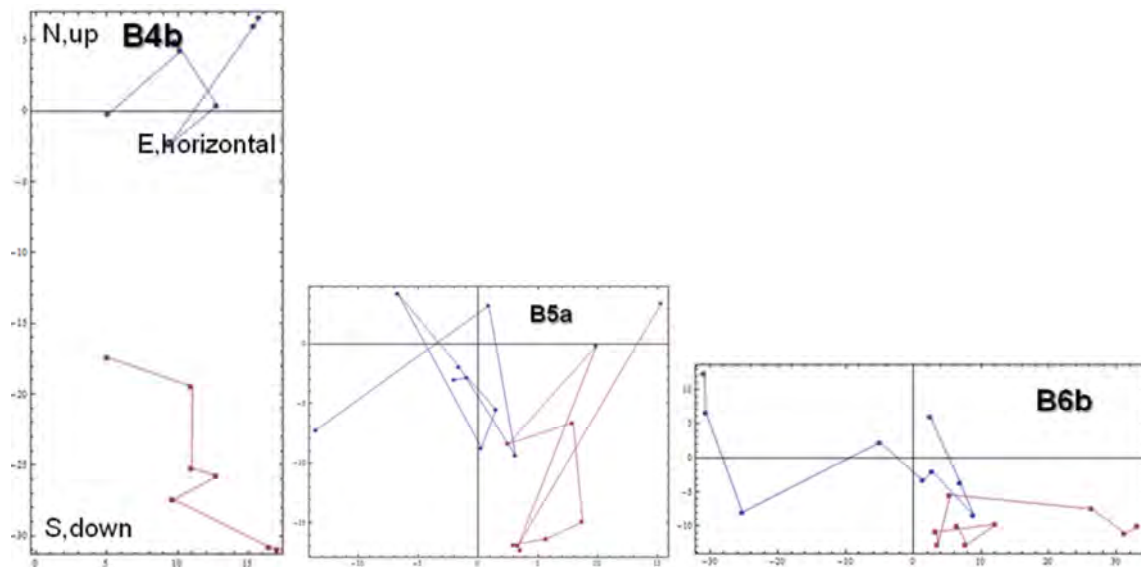


Figure 6.9 Zijderveld diagrams of AF demagnetisation results on three solid rock specimens from holes 4, 5, and 6 at site B on Hadseløya. Red: inclination plots of up-component versus horizontal component. Blue: declination plots of E-W component versus N-S component of the horizontal projection of the magnetisation.

As seen in Fig. 6.13, again the demagnetisation behaviour of these samples is very unstable, and no clear consistent direction can be derived. If at all, specimens B5a and B6b indicate a shallow direction rather remote from today's steep inclination.

The specimens B7b, B8b, and B9b come from three drillcores from different solid rock faces, but show a more consistent directional behaviour, which also roughly coincides with B5a and B6b, although the inclination seems to be somewhat steeper, yet not steep enough for the recent field (Fig. 6.14). All six solid rock specimens represent normal field directions with respect to a northern hemisphere location.

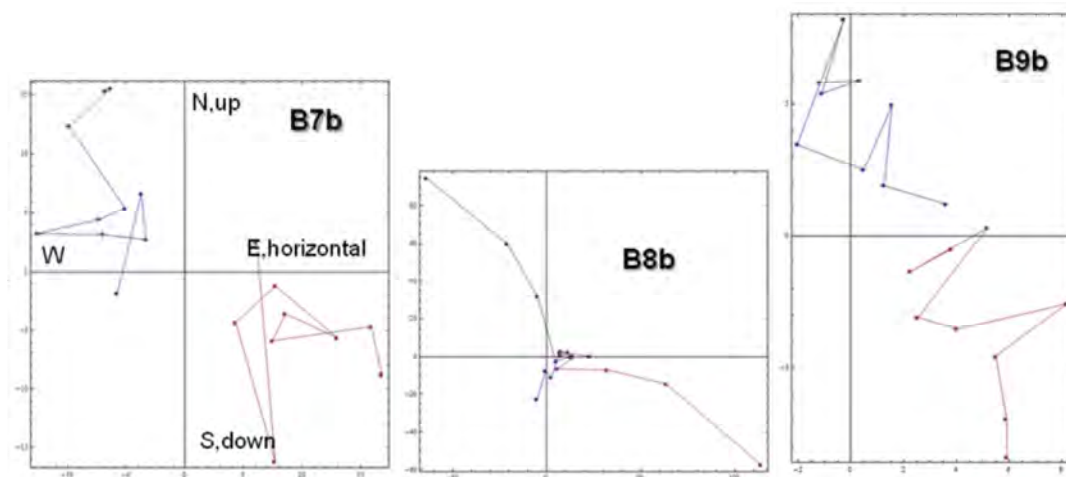


Figure 6.10 Zijderveld diagrams of AF demagnetisation results on three solid rock specimens from holes 7, 8, and 9 at site B at Hadseløya. Red: inclination plots of up-component versus horizontal component. Blue: declination plots of E-W component versus N-S component of the horizontal projection of the magnetisation.

Weathered rock samples

The magnetic directions at the two weathered rock samples from unconsolidated rocks are shown in Fig. 6.15. Both coincide closely with the magnetisations of the solid rock specimens.

B11a, resembling B6b, has a shallower inclination than B12a, which is closer to B8b. An overprint of a later magnetisation in the weathered rocks cannot be recognised by these results. This means either that no alteration occurred, or that alteration influenced the magnetic remanence of the solid and unconsolidated rocks in the same way.

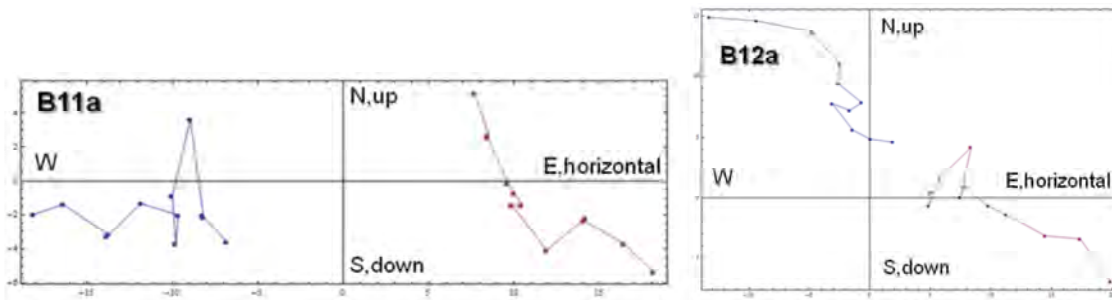


Figure 6.11 Zijdeveld diagrams of AF demagnetisation results on the two weathered rock specimens from casts 11 and 12 at site B at Hadseløya. Red: inclination plots of up-component versus horizontal component. Blue: declination plots of E-W component versus N-S component of the horizontal projection of the magnetisation.

6.5 Sortland

For the Sortland area and the island of Langøya, no deep weathering site could be found which was comparable in size to the ones observed on Vestvågøya, Andøya and Hamarøya. Nevertheless, deep weathering has also been reported from Langøya (Peulvast 1985, Paasche *et al.* 2006), but the sites with exposed deep weathering were rather small and mainly situated at higher elevation on top or along steep flanks of the mountains, where erosion is greater and such unconsolidated remnants of saprolites are less protected. However, most of Langøya was measured with high-resolution aeromagnetic data, acquired in 1988 (Mogaard *et al.* 1988), which we processed using the AMAGER technique (Chapter 2.3) to map possible weathering locations in valleys and topographic depressions on the island. A resistivity profile southwest of Sortland, which was measured to test whether there is an onshore extension of weathered basement from underneath the Mesozoic Sortlandsundet basin, which has been observed offshore (Davidsen *et al.* 2001), was used to correlate the AMAGER results. We carried out an excavation to check if deeply weathered bedrock coincides with a low-resistivity zone.

6.5.1 AMAGER results

The high-resolution aeromagnetic survey of Langøya was used together with a 50 m DEM grid to locate indications of fracturing and deep weathering in this area. The technique was applied as described in Chapter 2.3 and correlated with observed deep-weathering sites from publications by Peulvast (1985) and Paasche *et al.* (2006) (Fig. 6.16).

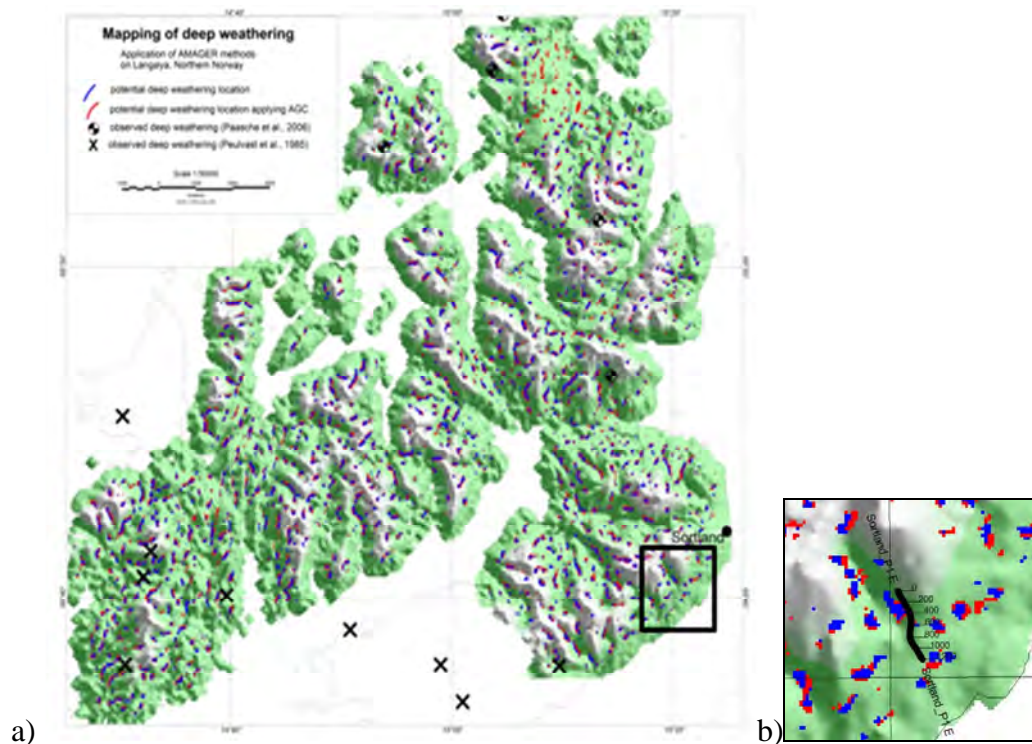


Figure 6.12 a) AMAGER results from Langøya and b) a zoomed in image to the position of the resistivity profile southwest of Sortland (shown by the black frame in Fig. a).

The result shows a fairly even distribution of possible weakness zones on Langøya. For an area in the northwestern part of Langøya, where the landscape is rather flat, the Automatic gain control (AGC) application reveals additional solutions (Fig. 6.16, in red). Correlation with the observed deep-weathering sites, however, is rather poor. We assume this is mostly because of the higher elevated positions of the sites at the tops and along flanks of the mountains, where the remnants of deep weathering are exposed to erosion, but also because the AMAGER technique is not well adapted to map deep weathering in such positions. However, correlations were found for sites located to the northwest, east and south.

6.5.2 Resistivity profiling

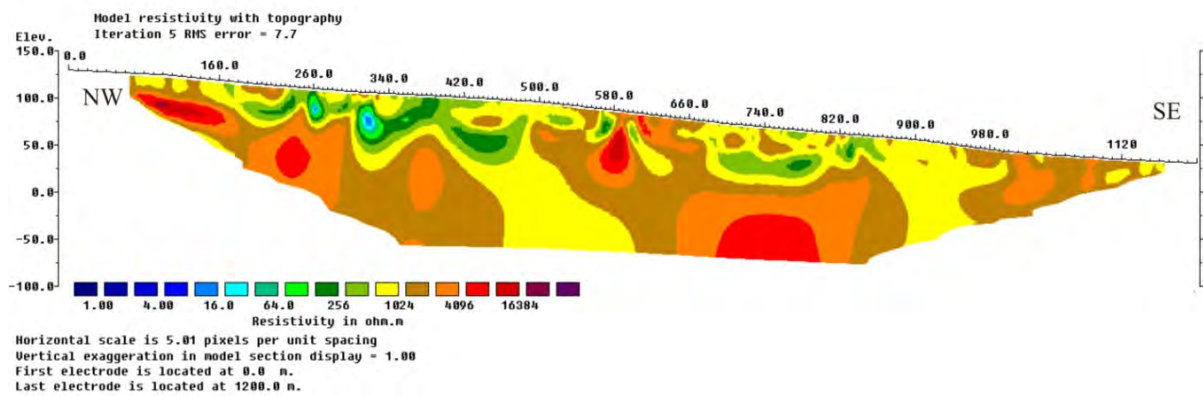
The resistivity profile (Fig. 6.17) confirms a layer of low resistivity and at least two major vertical zones of low resistivity. The two vertical low-resistivity zones, as well as the irregular top of the high-resistivity segments underneath, are compatible to what we have observed on the other profiles in the Lofoten-Vesterålen area, and suggest the existence of deep weathering and/or fractured basement.



b)

Profile 1

Resistivity
Gradient, el.spacing 10 m.
V/H-filter 1



Resistivity
Gradient, el.spacing 10 m.
V/H-filter 1

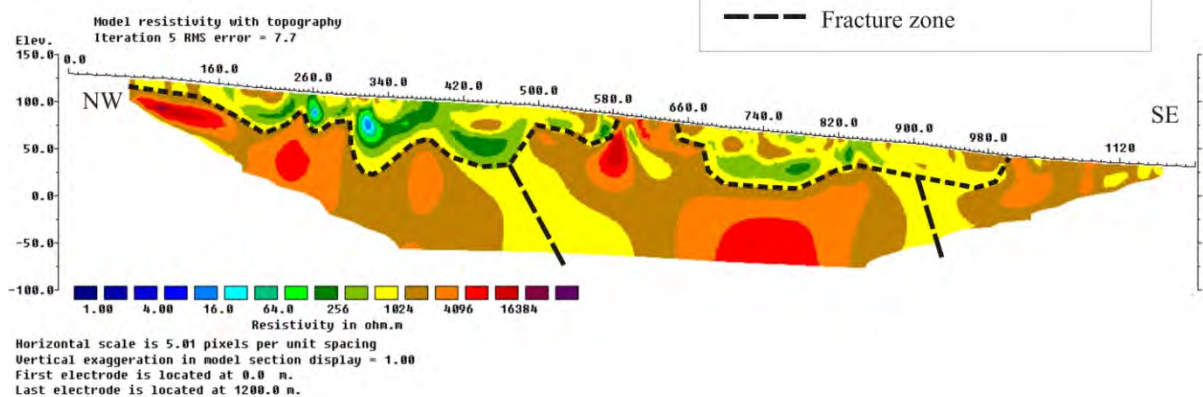


Figure 6.13 a) Location of the resistivity profile P1 to the southwest of Sortland. b) Result of the resistivity measurements. A low-resistivity layer is underlain by segments of high-resistivity bedrock. Two steep zones with low resistivity are observed and indicate major fracture zones.

Comparison of the resistivity profiling and the results of the AMAGER method shows a correlation for the area of the northwestern low-resistivity zone (pos. c. 200-600 m), whilst the second one to the south could not be identified. An explanation is likely due to the fine tuning of the AMAGER parameters, which is difficult to make for such a large area with varying susceptibility.



Figure 6.14 Excavation at Sortland. We observed fractured basement with minor signs of weathering.

An excavation of this site was carried out to a depth of c. 3 m and we found fractured and partly weathered basement under a thin layer of soil (Fig. 6.18).

6.6 Hamarøya

On Hamarøya, deep weathering was found in a quarry. The site is located in the southeast of the island and shows exposures along a rather broad area of a few hundred square metres. The largest exposure was c. 20 m high (Fig. 6.19b) and showed the same type of weathering observed on Hadseløya. The saprolite is of clay-poor, granular material highly mixed with corestones of various sizes. The primary bedrock, which could be observed from on-site corestones, is mangerite. The crystalline fabric of the original bedrock is well preserved, which again confirms the *in situ* state of the weathered material.

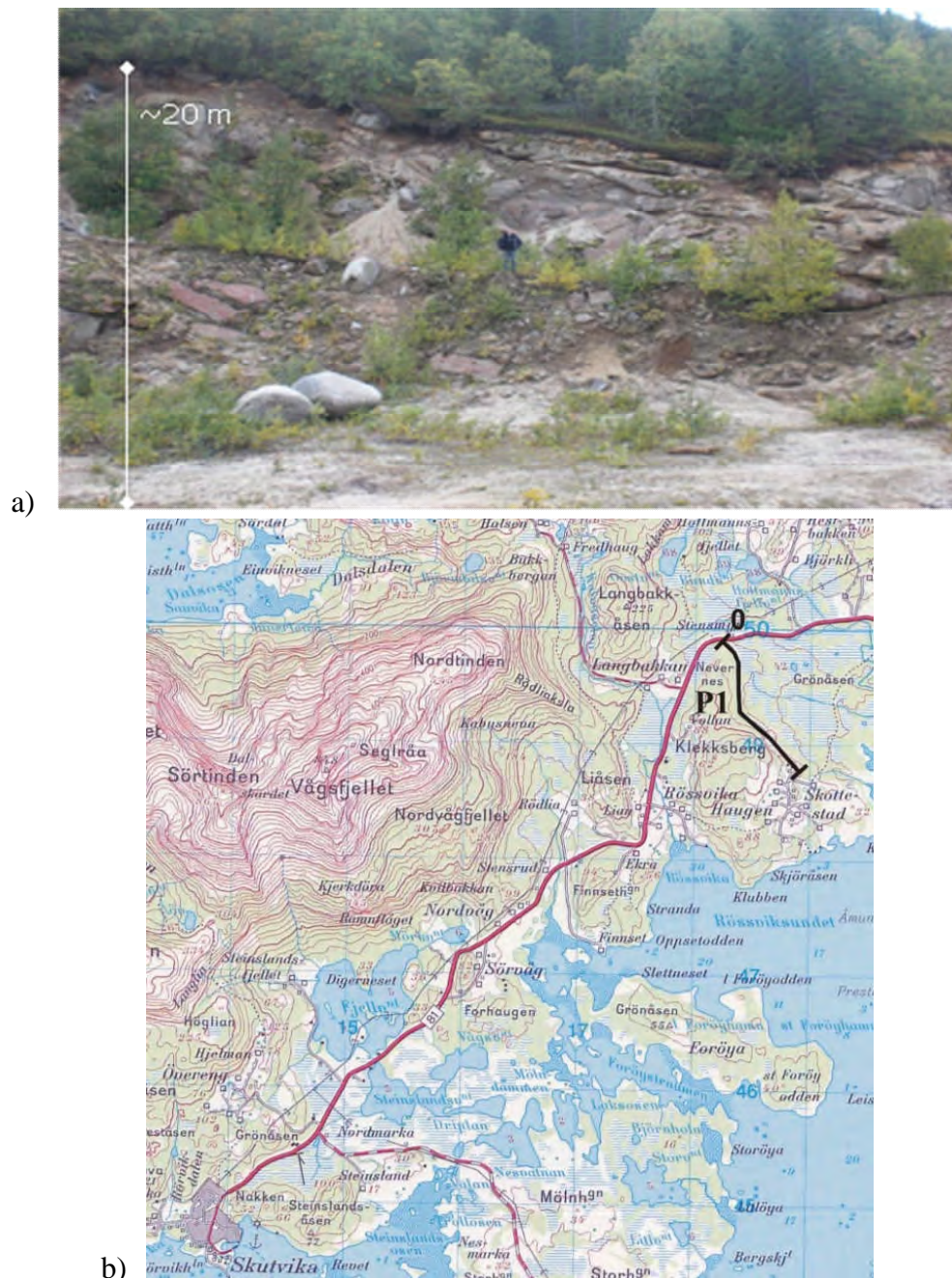


Figure 6.15 a) Picture of the c. 20 m-thick layer of saprolite in a quarry on Hamarøya. b) Map showing location of quarry and resistivity profiles. In contrast to Hadseløya the outcrop is dominated by an abundance of corestones in a matrix of highly weathered, clay-poor material.

A geochemical analysis from this site shows a mass loss between 40% and 62%, which is comparable to the Hadseløya locality.

6.6.1 Resistivity profiling

On Hamarøya, a single resistivity profile was measured in a southeast direction along an existing gravel road located adjacent to the quarry. The results are similar to the data obtained along Profile P1 on Hadseløya (Fig. 6.20). A layer of relatively low resistivity lies on top of segments with continuous high resistivity showing irregular surfaces, and is truncated by almost vertical zones with low resistivity. Noticeably different to Hadseløya is the occurrence of small high-resistivity zones within the shallow layer that might represent the dense distribution of corestones, as has already been observed in the exposures. Furthermore, the measured resistivity values are about one order of magnitude higher than the ones obtained on any of the other sites in the Lofoten-Vesterålen area. Since the observed bedrock type is similar, we tentatively explain this fact by inferring a better drained system for the Hamarøya site with consequently a dry subsurface.

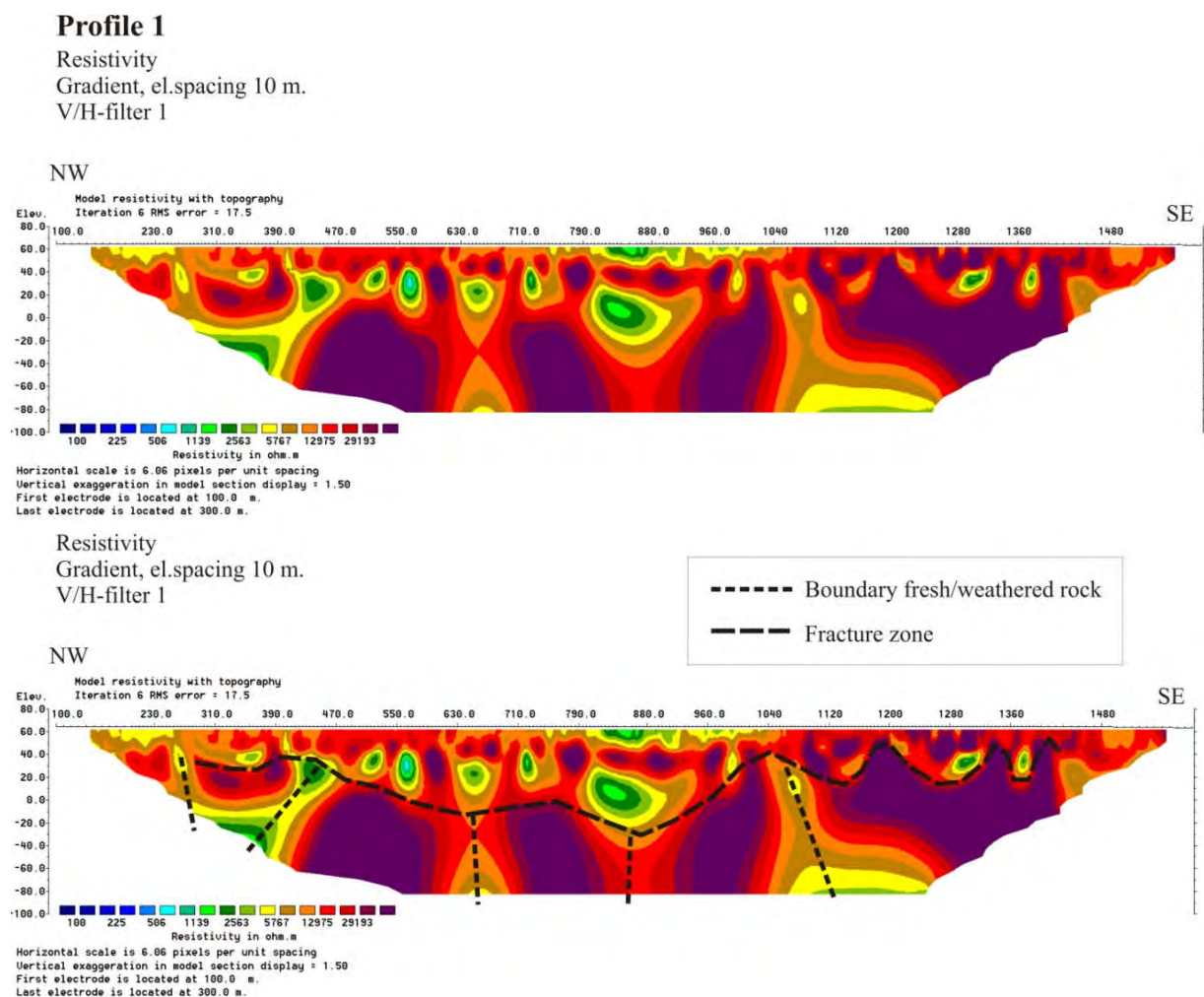


Figure 6.16 Resistivity profile from Hamarøya. A low-resistivity layer lies on top of segments with high resistivity. Deep, almost vertical zones with low resistivity indicate large fractures filled with deep-weathered saprolite.

The irregular surface probably reflects the transition between weathered and unweathered basement, whilst the low-resistivity zones might be expected to show deep fractures filled with deeply weathered bedrock. Compared to Hadseløya, it seems that the site on Hamarøya provides an insight into a deeper stage of a weathering zone, deeper in the saprorock and closer to the unweathered and non-fractured basement.

6.7 Andøya

The fourth location is in one of the best developed strandflats in Norway, and is situated on northeast Andøya in the vicinity of the Ramså Basin, the only known Mesozoic basin onshore Norway. Deeply weathered material can be found exposed on the beach and also from well cores which were drilled through the sedimentary succession of the Ramså Basin into the basement (Fig. 6.21). The weathered layer beneath the basin is overlain by Jurassic and Cretaceous sedimentary rocks.

The burial of the weathered basement below Mesozoic sediments proves the weathering to be rather old and most likely of Mesozoic age or older. Nevertheless geochemical analysis of the weathered material shows a rather low mass loss value, c. 28%, which is significantly lower than the one determined on Hadseløya and Hamarøya.

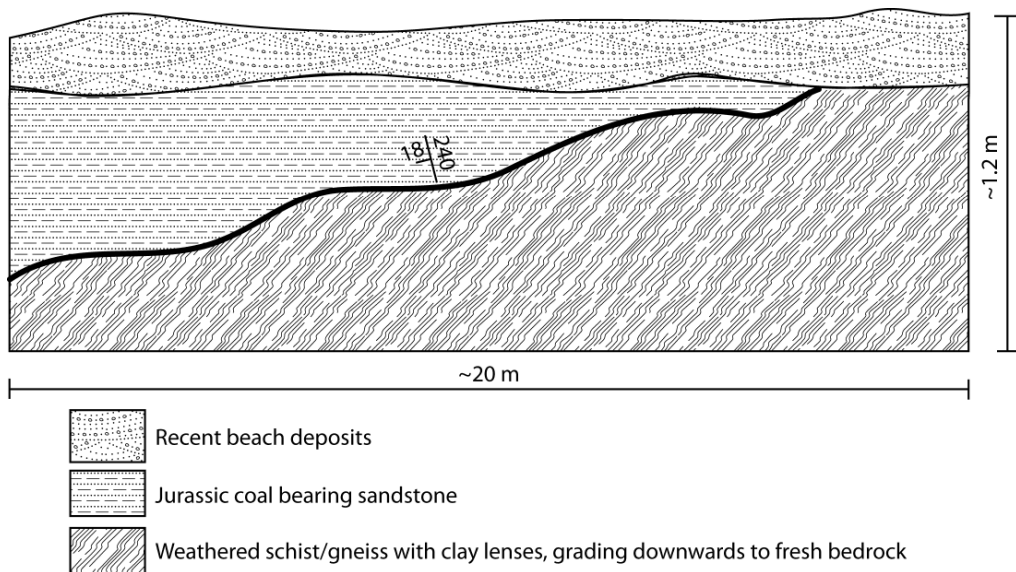


Figure 6.17 a) Map of the Ramså area with the positions of the six resistivity profiles. b) The Ramså Basin is situated on the strandflat on the eastern side of Andøya, where the Mesozoic rocks are visible at low tide; c) Deeply weathered basement is exposed on the present-day beach along the southernmost margin of the Ramså Basin.

The primary rock is mainly gneiss and the weathered material, which is found at the southern flank of the Ramså Basin at the surface, is of greyish colour and relatively clay-rich. It differs greatly from the ones observed at the three other locations in Lofoten-Vesterålen and Hamarøya and we could no longer recognise the fabric of the parent rock. Sturt *et al.* (1979) excavated a trench and studied the weathering profile at this location. They found at least two different types of altered bedrock. They concluded that a reasonable amount of weathered basement has been eroded from the nearby mountains and deposited on top of the saprolite that most probably occurs in an *in situ* position.



a)



b)

Figure 6.18 a) Excavating the basement-sediment contact at the margin of the Ramså Basin on Andøya. Underneath the greyish weathering layer, a brownish, clay-poor type of weathered basement is observed. b) Geological log of the trench at Ramså.

During the TWIN project six resistivity profiles were measured around the Ramså Basin and samples were tested for palaeomagnetic age dating and geochemical and mineralogical analysis. Furthermore we were following in Sturt's and Dalland's footsteps and excavated a trench at the beach of Ramså close to the southern basin edge and investigated the deep weathering and the sediment-basement transition (Fig. 6.22).

6.7.1 Resistivity profiling

The thickness of observed weathered basement in the drillcores is up to 30 m but resistivity data along at least two profiles indicate a much thicker regolith. The boundary of the basin can be observed on three of the six resistivity profiles as a rather sharp and significant resistivity contrast. On Profiles 3 and 5, however, no resistivity contrast is visible. The reasons for the lack of resistivity contrast in these particular profiles differ, however. Profile 3 (Fig. 6.23) is situated across a gabbroic body within a basement high that separates the basin into two. The gabbro is exposed to the west of the basin, but also seems to be rather shallow within the Ramså Basin. Furthermore, the resistivity values along that profile are rather low indicating that the gabbro itself might be deeply weathered or at least fractured. It is difficult to distinguish between unweathered basement and saprolite because the resistivity values are ambiguous and could indicate the presence of both kinds of rocks.

A possible near-top-basement is marked as dashed lines in the profile, but is highly speculative. Different vertical low resistivity zones were marked as possible faults, but none of them correlates with the indicated western basin boundary on the geological map (Henningsen & Tveten 1998).

Profile 5 (Fig. 6.24) is situated to the north of the basin and is measured in a southeast direction, and displays a significantly different picture as compared to the other profiles. The resistivity profile shows a wedge-shaped, low-resistivity zone, where the northwestern flank correlates with the basin boundary from the magnetic map and the southeastern one correlates with an observed fault, indicated on the geological map (Henningsen & Tveten 1998). This structure can be interpreted in terms of a sediment-filled wedge on top of a rotated fault block. Profile 5 shows outcropping, possibly fractured basement in the northwest. In between positions 200 m and 750 m, the top basement is rather flat with some fault zones indicated by vertical low-resistivity zones.

Profile 3

Resistivity
Gradient, el.spacing 10 m.
V/H-filter 1

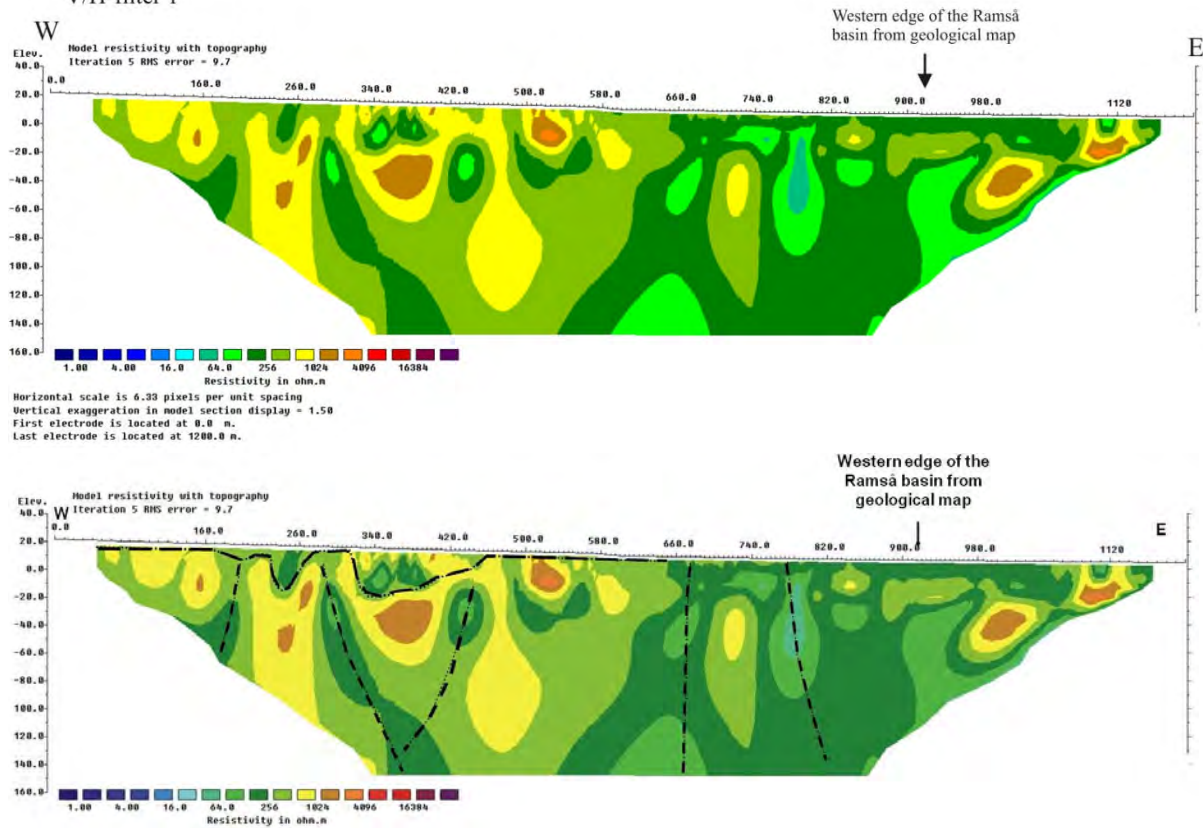


Figure 6.19 Resistivity along Profile 3 on Andøya. The vertical lines mark possible faults, indicated by vertical low resistivity zones. The horizontal dashed line represents the rather diffuse near-top-basement surface.

The basement is covered by a c. 10-20 m thick layer with lower resistivity, above a wedge-shaped, low-resistivity zone (position 750-1100 m). It remains unclear whether this low-resistivity unit represents sedimentary rocks or weathered basement. There seems to be an internal boundary (dashed line) dipping southeastwards towards the basin, indicating a possible base of the sedimentary rock succession on top of the saprolite.

Profile 5

Resistivity
Gradient, el.spacing 10 m.
V/H-filter 1

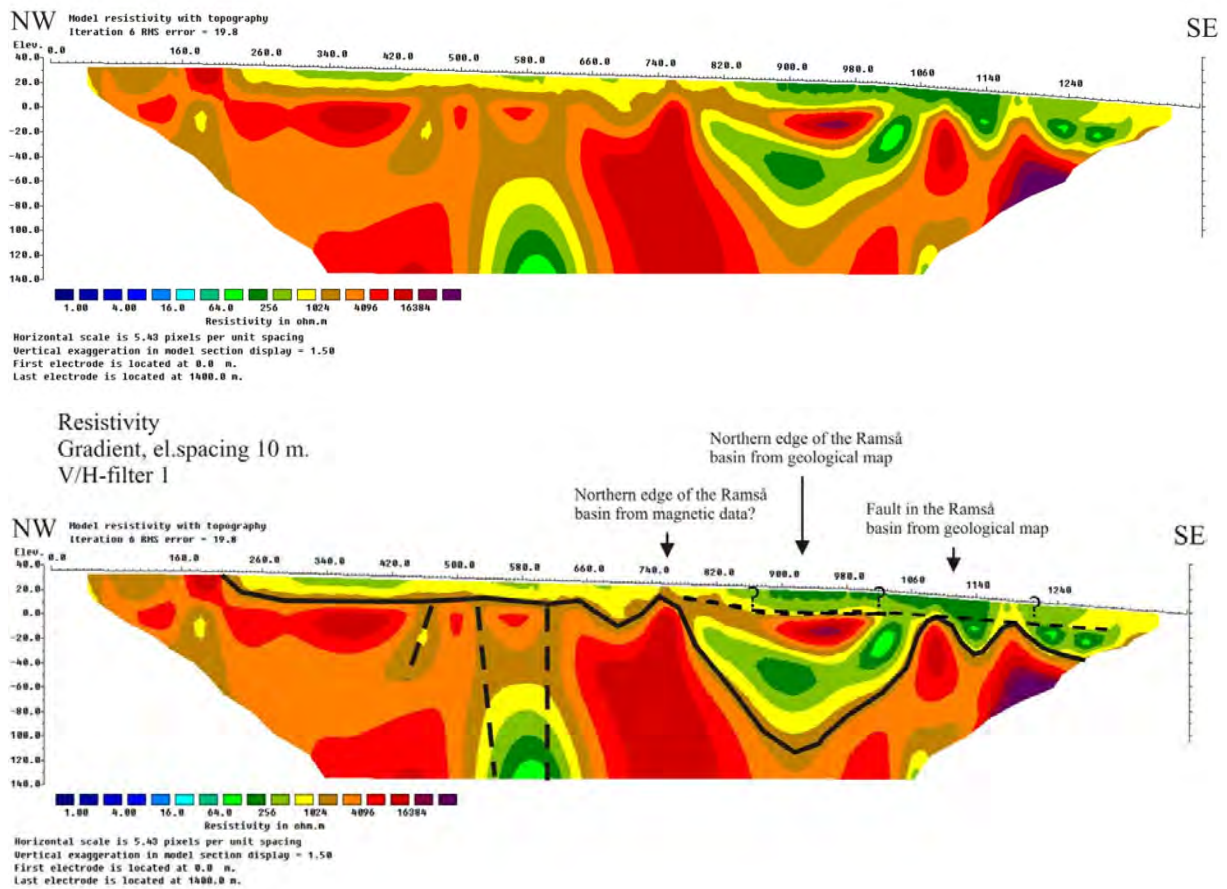


Figure 6.20 Resistivity along Profile 5 across the northern margin of the Ramså Basin, Andøya. The vertical dashed lines indicate possible faults, interpreted from the vertical low-resistivity zones. The near horizontal line represents a near-top-basement surface. The dashed line indicates a diffuse internal surface that may represent an alternative interpretation of the basement surface.

Profile 1, however, shows a transition zone, where the resistivity seems to change gradually and rather irregularly, which might indicate thick packages of deeply weathered basement on top of fractured basement, possible with layers of Mesozoic sediments on top (Fig. 6.25). A noticeable structural change at c. 800 m correlates with the basin boundary on the geological map. Southwards from here, a high-resistivity layer with a rather irregular surface is observed, overlain by an up to c. 70 m-thick low-resistivity sequence.

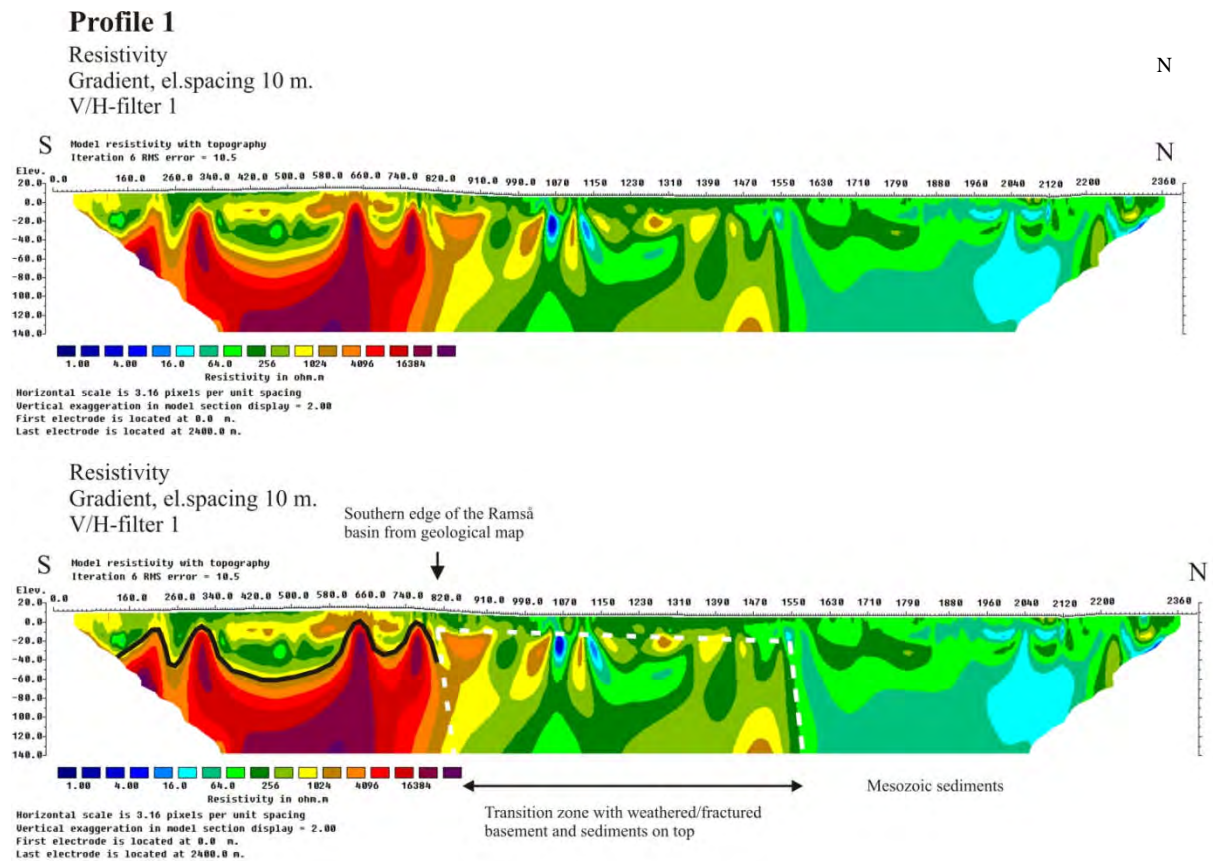
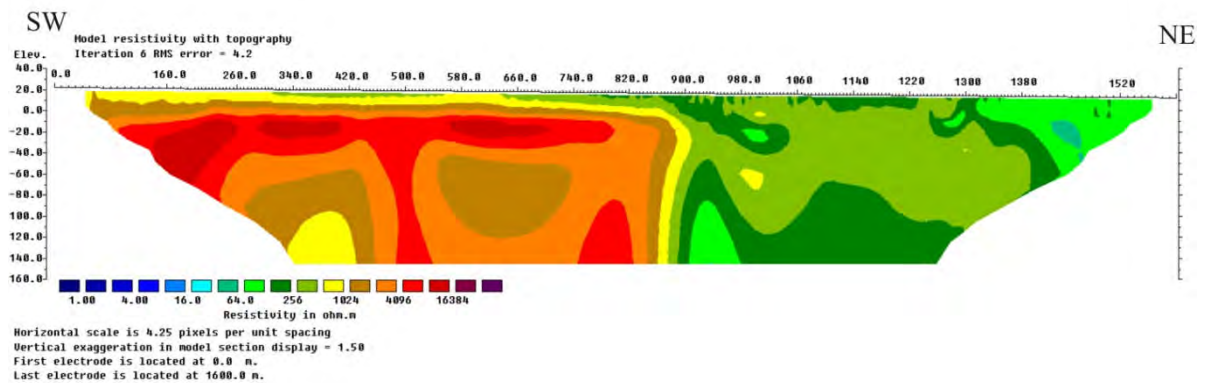


Figure 6.21 Resistivity along Profile 1 across the southern margin of the Ramså Basin, Andøya. The vertical lines indicate possible faults, represented by vertical low-resistivity zones. The horizontal line shows a near-top-basement interpretation. The hatched area marks a transition zone with possibly saprolite and/or sedimentary rocks.

Only a few metres to the west, Profile 6 shows an entirely different picture of the subsurface (Fig. 6.26). Here, the top surface of unweathered basement is rather flat below a c. 20 m-thick, low-resistivity layer. According to the geological map (Henningsen & Tveten 1998), this part of the profile should be located outside the sedimentary basin, but the resistivity is too low to represent unweathered basement rocks. The basin boundary, however, is clearly observed to the east at a depth greater than 20 m. Potential Mesozoic sedimentary rocks are characterised by rather low resistivity.

Profile 6

Resistivity
Gradient, el.spacing 10 m.
V/H-filter 1



Resistivity
Gradient, el.spacing 10 m.
V/H-filter 1

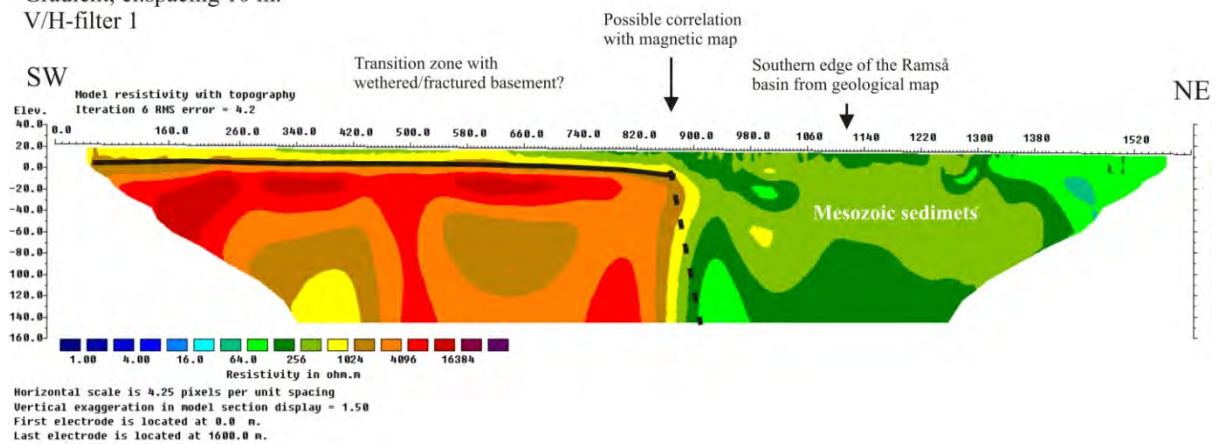


Figure 6.22 Resistivity along Profile 6 on Andøya. The vertical dashed line marks the basin flank. The horizontal line is a near-top-basement interpretation.

A similar picture is observed on Profile 2 (Fig. 6.27), located slightly to the north and measured from the west to the east. High-resistivity values are observed along the western 2/3 of the profile. The interpreted near-top-basement horizon is shallow or even outcropping at the western end of the line. In position 70-1020 m, a continuous low-resistivity layer appears and is dipping towards the northeast, whilst the resistivity values beneath are gradually decreasing. We interpret this zone as a transition zone, similar to the one we observed on Profile 1, but much less developed. At c. position 1020 m, a sharp vertical boundary occurs with much lower resistivity values to the east of this position. This boundary occurs on the magnetic data as a lineament, whilst the margin of the basin, according to the geological map (Henningsen & Tveten 1998), is located c. 150 m farther to the northwest, where the resistivity data indicate a fault or a contact. It remains questionable whether this indicates weathering or perhaps normal faulting, similar to Profile 5 (Fig. 6.24), with a slightly westward shifted basin flank.

Profile 2

Resistivity
Gradient, el.spacing 10 m.
V/H-filter 1

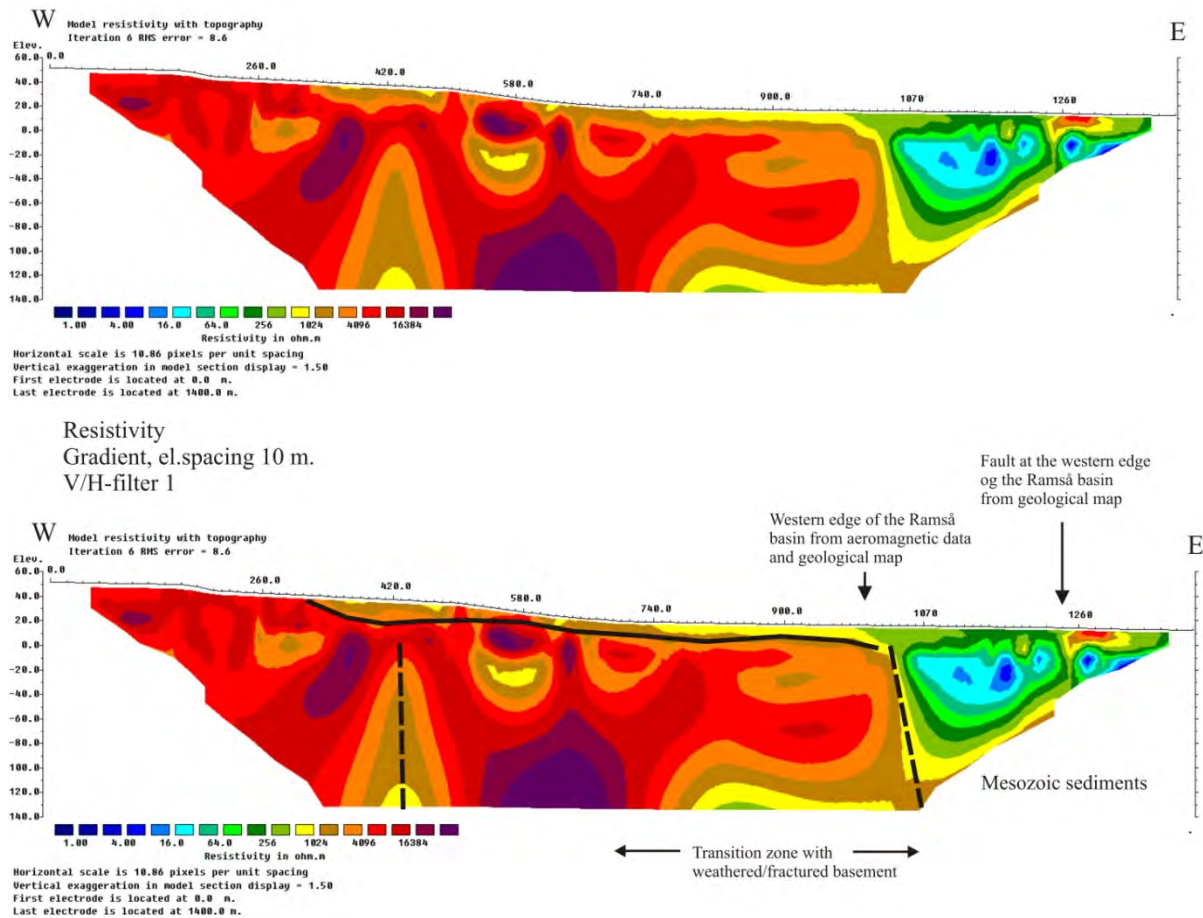


Figure 6.23 Resistivity along Profile 2 on Andøya. The vertical lines mark possible faults, indicated by vertical low-resistivity zones. The horizontal line represents a near-top-basement interpretation – the dashed line indicates a diffuse surface. The hatched area below the dashed line indicates a transition zone with lateral and gradually decreasing resistivity.

Profile 4 is positioned at the northern part of the basin and trends E-W. The basin boundary is clearly visible at the eastern end of the profile (pos. c. 1240 m) as a sharp resistivity boundary. To the west the resistivity data show strong resistivity variations with a very irregular near top-basement geometry, similar to the one we have observed on Hamarøya and the Lofotens. The thickness of weathered and fractured basement rocks as indicated from the resistivity profile is very large locally exceeding 150 m, and might be related to a fracture zone extending to a great depth (pos. 660 m).

Profile 4

Resistivity
Gradient, el.spacing 10 m.
V/H-filter 1

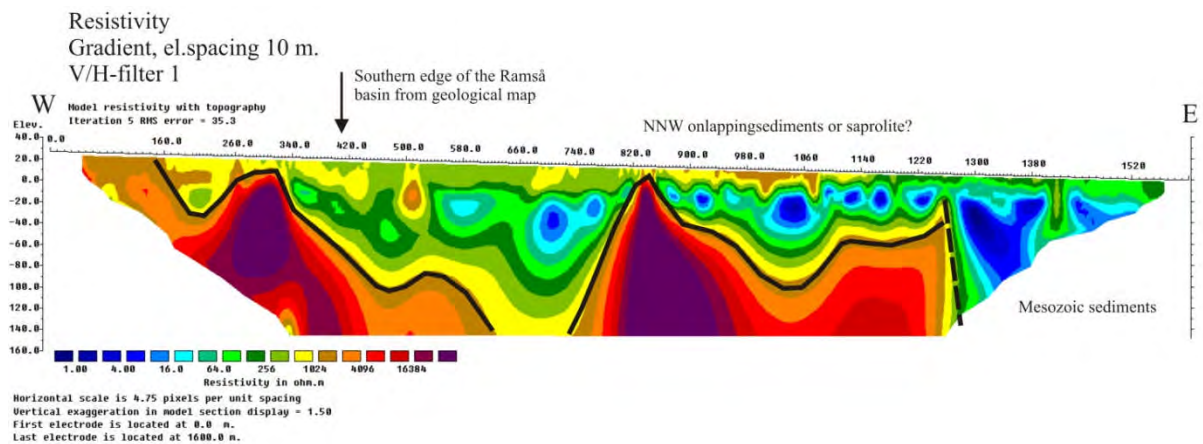
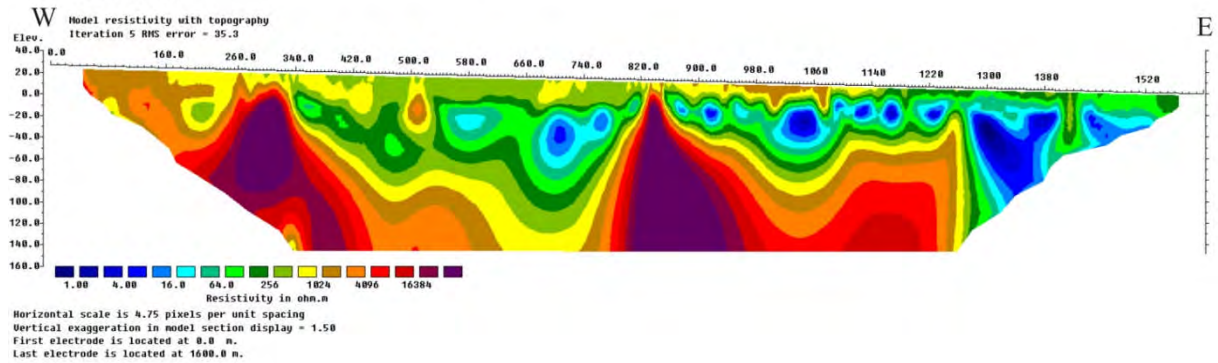


Figure 6.28 Resistivity along Profile 4 located across the northwestern margin of the Ramså Basin, Andøya. The vertical line indicates the possible basin flank. The sub-horizontal line represents a near-top-basement interpretation.

6.7.2 Palaeomagnetic sampling, Ramså

Sites C and D

On the island of Andøya we sampled weathered bedrock beneath a recent fluvial sand layer at Site C near Ramså (Fig. 6.29). Because no solid rocks were visible at this site, drillcore samples of solid bedrock from a nearby site D were taken as reference.



Figure 6.29 Relative position of weathered bedrock (site C) and solid rock samples (site D) in the river bed near Ramså, Andøya.

Weathered site C

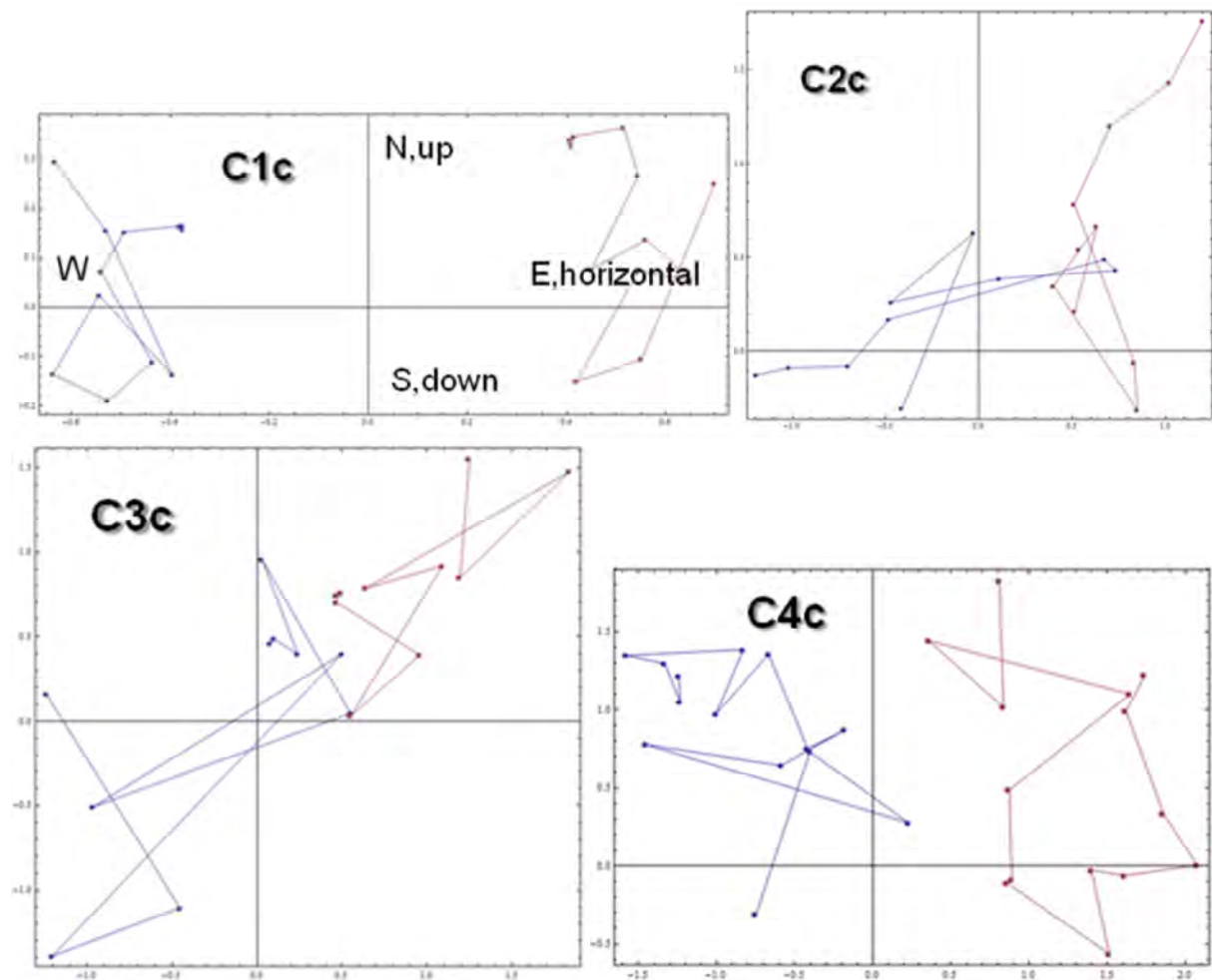


Figure 6.30 Zijdeveld diagrams of AF demagnetisation results on the weathered rock specimens from aluminium tubes 1, 2, 3 and 4 at site C. Red: inclination plots of up-component versus horizontal component. Blue: declination plots of E-W component versus N-S component of the horizontal projection of the magnetisation.

Solid bedrock site D

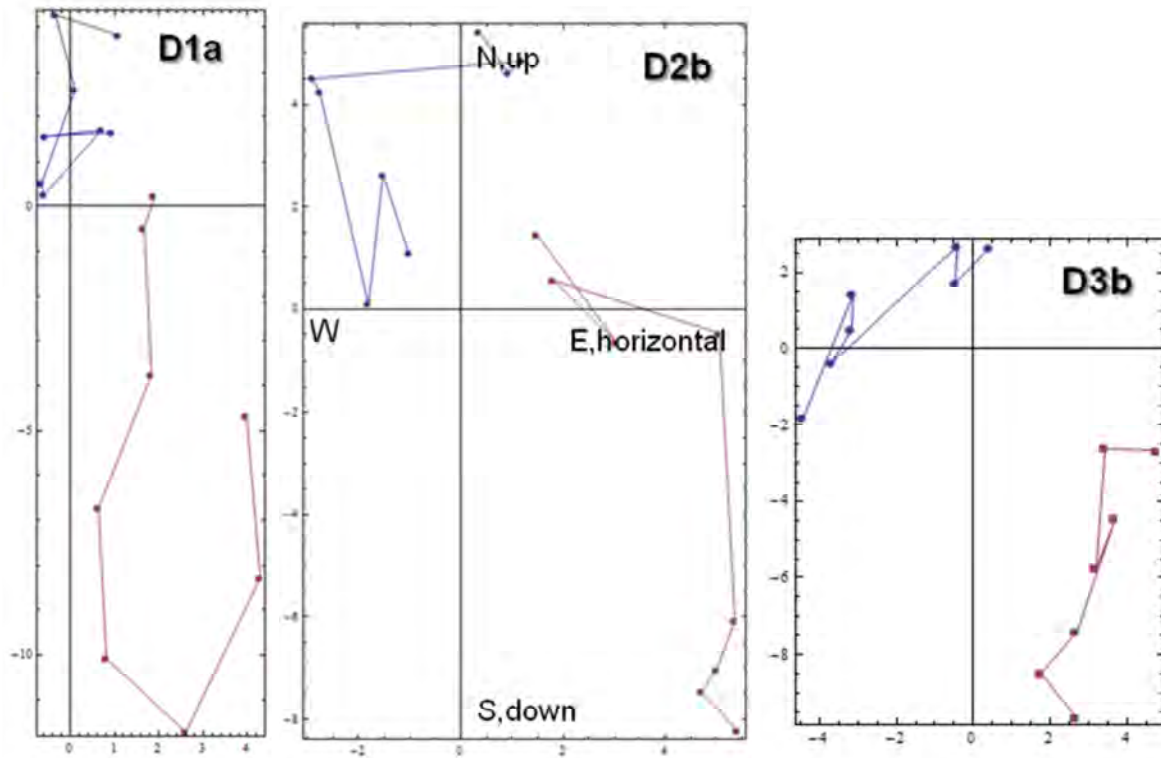


Figure 6.31 Zijdeveld diagrams of AF demagnetisation results on the solid rock specimens from drillcores 1, 2 and 3 at site D. Red: inclination plots of up-component versus horizontal component. Blue: declination plots of E-W component versus N-S component of the horizontal projection of the magnetisation.

Although all demagnetisation plots yield noisy and irregular palaeomagnetic directions, the results rather indicate a shallower magnetisation direction at site C as compared to site D. In any case, it can be concluded that even if the weathering process generated a new magnetic component, this definitely does not point in a recent steep north direction. The data therefore indicate a scenario of old weathering rather than a recent one (Fig. 6.31).

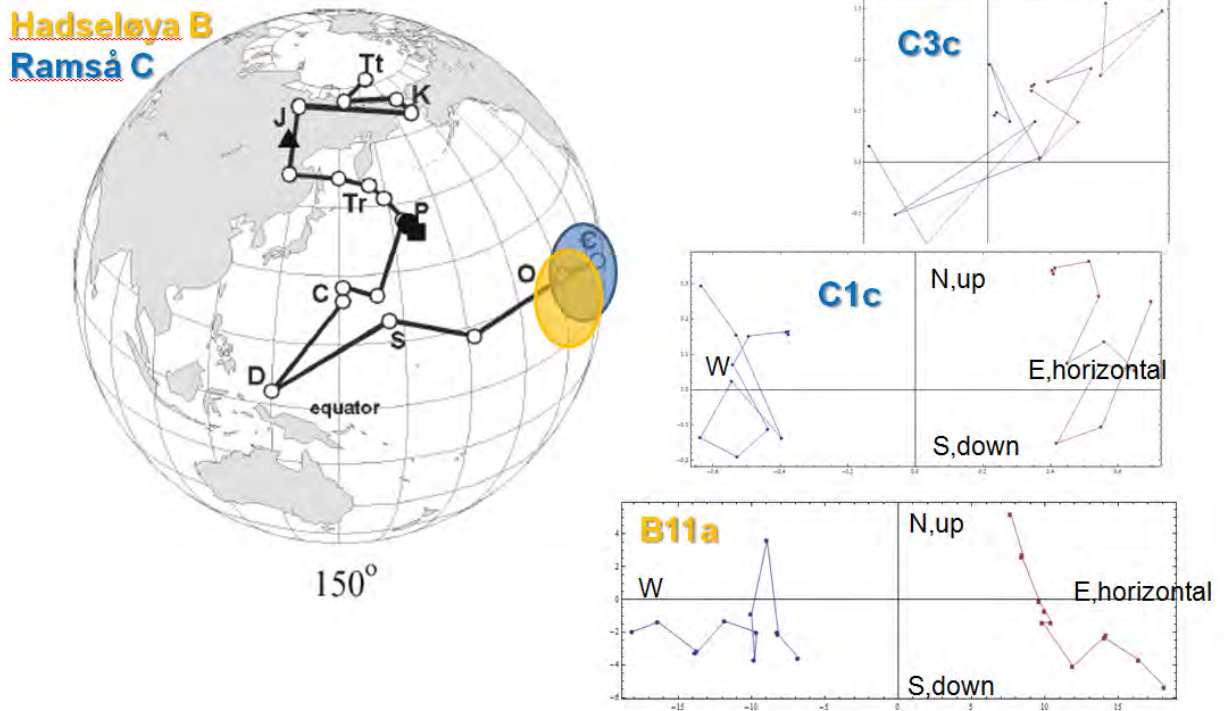


Figure 6.24 Palaeomagnetic directions from the weathered parts of Hadseløya (yellow) and Ramså (blue) are very unstable. When plotting them in relation to the polar wander curve from Parnell *et al.* (2004), the positions best correspond to the Ordovician or Cambrian period. This result either indicates that no remanent magnetisation is acquired during weathering, or it supports a scenario of old weathering.

6.7.3 Seismic profiling, Staveheia,

To map possible weathered bedrock at Staveheia, south of Bleik on Andøya, northern Norway, refraction seismic measurements were carried out back in 1986 (Hillestad 1987). The location of the area is shown in Fig. 6.33. The studies were carried out in close cooperation with geologist Jakob Møller at the Tromsø Museum, who had earlier studied weathered bedrock in the area.



Figure 6.33 Location of refraction seismic lines at Staveheia (Trolldalsheia) shown with grey hatching. The survey area is situated 4 km to the south-southwest of the fishing village Bleik. Other refraction seismic lines registered in NGUs database are shown in blue. The swamps to the southwest covers part of the Ramså Basin. See Fig. 6.21a.

6.7.3.1 Method and performance

A general description of the refraction seismic method is given in Section 2.2 and at <http://www.ngu.no/no/hm/Norges-geologi/Geofysikk/Bakkegeofysikk/Seismiske-metoder/> Altogether, 4 short lines were measured using an analogue seismograph (ABEM TRIO) and 12 geophones. The geophone spacing was mostly 10 metres but reduced to 5 metres at the end of the profiles. Small charges of dynamite were used as the energy source. At the time of the measurements, no electronic positioning was available, and profiles were plotted on a map at the scale of 1: 50,000. The altitude above sea level was read from the topographical map. This means that both the positions and the heights in the seismic sections are somewhat uncertain. The locations of the lines are shown in Fig. 6.34.

The data quality was good, but it was difficult to interpret the data due to the complicated geology.

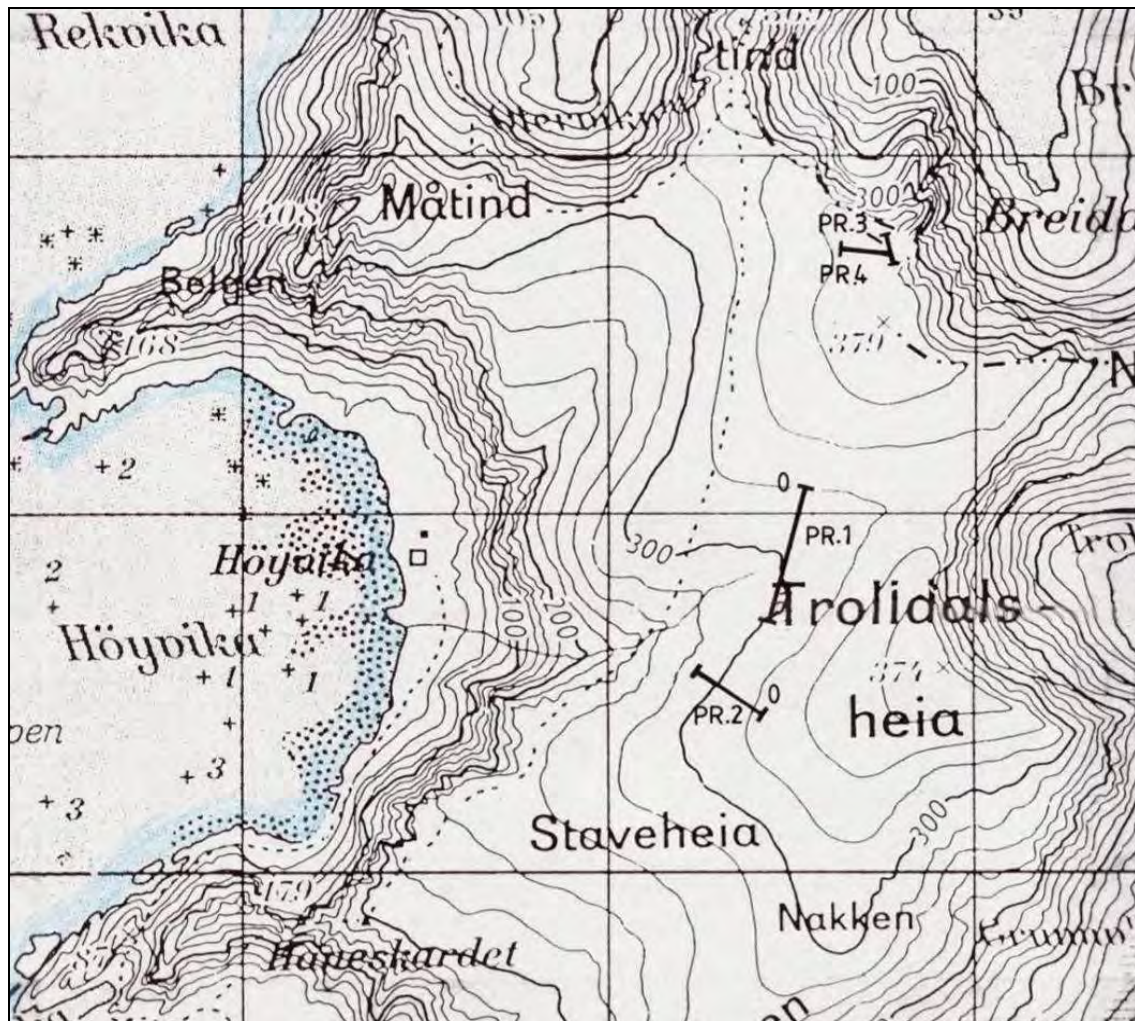


Figure 6.34 Detailed locations of the four seismic lines at Staveheia.

6.7.3.2 Results

The results from the refraction seismic survey at Staveheia are shown in Figs. 6.35-6.37. All four lines indicate a four-layer model. Layer 1 with P-wave velocity 350 – 450 m/s represents loose and dry sediments. Normally the second layer, with P-wave velocities from 900 to 1280 m/s, could be interpreted as more compacted sediments but still not fully water-saturated. The third layer, with P-wave velocities from 1850 to 2500 m/s, would in most other places in Norway be interpreted in terms of a till. The fourth layer is interpreted as unweathered bedrock.

During the fieldwork at Staveheia, a trench was dug at position 270 m along Profile 1. At two metres depth, they found material which looked 'suspiciously like bedrock' (Hillestad 1987). At the end of Profile 3, in the steep hillside below, weathered bedrock is exposed. Based on this, layers 2 and 3 in these two profiles were interpreted as weathered bedrock, whilst layer 4 was interpreted as unweathered bedrock. Depth to unweathered bedrock varies from less than five metres in Profile 2 to a maximum of 35 metres in Profile 3.

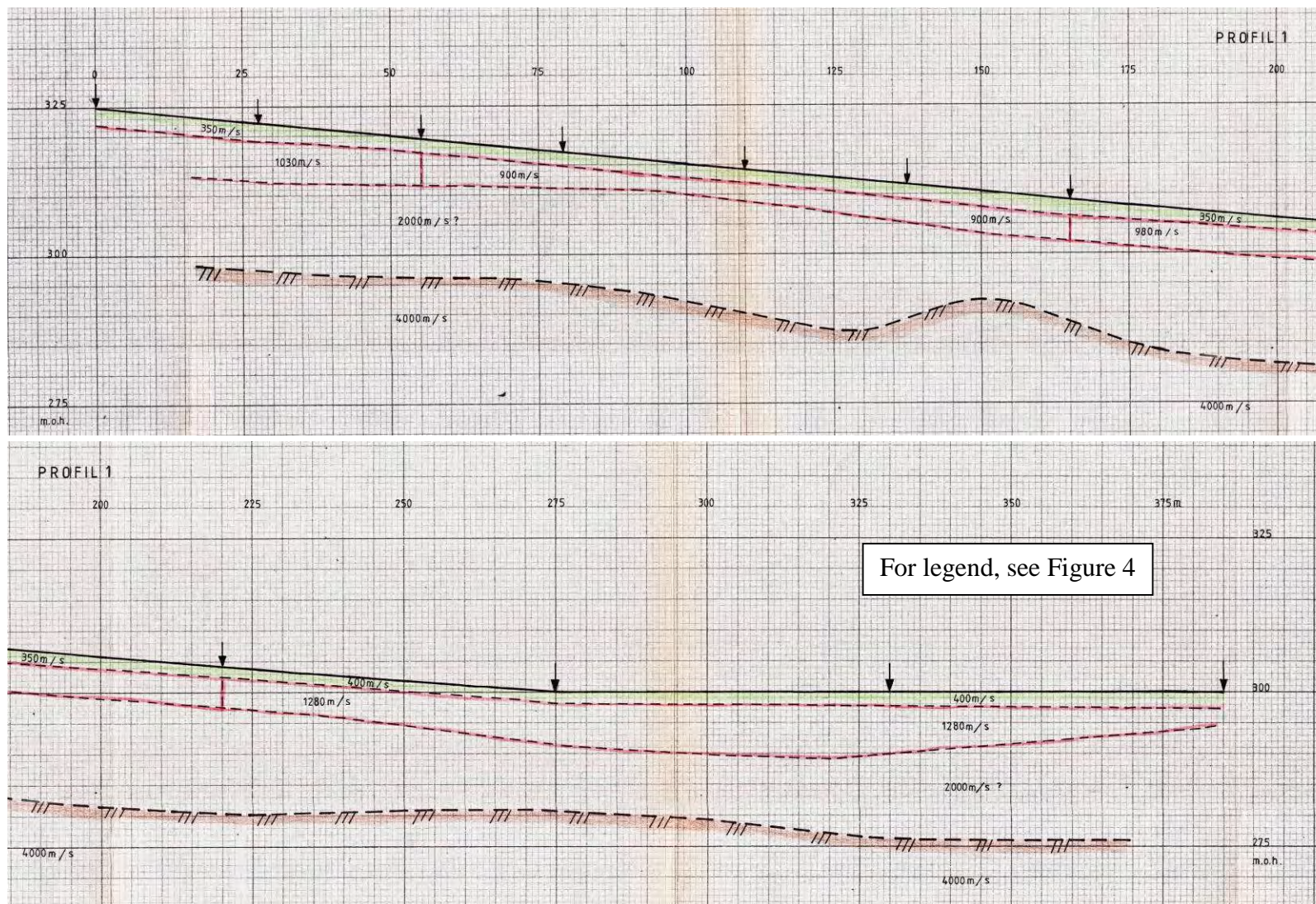


Figure 6.35 Interpreted seismic sections from Staveheia, Profile 1.

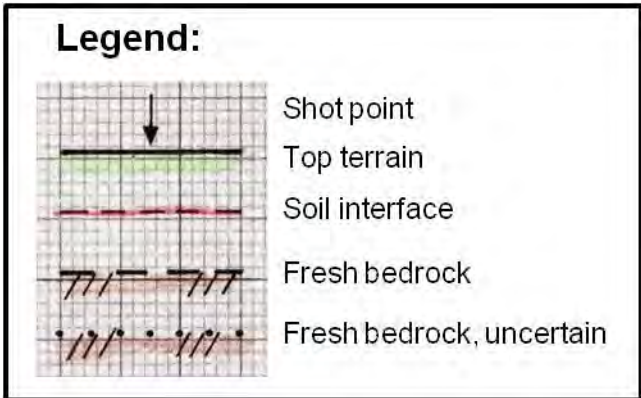
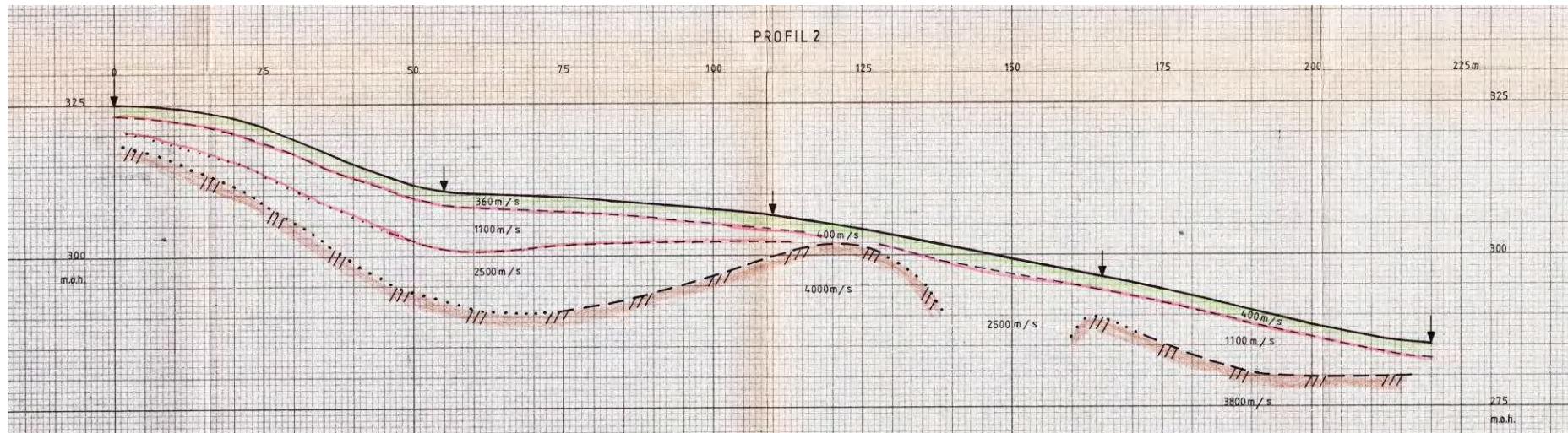


Figure 6.36 Interpreted seismic sections from Staveheia, Profile 2.

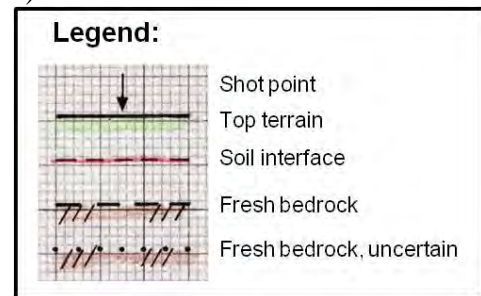
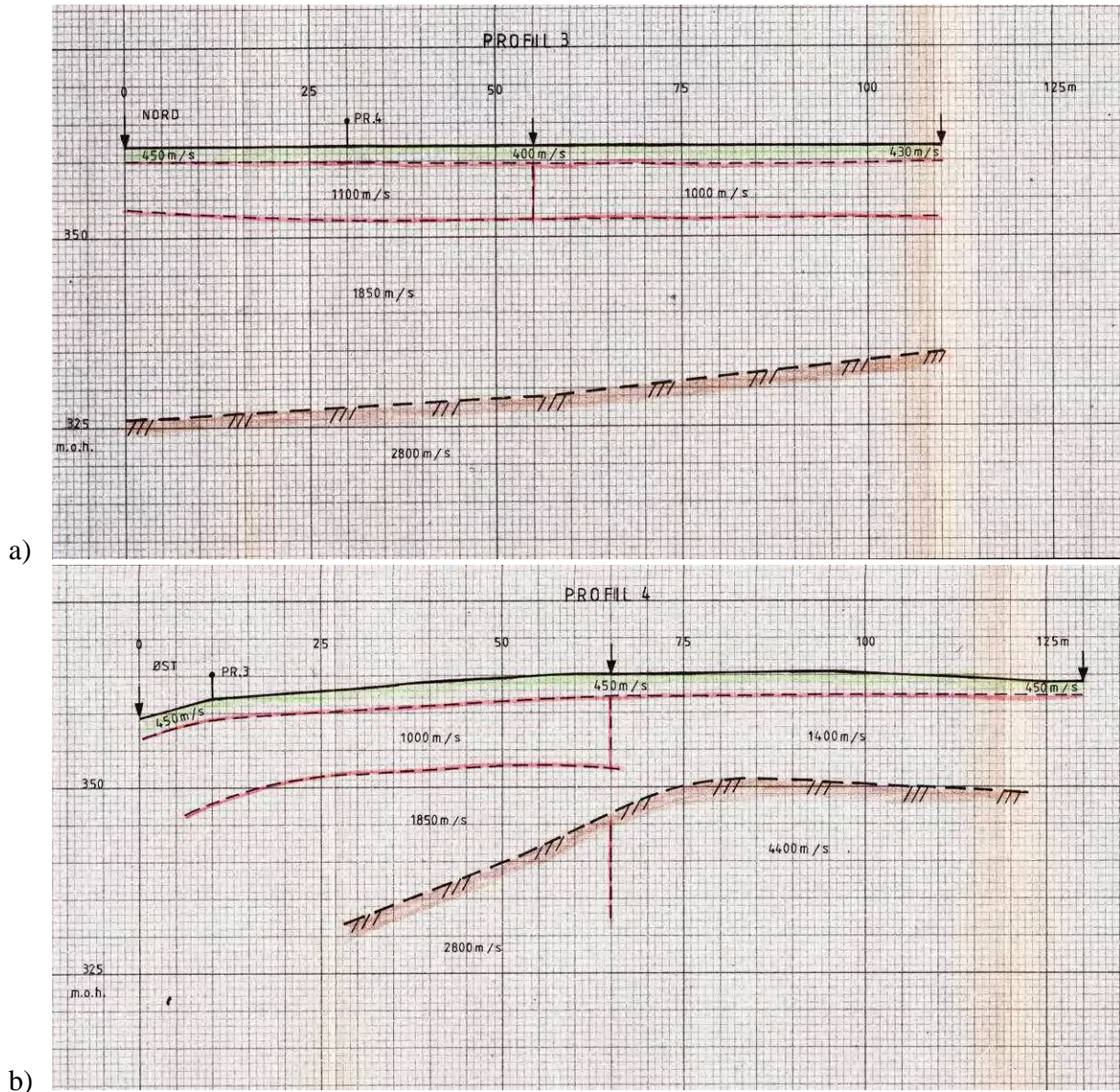


Figure 6.37 Interpreted seismic sections from Staveheia, Profiles 3(a) and 4 (b).

6.7.3.3 Discussion

As indicated above, layers 2 and 3 in Profiles 1 and 3 (Figs. 6.35 & 6.37) are interpreted as weathered bedrock. Since Profiles 3 and 4 lie next to each other, are very short (110 – 125 metres) and have almost similar velocities, we expect the weathered bedrock to extend into Profile 4. However, this is mainly based on the two field observations of weathered bedrock.

Layer 2 in Profile 1 has velocities from 900 to 1280 m/s. This is extremely low to represent weathered bedrock. As a reference, weathered bedrock at Leknes in Lofoten (see section 6.3.2 of the present report) has velocities from 4000 to 4500 m/s. If we compare this with experience from tunnelling in Norway, velocities between 2000 and 2500 m/s represent an extremely poor bedrock quality (Barton 2007). As indicated by Hillestad (1987), the three uppermost layers can also be interpreted as soil material of different kinds, mostly till.

The velocity of the material that Hillestad (1987) refers to as unweathered or fresh bedrock, varies from 2800 m/s up to a maximum of 4400 m/s. Along Profiles 1 and 2, the velocity is about 4000 m/s. Along Profiles 3 and 4 we find seismic velocities as low as 2800 m/s and also the highest in the area, 4400 m/s, in the western part of Profile 4. The bedrock in the area consists of amphibolite and different types of gneiss (www.ngu.no, Zwaan *et al.* 1998). Based on recent results from borehole logging (Elvebakk 2011), we can expect velocities above 5000 m/s in fresh bedrock like this. The relatively low velocities found in the bedrock at Staveheia indicate weathering to a depth of more than 25 metres.

Hillestad & Melleby (1967) carried out a similar refraction seismic survey in the southern part of Andøya for the planning of the new bridge to Hinnøya. They detected similar bedrock with low velocities in the order of 3150-4500 m/s. The bulk of the bedrock has a velocity of 3400-4100 m/s indicating that fractured and weathered bedrock is quite common in Vesterålen.

Chroston & Brooks (1989) measured the seismic velocity on 80 rock samples from the Lofoten-Vesterålen area and concluded that the mean velocities for the six main lithologies are all in the range from 6230 to 7130 m/s. Sellevoll (1983) carried out a regional seismic refraction line from Å in Lofoten to Stø on Langøya. They found a seismic velocity of 6050 m/s in the uppermost four kilometres of the crust, indicating that the bedrock in the Lofoten-Vesterålen area is generally highly fractured. Such a fracturing could have facilitated the tropical deep weathering during the Late Triassic to Early Jurassic period with a favourable warm and humid climate.

6.8 Conclusions from Lofoten-Vesterålen and Hamarøya

Based on our observations we conclude that there are still thick piles of weathered basement rocks onshore the Lofoten-Vesterålen islands and on Hamarøya. All observed, major, deep-

weathering locations occur in rather flat low-lying areas where erosion is considered to be low to moderate. Considering a generally much higher amount of erosion in the mountainous areas where glacial erosion occurs to a large degree as plucking, deep weathering is likely to still have considerable impact on the topography of the Norwegian landscape.

The different characteristics of the two exposed deep-weathering profiles with a rather homogeneous saprolite and only a few corestones on Hadseløya and a rather dense distribution of corestones with granular weathered material in between on Hamarøya could be interpreted as two insights into different stages or depths of the regolith. Whilst Hadseløya shows a sequence within the saprolite, the exposure on Hamarøya was much deeper seated, and is within or close to the saprock and consequently closer to the unweathered basement rock. It remains unclear whether or not the rate of erosion on Hamarøya was higher or the weathering process was slower and/or initiated at a later time.

Previous measurements of seismic velocity on fresh rock samples in the Lofoten-Vesterålen area are significantly higher than seismic velocities deduced from both shallow and deep refraction experiments revealing that the crust in the Lofoten-Vesterålen is highly fractured. A high fracture density could help to accelerate weathering downwards.

The AMAGER method was applied for the island of Langøya and indicated further amounts of deeply weathered and/or fractured basement in this area. Resistivity profiling and direct observation on site proved the capability of this technique to map such structures, but also indicated its uncertainties and its strong dependence on the data resolution.

Weathering of rocks during different climatic conditions is rather complex and is poorly understood. The initial trigger for the weathering, the actual type and finally the weathering rate are commonly considered to depend on several external factors such as climate, temperature, humidity and CO₂ content in the atmosphere (Brantley *et al.* 2007, Andersson *et al.* 2007, Riebe *et al.* 2004, West *et al.* 2004), but also on geotectonic processes like uplift and erosion (Raymo & Rudiman 1992, Amundson *et al.* 2007, Rasmussen *et al.* 2011). Knowledge of the age of weathering could consequently account for a better understanding of the geotectonic history of a region and also be helpful for an advanced mapping of deep weathering onshore Norway and offshore on the Norwegian shelf. For the TWIN project the clay mineral content was too low to give a hint on the chemical processes involved and possibly climatic conditions, which could otherwise have pointed to a specific epoch. The palaeomagnetic data were also inconclusive and Ar/Ar dating could not be performed because of a lack of datable material. However, the large percentage of leached minerals on Hamarøya and Hadseløya and at some locations in southern Norway (Chapter 5) could suggest a fairly old age for this type of weathering. This is intriguing

since this kind of clay-poor weathering has commonly been considered to be rather young, e.g. Cainozoic times (Migon 1997).

The observed saprolite is mostly a clay-poor and brownish material. The large amounts of observed deep-weathered material together with the indicated even greater thickness of the existing regolith raise the question about a possible maximum thickness of regolith and, consequently, the possible thickness of a transition zone from soil or the sedimentary succession to unweathered basement. Moreover, what is the nature of the transition from fresh to weathered bedrock? Gerrard (1988) described this transition to be *usually quite sharp* for crystalline rocks like granite. We did not observe the direct boundaries at the main locations, but we observed some smaller exposures where the boundary was sharp (Fig. 6.38), but did not represent the base of the weathering. On the other hand, from the resistivity profiles there was none that showed a transition front above a continuous unweathered basement. The corestones of fresh basement became larger with depth, but they were still truncated by large fracture zones with a significant low resistivity. This is definitely an important point which should be investigated further.



Figure 6.38 Example of a very sharp transition between weathered and fresh bedrock at a road-cut on Hamarøya.

The mapped remnants of weathering on Lofoten-Vesterålen and Hamarøya were located in the vicinity of major faults on the proximal flank of the hangingwall of rotated fault blocks, which can possibly be used as a link to develop a schematic pattern for finding new weathering sites and extrapolating deep-weathering occurrences along major faults.

7 REGIONAL GEOMORPHOLOGY AND DEEP WEATHERING

Ola Fredin

The main purpose of the TWIN deep-weathering database is to obtain a spatial overview of deep weathering in Norway. From Fig. 7.1 it is clear that many of the significant weathering localities are situated relatively close to the coast. Relatively few occurrences of clay or grus weathering can be found in inland areas of Norway. However, many dubious or nondescript occurrences can be found in central parts of Norway.

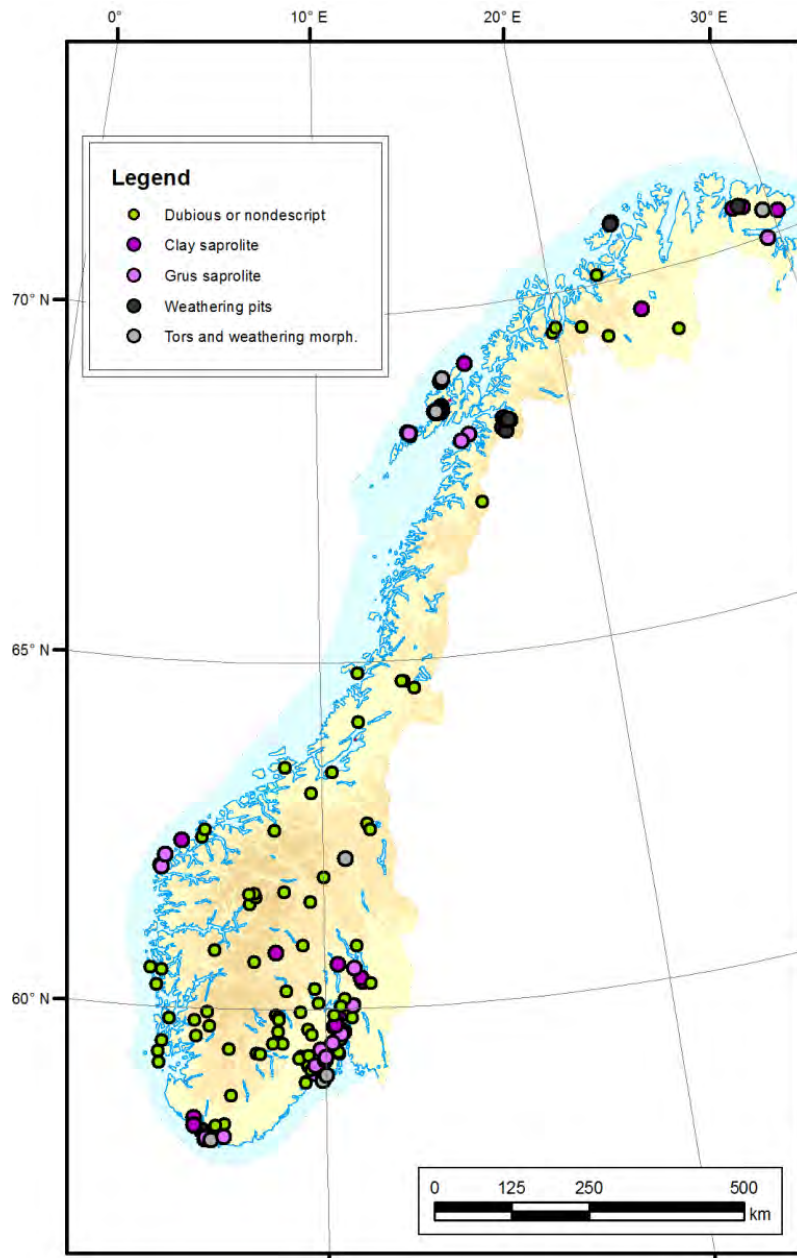


Figure 7.1 Known weathering localities in Norway. Excerpt from the TWIN weathering database.

In this study we will put relatively little emphasis on inland locations with nondescript occurrences of saprolite, since these quite likely reflect tectonic fault- or hydrothermal alteration zones with little signs of subaerial deep-weathering characteristics. However, we acknowledge that the sometimes poor description of these occurrences may hide some true deep-weathering localities.

The TWIN weathering database also contains information about bedrock derived from the NGU bedrock database. A pronounced common feature of the confirmed deep-weathering localities is that they occur in intermediate to mafic bedrock types such as monzonite/mangerite (e.g. Vesterålen and Hamarøy), gabbro (Vågsøy), syenite (Kjose) with the most acidic rocks being gneisses at Lista. In many cases the weathering thus seems to be conditioned by an abundance of relatively easily weathered feldspars, micas, pyroxenes and amphiboles. Two fundamental controls on weathering rate and characteristics are climate and vadose zone/groundwater conditions. It is clear that temperature and humidity play a critical role since reaction kinematics are dependent on these parameters (e.g. Nesbitt & Young, 1989). Recent studies also show that vadose zone dynamics also fundamentally influence how bedrock is weathered. It appears as if matrix permeability (low flow rates) in bedrock causes oxidation of biotite and granular (gravelly) disintegration of rock, little chemical alteration, clay formation and mass loss (Goodfellow *et al.* 2011). On the other hand, high vadose zone flow rates such as in bedrock fractures cause chemical alteration, mass loss and clay formation (Goodfellow *et al.* 2011).

Lidmar-Bergström (1995) characterised Scandinavia in seven different landscape (erosion) generations. This is a relatively crude classification but gives an impression as to when different areas were exposed to major exhumation episodes, which are reflected in the gross geomorphology. If the weathering occurrences are plotted on the map of Lidmar-Bergström (1995) (Fig. 7.2), the best developed weathering localities occur in the following landscape generations 1) the Sub-Cretaceous, 2) Tertiary surfaces, 3) Glacial erosion and 4) 'Paleic surfaces'. From this we infer that several localities around the Oslofjord and on the south coast of Norway belong to the 'Sub-Cretaceous landscape' that dominates South Norway, SW Sweden and central/NW Sweden. Although this landscape has no cover rocks in Norway that can prove its pre-Cretaceous origin, it can be correlated morphologically to very similar landscapes in southern Sweden with Mesozoic cover rocks (Lidmar-Bergström 1989). In addition, this landscape dips down beneath Mesozoic strata on the Norwegian shelf (Riis 1996). It thus seems likely that the deep weathering found in south Norway was initiated mainly in pre-Cretaceous time. Sørensen (1988), however, argued that the weathering characteristics in the Kjose area indicate a rejuvenation of weathering processes when the landscape was re-exposed in Plio-/Pleistocene time, with ongoing weathering also in the Holocene.

Many of the other known saprolites occur in what Lidmar-Bergström (1995) has classified as landscape dominated by glacial erosion (Fig. 7.2). The major landforms, for example U-shaped

valleys and fjords, are thus formed by Quaternary erosion but pockets of pre-Quaternary weathering might remain in certain locations. There is no clear relationship between topography and localities with deep weathering. It also appears that small topographic differences and lee-side processes were enough to protect pre-Quaternary weathering sites from the erosive effects of ice sheets. Thus, at this stage we cannot predict locally with any confidence where we are likely to find deep weathering.

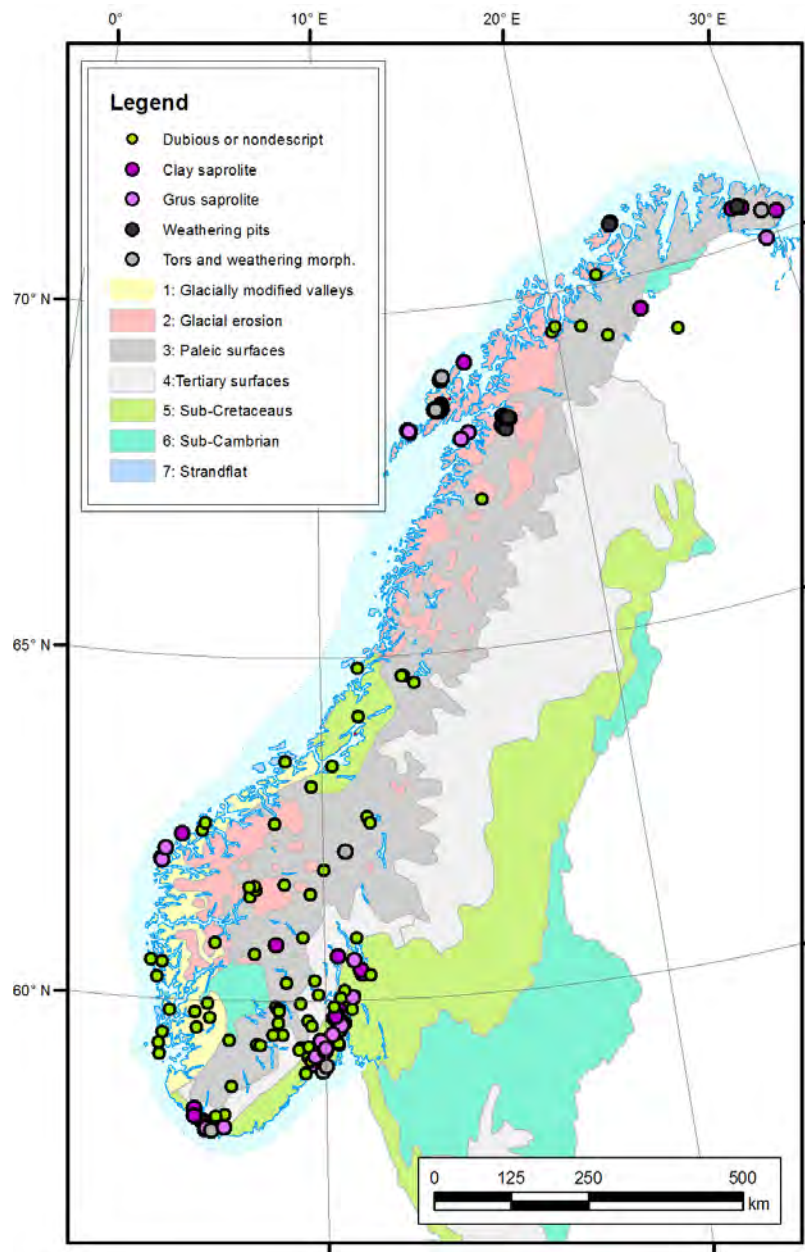


Figure 7.2 Known weathering localities and saprolites in Norway and landscape generations after Lidmar-Bergström (1995). Note that Fjellanger & Nystuen (2007) classify Varanger Peninsula as representing a Tertiary surface.

Another phenomenon in these areas that has been reported in the literature and the TWIN database is that of autochthonous blockfields. At the moment it is not fully understood how autochthonous blockfields relate to the long term topographic history of Norway and the Paleic surface (Gjessing 1967). Some workers have reported finds of clay minerals such as kaolinite in the autochthonous blockfields (Rea *et al.* 1996, Paasche *et al.* 2006). Other studies indicate that the Paleic surface is undergoing steady-state erosion, with the weathering soil being eroded at the same pace as it is created, and very little saprolite older than the Quaternary can be found (Goodfellow *et al.* 2009). The gross landforms of the Paleic surface may thus be ancient but the actual soils might be younger. Because of this we largely omit autochthonous blockfields from this study.

Overall, it appears difficult to assign a definitive age to the weathering in Norway based on weathering characteristics, position in the terrain or bedrock type. The most compelling regional correlation that indicates that the saprolites might have been formed in Mesozoic time is correlation of 'envelope surfaces' of topography and the fact that these dip down under Mesozoic strata offshore Norway (e.g. Riis 1996, Lidmar-Bergström *et al.* 2007). At several locations in South Sweden and Denmark, this relationship can also be observed onshore (Lidmar-Bergström *et al.* 1999). Most of these localities exhibit extensive saprolite profiles with clay-rich kaolinitic weathering with, in places, pure kaolinite and quartz sand (Lidmar-Bergström 1989), indicative of intense leaching of feldspars in a hot and humid climate with acidic meteoric water (Fig. 7.3). These saprolites are found in landscapes termed as 'Sub-Cretaceous undulating hilly relief' or 'Sub-Cretaceous joint valley landscape'.

On the other hand, also in southern Sweden, areas with grassy saprolites can be found. These are associated with little mass loss, mechanical disintegration, and an almost complete absence of clay (Lidmar-Bergström *et al.* 1997). These saprolites are found in a landscape correlated with etching and erosion of the sub-Cambrian peneplain during the Tertiary (Lidmar-Bergström 1995), and the weathering must thus have taken place during the Tertiary in a cooler climate (Fig. 7.3).

landmass commenced in Mesozoic time, possibly as clay-rich, kaolinitic, deep-weathering zones. By latest Cretaceous time the saprolites were covered by sedimentary strata and thus protected. Later on, possibly as late as during Neogene uplift and erosion events, most of the cover rocks and saprolites were stripped from the bedrock and rejuvenation of bedrock weathering could take place. This new weathering episode took place in 1) a cooler climate and 2) in bedrock already weakened by the previous weathering episode. Both of these factors favour plain oxidation of biotite (cool climate and matrix permeability in vadose zones and formation of grussy saprolites). During the Quaternary, most of these newly formed saprolites were once more stripped except for small pockets shielded by topographic effects or non-erosive, cold-based, ice sheets. The Norwegian landscape wherein the saprolites remain thus have a Mesozoic origin but with strong imprint of erosive processes in the Cainozoic (Fig. 7.4). Most of the investigated saprolites appear young but their formation was preconditioned by processes in the Mesozoic. This also suggests that it will be very difficult to obtain an absolute age of the weathering events, since they are interlocked with each other but of different character.

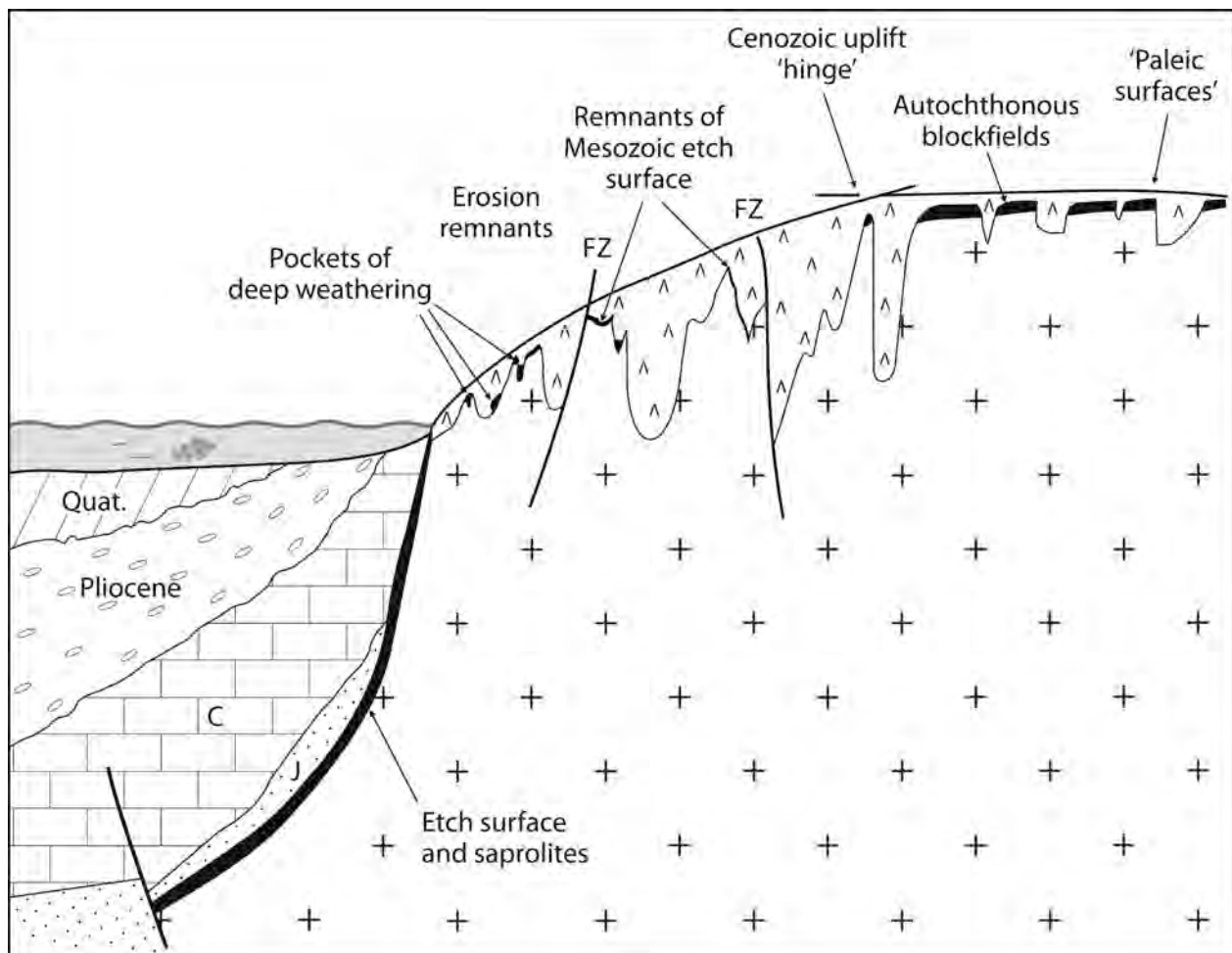


Figure 7.4 Overview of Norwegian saprolites and landscape, correlation to offshore sedimentary successions and Cainozoic erosion.

8 DISCUSSION

The present-day seismicity provides a means to estimate the timing of Neogene erosion and sedimentation and consequently the exhumation of a pre-existing deep weathering. Byrkjeland *et al.* (2000) demonstrated that large Pleistocene wedges (i.e. rapidly accumulating depocentres) also attract seismicity (see also Fejerskov & Lindholm 2000). This occurs even in oceanic crust, which is normally aseismic, and prominent examples are provided by the Lofoten Basin and the Norway Basin. Along the coast of northern Norway there is also a parallel, shallow seismicity delineation which largely reflects extensional stress conditions (Hicks *et al.* 2000 a,b, Fjeldskaar *et al.* 2000).

Fig. 8.1a shows an ice-sheet model for the last glacial maximum (Ottesen *et al.* 2005). The major glaciations during the last 600,000 years extended all the way to the continental margin. Fig. 8.1b denotes interpreted Plio-Pleistocene depositions and erosion along the Norwegian continental margin with superimposed earthquakes (from Bungum *et al.* 2010, Kukkonen *et al.* 2010 and Olesen *et al.* in press). One dominant feature is the late Pliocene–Pleistocene Bjørnøya Fan, which is 400 km wide and up to 3.5 km thick and is, moreover, co-located with seismic activity that is higher than anywhere else in Fennoscandia (Byrkjeland *et al.* 2000), even though it is located in oceanic crust which normally is aseismic. The stress is expected to be compressional under the load and tensional features noted on the continental flanks (Stein *et al.* 1989), as also modelled by Engen & Watts (2008).

Because very recent erosion has taken place in the Vestfjorden area (Riis 1996), the crust in the greater Helgeland-Lofoten region may be flexured, which would result in coast-perpendicular extension as shown by Atakan *et al.* (1994), Bungum & Husebye (1979) and Hicks *et al.* (2002a) in the Rana, Meløy and Steigen districts. Considering that the Plio-Pleistocene loading of the relatively stiff oceanic crust causes relatively high seismicity in the Norwegian Sea, it is also likely that a comparable unloading of the coastal areas in western and northern Norway may induce earthquake activity (Olesen *et al.* in press). This scenario is likely because continental crust is generally weaker than oceanic crust. Fig. 8.1b shows that the seismicity in Norway is to a large extent located in areas of either Plio-Pleistocene erosion or sedimentation. The major exception is the Barents Sea region, which is almost void of earthquakes. This may, however, be caused by the wide area of erosion and uniform unloading, thus not creating sufficient differential stress in the crust (Bungum *et al.* 2010, Olesen *et al.* in press). We suggest that the deep weathering in the Hamarøya, Lofoten and Vesterålen areas is preserved because of the young Late Pleistocene uplift and erosion of this area. Most of the ice was transported in ice streams through Vestfjorden and Andfjorden (Fig. 8.1a) leaving the interior of the mainland and the Lofoten-Vesterålen archipelago relatively unaffected. The inland ice in this area was most likely thin and the erosion was concentrated to local cirques. Some of the palaeosurfaces on the uplifted and rotated fault blocks were therefore relatively undisturbed. The little consolidated Mesozoic

rocks were easily removed by the enormous amounts of meltwater following each glacial cycle. This interpretation is consistent with the observed deep weathering on mountainous areas of Hadseløya, Langøya and Andøya.

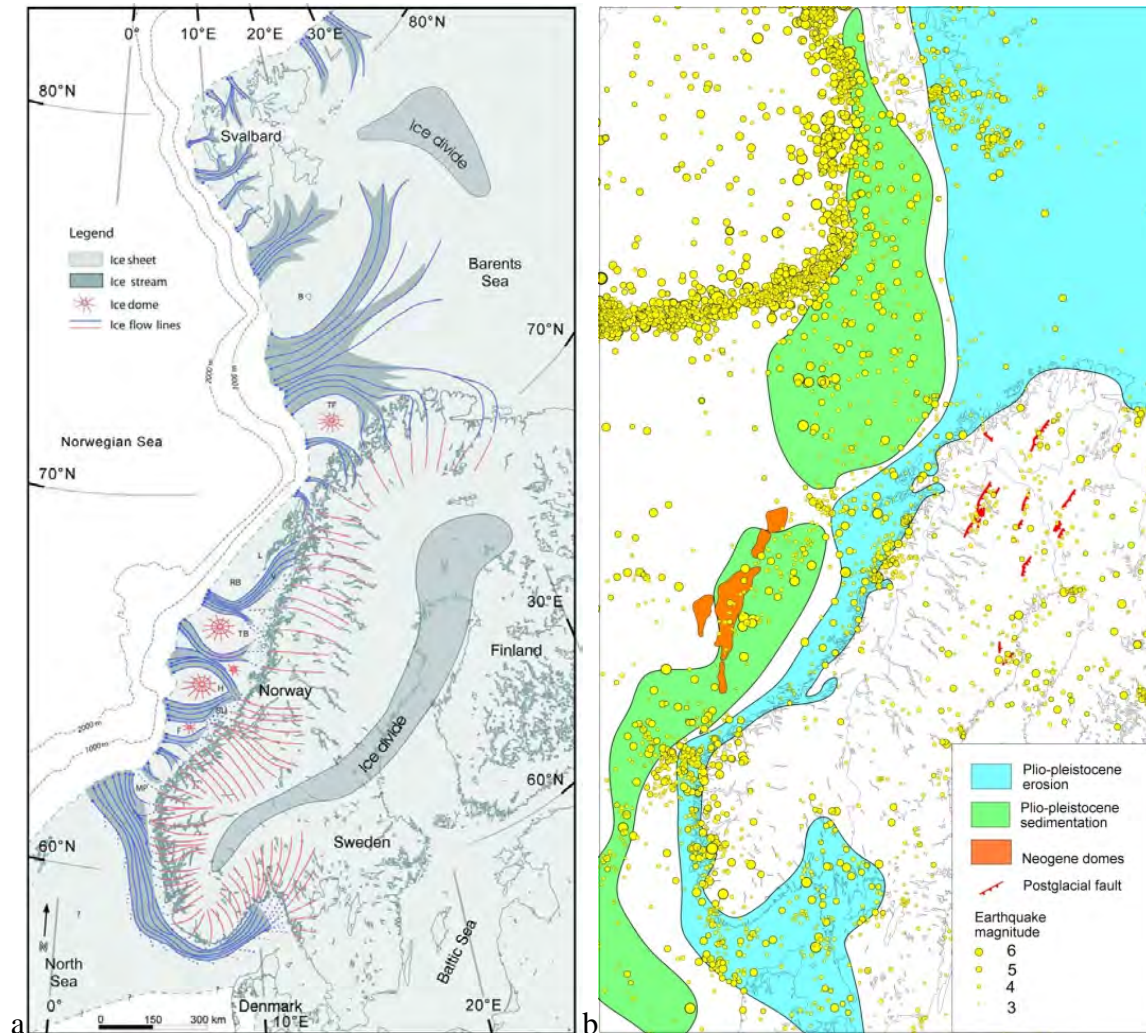


Figure 8.1 a) Ice-sheet model for the last glacial maximum (from Ottesen et al. 2005). b) Earthquakes, postglacial faults, Neogene domes and areas of interpreted Plio-Pleistocene deposition and erosion along the Norwegian continental margin (modified from Blystad et al. 1995, Riis 1996, Lidmar-Bergström et al. 1999, Bungum et al. 2000, Dehls et al. 2000b). The areas of Plio-Pleistocene sedimentation and erosion are coinciding with present-day seismicity indicating that recent loading/unloading is causing flexuring and faulting in the lithosphere. The major exception is the Barents Sea region, which is almost devoid of earthquakes. This may, however, be caused by the wide area of erosion and uniform unloading not creating sufficient differential stress in the crust (Bungum et al. 2010, Olesen et al. in press). Focal-plane solutions (Dehls et al. 2000b, Hicks et al. 2000b) indicate dominating compressional events in the areas with loading while the regions with recent unloading have dominating extensional or strike-slip events (Fig. 8.2).

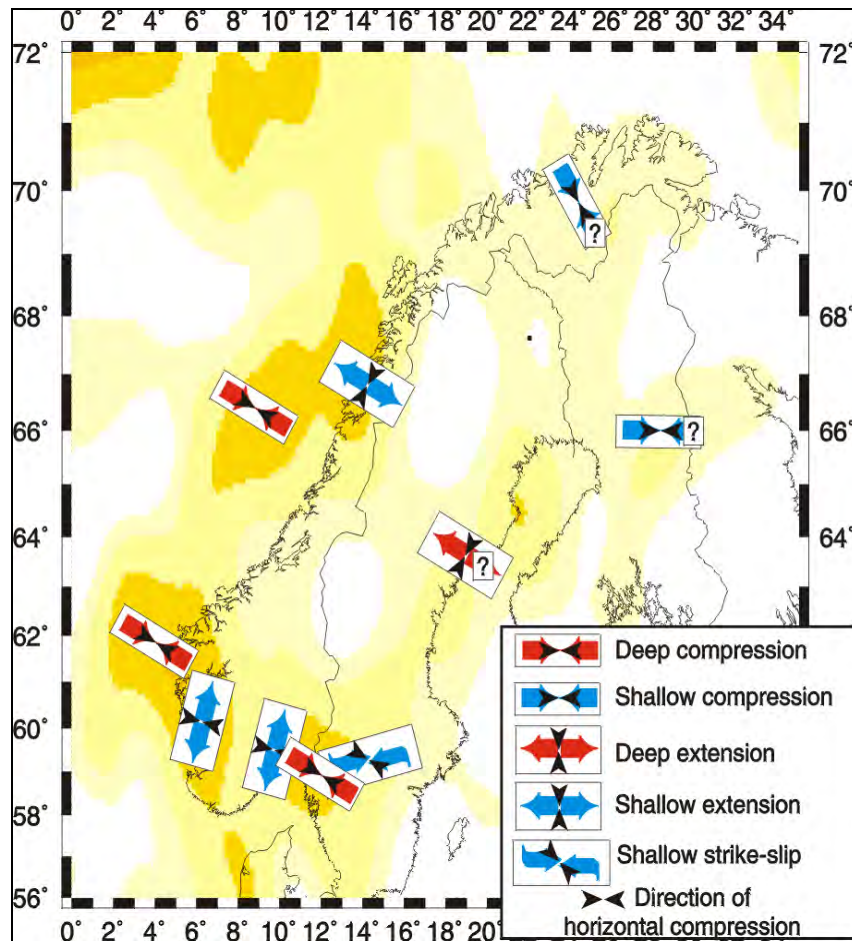


Figure 8.2 Contemporary stress directions, type of faulting and focal depth synthesised from earthquake focal mechanisms and *in situ* stress measurements (Fjeldskaar *et al.* 2000). Areas of sparse data are indicated with question marks. Intensity of yellow colour indicates intensity of seismicity. Regions under compression seem to coincide with areas of Plio-Pleistocene loading, whereas regions under extension agree fairly well with erosional areas.

A similar model is also applicable for the Oslofjord-Sørlandet region where there is an abundance of reported locations of deep weathering (Sections 5.1 and 5.2 and Chapter 7 in the present report). The erosion of the Mesozoic cover in this region was also dependent on means of transportation. The ice stream in the Norwegian Channel (Fig. 8.1a) that was established in the Late Pleistocene provided both the erosion agent and the transportation mechanism for the eroded Mesozoic rocks which accumulated as sedimentary wedges along the Møre margin (the North Sea Fan). We therefore suggest that a model similar to that for the greater Vestfjorden-Andfjorden region can be applied for the Oslofjord-Sørlandet region, the main difference being the location relative to the active rifting in the North Sea and the Norwegian Sea. The greater Vestfjorden region constitutes a part of the Mesozoic rift system with an abundance of uplifted and rotated fault blocks (Blystad *et al.* 1995, Løseth & Tveten 1996, Olesen *et al.* 1997, 2002,

Bergh *et al.* 2007) whilst the Oslofjord-Sørlandet region was located in the flat-lying hinterland. Consequently, we find the remnants of deep weathering on rotated fault blocks in Lofoten-Vesterålen whilst similar regoliths occur in the relatively gentle landscape along the coast of southern Norway. The Vågsøy, Stad and Inderøya areas were most likely uplifted and exposed to intensive erosion at an earlier stage (e.g. in the Late Miocene og Early Pliocene during the deposition of the Utsira and Molo formations (Riis 1996, Eidvin *et al.* 2007).

9 CONCLUSIONS

- 1) Deeply weathered fracture zones extend to a depth of more than 200 m in Norway. This conclusion is supported by geophysical studies (2D resistivity and refraction seismic) and observations of clay-rich fracture zones in tunnels.
- 2) Geophysical studies also reveal more continuous saprolite layers with a thickness up to 100 metres in Vestfold, Lofoten-Vesterålen, Hamarøya and Varangerhalvøya.
- 3) XRF analysis and mass balance calculations show a high degree of mineral alteration with bulk leaching of main elements (Si, Al, Na and K) in the range of 30 - 65%. The upper range can be considered indicative of intense weathering.
- 4) The porosity and permeability of the grus weathering at Vestvågøya in Lofoten were measured to 24.3 % and c. 300 mD, respectively.
- 5) It is difficult to assign a definitive age to the weathering in Norway based on weathering characteristics, position in the terrain or bedrock type. The best evidence for a Mesozoic age is the correlation of 'envelope surfaces' of topography and the fact that these dip down under Mesozoic strata offshore Norway
- 6) Even though most of the investigated saprolites appear young, their formation was probably preconditioned by processes in the Mesozoic. The partial or total alteration of bedrock to grus aggregates and clay minerals is to a large extent the result of chemical weathering caused by percolating acidic groundwater in a humid climate, most probably during tropical to sub-tropical conditions in the Mesozoic.
- 7) The degree of weathering varies extensively within several of the investigated sites. An offshore petroleum reservoir consisting of weathered basement rocks is most likely equally heterogeneous.
- 8) The deep weathering in the Lofoten-Vesterålen and Hamarøya areas most likely occurs on surfaces of basement rocks in rotated fault blocks, whereas the weathering in southeastern Norway and eastern Finnmark seems to occur in a stable and more distal area relative to the Mesozoic rift basins.
- 9) The landscape of southeastern Norway and eastern Finnmark is dominated by palaeosurfaces (paleic surface) with glacially eroded inselbergs consisting of competent rocks such as quartzite and gabbro.
- 10) Some of the alpine terrains in Norway such as Jotunheimen, Rondane, Dovrefjell, Lyngen and Øksfjord-Stjernøy-Seiland most likely represent glacially eroded inselbergs.

11) Deep weathering processes may explain some of the anomalous high concentrations of heavy metals and REE in Fennoscandian till.

10 RECOMMENDATION FOR FURTHER WORK

- 1) Detailed study of the Ramså Basin using geophysical techniques such as reflection seismic, helicopter EM and airborne FTG (full tensor gravity), and chemical and mineralogical studies of existing drill cores.
- 2) Establish a regional project to sample and analyse till in eastern Norway, Trøndelag and Finnmark. The chemistry and mineralogy of the till should be compared with the results from the Lito Project to unravel the possible content of deep-weathering material.
- 3) Establish a research project within the MINFORSK programme to improve the understanding of deep weathering processes in Norway and consequently improve the geophysical and geochemical exploration techniques for mineral resources.
- 4) Continue airborne geophysical mapping of the coastal areas of Norway to map the extent of deep-weathered bedrock.
- 5) Mineralogical and chemical studies of the weathered schistose rocks in the Nord-Trøndelag region (reported in Section 5.3.3 in the present report).
- 6) Geophysical and geological studies of extensive grus weathering observed in the Misvær area to the southeast of Bodø (P. Ihlen, pers. comm. 2012).

Acknowledgements

This study was funded by the Norwegian Petroleum Directorate and the Geological Survey of Norway. Alf Olav Larsen carried out the XRD-analyses on samples from the Lista area. Consulting Engineer Ragnar Hagen in Måløy and Maria Göthfors, Bergab Berggeologiska Undersökningar AB in Gothenburg, provided data on drillcores from construction sites for the Mehuken wind power park. Bart Hendriks at NGU participated in the sampling of the deep weathering material in northern Norway and tested different isotope dating methods. David Roberts read the report and corrected the English text. We express our thanks to these institutions and persons.

11 REFERENCES

- ABEM 1999: *ABEM Terrameter SAS 4000/SAS 1000. Instruction Manual*. ABEM Printed Matter 93101. ABEM, Sweden.
- Acworth, R.I. 1987: The development of crystalline basement aquifers in a tropical environment. *Quarterly Journal of Engineering Geology* 20, 265-272.
- Ahlmann, H.W. 1919: Geomorphological studies in Norway. *Geografiska annaler* 1, 151-205.
- Ahnert, F. 1998: *Introduction to geomorphology*. John Wiley and Sons, Chichester, 352 pp.
- Alnæs, L. & Hillestad, G. 1989: Preliminary investigation on Kaolinite in the Komagelv valley, Finnmark. *Norges geologiske undersøkelse Report 89.002*, 83 pp.
- Amos, B.J. & Greenbaum, D. 1989: Alteration detection using TM imagery: The effects of supergene weathering in an arid climate. *International Journal of Remote Sensing* 10, 515-527.
- Amundson, R., Richter, D.D., Humphreys, G.S., Jobbágy, E.G. & Gaillardet, J. 2007: Coupling between biota and Earth materials in the Critical Zone. *Elements* 3, 327-332
- Andersen, B.G.: 1960: Sørlandet i sen- og postglasial tid. *Norges geologiske undersøkelse* 210, 142 pp.
- Anderson, S.P., von Blanckenburg, F. & White A.F. 2007: Physical and chemical controls on the critical zone. *Elements* 3, 315-319
- Atakan, K., Lindholm, C.D. & Havskov, J. 1994: Earthquake swarm in Steigen, northern Norway: an unusual example of intraplate seismicity. *Terra Nova* 6, 180-194.
- Banks, D., Solbjørg, M.L. & Rohr-Torp, E. 1992a: Permeability of fracture zones in a Permian granite. *Quarterly Journal of Engineering Geology* 25, 377-388.
- Banks, D., Rohr-Torp, E. & Skarphagen, H. 1992b: An integrated study of a Precambrian granite aquifer, Hvaler, southeastern Norway. *Norges geologiske undersøkelse Bulletin* 422, 47-66.
- Banks, D., Rohr-Torp, E. & Skarphagen, H. 1994: Groundwater resources in hard rock; experiences from the Hvaler study, southeastern Norway. *Applied Hydrogeology* 2/94, 33-42.
- Barth, T.F.W. 1939a: Norske mineraler av Beidellit-gruppen. *Norsk Geologisk Tidsskrift* 19, 300-310.
- Barth, T.F.W. 1939b: Geomorphology of Vest-Agder Fjord-Land. *Norsk Geografisk Tidsskrift* 7, 34-48
- Barton, N. 2007: *Rock quality, seismic velocity, attenuation and anisotropy*. Taylor & Francis Group. London, 729 pp.
- Beard, L.P. & Lutro, O. 2000: Airborne geophysics and infrastructure planning – A case study. *Journal of Environmental and Engineering Geophysics* 5, 1-10.
- Bergh, S.G., Eig, K., Kløvjan, O.S., Henningsen, T., Olesen, O. & Hansen, J.A. 2007: The Lofoten-Vesterålen continental margin: a multiphase Mesozoic- Palaeogene rifted shelf as shown by offshore-onshore brittle fault-fracture analysis. *Norwegian Journal of Geology* 87, 29-58. ISSN 029-196X.

- Bergseth, H., Låg, J. & Tungesvik, K. 1980: Smectite formed as a weathering product of granite at Holmsbu, southern Norway. *Norsk Geologisk Tidsskrift* 60, 279-281.
- Bingen, B., Birkeland, A., Nordgulen, Ø. & Sigmond, E.M.O. 2001: Correlation of supracrustal sequences and origin of terranes in the Sveconorwegian orogen of SW Scandinavia: SIMS data on zircon in clastic sediments. *Precambrian Research* 108, 293-318.
- Bjørlykke, H. 1929: Jordbunnen på Lista. *Meldinger fra Norges Landbrukshøiskole IX* (3), 76 pp.
- Blystad, P., Brekke, H., Færseth, R.B., Larsen, B.T., Skogseid, J. & Tørudbakken, B. 1995: Structural elements of the Norwegian continental shelf, Part II. The Norwegian Sea Region. *Norwegian Petroleum Directorate Bulletin* 8, 45 pp.
- Bollingmo, P. 1999: 'Romeriksporten'. Kursdagene ved NTNU, Konferanse om trafikktunneler, Trondheim.
- Bonow, J., Lidmar-Bergström, K. & Näslund, J.-O. 2003: Palaeosurfaces and major valleys in the area of Kjølén Mountains, southern Norway - consequences for uplift and climate change. *Norwegian Journal of Geography* 57, 83-101.
- Bonow, J.M., Lidmar-Bergström, K., Japsen, P., Chalmers, J.A. & Green, P.F. 2007: Elevated erosion surfaces in central West Greenland and southern Norway: their significance in integrated studies of passive margin development. *Norwegian Journal of Geology* 87, 197-206. ISSN 029-196X.
- Brantley, S.L., Goldhaber, M.B. & Ragnarsdottir, K.V. 2007: Crossing disciplines and scales to understand the critical zone. *Elements* 3, 307-314
- Brimhall, G.H., Alpers, C.N. & Cunningham, A.B. 1985: Analysis of supergene ore-forming processes and ground water solute transport using mass balance principles. *Economic Geology* 80, 1227-1256
- Brimhall, G.H. & Dietrich, W.E. 1987: Constitutive mass balance relations between chemical composition, volume, density, porosity, and strain in metasomatic hydrochemical systems: Results on weathering and pedogenesis. *Geochimica et Cosmochimica Acta* 51, 567-587.
- Buckingham, W.F. & Sommer, S.E. 1983: Mineralogical characterization of rock surfaces formed by hydrothermal alteration and weathering; application to remote sensing. *Economic Geology* 78, 664-674.
- Bugge, C. 1917: Kongsbergfeltets geologi. *Norges geologiske undersøkelse* 82, 272 pp.
- Butler, J.R. 1954: The *geochemistry and mineralogy* of rock weathering. 2: the Nordmarka area, Oslo. *Geochimica et Cosmochimica Acta* 6, 268-281.
- Bungum, H. & Husebye, E.S. 1979: The Meløy, northern Norway, earthquake sequence - a unique intraplate phenomenon. *Norsk Geologisk Tidsskrift* 59, 189-193.
- Bungum, H., Lindholm, C.D., Dahle, A., Woo, G., Nadim, F., Holme, J.K., Gudmestad, O.T., Hagberg, T. & Karthigeyan, K. 2000: New seismic zoning maps for Norway, the North Sea and the UK. *Seismological Research Letters* 71, 687-697.
- Bungum, H., Olesen, O., Pascal, C., Gibbons, S., Lindholm, C.D. & Vestøl, O. 2010: To what extent is the present seismicity of Norway driven by postglacial rebound? *Journal of the Geological Society, London* 167, 373-384.

- Byrkjeland, U., Bungum, H. & Eldholm, O. 2000: Seismotectonics of the Norwegian continental margin. *Journal of Geophysical Research* 105, 6221–6236.
- Bøe, R. 1989: A pre-Devonian pediment in the lowermost Old Red Sandstone Hitra Group, Western Norway. *Norsk Geologisk Tidsskrift* 69, 21-28.
- Bøe, R. & Bjerkli, K. 1989: Mesozoic sedimentary rocks in Edøyfjorden and Beitstadfjorden, Central Norway: Implications for the structural history of the Møre-Trøndelag fault zone. *Marine Geology* 87, 287-299.
- Bøe, R., Fossen, H. & Smelror, M. 2010: Mesozoic sediments and structures onshore Norway and in the coastal zone. *Norges geologiske undersøkelse Bulletin* 450, 15-32.
- Carstens, H. 2011: Reservoaranalog – midt inne i skauen. *GEO* 14, 8, 10-15.
- Chadwick, O.A., Brimhall, G.H. & Hendricks, D.M. 1990: From a black to a gray box - A mass balance interpretation of pedogenesis. *Geomorphology* 3, 369-390.
- Chroston, P.N. & Brooks, S.G. 1989: Lower crustal seismic velocities from Lofoten–Vesterålen, North Norway. *Tectonophysics* 157, 251– 269.
- Clark, D. A. 1997: Magnetic petrophysics and magnetic petrology: aids to geological interpretation of magnetic surveys. *AGSO Journal of Geology & Geophysics* 17, 83-103.
- Cunningham, C.G., Rye, R.O., Rockwell, B.W., Kunk, M.J. & Councell, T.B. 2005: Supergene destruction of a hydrothermal replacement alunite deposit at Big Rock Candy Mountain, Utah: mineralogy, spectroscopic remote sensing, stable-isotope, and argon-age evidence. *Chemical Geology* 215, 317-337
- Dahl, E. 1948: Studier over forvitringstyper i strøket Nordfjord-Sunnmøre, og deres relasjon til istidene. *Norsk Geologisk Tidsskrift* 27, 242–244.
- Dahl, E 1954: Weathered gneisses at the island of Runde, Sunnmøre, Western Norway and their geological interpretation. *Nytt Magasin for Botanikk* 3, 5-23
- Dahl, E. 1987: The nunatak theory reconsidered. *Ecological Bulletins* 38, 77-94.
- Dahl, E. 1992: Nunatakkeori: IV. Hvor fantes isfrie områder og hva slags planter kunne leve på dem? *Blyttia* 1, 115-137.
- Dahl, R. 1961: Refugieproblemet og de kvartærgeologiske metodene. *Svensk Naturvetenskap* 14, 81-96
- Dahl, R. 1966: Block fields, weathering pits and tor-like forms in the Narvik mountains, Nordland, Norway. *Geografiske Annaler Ser. A.48* (2), 55-85.
- Dahl, R., Sveian, H. & Thoresen, M.K. 1997: *Nord-Trøndelag og Fosen – geologi og landskap*. Norges geologiske undersøkelse, Trondheim, 136 pp.
- Dahlin, T. 1993: *On the automation of 2D resistivity surveying for engineering and environmental applications*. PhD thesis, Department of Engineering Geology, Lund Institute of Technology, Lund University. 187 pp, ISBN 91-628-1032-4.
- Dalsegg, E., Olesen, O. & Sandstad, J.S. 1986: Geofysiske og geologiske undersøkelser av et sulfidmineralisert område ved Riednjav'ri, Kautokeino, Finnmark. *NGU Report* 85.061, 32 pp.
- Dalsegg, E. 1987: Geofysiske bakkemålinger Sargejåk-Vest, Karasjok, Finnmark. *NGU Report* 87.145, 22 pp.

- Davidsen, B., Sommaruga, A. & Bøe, R. 2001: Final Report: Sedimentation, tectonics and uplift in Vesterålen. Phase 1 – Localizing near-shore faults and Mesozoic sediment basins. *NGU Report 2001.111*, 16 pp.
- Dehls, J.F., Olesen, O., Olsen, L. & Blikra, L.H. 2000a: Neotectonic faulting in northern Norway; the Stuoragurra and Nordmannvikdalen postglacial faults. *Quaternary Science Reviews* 19, 1447-1460.
- Dehls, J.F., Olesen, O., Bungum, H., Hicks, E., Lindholm, C.D. & Riis, F. 2000b: Neotectonic map, Norway and adjacent areas 1:3 mill. *Geological Survey of Norway, Trondheim*.
- Dixon, J.C. & Thorn, C.E. 2005: Chemical weathering and landscape development in mid-latitude alpine environments. *Geomorphology* 67(1-2), 127-145.
- Dixon, J. C., Campbell, S. W., Thorn, C. E. & Darmody, R. G. 2006: Incipient weathering rind development on introduced machine-polished granite discs in an Arctic alpine environment, northern Scandinavia. *Earth Surface Processes and Landforms* 31(1), 111-121.
- Dixon, J.L., Heimsath, A.M. & Amundson, R. 2009: The critical role of climate and saprolite weathering in landscape evolution. *Earth Surface Processes and Landforms*, 34(11), 1507-1521.
- Doré, A.G. 1992: The base Tertiary surface of southern Norway and the northern North Sea. *Norsk Geologisk Tidsskrift* 72, 259–265.
- Ebbing, J., Skilbrei, J.R. & Olesen, O. 2007: The magmatic system of the Oslo Graben revealed by forward and inverse modeling of potential fields. *Journal of Geophysical Research* 112, B04404, doi:10.1029/2006JB004694.
- Eggleton, R.A. (Ed.) 2001: *The regolith glossary: Surficial geology, soil and landscapes*. CRC LEME, Perth, 86 pp.
- Eidvin, T., Bugge, T. & Smelror, M. 2007: The Molo Formation, deposited by coastal progradation on the inner Mid-Norwegian continental shelf, coeval with the Kai Formation to the west and the Utsira Formation in the North Sea. *Norwegian Journal of Geology* 87, 75-142.
- Elmore, R. D., Burr, R., Engel, M. & Parnell, J. 2010: Paleomagnetic dating of fracturing using breccia veins in Durness Group carbonates, NW Scotland. *J. Struct. Geology* 32, 1933-1942.
- Elvebakk, H. 2011: Sammenstilling av resistivitet, seismiske hastigheter og naturlig gammastråling i norske bergarter. *NGU Rapport 2011.042*, 60 pp.
- Engen, Ø. & Watts, A.B. 2008: Submarine fans on the western Barents Sea continental margin— A test of the Earth's response to young sediment loads. Poster. *European Geosciences Union General Assembly, Vienna, 13–18 April 2008, Abstract No. EGU2008-A-03471*.
- Englund, J.O. & Jørgensen, P. 1975: Weathering and hydrogeology of the Brumunddal sandstone, Southern Norway. *Nordic Hydrology* 6 (1), 43–62
- Fejerskov, M. & Lindholm, C.D. 2000: Crustal stress in and around Norway; an evaluation of stress-generating mechanisms. In Nøttvedt, A., Brekke, H., Birkeland, Ø., *et al.* (eds.)

- Dynamics of the Norwegian Margin*. Geological Society, London, Special Publications, 167, 451–467.
- Fenner, J. 1988: Occurrences of pre-Quaternary diatoms in Scandinavia reconsidered. *Meyniana* 40, 133-141.
- Fjeldskaar, W., Lindholm, C.D., Dehls, J.F. & Fjeldskaar, I. 2000: Postglacial uplift, neotectonics and seismicity in Fennoscandia. *Quaternary Science Reviews* 19, 1413-1422.
- Fjellanger, J. & Etzelmüller, B. 2003: Stepped palaeosurfaces in southern Norway: Interpretation from DEM-derived topographic profiles. *Norwegian Journal of Geography* 57, 102-110.
- Fjellanger, J. & Sørbel, L. 2007: Origin of the palaeic landforms and glacial impact on the Varanger Peninsula, northern Norway. *Norwegian Journal of Geology* 87, 223-238
- Fjellanger, J. & Nystuen, J.P. 2007: Diagenesis and weathering of quartzite at the palaeic surface on the Varanger Peninsula, northern Norway. *Norwegian Journal of Geology* 87, 239-251.
- Fjellanger, J., Sørbel, L., Linge, H., Brook, E.J., Raisbeck, G.M. & Yiou, F. 2006: Glacial survival of blockfields on the Varanger Peninsula, northern Norway. *Geomorphology* 82 (3-4), 255-272.
- Fugelli, E.M.F. 1992: Clay minerals in some samples from Opstad and Høgemork on Jæren, southwest Norway. *Norsk Geologisk Tidsskrift* 72, 217-219.
- Fugro Airborne Surveys 2003: Logistics report, fixed-wing borne magnetic, radiometric and VLF-EM survey in the Oslo region, southern Norway. *Report FCR 2241*, 124 pp.
- Geosoft 2004: *OASIS Montaj v6.0 Mapping and processing system, The core software platform for working with large volume spatial data. Quick start tutorials*. Geosoft Incorporated, 258 pp.
- Geosoft 2005a: *Montaj GridKnit, Grid extension for OASIS Montaj v6.1, Tutorial and user guide*, Geosoft Incorporated, 27 pp.
- Geosoft 2005b: *Montaj MAGMAP filtering, 2-D frequency domain processing of potential field data, Extension for Oasis Montaj v6.1*. Geosoft Incorporated, 66 pp.
- Gerrard, A.J. 1988: *Rocks and landforms*. Allen & Unwin, London, Boston, 319 pp.
- Gjelsvik, T. 1956: Pre-glaciale forvitningsfenomener i kopperforekomster i den syd-vestlige del av Finnmarksvidda. *Geologiska föreningens i Stockholm förhandlingar* 78, 659-665.
- Gjems, O. 1963: Kaolin as a weathering of Eocambrian sandstone (sparagmite) in the Rondane Mountains, East Norway. *Norsk Geologisk Tidsskrift* 43, 537-538.
- Gjessing J. 1967: Norways paleic surface *Norsk Geografisk Tidsskrift* 21, 69-13.
- Goldschmidt V.M. 1911: Die Kontakt-metamorphose in Kristianiagebiet. *Videnskapselskapets skrifter* 1, 11, 483 pp.
- Goldschmidt V.M. 1928: *Om dannelse av lateritt som forvitningsprodukt av norsk labradorsten*. (The formation of laterite as a weathering product of Norwegian labradorite). Comemorative writing for H. Sørli, Oslo. p. 21-24
- Goldstein, J., Newbury, D. E., Joy, D. C., Lyman, C. E., Echlin, P., Lifshin, E., Sawyer, L.C. & Michael, J.R. 2003: *Scanning electron microscopy and X-ray Microanalysis, 3rd Edition*. Kluwer Academic/Plenum Publishers, New York, 689 pp.

- Goodfellow B.W., Fredin O., Derron M.-H. & Stroeven A.P. 2009: Weathering processes and Quaternary origin of an alpine blockfield in Arctic Sweden. *Boreas* 38, 379-398.
- Goodfellow B.W., Hilley G.E. & Schulz M.S. 2011: Vadose zone controls on weathering intensity and depth: Observations from grussic saprolites. *Applied Geochemistry* 26, 36-39.
- Grant, F.S. 1984: Aeromagnetism, geology and ore environments, I. Magnetite in igneous, sedimentary and metamorphic rocks: an overview. *Geoexploration* 23, 303-333.
- Griffin, W.L., Taylor, P.N., Hakkinen, J.W., Heier, K.S., Iden, I.K., Krogh, E.J., Malm, O.A., Olsen, K.I., Ormaasen, D.E. & Tveten, E. 1978: Archaean and Proterozoic crustal evolution in Lofoten-Vesterålen, North Norway. *Journal of Geological Society, London* 135, 629-647.
- Gundersen, P. & Gaut, S. 2005: Grunnvann, del II. *VA-Bulletin. Nyheter og notiser fra NORVAR BA4*, 12-13.
- Grønhaug, A. 1975: *Drift av vegtunnel gjennom leirsonen i Rørvikskaret*. Intern rapport nr. 616. Vegdirektoratet, Veglaboratoriet, Oslo.
- Göthfors, M. 2010: Mehuken wind power park, mapping of drill cores from five sites for wind power plants. *Bergab – Berggeologiska Undersökningar AB Report*, 30 pp.
- Hendriks, B.W.H. & Andriessen, P.A.M. 2002: Pattern and timing of the post-Caledonian denudation of northern Scandinavia constrained by apatite fission-track thermochronology In Doré, T., Cartwright, J.A., Stoker, M.S., Turner, J.P. & White, N. (eds.) *Exhumation of the North Atlantic margin: Timing, mechanisms and implications for petroleum exploration*. Geological Society, London, Special Publications, 196, 117-137.
- Henkel, H. & Guzmán, M. 1977: Magnetic features of fracture zones. *Geoexploration* 15, 173-181.
- Henningsen, T. & Tveten, E. 1998: Geologisk kart over Norge. Berggrunnskart ANDØYA, M 1:250 000. *Norges geologiske undersøkelse, Trondheim, Norway*.
- Hicks, E., C., Bungum, H. & Lindholm, C.D. 2000a: Seismic activity, inferred crustal stresses and seismotectonics in the Rana region, northern Norway. *Quaternary Science Reviews* 19, 1423-1436.
- Hicks, E.C., Bungum, H. & Lindholm, C.D. 2000b: Stress inversion of earthquake focal mechanism solutions from onshore and offshore Norway. *Norsk Geologisk Tidsskrift* 80, 235-250.
- Hillestad, G. 1987: Seismiske målinger på Staveheia, Andøya. *NGU Report 87.041*, 8 pp.
- Hillestad, G. 1967: Seismiske målinger ved Møsjevann og Nedre Æråsvann, Andøy. *NGU Report 87.042*, 9 pp.
- Hillestad, G. & Melleby, P. 1967: Seismiske undersøkelser Risøyhamn/Andøy. *NGU Report 785A*, 9 pp.
- Hirvas, H., Lagerbäck, R., Mäkinen, K., Nenonen, K., Olsen, L., Rodhe, L. & Thoresen, M. 1988: The Nordkalott Project: Studies of Quaternary geology in northern Fennoscandia. *Boreas* 17, 431-437.

- Homan, C.H: 1890: Kaolinforekomst i Hurdalen. *Norges geologiske undersøkelse Årbok 1891*. p 89.
- Holtedahl, O. 1939: From the northern Randsfjord district. *Norsk Geografisk Tidsskrift* 7, 441-451.
- Holtedahl, O. 1953a: Norges geologi, Bind II. *Norges geologiske undersøkelse 164*, 604-606.
- Holtedahl, H. 1953b: A petrographical and mineralogical study of two high altitude soils from Trollheimen, Norway. *Norwegian Journal of Geography* 32, 191-226.
- Holtedahl, H. 1958: Den norske strandflate. *Norsk Geografisk Tidsskrift* 16, 286-303
- Holtedahl, H. 1988: Bedrock geology and Quaternary sediments in the Lista basin, S. Norway. *Norsk Geologisk Tidsskrift* 68, 1-20.
- Huseby, F.C.A. 1968: Lieråsen tunnel. Del II: Geofysiske og videre geologiske undersøkelser. *Tekniske meddelelser – NSB, Teknisk tidsskrift for Norges Statsbaner* 3. 11 pp.
- Ihlen, P.M. & Martinsen, M. 1986: Ore deposits spatially related to the Drammen granite batholith. In S. Olerud & P.M. Ihlen (eds): *Metallogeny associated with the Oslo paleorift*. Sveriges geologiska undersökning Ca 59, 38-42.
- Ihlen, P.M., Trønnes, R. & Vokes, F.M. 1982: Mineralization, wall rock alteration and zonation of ore deposits associated with the Drammen Granite in the Oslo Region, Norway. In Evans, A.M. (ed.) *Metallization associated with Acid Magmatism*. John Wiley & Sons, Chichester, 111-136.
- Isachsen, F. & Rosenquist, I.Th. 1949: Forvittringsleire og blekejord på Karmøy. *Norsk Geologisk Tidsskrift* 27, 175-186
- Itaya, T., Arribas, Jr.A. & Okada, T. 1996: Argon release systematic of hypogene and supergene alunite based on progressive heating experiments from 100 to 1000°C. *Geochimica et Cosmochimica Acta* 60, 4525-4535.
- Japsen, P., Bidstrup, T. & Lidmar-Bergström, K. 2002: Neogene uplift and erosion of southern Scandinavia induced by the rise of the South Swedish Dome In Doré, A.G., Cartwright, J.A., Stoker, M.S., Turner, J.P., and White, N.J. (eds.) *Exhumation of the North Atlantic Margin: Timing, mechanisms and implications for petroleum exploration*. Geological Society, London, Special Publications 196, 183-207.
- Japsen, P., Bonow, J.M., Chalmers, J.A. & Rasmussen, E.S. 2008: Norges fjelde - rodløse realiteter. *Geologisk Nyt* 2, 38-40.
- Jensen, L.N. & Schmidt, B.J. 1972: *Kjemisk forvitring i prekambriske, kambro-silurske og permiske bergarter i Numedalen*. Thesis Institute of Limnology Universitetet i Oslo.
- Jørgensen, P. 1964: Mineralogical composition of two Silurian bentonite beds from Sundvollen, southern Norway. *Norsk Geologisk Tidsskrift* 44, 227-234
- Kirkemo, K. 2000: Tunneldrift for 88 år siden. *GEO* 5, 40-41
- Kleman, J. 1994: Preservation of landforms under ice sheets and ice caps. *Geomorphology* 9, 19-32.
- Kleman, J. & Hättestrand, C. 1999: Frozen-bed Fennoscandian and Laurentide ice sheets during the Last Glacial Maximum. *Nature* 402 (6757), 63-66.

- Kleman, J., Stroeven, A.P. & Lundqvist, J. 2008: Patterns of Quaternary ice sheet erosion and deposition in Fennoscandia and a theoretical framework for explanation, *Geomorphology* 97(1-2), 73- 90.
- Kocheise, R.-C. 1994: *Svelleleire i undersjøiske tunneler*. Ph.D. thesis, Norwegian University of Science and Technology, Trondheim, Norway, 420 pp.
- Larsen, E. & Longva, O. 1979: *Jordartskartlegging, glacialgeologi og kvartær stratigrafi på Stad og Vågsøy, ytre Nordfjord*. Cand. real thesis, Univ. of Bergen, 305 pp.
- Larsen, M.L. 1990: Riksvei 108, Hvalertunnelen, geologisk sluttrapport. *Statens Vegvesen, Østfold Report 88/3744*, 31 pp.
- Lidmar-Bergström, K. 1982: Pre-Quaternary geomorphological evolution in southern Fennoscandia. *Sveriges Geologiska Undersökning C785/Meddelanden från Lunds Universitets Geografiska Institution, Avhandlingar XCI*, 202 pp.
- Lidmar-Bergström, K. 1988: Preglacial weathering and landform evolution in Fennoscandia. *Geografiska Annaler, Serie A. 70*, 273-276.
- Lidmar-Bergström, K. 1989: Exhumed Cretaceous landforms in south Sweden. *Zeitschrift für Geomorphologi, N.F. Suppl. 72*, 21-40.
- Lidmar-Bergström, K. 1995: Relief and saprolites through time on the Baltic Shield. *Geomorphology* 12, 45-61.
- Lidmar-Bergström, K. 1999: Uplift histories revealed by landforms of the Scandinavian domes. In Smith, B.J., Whalley, W.B. & Warke, P.A. (eds.) *Uplift, erosion and stability: Perspectives on long-term landscape development*. Geological Society, London, Special Publications 162, 85-91.
- Lidmar-Bergström, K. & Näslund, J. 2005: Fennoscandia – Major landforms and bedrock. In Seppälä, M. (ed.): *The Physical Geography of Fennoscandia*. The Oxford Regional Environments Series, Oxford University Press, 3-16.
- Lidmar-Bergström, K. & Bonow, J.M. 2009: Hypotheses and observations on the origin of the landscape of southern Norway - A comment regarding the isostasy-climate-erosion hypothesis by Nielsen *et al.* 2008, *Journal of Geodynamics*, 48 (2), 95-100.
- Lidmar-Bergström, K., Olsson, S. & Olvmo, M. 1997: Palaeosurfaces and associated saprolites in Southern Sweden. In Widdowson, M. (ed.) *Palaeosurfaces: Recognition, Reconstruction and Interpretation*. Geological Society of London Special Publications 120, 95–123.
- Lidmar-Bergström, K., Olsson, S. & Roaldset, E. 1999: Relief features and palaeoweathering remnants in formerly glaciated Scandinavian basement areas. In Thiry, M. & Simon-Coinçon, R. (eds.) *Palaeoweathering, palaeosurfaces and related continental deposits*. International Association of Sedimentologists (IAS) Special publication 27, 275-301.
- Lidmar-Bergström, K., Ollier, C.D. & Sulebak, J.R. 2000: Landforms and uplift history of Southern Norway. *Global and Planetary Change* 24, 211–231.
- Lidmar-Bergström, K., Näslund, J.O., Ebert, K., Neubeck, T. & Bonow, J.M. 2007: Cenozoic landscape development on the passive margin of northern Scandinavia, *Norwegian Journal of Geology* 87 (1-2), 181-196.

- Lindahl, I. 1983: Classification of uranium mineralization in Norway. *Norges geologiske undersøkelse* 380, 125-142.
- Lipponen, A. & Airo, M.-L. 2006: Linking regional-scale lineaments to local-scale fracturing and groundwater inflow into the Pääjänne water-conveyance tunnel, Finland. *Near Surface Geophysics 2006*, 97-111.
- Loke, M.H. 2007: *RES2INV ver. 3.56. Geoelectrical Imaging 2D & 3D. Instruction manual.* www.geoelectrical.com.
- Lundin, E., Olesen, O., Kihle, O. & Skilbrei, J.R. 2005: Interpretation of the magnetic anomaly pattern in the Oslo region. *NGU Report 2005.044*, 43 pp.
- Lutro, O. & Nordgulen, Ø. 2004: *Oslofeltet, berggrunnskart, 1.250.000*, Norges geologiske undersøkelse, Trondheim.
- Løseth, H. & Tveten, E. 1996: Post-Caledonian structural evolution of the Lofoten and Vesterålen offshore and onshore areas. *Norwegian Journal of Geology* 76, 215-230.
- Låg, J. 1945: Weathering of syenite in Kjøse, Vestfold. *Norsk Geologisk Tidsskrift* 25, 216-224.
- Låg, J. 1948: Undersøkelser over opphavsmaterialet for Østlandets morenedekker. *Meddelelser fra Det norske Skogforsøksvesen* 10, 223 pp. (p. 79-84 & 194)
- Låg, J. 1963: Notes on geological features of importance for the productivity of the soils of Norway. *Soil Science* 95, 1-8.
- Malmström, B. & Palmer, O. 1984: Glacial och periglacial geomorfologi på Varangerhalvön, Nordnorge. *Medd. Lunds Univ. Geogr. Inst. Avh.* 39, 351 pp.
- Mangerud, J. 1973: Isfrie refugier i Norge under istidene. *Norges geologiske undersøkelse* 297, 1-23
- Markgren, M. 1962: *Detaljmorfologiska studier i fast berg och blockmaterial. I. Vittringsprosesser.* Svensk Geografisk Årsbok, Lund.
- McQueen, K.G. 2008: *A guide for mineral exploration through the regolith in the Cobar Region, Lachlan Orogen, New South Wales.* Cooperative Research Centre for Landscape Environments and Mineral Exploration (CRC LEME) Explorers' Guide Series, Australian National University, Canberra, 110 pp.
- Migon, P. 1997: Palaeoenvironmental significance of grus weathering profiles: a review with special reference to northern and central Europe. *Proceedings of the Geologists' Association.* J08, 57-70
- Migon, P. & Thomas, M.F. 2002: Grus weathering mantles - problems of interpretation, *Catena*, 49 (1-2), 5-24.
- Migon, P. & Lidmar-Bergström, K. 2001: Weathering mantles and their significance for geomorphological evolution of central and northern Europe since the Mesozoic. *Earth-Science Reviews*, 56 (1-4), 285-324.
- Migon, P. & Lidmar-Bergström, K. 2002: Deep weathering through time in central and northwestern Europe: problems of dating and interpretation of geological record. *Catena* 49, 25-40.
- Moen, K. 2007: Ras på stuff i Ravneheitunnelen, Fjellsprengningsteknikk, bergmekanikk og geoteknikk 2007, 5.1-5.19.

- Mogaard, J.O., Olesen, O., Rønning, S. & Blokkum, O. 1988: Geofysiske målinger fra helikopter over Langøya, Vesterålen. *NGU Report 88.151*, 32 pp.
- Moore, D. & Reynolds, Jr., R. C. 1997: *X-Ray diffraction and the identification and analysis of clay minerals, 2nd ed.* Oxford University Press, New York.
- Møller, J.J. & Sollid, J.L. 1973: Geomorfologisk kart over Lofoten – Vesterålen. *Norsk Geologisk Tidsskrift* 27, 195-205.
- Mørk, M.B.E., Vigran, J.O., Smelror, M., Fjerdingsstad, V. & Bøe, R. 2003: Mesozoic mudstone compositions and the role of kaolinite weathering – shallow cores in the Norwegian Sea (Møre to Troms). *Norwegian Journal of Geology* 83, 61-78.
- Nesbitt, H.W. & Young, G.M. 1989: Formation and diagenesis of weathering profiles. *Journal of Geology* 97, 129-147.
- Nesje, A. 1988: Block fields in southern Norway: significance for the late Weichselian ice sheet. *Norsk Geologisk Tidsskrift* 68, 149-169
- Nettleton, W.D., Flach, K.W. & Nelson, R.E. 1970: Pedogenic weathering of tonalite in Southern California. *Geoderma* 4, 387-415.
- Neuman, H. 1985: Norges Mineraler. *Norges geologiske undersøkelse Skrifter* 68, 278 pp.
- Nielsen, S.B., Gallagher, K., Leighton, C., Balling, N., Svenningsen, L., Jacobsen, B.H., Thomsen, E., Nielsen, O.B., Heilmann-Clausen, C., Egholm, D.L., Summerfield, M.A., Clausen, O.R., Piotrowski, J.A., Thorsen, M.R., Huuse, M., Abrahamsen, N., King, C., Lykke-Andersen, H. 2009: The evolution of western Scandinavian topography: A review of Neogene uplift versus the ICE (isostasy-climate-erosion) hypothesis, *Journal of Geodynamics* 47 (2-3), 72-95.
- Nilsen, B. 1988: Norwegian sub-sea tunnels – A review with emphasis on water leakages. In Serrano, J.M. (ed.) *Proc. Int. Congr. On Tunnels and Water, Madrid, 12-15 June 1988*, Balkema, Rotterdam, 913-918.
- Often, M., Olsen, L., Lyså, A. 1990: Statusrapport over undersøkelsene i Sargejåk gullfelt, Finnmark. *Norges geologiske undersøkelse Rapport 90.045*, 120 s.
- Olaussen, S., Larsen, B.T. & Steel, R. 1994: The upper Carboniferous-Permian Oslo Rift; basin fill in relation to tectonic development, *Canadian Society of Petroleum Geologists, Memoir* 17, 175-197.
- Olerud, S. & Ihlen, P.M. (eds) 1986: Metallogeny associated with the Oslo Paleorift. 7th IAGOD Symposium and Nordkalott Project Meeting, Excursion guide no. 1. *Sveriges geologiska undersökning Serie Ca. 59*, 52 pp.
- Olesen, O. 2004a: Problemene skyldes dypforvitring. *GEO* 7, 18-20.
- Olesen, O. 2004b: Ny metode for kartlegging av dypforvitring. *GEO* 7, p. 20.
- Olesen, O. 2006: Aktsomhetskart for tunnelplanlegging, Østlandsområdet, Geofysisk tolkning av dypforvitring, M 1:100.000. *Norges geologiske undersøkelse*, Trondheim.
- Olesen, O. & Rønning, J.S. 2008: Deep weathering: The climate of the past causes tunnel problems. In Slagstad, T. & Dahl, R. (eds.) *Geology for society for 150 years – The legacy after Kjerulf*. Gråsteinen 13, 101-110.

- Olesen, O., Lundin, E., Nordgulen, Ø., Osmundsen, P.T., Skilbrei, J.R., Smethurst, M.A., Solli, A., Bugge, T. & Fichler, C. 2002: Bridging the gap between the Nordland onshore and offshore geology. *Norwegian Journal of Geology* 82, 243-262.
- Olesen, O., Dehls, J.F., Ebbing, J., Henriksen, H., Kihle, O. & Lundin, E. 2007: Aeromagnetic mapping of deep-weathered fracture zones in the Oslo Region – a new tool for improved planning of tunnels. *Norwegian Journal of Geology* 87, 253-267.
- Olesen, O., Bungum, H., Lindholm, C., Olsen, L., Pascal, C. & Roberts, D. in press: Neotectonics, seismicity and contemporary stress field in Norway – mechanisms and implications. In: L. Olsen, L. (ed.) *Quaternary Geology of Norway*. Norges geologiske undersøkelse Special Publications, Trondheim, Norway.
- Olsen, L. 1985: Quaternary palaeosols in Norway – examples from selected areas. *Norges geologiske undersøkelse Bull.* 427, 12-15.
- Olsen, L. 1993: Last glaciation elucidated by dates from some localities on the Norwegian mainland. Abstract, *Geonytt* 93, p. 37.
- Olsen, L. 1998: Pleistocene paleosols in Norway: Implications for past climate and glacial erosion. *Catena* 34, 75-103.
- Olsen, L., Mejdahl, V., & Selvik, S.F. 1996: Middle and late Pleistocene stratigraphy, chronology and glacial history in Finnmark, North Norway. *Norges geologiske undersøkelse Bulletin* 429, 111 pp.
- Olsen, L., Reite, A., Riiber, K., & Sørensen, E. 1996: *Finnmark County. Map of Quaternary geology 1: 500 000 with description*. Norges geologiske undersøkelse, Trondheim.
- Ottesen, D., Dowdeswell, J.A. & Rise, L. 2005: Submarine landforms and the reconstruction of fast-flowing ice streams within a large Quaternary ice sheet: The 2500-km-long Norwegian-Svalbard margin (57° - 80°N). *Geological Society of America Bulletin* 117, 1033-1050.
- Palacky G.V. 1987: Resistivity characteristics of geologic targets. In *Electromagnetic Methods in Applied Geophysics 1, Theory*, 1351 pp.
- Palmstrøm, A., Nilsen, B., Borge Pedersen, K. & Grundt, L. 2003: Miljø- og samfunnstjenlige tunneler. Riktig omfang av undersøkelser for berganlegg. *Vegdirektoratet, Teknologiavdelingen Publikasjon* 101, 132 pp.
- Parnell, J., Watt, G., Chen, H., Wycherley, H., Boyce, A., Elmore, D., Blumstein, R.M. & Green, P. 2004: Kaolin polytype evidence for a hot-fluid pulse along Caledonian thrusts during rifting of the European Margin. *Mineral. Mag.* 68, 419–432.
- Peulvast, J.-P. 1985: In situ weathered rocks on plateaus, slopes and strandflat areas of the Lofoten-Vesterålen, North Norway. *Fennia* 163, 333-340.
- Peulvast, J.-P. 1986: Structural Geomorphology and morphological development in the Lofoten-Vesterålen area, Norway. *Norsk Geografisk Tidsskrift* 40, 135–161.
- Peulvast, J.-P. 1988: Pre-glacial landform evolution in two coastal high latitude mountains: Lofoten-Vesterålen (Norway) and Scoresby Sund area (Greenland). *Geografiska Annaler* 70A, 351–360.

- Pluijm, B.A., van der Hall, C.M., Vrolijk, P.J., Pevear, D.R. & Covey, M.C. 2001: The dating of shallow faults in the Earth's crust. *Nature* 412, 172-175.
- Polak, S., Lundin, E., Bøe, R., Lindeberg, E., Olesen, O. & Zweigel, P. 2004: Storage potential for CO₂ in the Beitstadfjord Basin, Mid-Norway. *NGU Report 2004.036*, 51 pp.
- Paasche, Ø., Strømsøe, J.R., Dahl, S.O. & Linge, H. 2006: Weathering characteristics of arctic islands in northern Norway. *Geomorphology* 82, 430-452.
- Ramberg, I.B. & Larsen, B.T. 1978: Tectonomagmatic evolution. In Dons, J.A., & Larsen, B.T. (eds.) *The Oslo Paleorift, a review and guide to excursions*. Norges geologiske undersøkelse 337, 55-73.
- Rasmussen, C., Brantley, S., Richter, D. de B., Blum, A., Dixon, J. & White, A.F. 2011: Strong climate and tectonic control on plagioclase weathering in granitic terrain. *Earth and Planetary Science Letters* 301, 521-530
- Raymo M.E. & Ruddiman W.F. 1992: Tectonic forcing of late Cenozoic climate. *Nature* 359, 117-122.
- Rea, B.R., Whalley, W.B., Rainey, M.M. & Gordon, J.E. 1996a: Blockfields, old or new? Evidence and implications from some plateaus in Northern Norway. *Geomorphology* 15, 109-121.
- Rea, B.R., Whalley, W.B. & Porter, E.M. 1996b: Rock weathering and the formation of summit blockfield slopes in Norway: examples and implications. In Anderson, M.G. & Brooks, S.M. (eds.) *Advances in Hillslope Processes*. Wiley, Chichester, 1257-1275,
- Redpath, B.B. 1973: Seismic refraction exploration for engineering site investigations. *U.S. Army Engineer Waterways Experiment Station Explosive Excavation Research Laboratory, Technical Report E-73-4*, Livermore, California, 51 pp.
- Reimann, C., Arnoldussen, A., Englmaier, P., Filzmoser, P., Finne, T.E., Garrett, R.G., Koller, F. & Nordgulen, Ø. 2007: Element concentrations and variations along a 120-km transect in southern Norway - Anthropogenic vs. geogenic vs. biogenic element sources and cycles. *Applied Geochemistry* 22, 851-871
- Reimann, C., Finne, T.E. & Filzmoser, P. 2011: New geochemical data from a collection of till samples from Nordland, Troms and Finnmark. *NGU Report 2011.045*.
- Reimann, C., Finne, T.E. & Filzmoser, P. 2012: Soil geochemical data from the Nordkinn peninsula, Finnmark. *NGU Report 2012.096*, 95 pp.
- Reite, A.J. 1997: *Verran 1622 I, kvartærgeologisk kart - M 1:50.000*. Norges geologiske undersøkelse, Trondheim.
- Rekstad, J. 1915: Helgelands ytre kyststrand. *Norges geologiske undersøkelse Årbok* 5, 1-53
- Reusch, H.H. 1878: Iagttagelser over isskuret Fjeld og forvitret Fjeld. *Christiania Videnskabs-Selskabs Forhandl.* 7, 1-28.
- Reusch, H.H. 1894: Strandflaten, et nyt trek i Norges Geografi. *Norges geologiske undersøkelse* 14, 1-14.
- Reusch, H.H. 1900: En forekomst af kaolin og ildfast ler ved Dydland nær Flekkefjord. *Norges geologiske undersøkelse* 32, 99-103.

- Reusch, H.H. 1901a: Nogle bidrag til forståelsen av hvorledes Norges dale og fjelde er blevne til. *Norges geologiske undersøkelse* 32, 124-263
- Reusch, H.H. 1901b: Høifjellet mellom Vangsmjøsen og Tisleia (Valdres). NGU Aarbog for 1900. *Norges geologiske undersøkelse* 31, 45–88.
- Reusch, H.H. 1902: Vore dale og fjelde. Hvordan formen af Norges overflade er dannet. *Naturen* 26, 29-142.
- Reusch, H.H. 1903a: Betrachtungen über das Relief von Norwegen. *Geographische Zeitschrift* Heft 8, 425-435.
- Reusch, H.H. 1903b: Norske kaolinforekomster. *Naturen* 27, 29-132.
- Reusch, H.H. 1910: Norges geologi. *Norges geologiske undersøkelse* 50, 1–196.
- Reynolds, R.C. 1971: Clay mineral formation in an alpine environment. *Clays and Clay Minerals*, 19(6), 361-374.
- Riebe C.S., Kirchner J.W. & Finkel R.C. 2004: Erosional and climatic effects on long-term chemical weathering rates in granitic landscapes spanning diverse climate regimes. *Earth and Planetary Science Letters* 224, 547-562
- Riis, F. 1996: Quantification of Cenozoic vertical movements of Scandinavia by correlation of morphological surfaces with offshore data. *Global and Planetary Change* 12, 331-357.
- Riis F. & Fjeldskaar, W. 1992: On the magnitude of the Late Tertiary and Quaternary erosion and its significance for the uplift of Scandinavia and the Barents Sea. In Larsen, R.M., Brekke, H., Larsen, B.T. & Talleraas, E. (eds.) *Structural and Tectonic Modeling and its application to Petroleum Geology*. Norwegian Petroleum Society Special Publication 1, 163-185
- Roaldset, E. 1975: Rare earth element distributions in some Precambrian rocks and their phyllosilicates, Numedal, Norway. *Geochimica et Cosmochimica Acta* 39, 4, 455-469.
- Roaldset, E., Pettersen, E., Longva, O. & Mangerud, J. 1982: Remnants of preglacial weathering in western Norway. *Norsk Geologisk Tidsskrift* 62, 169-178.
- Roaldset, E., Riis, F., & Johnsen, S.O. 1993: Weathered basement rocks below Mesozoic sediments, Norwegian North Sea. In Ford, D. McCann, B. & Vajoczki, S. (eds.) *Third International Geomorphology Conference, 23-28 August, Hamilton, Ontario, Canada, Programme with Abstracts*, p. 229.
- Rohrman, M.H.E.J., van der Beek, P.A., Andriessen, P.A.M. & Cloetingh, S. 1995: Meso-Cenozoic morphotectonic evolution of southern Norway: Neogene domal uplift inferred from apatite fission-track thermochronology. *Tectonics* 14, 704-718
- Rokoengen, K. 1973: *Svelleegenskaper hos leirsoner i fjell*. Ph.D. thesis. Norwegian University of Science and Technology, Trondheim, Norway, 243 pp.
- Rosenquist, I.Th. 1949: En forekomst av montmorillonitt i Norge og undersøkelser over absorpsjonsevne og blekevirkning av blekejord. *Norsk Geologisk Tidsskrift* 27, 179-186.
- Rosenquist, I.Th. 1952a: Kaolin fra Hurdal. *Norges geologiske undersøkelse* 183, 5-9
- Rosenquist, I.Th. 1952b: Montmorillonitt fra Fortun i Sogn. *Norsk Geologisk Tidsskrift* 37, 403-414.

- Rosenquist, I.Th. 1960: Montmorillonitt fra Skyrvedalen i Hemsedal. *Norsk Geologisk Tidsskrift* 39, 350-354. .
- Rueslåtten, H.R., Lile, O.B., Veslegard, G. & Fjeld, O.C. 1984: *Vann i fjell prosjektet, sluttrapport*. Norges tekniske høgskole Report, Trondheim.
- Rønning, J. S., Dalsegg, E., Heincke, B., Olesen, O. & Tønnesen, J.F. 2009: Geofysiske målinger over tunneler ved Hanekleiv, Ravneheia og Vadfoss. *NGU Report 2009.040*, 36 pp.
- Samuelsson, L. 1973: Selective weathering of igneous rocks. *Sveriges Geologiske Undersøkelse Ser. C 690*, 16 pp
- Schetelig, J. 1918: Natur og fjeldgrund. In Berg, L. (ed.) *Sandherred. En Bygdebok*. Kristiania (Oslo), 36-50.
- Schnepp, E., Worm, K. & Scholger, R. 2008: Improved sampling techniques for baked clay and soft sediments. *Phys. Chem. Earth* 33, 407-413, doi: 10.1016/j.pce.2008.02.030, 2008.
- Schuster, D.L., Vasconcelos, P.M., Heim, J.A. & Farley, K.A. 2005: Weathering geochronology by (U-Th)/He dating of goethite. *Geochimica et Cosmochimica Acta* 69, 659-673.
- Scott, K.M. & Pain, C.F. 2008 (eds.): *Regolith science*. CSIRO Publishing, Collingwood, Australia and Springer, Dordrecht, The Netherlands, 461 pp.
- Sellevoll, M.A. 1983: A study of the Earth's crust in the island area of Lofoten–Vesterålen, northern Norway. *Norges geologiske undersøkelse Bulletin* 380, 235-243.
- Selmer-Olsen, R. 1964: *Alminnelig geologi og ingeniørgeologi*. Tapir forlag, Trondheim, 409 pp.
- Sernander, R. 1896: *Nogra ord med anledning av Gunnar Andersson*. Svenska Växtvärldens Historia, Botaniska, p. 114
- Siedlecka, A. & Roberts, D. 1996: *Finnmark fylke. Berggrunnsgeologi M 1:500 000*. Norges geologiske undersøkelse, Trondheim.
- Stein, S., Cloetingh, S., Sleep, N.H. & Wortel, R. 1989: Passive margin earthquakes, stresses and rheology. In Gregersen, S. & Basham, P.W. (eds) *Earthquakes at North-Atlantic Passive Margins; Neotectonics and Postglacial Rebound*. NATO ASI Series, Series C: Mathematical and Physical Sciences 266, 231–259.
- Steltenpohl, M.G., Hames, W.E. & Andresen, A. 2004: The Silurian to Permian history of a metamorphic core complex in Lofoten, northern Scandinavian Caledonides. *Tectonics* 23, 1-23. doi:10.1029/2003TC001522.
- Steltenpohl, M.G., Carter, B.T., Andresen, A. & Zeltner, D.L. 2009: $^{40}\text{Ar}/^{39}\text{Ar}$ thermochronology of late- and postorogenic extension in the Caledonides of northcentral Norway. *Journal of Geology* 117, 399-414. doi:10.1086/599217.
- Steltenpohl, M.G., Moecher, D., Andresen, A., Ball, J., Mager, S. & Hames, W.E. 2011: The Eidsfjord shear zone, Lofoten-Vesterålen, north Norway: An Early Devonian, paleoseismogenic low-angle normal fault. *Journal of Structural Geology* 33, 1023-1043.
- Strøm, K.M. 1948: The geomorphology of Norway. *Geogr. Journ.* 112, 19-27.
- Strömquist, L. 1973: *Geomofologiska studier av blockhav ock blockfält i norra Scandinavien*. PhD thesis, Uppsala University Report 22.
- Strømsøe, J.R. 2011: Weathering patterns in high latitude regolith *Journal of Geophysical Research* 116, F03021, 17 pp.

- Sturt, B.A., Dalland, A. & Mitchell, J.L. 1979: The age of the sub Mid-Jurassic tropical weathering profile of Andøya, northern Norway, and the implications for the Late Palaeozoic paleogeography in the North Atlantic region. *Geologische Rundschau* 68, 523–542.
- Sundvoll, B. & Larsen, B.T. 1994: Architecture and early evolution of the Oslo Rift. *Tectonophysics* 240, 173-189.
- Svenonius, F. 1909: Om skärf- eller blockhafven på våra högfjell. *Geologiska Föreningens i Stockholm Förhandlingar* 31, 169-181
- Sveian, H. 1985: *Stiklestad 1722 IV, kvartærgeologisk kart - M 1:50.000*. Norges geologiske undersøkelse, Trondheim.
- Sveian, H. & Solli, A. 1997: Tid og form – geologisk historie – kapittel 4. In Dahl, R., Sveian, H. & Thoresen, M.K. (eds.) *Nord-Trøndelag og Fosen – geologi og landskap*. Norges geologiske undersøkelse, Trondheim, 111-130.
- Sveian, H., Bergstrøm, B., Reite, A.J., Olsen, L. & Riiber, K. in press: *Nord-Trøndelag fylke. Kvartærgeologisk kart M 1:250.000*. Norges geologiske undersøkelse, Trondheim.
- Sørensen, R. 1988: In-situ rock weathering in Vestfold, southeastern Norway. *Geografiska annaler* 70, 299-308.
- Sæther, E. 1964: Clay veins in rocks in Norway. *Norsk Geologisk Tidsskrift* 44, 385-429.
- Taylor, G. 2008: Landscape and regolith. In Scott, K.F. & Pain, C.F. (eds.) *Regolith science*. CSIRO Publishing, Collingwood, Australia and Springer, Dordrecht, The Netherlands, 31-43.
- Thomas, M. F. 1989: The role of etch processes in landform development II. Etching and the formation of relief. *Zeitschrift für Geomorphologie NF*. 33, 257-274.
- Torsvik, T.H. & Cocks, L.R.M. 2005: Norway in space and time: A Centennial cavalcade. *Norwegian Journal of Geology* 85, 73-86, ISSN 029-196X.
- Tveten, E. 1978: *Geologisk kart over Norge, berggrunnskart Svolvær M 1:250 000*. Norges geologiske undersøkelse, Trondheim.
- Tynni, R. 1982: The reflection of geological evolution in Tertiary and interglacial diatoms and silicoflagellates in Finnish Lapland. *Geological Survey of Finland Bulletin* 320, 4-40.
- Undås, I. 1945: Drag av Bergensområdets kvartærgeologi. *Norsk Geografisk Tidsskrift* 25, 441-445.
- Vasconcelos, P.M., Becker, T.A., Renne, P. R. & Brimhall, G.H. 1992: Age and duration of weathering by ^{40}K - ^{40}Ar and $^{40}\text{Ar}/^{39}\text{Ar}$ analysis of potassium manganese oxides. *Science* 258, 451-455.
- Vasconcelos, P.M., Brimhall, G.H., Becker, T. A. & Renne, P.R. 1994: $^{40}\text{Ar}/^{39}\text{Ar}$ analysis of supergene jarosite and alunite: Implications to the paleoweathering history of western USA and West Africa. *Geochimica et Cosmochimica Acta* 58, 401-420.
- Velde, B. & Meunier, A. 1987: Petrologic phase equilibria in natural clay systems. In Neuman, A.C.D. (ed.) *Chemistry of Clays and Clay minerals*. Mineralogical Society Monograph 6, Longman Scientific & Technical, Harlow, 423-458.

- Vogt, Th. 1912: Landskapsformene i det ytterste av Lofoten. *Norsk Geografisk Selskap Aarbok* 23, 1-50
- West, A.J., Galy, A. & Bickle, M. 2005: Tectonic and climatic controls on silicate weathering. *Earth and Planetary Science Letters* 235, 211 – 228.
- Whalley, W.B., Rea, B.R., Rainey, M.M. & McAllister, J.J. 1997: Rock weathering in blockfields: some preliminary data from mountain plateaus in North Norway. In Widdowson, M. (ed.) *Palaeosurfaces: Recognition, Reconstruction, and Interpretation*. Geological Society of London Special Publications 120, 133-145.
- Zwaan, K.B., Fareth, E. & Grogan, P.W. 1998: *Geologisk kart over Norge, berggrunnskart Tromsø, M 1:250.000*. Norges geologiske undersøkelse, Trondheim.
- Øverland, J.A. 2011: 'Mitt geofunn': Kjelen – forvittringsgrop som endestav. *GEO* 14, 6, p. 70.
- Åm, K. 1975: Aeromagnetic basement complex mapping north of latitude 62°N, Norway. *Norges geologiske undersøkelse* 316, 351-374.
- Åm, M. 1994: *Mineralogisk og petrologisk karakterisering av vitrings-/sleppematreiale fra Stuoragurraforkastningen, Finnmark*. Project Report, University of Trondheim, NTH, 102 pp.

Appendix 1

XRD-analysis by Alf Olav Larsen

Hei Dag.

Har undersøkt prøvene vha XRD og kommet til følgende resultater:

Sort mineral på sprekker i Ravnefjelltunellen

XRD-analysen viser at sort mineral på sprekker i Ravnefjelltunellen er hisingeritt. Dette er et dårlig krystallinsk mineral med den enkle formelen $\text{FeSiO}_3 \cdot \text{H}_2\text{O}$, ofte delvis substituert med Ca, Mg, Al, Fe, CO_2 m.fl. Mineralen dannes som et dekomponeringsprodukt etter Fe-holdige mineraler. Jeg har relativt nylig skrevet en artikkel om dette mineralet fra syenittpegmatittgangene i Tvedalen, se vedlagte kopi.

Dypvitret bergart fra Ravnefjelltunellen

Prøven er delvis nedknust og slemmet i vann. Finpartikulært materiale i suspensjon er dekantert, filtrert og analysert vha XRD. Hovedbestanddelen er montmorillonitt (smektitt) samt mindre mengder albitt, biotitt (annitt) og spor av kaolin. Sistnevnte mineral kan være noe usikker da sterkeste refleks fra kaolin og kloritt er sammenfallende. Identifikasjonen av montmorillonitt er verifisert ved glykolbehandling (svelling av basisrefleksene fra 15 Å til 17 Å).

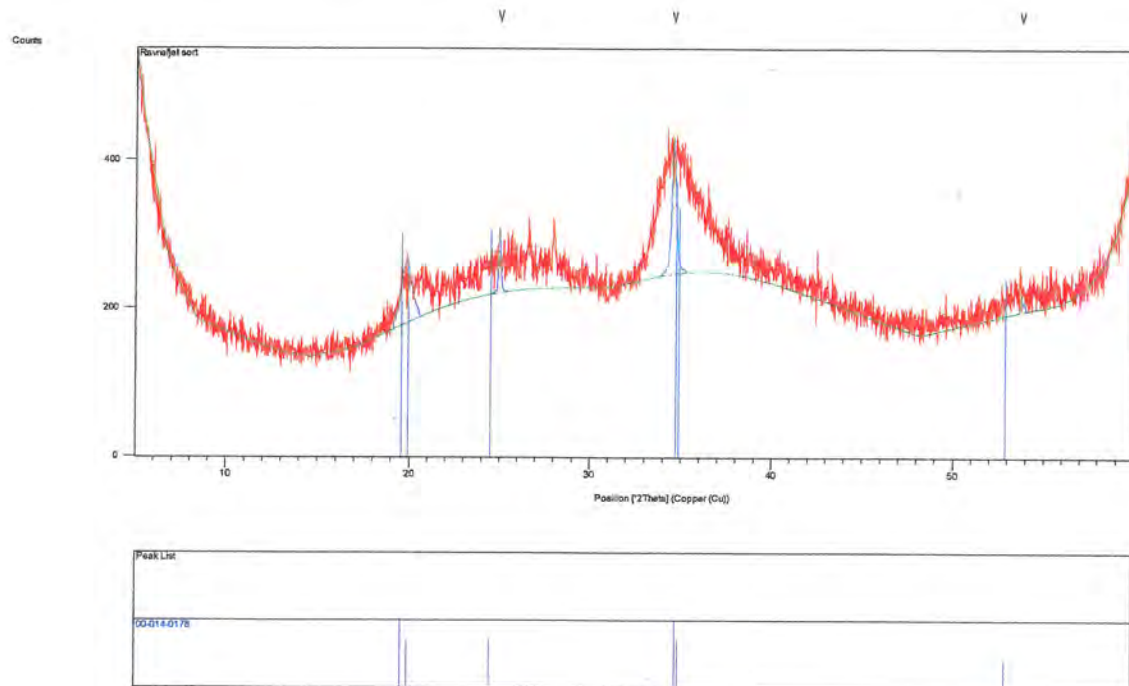
Dypvitret bergart fra Sigerslottet

Prøven er finknust og analysert vha XRD. Hovedbestanddelen er montmorillonitt (smektitt) samt endel illitt, kvarts og spor av kaolin. Sistnevnte mineral kan være noe usikker da sterkeste refleks fra kaolin og kloritt er sammenfallende. Prøven inneholder også noe goethitt, som er hovedårsaken til prøvens gulbrune farge. Identifikasjonen av montmorillonitt er verifisert ved glykolbehandling (svelling av basisrefleksene fra 15 Å til 17 Å).



Ravnefjell sort

Graphics, Analyze + Pattern View:

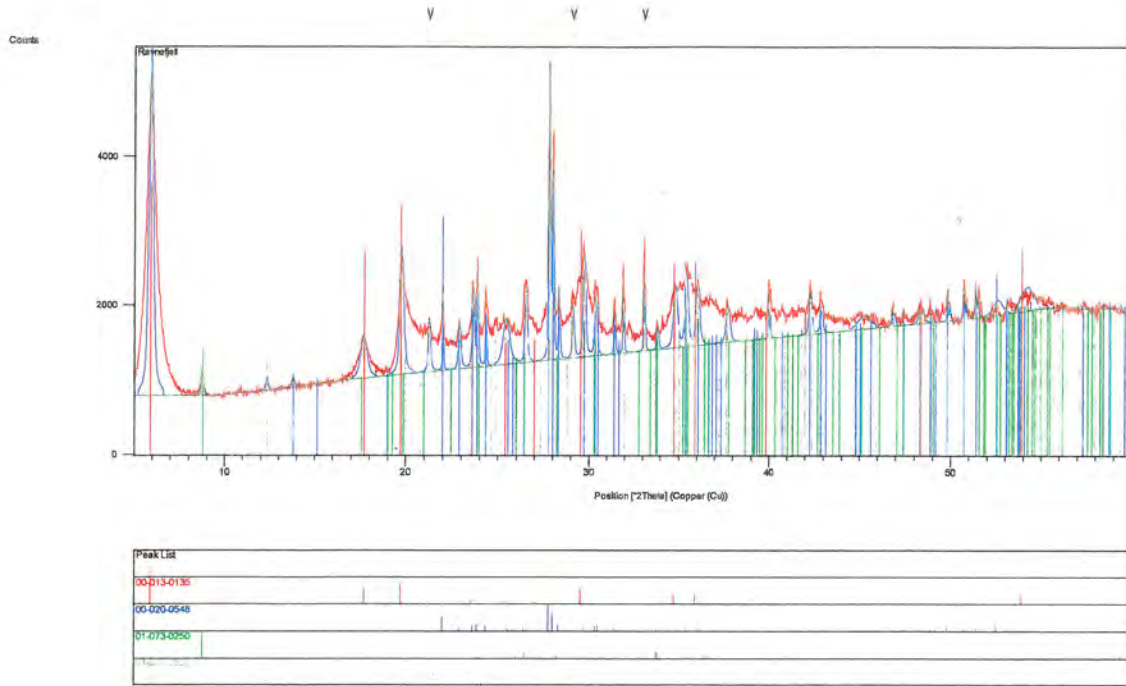


Pattern List:

Ref. Code	Compound Name	Chemical Formula
00-014-0178	Hisingerite	(Fe1.53 Mg0.48 Fe0.17) (Si3.03 Fe0.77 Al0.20) O10 ·x H2 O

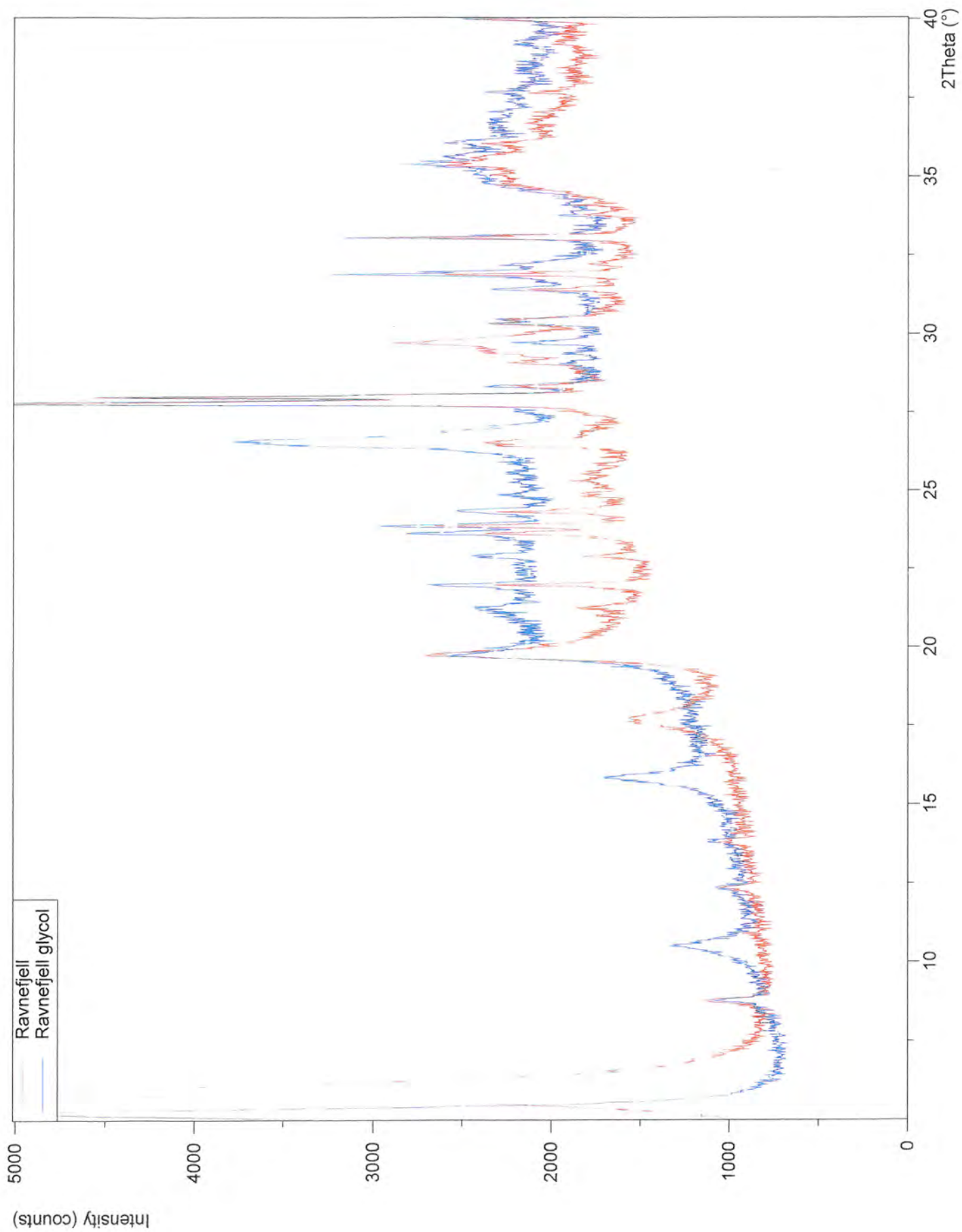
Ravnefjell

Graphics, Analyze + Pattern View:



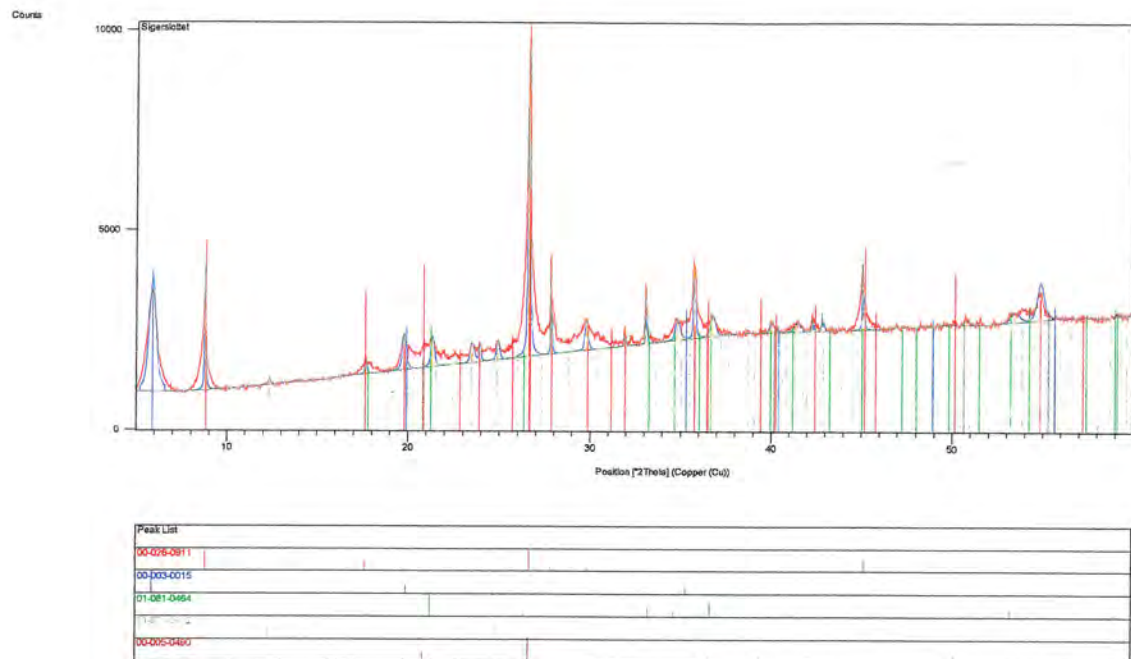
Pattern List:

Ref. Code	Compound Name	Chemical Formula
00-013-0135	Montmorillonite	Ca _{0.2} (Al , Mg) ₂ Si ₄ O ₁₀ (O H) ₂ · 4 H ₂ O
00-020-0548	Albite	(Na , Ca) (Si , Al) ₄ O ₈
01-073-0250	Annite	K Fe ₃ Al Si ₃ O ₁₀ (O H , F) ₂
01-076-0632	Kaolinite	Al ₂ Si ₂ O ₅ (O H) ₄



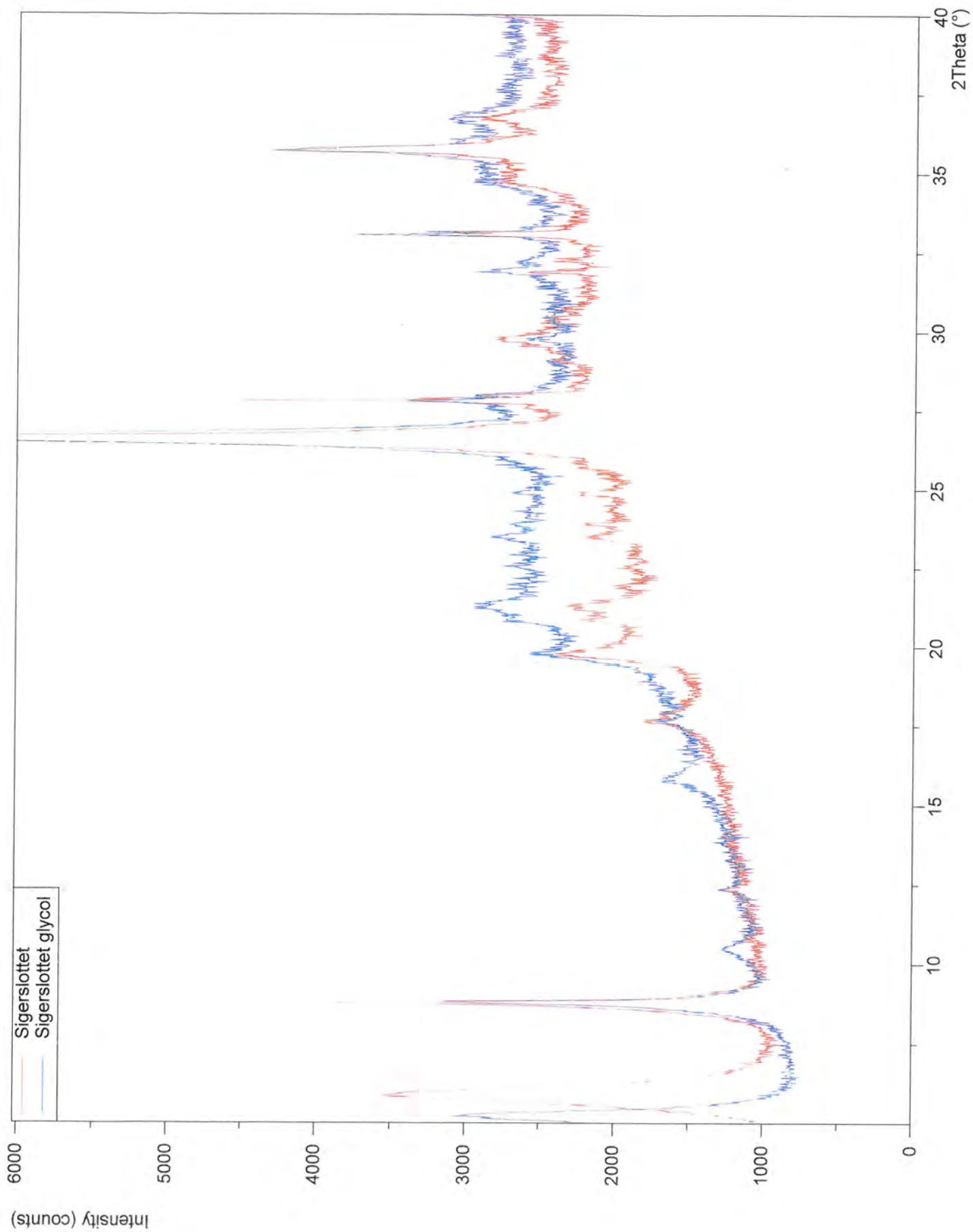
Sigerslottet

Graphics, Analyze + Pattern View:



Pattern List:

Ref. Code	Compound Name	Chemical Formula
00-026-0911	Illite	(K , H3 O) Al2 Si3 Al O10 (O H)2
00-003-0015	Montmorillonite	(Na , Ca)0.3 (Al , Mg)2 Si4 O10 (O H)2 · x H2 O
01-076-0632	Kaolinite	Al2 Si2 O5 (O H)4
01-081-0464	Goethite	Fe O (O H)
00-005-0490	Quartz	Si O2



Appendix 2

Mehuken windpower park, mapping of drillcores from five sites for windpower plants. Bergab –
Berggeologiska Undersökningar AB

Maria Göthfors, 2010



For
Norconsult AB

Mehuken wind power park

Mapping of drill cores from five sites for wind power plants

Bergab – Berggeologiska Undersökningar AB

Project leader
Elisabeth Olsson

Administrator
Maria Göthfors

Mapping of drillcores, Mehuken, Norway

Five drill cores have been investigated during the time of January the 18 to 22, 2010. The drill cores have been investigated in regard to rock type, foliation, fractures and fracture fillings. The fracture intensity has been analysed by means of RQD. The drill core holes have been analysed in water permeability by packer test valves. Four of the drill cores have been chosen for analysis of nordic abrasion value. Four samples have been chosen for uniaxial compression test and modulus of elasticity.

RQD

Fracture intensity also denotes RQD (Rock Quality Designation). RQD is a quality measure that defines the proportion intact core pieces longer than 10 cm from 1 meter core. Consequently it gives a measure on the fracture intensity in the rock by the following scale in percent.

RQD	Rating
90-100	Excellent
75-90	Good
50-75	Fair
25-50	Poor
0-25	Very poor

Packer test valves

Packer test valves are carried out by placing a packer in the bore hole. The packer is used to seal of the hole in sections, in this case in 300 mm sections starting from the bottom.

Water is injected through the packer with a known pressure and the flow rate is measured. In this case the flow rate is measured with three pressure stages, 2 bars, 5 bars and 2 bars. The three pressure stages are repeated for every section. Water is injected until a steady flow is reached for each pressure stage.

Site 2:1

The bedrock was investigated at depth through a 20,75 m drill core that has been drilled towards the northeast with an inclination of 70 degrees from the horizontal. The drill core consists of amphibolite, but there are also some smaller segments of gneiss. The amphibolite varies in colour from grey to carbon black. The carbon black amphibolite is soft and very crumbly. The dominant joint set is parallel to the foliation in the core. The foliation strikes N20-35E direction and dips 40-70° to E and W.

The core indicates a relatively heavily fractured bedrock, especially in the upper 12 meters. There are several zones where the drill core is very heavily fractured or totally crushed.

Joint surfaces in the upper meter of the core are rust covered. Below the depth of one meter, clay minerals on joint surfaces are common and especially in the fracture zones. Chlorite is another common mineral occurring on joint surfaces.

The RQD value indicates that the core is primarily of fair and good quality, but there are also a few meters of poor and very poor quality, as well as excellent quality (see figure 1).

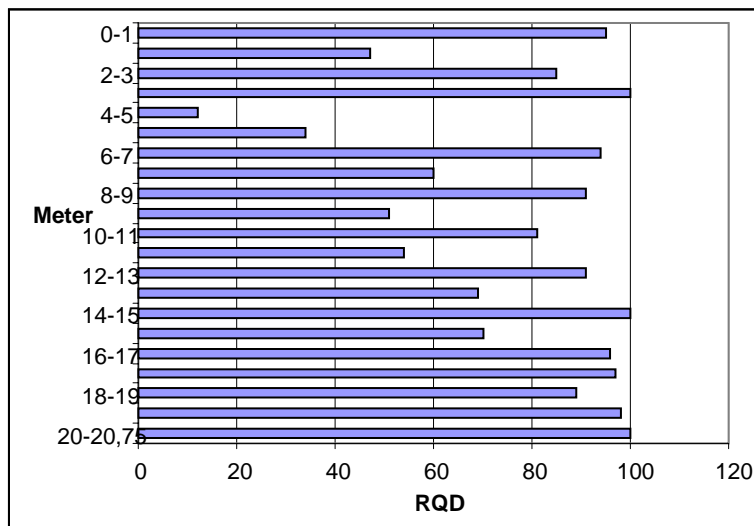


Figure 1

Packer test valves indicate that permeability in most of the borehole is slight, except between core meter 0 and 5, where permeability is high. Between core depth 14 and 17 meter, there is no permeability.

The uniaxial compression test and the modulus of elasticity test indicate a very strong rock mass between fractures (S_{a_max} [MPa] 303,9 and E [GPa] 135,2). The rock piece on which the tests have been performed is primarily amphibolitic.

The Nordic abrasion value indicates a fair abrasion resistance (19,1).

However the test results indicate a strong rock mass, the tests have only been performed on a small piece of the drill core with no fractures. The tests have not considered fractures or fracture zones in other parts of the drill core. Thus the modulus of elasticity can be lower than the tests indicate due to fractures or other weakening features in the rock mass.

In the case of site 2:1 the uniaxial compression test and the modulus of elasticity test indicate a strong rock mass. At the same time the drill core is relatively heavily fractured.

The recommendation is to stick to the results from the in-situ deformation modulus that has been estimated with an empirical relationship suggested by Serafim and Pereira (1983). In this case a value of 8 GPa.

Photos and analysis results site 2-1, see attachment 1

Site 2-4

The bedrock was investigated at depth through a 19,90 m drill core that has been drilled towards the southwest with an inclination of 70 degrees from the horizontal. The drill core consists of grey foliated augen gneiss. The eyes are light in colour and often slightly extended in the foliation direction. Between core depth 15,80 and 19,90 meters, the core consists of amphibolite.

The dominant joint set is parallel to the foliation in the core. The foliation strikes N50-80W direction and dips 25-50° to N. Other occurring joint sets strike NS and dip ~30° to E.

The core indicates a nearly intact bedrock. There are not much fillings in the fractures. Occuring fracture minerals are micas, chlorite, rust and clay minerals. Some of the fractures are weathered.

The RQD value indicates that the core is primarily of good and excellent quality (see figure 2). Although the core seems to be intact, planes of weakness occurs regularly and do quite easy break into two parts.

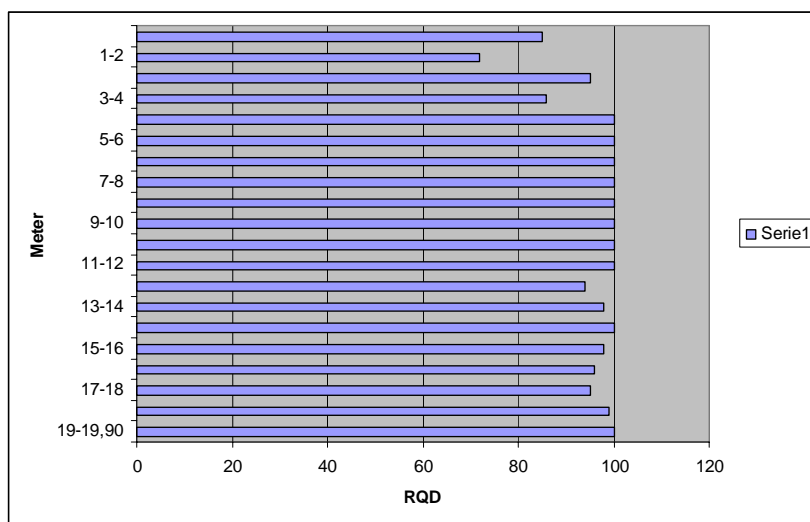


Figure 2

Packer test valves indicate that permeability is nonexistent except for a large shallow leakage between core depth 0 and 8 meters.

The uniaxial compression test and the modulus of elasticity test indicates a strong rock mass between fractures (σ_{max} [MPa] 76,6 and E [GPa] 34,8). The rock piece on which the tests have been performed is augen gneiss.

The Nordic abrasion value indicates a fair abrasion resistance (18,9).

Howsoever the test results indicate a strong rock mass, the tests have only been performed on a small piece of the drill core with no fractures. The tests have not considered fractures or fracture zones in other parts of the drill core. Thus the modulus of elasticity can be lower than the tests indicate due to fractures or other weakening features in the rock mass.

In the case of site 2:4 the uniaxial compression test and the modulus of elasticity test indicate a strong rock mass. At the same time the drill core indicates a nearly intact bedrock. Although the core seems to be intact, planes of weakness occurs regularly and do quite easy break into two parts.

The recommendation is to stick to the results from the in-situ deformation modulus that has been estimated with an empirical relationship suggested by Serafim and Pereira (1983). In this case a value of 13 GPa.

Photos and analysis results site 2-4, see attachment 2

Site 2:6

The bedrock was investigated at depth through a 21,75 m drill core that has been drilled towards the southwest with an inclination of 70 degrees from the horizontal. The drill core consists of grey foliated augen gneiss. There are also some smaller segments of amphibolite. The augen gneiss is rich in mica minerals. The eyes are light in colour and often slightly extended in the foliation direction. The colour of the amphibolite varies from grey to greyish green to carbon black. The carbon black amphibolite is soft and crumbly. The dominant joint set is parallel to the foliation in the core. The foliation strikes NS direction and dips 70° to the north. Other occurring joint sets strike NE and NW and dip 30-60° to NE and NW.

The core indicates a relatively intact bedrock, but there are a few zones where the drill core is very heavily fractured or totally crushed.

There are not much fillings in the fractures. Occurring fracture minerals are chlorite and calcite.

The RQD value indicates that the core is primarily of good and excellent quality, but there are also a few meters of poor and fair quality, especially between core depth 13 and 16 meters (see figure 3).

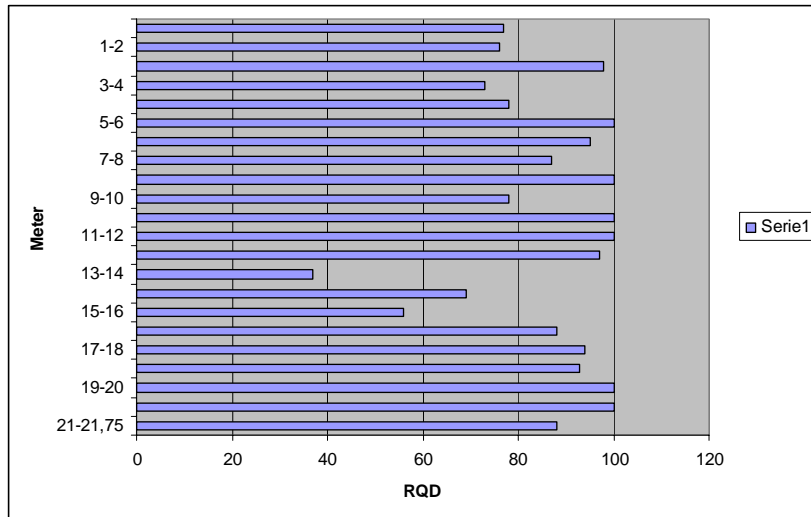


Figure 3

Packer test valves indicate that permeability is large between core depth 0 and 6 meters, small between core depth 6 and 9 meters and nonexistent in the remaining core, which indicates an impenetrable rock under core depth 9 meters.

The Nordic abrasion value indicates a good abrasion resistance (22,6).

Photos and analysis results site 2-6, see attachment 3

Site 2-7

The bedrock was investigated at depth through a 20,62 m drill core that has been drilled towards the southwest with an inclination of 70 degrees from the horizontal. The drill core consists of grey foliated gneiss that has been affected of the amphibolite that occurs as segments in core. The colour of the amphibolite varies from grey to greyish green.

The dominant joint set is parallel to the foliation in the core. The core has not been oriented thus you can not say anything about the direction of the fractures.

The core indicates a relatively intact bedrock, except for the zones where the rock is heavily fractured or totally crushed. The joint surfaces are chlorite- and clay covered. Above 12 meter the joint sets are rust-covered. Some of the fractures are weathered.

The RQD value indicates that the the core is primarily of good to excellent quality, but there are also a few meters of fair quality (see figure 4).

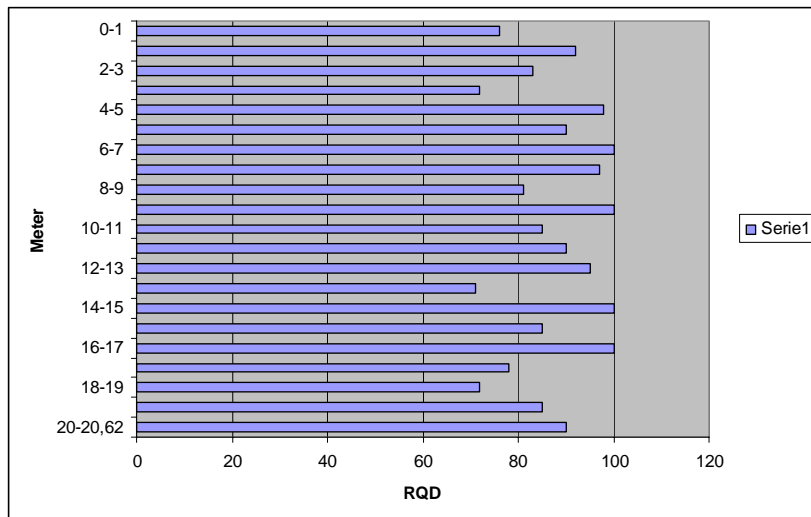


Figure 4

Packer test valves indicate that permeability in the bore hole is quite big close to the surface and also in core depth 17-20 meters.

The uniaxial compression test and the modulus of elasticity test indicates a very strong rock mass between fractures (Sa_{max} [MPa] 261,0 and E [GPa] 97,0). The rock piece on which the tests have been performed is primarily granitic amphibolite.

The Nordic abrasion value indicates a good abrasion resistance (16,1).

Howsoever the test results indicate a strong rock mass, the tests have only been performed on a small piece of the drill core with no fractures. The tests have not considered fractures or fracture zones in other parts of the drill core. Thus the modulus of elasticity can be lower than the tests indicate due to fractures or other weakening features in the rock mass.

In the case of site 2:7 the uniaxial compression test and the modulus of elasticity test indicate a very strong rock mass. At the same time the core indicates a relatively intact bedrock, except for the zones where the rock is heavily fractured or totally crushed.

The recommendation is to stick to the results from the in-situ deformation modulus that has been estimated with an empirical relationship suggested by Serafim and Pereira (1983). In this case a value of 15 GPa.

Photos and analysis results site 2-7, see attachment 4

Site 2-8

The bedrock was investigated at depth through a 21,60 m drill core that has been drilled towards the southwest with an inclination of 70 degrees from the horizontal. The drill core consists of grey foliated augen gneiss. There are also reoccurring segments of amphibolite. The eyes are light in colour and often slightly extended in the foliation direction. The colour of the amphibolite varies from grey to greyish green to carbon black. The carbon black amphibolite is soft and crumbly.

The dominant joint set is parallel to the foliation in the core. The foliation strikes N40-60W direction and dips 30-70° to NE. Other occurring groups of fractures strike EW and dip ~25° to N.

The core indicates a relatively intact bedrock, except for a few zones where the drill core is very heavily fractured or totally crushed. In these zones there are a lot of clay minerals. Otherwise there are not much fillings in the fractures. Occuring fracture minerals are clay minerals and chlorite. Some of the fractures are weathered.

The RQD value indicates that the core is primarily of fair to excellent quality, but there are also a few meters of poor quality (see figure 5).

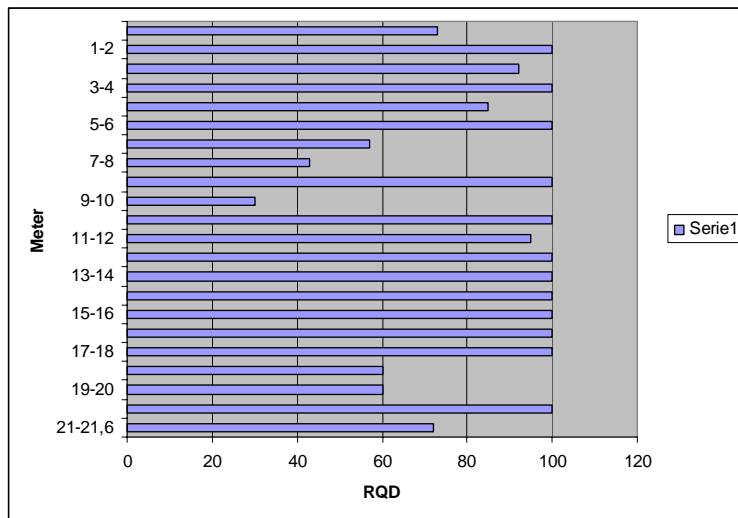


Figure 5

Packer test valves indicate that permeability is quite small except for some shallow leakage between core depth 0 and 6 meters, and some intermediate losses between 9 and 15 meters.

The uniaxial compression test and the modulus of elasticity test indicate a quite strong rock mass between fractures (S_{a_max} [MPa] 120,8 and E [GPa] 21,1). The rock piece on which the tests have been performed is primarily amphibolitic.

Howsoever the test results indicate a strong rock mass, the tests have only been performed on a small piece of the drill core with no fractures. The tests have not considered fractures or fracture zones in other parts of the drill core. Thus the modulus of elasticity can be lower than the tests indicate due to fractures or other weakening features in the rock mass.

In the case of site 2:8 the uniaxial compression test and the modulus of elasticity test indicate a quite strong rock mass. At the same time the core indicates a relatively intact bedrock, except for a few zones where the drill core is very heavily fractured or totally crushed.

The recommendation is to stick to the results from the in-situ deformation modulus that has been estimated with an empirical relationship suggested by Serafim and Pereira (1983). In this case a value of 15 GPa.

Photos and analysis results site 2-8, see attachment 5

	Site 2:1	Site 2:4	Site 2:6	Site 2:7	Site 2:8
Rock type	Amphibolite	Augen gneiss	Amphibolite	Granitic amphibolite	Augen gneiss and amphibolite
Petrography	Not investigated	Not investigated	Not investigated	Not investigated	Not investigated
Uniaxial compression test (MPa)	303,9	76,6	Test not performed	261,0	120,8
Modulus of elasticity (GPa)	135,2	34,8	Test not performed	97,0	21,1
Nordic abrasion value	19,1	18,9	22,6	16,1	Test not performed
Unweathered rock surface	Not investigated	Not investigated	Not investigated	Not investigated	Not investigated
Quality of surface rocks in drill core	0-13,5 meters very poor quality, 13,5-20,75 good quality	0-8 meters poor quality, 8-19,90 meters good quality	0-6 meters poor quality, 6-13 meters good quality, 13-21,75 poor quality	0-9 meters poor quality, 9-20,62 meters good quality.	0-6meters poor quality, 6-20 meters fair quality, 20-21,60 meters good quality.
Water loss in bore hole	0-14 m, 17-20 m	0-8 m	0-9 m	0-5 m, 14-20 m	0-6 m, 9-15 m
Occurrence of sliding surfaces	Not investigated	Not investigated	Not investigated	Not investigated	Not investigated
Supporting rock around foundation	Not investigated	Not investigated	Not investigated	Not investigated	Not investigated
Fresh, recently blasted rock surface.	Not investigated	Not investigated	Not investigated	Not investigated	Not investigated
Optimized foundation location	Not investigated	Not investigated	Not investigated	Not investigated	Not investigated
Rock surface gradient	Not known	Not known	Not known	Not known	Not known
Empirical deformation modulus	3/8 GPa	9/13 GPa	7/15 GPa	10/15 GPa	7/15 GPa
Maximum allowed soil pressure on rock surface	0,6 MPa	1,3 MPa	1,3 MPa	0,6 MPa	1,3 MPa

Attachments:

- 1 Results site 2-1
- 2 Results site 2-4
- 3 Results site 2-6
- 4 Results site 2-7
- 5 Results site 2-8

Maria Göthfors

Bergab- Berggeologiska Undersökningar AB

Gothenburg 2010-03-02

Attachment 1. Site 2-1 Mehuken

Drill core 2-1, box 1



Drill core 2-1, box 2



Drill core 2-1, box 3



Drill core 2-1, box 4



GEO-gruppen AB

Vattenförlustmätning

Uppdrag: Mehuken

Ärende nr: _____

Kärnbrorrhål: Verk 2:1 Nord-öst 240°

Utförd av: L. Thomsson

Datum: 11-1

Djup (m)	2 bar	5 bar	2 bar	Noteringar
	vattenförlust (l/5min)			
17-20	6,6	23,2	10,4	
14-17	0	0	0	
11-14	8,7	16,6	12,1	
8-11	25,0	38,5	25,0	
5-8	20,4	39,7	28,2	
2-5	22,5	Max 2Bar 300	22,5	
				0,00-1,73 Tappar allt Spol vatten-retur.

Stenmaterial

Sidan 1 av 1

Beställare Bergab Maria Göthfors Stampgatan 15 416 64 GÖTEBORG	Provtagningsdatum Ankomstdatum 2010-02-03	Analys start 2010-02-04 Analys slut 2010-02-05
Produkt Borrkärnor, labkrossat 2 steg Leverantör	Referens nr Provtagningsplats Verk 2:1, prov taget mellan 11,85 och 19,23 m Provtagare	Id-nummer
Entreprenör	Märkning	
Objekt Grundläggning av vindkraftverk, Mehuken		

Provresultat Kommentar	Medel- värde	Fraktion (mm)
SS-EN 1097-6/A1:2005 Korndensitet och Vattenabsorption		11,2/16
Korndensitet - skenbar (Mg/m ³)	3,12	
Använd provningsmetod	Bil. A.4	
SS-EN 1097-9/A1:2005 (Nordiska kulkvarnsmetoden)	19,1	11,2/16

Notering	Ort och datum KUNGÄLV 2010-02-08
	 Amir Rajabi, Laborarietekniker Utskriften är med en elektronisk signatur

Provresultat avser endast till laboratoriet inkommet prov. För information om mätosäkerhet kontaktas laboratoriet.

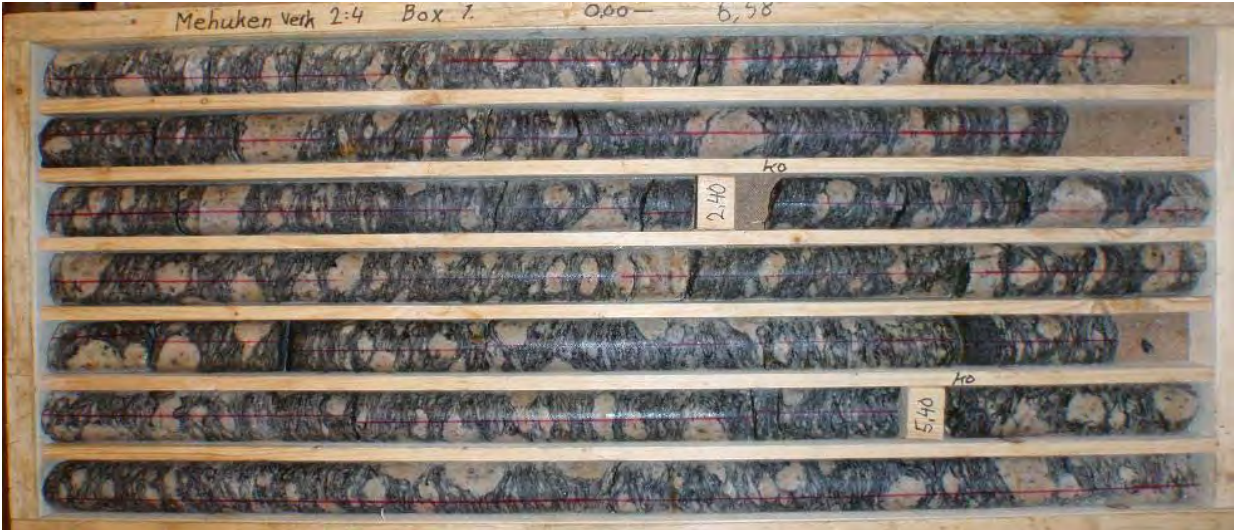
[EA] = Ej ackrediterad metod. [E] = Enkelprov

Vid best. av kornstorleksfördelning används stansade siktar >= 4,0 mm

Ackrediterat laboratorium utses av styrelsen för teknisk ackreditering (SWEDAC) enligt lag. Verksamheten vid de svenska ackrediterade laboratorierna uppfyller kraven enligt ISO/IEC 17025 samt enligt ISO 9001:2000 och 14001:1996 certifierat laboratorium. Denna rapport får endast återges i sin helhet, om inte utfärdande laboratorium i förväg skriftligen godkänt annat.

Attachment 2. Site 2-4 Mehuken

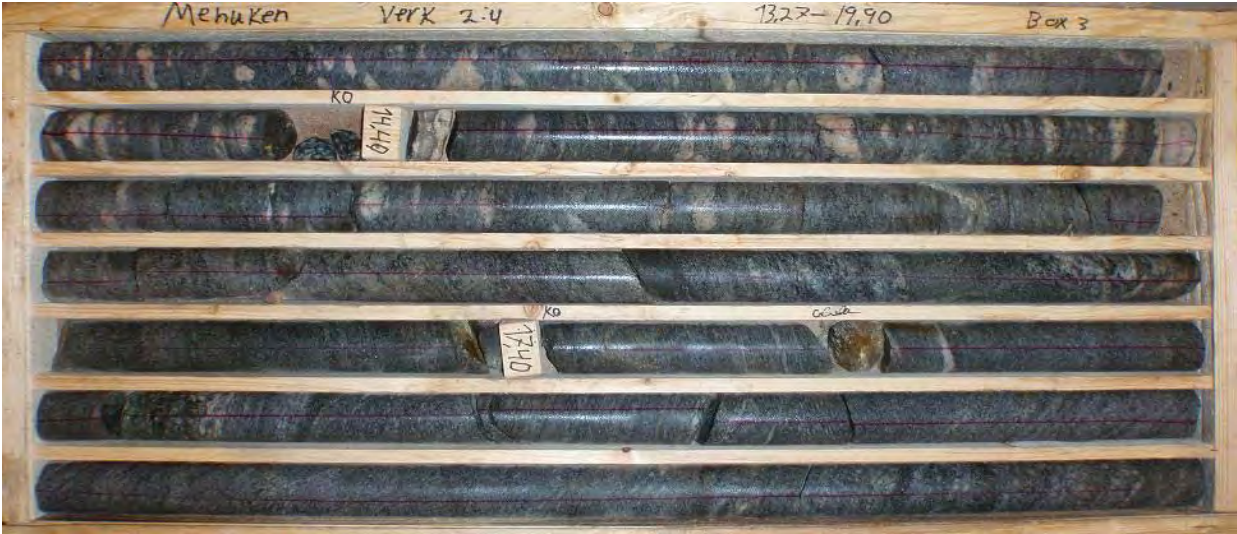
Drill core 2-4, box 1



Drill core 2-4, box 2



Drill core 2-4, box 3



GEO-gruppen AB

Vattenförlustmätning

Uppdrag: Mehuken

Ärende nr: _____

Kärnborrhål: Verk 2:4 syd-väst

Utförd av: L. Thomsson

Datum: 12-1


Djup (m)	2 bar	5 bar	2 bar	Noteringar
	vattenförlust (l/5min)			
17-19	0	0	0	
14-17	0	0	0	
11-14	0	0	0	
8-11	0	0	0	
5-8	138	^{2Bar} 300 x	140	x Får ej upp högre tryck
2-5	107	203	110	

Stenmaterial

Sidan 1 av 1

Beställare Bergab Maria Göthfors Stampgatan 15 416 64 GÖTEBORG	Provtagningsdatum 2010-02-03	Analys start 2010-02-04
Produkt Borrkärnor, labkrossat 2 steg	Referens nr	Id-nummer
Leverantör	Provtagningsplats Verk 2:4, prov taget mellan 9,47 och 16,07 m	Provtagare
Entreprenör	Märkning	
Objekt Grundläggning av vindkraftverk, Mehuken		

Provresultat Kommentar	Medel- värde	Fraktion (mm)
SS-EN 1097-6/A1:2005 Korndensitet och Vattenabsorption		11,2/16
Korndensitet - skenbar (Mg/m ³)	2,72	
Använd provningsmetod	Bil. A.4	
SS-EN 1097-9/A1:2005 (Nordiska kulkvarnsmetoden)	18,9	11,2/16

Notering	Ort och datum KUNGÄLV 2010-02-08
	 Amir Rajabi, Laborrietekniker Utskriften är med en elektronisk signatur

Provresultat avser endast till laboratoriet inkommet prov. För information om mätosäkerhet kontaktas laboratoriet.
[EA] = Ej ackrediterad metod. [E] = Enkelprov
Vid best. av kornstorleksfördelning används stansade siktar >= 4,0 mm

Ackrediterat laboratorium utses av styrelsen för teknisk ackreditering (SWEDAC) enligt lag. Verksamheten vid de svenska ackrediterade laboratorierna uppfyller kraven enligt ISO/IEC 17025 samt enligt ISO 9001:2000 och 14001:1996 certifierat laboratorium.
Denna rapport får endast återges i sin helhet, om inte utfärdande laboratorium i förväg skriftligen godkänt annat.

Attachment 3. Site 2-6 Mehuken

Drill core 2-6, box 1



Drill core 2-6, box 2



Drill core 2-6, box 3



Drill core 2-6, box 4



GEO-gruppen AB

Vattenförlustmätning

Uppdrag: Mehuken

Ärende nr: _____

Kärnbrorrhål: Verk 2:6 Syd-väst

Utförd av: L. Thomsson

Datum: 12-1


Djup (m)	2 bar	5 bar	2 bar	Noteringar
	vattenförlust (l/5min)			
21-18	0	0	0	
18-15	0	0	0	
15-12	0	0	0	
12-9	0	0	0	
9-6	6,1	15,3	3,1	
6-3	162	300	171	

Stenmaterial

Sidan 1 av 1

Beställare Bergab Maria Göthfors Stampgatan 15 416 64 GÖTEBORG	Provtagningsdatum Ankomstdatum 2010-02-03	Analys start 2010-02-04 Analys slut 2010-02-08
Produkt Borrkärnor, labkrossat 2 steg Leverantör	Referens nr Provtagningsplats Verk 2:6, prov taget mellan 0 och 6,5 m Provtagare	Id-nummer
Entreprenör	Märkning	
Objekt Grundläggning av vindkraftverk, Mehuken		

Provresultat Kommentar	Medel- värde	Fraktion (mm)
SS-EN 1097-6/A1:2005 Korndensitet och Vattenabsorption		11,2/16
Korndensitet - skenbar (Mg/m ³)	2,77	
Använd provningsmetod	Bil. A.4	
SS-EN 1097-9/A1:2005 (Nordiska kulkvarnsmetoden)	22,6	11,2/16

Notering	Ort och datum KUNGÄLV 2010-02-08
	 Amir Rajabi, Laborrietekniker Utskriften är med en elektronisk signatur

Provresultat avser endast till laboriet inkommet prov. För information om mätosäkerhet kontakta laboriet.

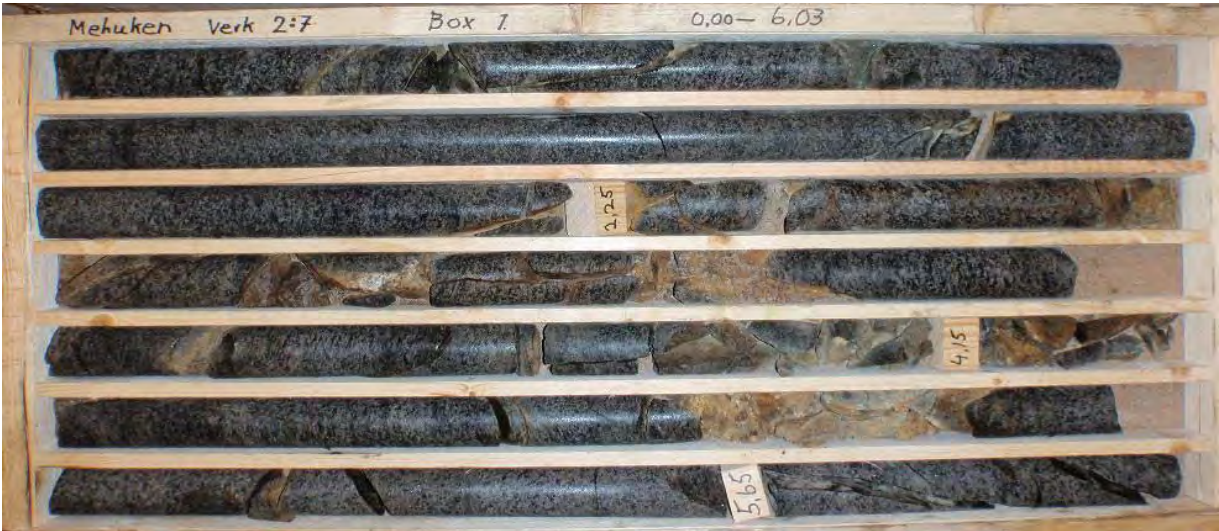
[EA] = Ej ackrediterad metod, [E] = Enkelprov

Vid best. av kornstorleksfördelning används stansade siktar >= 4,0 mm

Ackrediterat laboratorium utses av styrelsen för teknisk ackreditering (SWEDAC) enligt lag. Verksamheten vid de svenska ackrediterade laborieterna uppfyller kraven enligt ISO/IEC 17025 samt enligt ISO 9001:2000 och 14001:1996 certifierat laboratorium. Denna rapport får endast återges i sin helhet, om inte utfärdande laboratorium i förväg skriftligen godkänt annat.

Attachment 4. Site 2-7 Mehuken

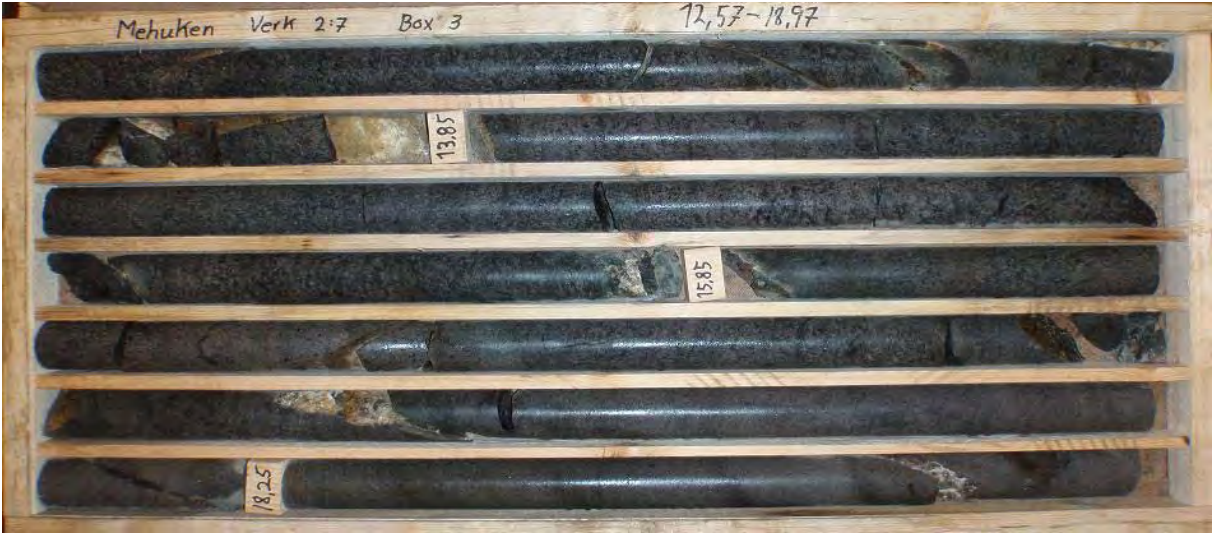
Drill core 2-7, box 1



Drill core 2-7, box 2



Drill core 2-7, box 3



Drill core 2-7, box 4



GEO-gruppen AB

Vattenförlustmätning

Uppdrag: Mehulen

Ärende nr: _____

Kärnbrorrhål: Verk 2:7 Syd-väst

Utförd av: L. Thomsson

Datum: 7-1-10

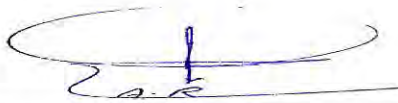
Djup (m)	2 bar	5 bar	2 bar	Noteringar
	vattenförlust (l/5min)			
17-20	12,6	300	13,7	
14-17	5,6	9,4	6,6	
11-14	0	0	0	
8-11	0	0	0	
5-8	0	0	0	
2-5	210	Max 2bar 300	210	x Får ej upp högre tryck
				0,00-2,35 Tappar allt
				Spolvatten-retur

Stenmaterial

Sidan 1 av 1

Beställare Bergab Maria Göthfors Stampgatan 15 416 64 GÖTEBORG	Provtagningsdatum Ankomstdatum 2010-02-03	Analys start 2010-02-04 Analys slut 2010-02-08
Produkt Borrkärnor, labkrossat 2 steg Leverantör	Referens nr Provtagningsplats Verk 2:7, prov taget mellan 6,03 och 12,57 m Provtagare	Id-nummer
Entreprenör	Märkning	
Objekt Grundläggning av vindkraftverk, Mehuken		

Provresultat Kommentar	Medel- värde	Fraktion (mm)
SS-EN 1097-6/A1:2005 Korndensitet och Vattenabsorption		11,2/16
Korndensitet - skenbar (Mg/m³)	3,30	
Använd provningsmetod	Bil. A.4	
SS-EN 1097-9/A1:2005 (Nordiska kulkvarnsmetoden)	16,1	11,2/16

Notering	Ort och datum KUNGÄLV 2010-02-08
	 Amir Rajabi, Laboratorietekniker Utskriften är med en elektronisk signatur

Provresultat avser endast till laboratoriet inkommet prov. För information om mätosäkerhet kontaktas laboratoriet.

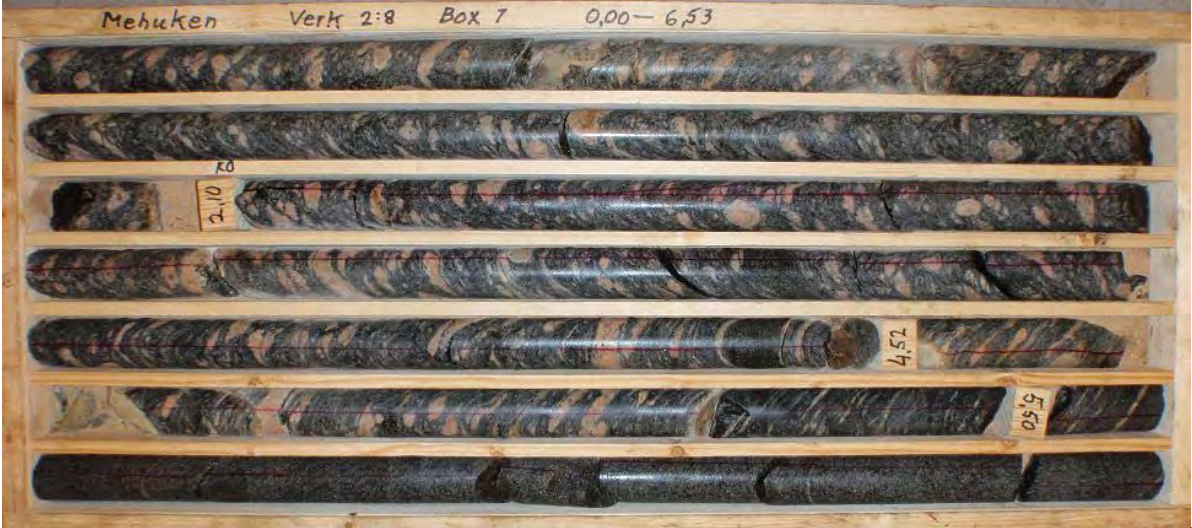
[EA] = Ej ackrediterad metod. [E] = Enkelprov

Vid best. av kornstorleksfördelning används stansade siktar >= 4,0 mm

Ackrediterat laboratorium utses av styrelsen för teknisk ackreditering (SWEDAC) enligt lag. Verksamheten vid de svenska ackrediterade laboratorierna uppfyller kraven enligt ISO/IEC 17025 samt enligt ISO 9001:2000 och 14001:1996 certifierat laboratorium. Denna rapport får endast återges i sin helhet, om inte utfärdande laboratorium i förväg skriftligen godkänt annat.

Site 5. Foundation 2-8 Mehuken

Drill core 2-8, box 1



Drill core 2-8, box 2



Drill core 2-8, box 3



Drill core 2-8, box 4



GEO-gruppen AB

Vattenförlustmätning

Uppdrag: Mehuken

Ärende nr: _____

Kärnborrhål: Verk 2:8 Syd-väst 225°

Utförd av: L. Thomsson

Datum: 10-1

Djup (m)	2 bar	5 bar	2 bar	Noteringar
	vattenförlust (l/5min)			
<u>3-6</u>	<u>ytläckage</u>			<u>Tappade spolvatten returen</u>
<u>6-9</u>	<u>0</u>	<u>0</u>	<u>0</u>	
<u>9-12</u>	<u>0</u>	<u>20,3</u>	<u>0</u>	
<u>12-15</u>	<u>21,6</u>	<u>53,1</u>	<u>20,8</u>	
<u>15-18</u>	<u>0</u>	<u>0</u>	<u>0</u>	
<u>18-21</u>	<u>0</u>	<u>0</u>	<u>0</u>	

SpecimenID	E[GPa]	Sa_max[MPa]	diam[m]	height[m]	gauge_length[m]
2_1	135.2	303.9	0.0448	0.1275	0.0640
2_4	34.8	76.6	0.0448	0.1279	0.0640
2_7	97.0	261.0	0.0451	0.1275	0.0640
2_8	21.1	120.8	0.0450	0.1274	0.0640